

# **Thermodynamics of Biomolecular Recognition**

**by Katherine E. McAuley-Hecht**

a thesis submitted in partial  
fulfilment for the degree of Ph.D.

ProQuest Number: 13815521

All rights reserved

INFORMATION TO ALL USERS

The quality of this reproduction is dependent upon the quality of the copy submitted.

In the unlikely event that the author did not send a complete manuscript and there are missing pages, these will be noted. Also, if material had to be removed, a note will indicate the deletion.



ProQuest 13815521

Published by ProQuest LLC (2018). Copyright of the Dissertation is held by the Author.

All rights reserved.

This work is protected against unauthorized copying under Title 17, United States Code  
Microform Edition © ProQuest LLC.

ProQuest LLC.  
789 East Eisenhower Parkway  
P.O. Box 1346  
Ann Arbor, MI 48106 – 1346

*Thesis*  
*9530*  
*Copy 1*

GLASGOW  
UNIVERSITY  
LIBRARY

## ACKNOWLEDGEMENTS

I would like to thank my supervisor Alan Cooper for suggesting this interesting project and for his support throughout. I am deeply indebted to Dr. Chris Johnson for his advice and encouragement and also to the remaining members of the biophysical laboratory- Margaret Nutley and Lorna Whytelaw.

I am also grateful to Dr A. Brown for the use of his lab facilities in the genetics department; Mr. I. Smith of the microbiology department for his advice and use of incubators, autoclaves, etc. and members of the biochemistry, mycology and cell biology departments for the use of their autoclaves.

Finally I must thank my friends at Glasgow and Edinburgh universities (particularly A. Gargaro, J. Thomson & family, C. Tedford and C. Mackellar), my family and especially Lutz for their support and encouragement.

Katherine McAuley-Hecht

## ABSTRACT

Thermodynamic aspects of molecular recognition have been studied using yeast phosphoglycerate kinase (PGK) and two antibiotics, ristocetin and vancomycin, as model systems.

The binding of 3 natural substrates, ADP, ATP and 3-phosphoglycerate to wild-type and two mutant forms of PGK was examined using kinetic techniques and isothermal titration microcalorimetry. The latter technique was also used to investigate the binding of various ligand molecules to PGK and to study the formation of the ternary complex- PGK.3-PG.ADP.

The thermodynamic parameters ( $K_a$ ,  $\Delta H^\circ$ ,  $\Delta G^\circ$ ,  $\Delta S^\circ$ ) relating to substrate binding to PGK are very sensitive to experimental conditions. Some of the factors which were found to influence the binding parameters include the buffer system, anion concentration, magnesium concentration and pH. For example, the  $\Delta H^\circ$  values for the binding of 3-phosphoglycerate to PGK were different for each buffer system investigated. This effect is due to protonation changes which occur when 3-phosphoglycerate binds to the enzyme.

The proposed binding sites for ADP and 3-phosphoglycerate are on separate domains and are some distance apart and therefore it might be expected that the binding of one substrate would not affect the binding of the other substrate. However the microcalorimetric experiments revealed that 3-phosphoglycerate binds much more weakly to the binary PGK.ADP complex than to PGK alone, whereas, the binding of

ADP is apparently enhanced by 3-phosphoglycerate. These results are consistent with ADP binding at two sites and displacing 3-phosphoglycerate at one of the sites.

The binding of bacterial cell-wall analogue peptides to ristocetin A and vancomycin was also studied by isothermal titration microcalorimetry. This work was in collaboration with Dr. Williams, Cambridge University. Four peptides were used in this study: one monopeptide (N-acetyl D-ala), two dipeptides (N-acetyl D-ala-D-ala, D-ala-D-ala) and one tripeptide (diacetyl L-lys-D-ala-D-ala). The ligand with the highest binding affinity for both antibiotics was the tripeptide. The trend in binding affinity continued with N-acetyl D-ala-D-ala followed by N-acetyl D-ala. The remaining peptide, D-ala-D-ala, did not bind to either antibiotic.

The thermodynamic parameters associated with the binding of the dipeptide and the tripeptide to vancomycin were dependent on antibiotic concentration. This is probably due to the tendency of the antibiotic to dimerise at higher concentrations. A model is proposed to explain the observed thermodynamic data, where we assume that an antibiotic dimer is formed which can bind two peptide molecules at two equivalent sites.

# CONTENTS

<b>Acknowledgements</b> .....	<b>I</b>
<b>Abstract</b> .....	<b>II</b>
<b>Chapter one Introduction</b> .....	<b>1</b>
1.1 Molecular recognition .....	1
1.2 Aims of thesis .....	4
1.3 Basic thermodynamics .....	5
1.4 Non-covalent forces (general) .....	7
1.4.1 Hydrogen bonding.....	8
1.4.2 Hydrophobic effects .....	9
1.4.3 Electrostatic forces .....	9
1.4.4 van der Waals forces .....	10
1.5 Non-covalent forces in biological complexes .....	11
1.5.1 Hydrogen bonding.....	11
1.5.2 Hydrophobic effects .....	13
1.5.3 Electrostatic effects .....	13
1.6 Methods for studying binding.....	14
1.6.1 Equilibrium dialysis .....	14

1.6.2	Equilibrium gel-filtration.....	15
1.6.3	Spectroscopic techniques.....	16
1.6.4	Kinetic experiments.....	16
1.6.5	Molecular mechanics, molecular dynamics and free energy perturbation methods.....	18
1.7	Phosphoglycerate kinase.....	19
1.8	The vancomycin group of antibiotics.....	34
<b>Chapter two Microcalorimetry.....</b>		<b>45</b>
2.1	Introduction to calorimetry.....	45
2.2	Calibration.....	53
2.3	Calculation of thermodynamic parameters from experimental data.....	53
2.4	Data analysis.....	56
2.4.1	Model for one set of sites.....	57
2.4.2	Model for two sets of independent sites.....	58
2.5	Associated heat effects.....	59
2.6	Recent uses of the Omega calorimeter.....	61
<b>Chapter three Materials and Methods.....</b>		<b>64</b>
3.1	Yeast cultures.....	64
3.2	Proteins.....	64

3.3	Substrates and ligands .....	65
3.4	SDS-PAGE chemicals.....	65
3.5	Fermentation and purification reagents.....	65
3.6	Antibiotics and cell wall analogues .....	65
3.7	General chemicals .....	66
3.8	Preparation of PGK, substrate and ligand samples for calorimetry .....	66
3.9	Preparation of antibiotic samples for calorimetry .....	67
3.10	Procedure for microcalorimetry using the LKB calorimeter .....	67
3.11	Procedure using Omega titration calorimeter.....	67
3.12	PGK enzyme activity measurements .....	69
3.12.1	Method A (Scopes, 1975) .....	69
3.12.2	Method B (Scopes, 1978a).....	70
3.12.3	Determination of <b>Michaelis</b> constants .....	71
3.12.4	Sulphate activation measurements .....	72
3.13	Determination of protein concentration .....	72
3.13.1	Estimation of protein concentration by UV absorption .....	73
3.13.2	Estimation of protein concentration by the Coomassie blue technique.....	73
3.14	SDS polyacrylamide gel electrophoresis.....	74

3.15	Wild-type and mutant PGK plasmids .....	76
3.16	Maintenance of yeast cultures .....	79
3.17	Yeast fermentation .....	81
3.18	Purification of Yeast PGK .....	81
<b>Chapter four</b>	<b>PGK Results .....</b>	<b>85</b>
4.1	PGK preparation .....	85
4.2	Kinetic studies of PGK.....	87
4.3	Microcalorimetry of substrate /ligand binding to PGK .....	92
4.3.1	The LKB titration calorimeter experiments.....	92
4.3.2	The Omega calorimeter experiments .....	95
4.3.3	Wild-type PGK .....	95
4.3.4	Mutant PGK.....	108
4.3.5	Buffer effects on the binding of 3-phosphoglycerate to wild-type PGK.....	116
4.3.6	Effect of anions on the binding of 3-phosphoglycerate .....	120
4.3.7	Sulphate effects on ligand binding.....	122
4.3.8	Studies of nucleotide binding to wild-type PGK.....	126
4.3.9	Wild-type ternary complex.....	134
4.3.10	H388Q ternary complex .....	140

<b>Chapter five Discussion (PGK experiments)</b> .....	144
<b>Chapter six Vancomycin and ristocetin results</b> .....	164
6.1 N-acetyl D-ala.....	164
6.2 N-acetyl D-ala-D-ala.....	168
6.3 D-ala-D-ala .....	173
6.4 Di-N-acetyl L-lys-D-ala-D-ala .....	173
6.5 Heat capacities .....	179
6.6 van't Hoff enthalpies .....	182
<b>Chapter seven Discussion (vancomycin &amp; ristocetin)</b> .....	185
7.1 Previous studies .....	185
7.2 Present work .....	188
7.3 Dimerisation effects .....	190
<b>Chapter eight Summary</b> .....	194
<b>Appendices</b> .....	196
Appendix A Site-directed mutagenesis.....	196
Appendix B Kinetic equations.....	202
Appendix C Abbreviations.....	203
<b>References</b> .....	204

## **Published work**

# 1 INTRODUCTION

## 1.1 Molecular recognition

Specificity is one of the most important features of biological reactions. Enzymes, in particular, achieve remarkable specificity and are able to distinguish between ligands that differ by just one functional group or between stereoisomers. This almost perfect recognition by enzymes for substrates is echoed by other biological macromolecules. For example, the immune system relies on the specific recognition of antigens by antibodies; hormones interact only with their target receptors; and regulatory proteins that control DNA transcription are able to bind to the correct site on the DNA molecule. All these biomolecular recognition processes are a result of the ligands having a structure which is complementary to the receptor in terms of size, shape and interactions.

Biological complexes are stabilised by multiple intermolecular non-covalent interactions, such as hydrogen bonding, van der Waals, electrostatic and hydrophobic effects. Non-covalent interactions although weaker than covalent bonds, have the advantage of allowing molecules to associate with high affinity and yet dissociate quickly (Frieden, 1975). Complex formation is usually a balance between favourable intermolecular interactions and unfavourable entropy effects resulting from restricting a ligand at a binding site. However, the major problem in predicting binding energies is that non-covalent forces are modified in aqueous solution, thus the solvation of both receptor and ligand and the changes in solvation which occur on complex formation must be considered. This problem cannot as yet be modelled theoretically and so

experimental techniques are used to study molecular recognition, and both the structural and thermodynamic aspects must be addressed.

Many molecular recognition experiments aim to investigate individual intermolecular interactions and provide an estimate of the stabilising energy for that particular interaction. This may be done, for example, by systematically varying functional groups on the ligand or macromolecule and noting effect on binding parameters. Ligands can be altered using chemical techniques, macromolecules by e.g. site-directed mutagenesis (Appendix A).

Structural techniques are used in molecular recognition studies to obtain a 3-dimensional view of the complex. NMR or X-ray crystallography are generally used. 2D-NMR techniques can provide well-resolved structures for proteins containing up to 100 amino acid residues, but for more than 100 amino acid residues peaks begin to overlap and the spectrum becomes difficult to interpret (Wright, 1989). X-ray crystallography can be used for any size of macromolecule providing that the macromolecule can be crystallized in a form suitable for X-ray diffraction studies and that heavy atom derivatives can be found. Hydrogen bonding interactions can be proposed from the structure of a complex using distance and geometric considerations, however, it is not yet possible to predict the stability of a complex from the structure, nor is it possible to quantify the relative importance of the many interactions involved in forming the complex. Therefore experiments that provide at least some of the thermodynamic binding parameters are required. These are usually estimated from direct binding studies, spectroscopic experiments or, in the case of enzymes, kinetic studies. Most of these experiments determine the equilibrium constant and free energy of binding, but few are conducted at different temperatures to allow the determination of enthalpy and entropy values.

An improved understanding of molecular recognition would be useful for rational drug design or modification of enzyme catalysis. Most drugs act either by inhibiting a target enzyme or by binding to a receptor protein; if the recognition phenomenon was better understood then it would be possible to develop structure-activity hypotheses and design new pharmaceutical compounds. An example of this type of work is the development of new trimethoprim analogues with improved selectivity. Trimethoprim, a drug used to treat bacterial infections, functions by inhibiting the enzyme dihydrofolate reductase (DHFR) effectively blocking the synthesis of some amino acids and purine and pyrimidine bases. Trimethoprim binds 3000 times more tightly to *E.coli* DHFR than to vertebrate DHFR (Davis *et al.*, 1990). Structural information (Matthews *et al.*, 1985, Oefner *et al.*, 1988) in conjunction with theoretical studies (Osguthorpe *et al.*, 1988) and free energy studies of the binding of trimethoprim to the binary complex of DHFR.NADH (Fleischman & Brooks, 1990) led to the development of the novel analogues, which have an increased selectivity of 50 000 times for bacterial enzymes.

Enzymes may act as catalysts by binding to the transition state for the reaction with higher affinity than the substrate (Pauling, 1946, Wolfenden, 1969, Kraut, 1988). A study of enzyme-substrate recognition could provide information on specificity requirements and catalysis. Enzyme catalysis could then be modified by altering the amino acid residues at the active site of the enzyme. The simplest strategy to alter the specificity of an enzyme is to swap functional groups, i.e. replace an enzyme side-chain with a residue containing the same functional group that is present in the substrate. The specificity of subtilisin was altered in this way. Subtilisin is a proteolytic enzyme which normally cleaves peptide bonds adjacent to amino acid residues with large side-chains such as phenylalanine. Subtilisin was made to recognise alanine and glycine residues instead of phenylalanine, by substituting a

phenylalanine residue for a glycine present in the active site (Estell *et al.*, 1986).

## 1.2 Aims of thesis

The aim of this thesis is to explore the basic thermodynamics of the interactions involved in molecular recognition using microcalorimetry. Two model systems were selected for investigation: the first involving an enzyme, yeast phosphoglycerate kinase (PGK) and its interaction with substrates; the second involves two antibiotics, vancomycin and ristocetin, binding to small peptides.

PGK is a monomeric enzyme comprising two domains of approximately equal size. The function of PGK is to transfer a phosphoryl group from 1,3-diphosphoglycerate to adenosine diphosphate (ADP) to give adenosine triphosphate (ATP) and 3-phosphoglycerate. The crystal structure of yeast PGK is known (Watson *et al.*, 1982) and several mutant forms are available; therefore PGK appeared to be a suitable candidate for molecular recognition studies. In particular, since PGK is a 2 substrate/2 product enzyme, it allows the possibility of examining the binding of actual substrates, one at a time, or non-productive ternary complexes, rather than simply inhibitors or substrate analogues. PGK is also of interest since a domain movement is believed to occur when both substrates bind to the enzyme; this would be expected to lead to some interesting thermodynamic properties, observable by microcalorimetry.

Vancomycin and ristocetin are antibiotics active against gram positive bacteria. Both antibiotics are small heptapeptides with rigid structures and well-defined binding cavities. This work is in collaboration with Dr.D.H. Williams, Cambridge University and extends previous microcalorimetric investigations by Rodriguez-Tebar *et al.* (1986) of the binding of cell-wall analogue peptides to the

antibiotics. Being smaller molecular systems, these offer potential advantages over the much larger protein system, which can be hard to interpret.

### 1.3 Basic thermodynamics

The thermodynamic quantities which are of interest in describing ligand binding are the standard Gibbs energy change  $\Delta G^\circ$ , the standard enthalpy change  $\Delta H^\circ$ , the standard entropy change  $\Delta S^\circ$  and the heat capacity change at constant pressure  $\Delta C_p^\circ$ .

For the formation of a simple 1:1 binding complex between a macromolecule, M, and a ligand, L, at equilibrium,



the equilibrium constant, K (which is equivalent to the association constant,  $K_a$ , and the reciprocal of the dissociation constant,  $K_d$ ) is given by:

$$K = \frac{a_{ML}}{a_M a_L} \quad (1.1)$$

where  $a_{ML}$ ,  $a_M$  and  $a_L$  are the activities of the corresponding species. Lack of knowledge of the activity co-efficients means that concentrations, [M], [L] and [ML], rather than activities are customarily used, therefore

$$K_a = \frac{[ML]}{[M][L]} \quad (1.2)$$

This is a reasonable approximation since activity coefficients in dilute solutions are usually close to unity.

The standard free energy change of binding is related to the equilibrium constant by the following equation:

$$\Delta G^\circ = -RT \ln K, \quad (1.3)$$

where R is the gas constant (equal to  $8.314 \text{ J mol}^{-1} \text{ K}^{-1}$ ) and T is temperature. For significant binding to occur,  $\Delta G^\circ$  must be negative. The free energy change has both enthalpic and entropic components as shown in equation 1.4.

$$\Delta G^\circ = \Delta H^\circ - T\Delta S^\circ. \quad (1.4)$$

$\Delta G^\circ$  represents a balance between the tendency of a system to minimise its energy and to maximise its entropy.

The enthalpy change for a process is equal to the heat evolved or absorbed by the system during that process under constant pressure, and is defined by

$$\Delta H^\circ = \Delta U^\circ + P\Delta V, \quad (1.5)$$

where P is pressure, V is volume and U is the internal energy of the system which includes contributions from the potential and rotational, vibrational and translational energies of all the molecules in the system. The  $P\Delta V$  term takes account of any work done on or by the system by volume changes. Exothermic processes which liberate heat are denoted by negative  $\Delta H^\circ$  values and endothermic processes have positive values.  $\Delta H^\circ$  can be measured directly by calorimetry or by measuring the association constant at several temperatures and then applying the van't Hoff relationship:

$$\frac{d \ln K_a}{d(1/T)} = - \frac{\Delta H^\circ}{R}. \quad (1.6)$$

However, errors in measuring  $K_a$  values consequently lead to high errors in  $\Delta H^\circ$  values.

The entropy change can be expressed at the molecular level as

$$\Delta S^\circ = -R \ln(w_{\text{free}}/w_{\text{bound}}),$$

The entropy change can be expressed at the molecular level as

$$\Delta S^\circ = -R \ln(w_{\text{free}}/w_{\text{bound}}), \quad (1.7)$$

where  $w_{\text{free}}/w_{\text{bound}}$  is the ratio of the number of ways that the system may exist in either the free or bound states. The entropy change can be calculated from the enthalpy change and the equilibrium constant using equations 1.3 and 1.4.

Both  $\Delta H^\circ$  and  $\Delta S^\circ$  are dependent on temperature because of heat capacity effects

$$\Delta H^\circ_{(T2)} - \Delta H^\circ_{(T1)} = \int_{T1}^{T2} \Delta C_p^\circ dT \quad (1.8)$$

$$\Delta S^\circ_{(T2)} - \Delta S^\circ_{(T1)} = \int_{T1}^{T2} (\Delta C_p^\circ/T) dT \quad (1.9)$$

The change in heat capacity ( $\Delta C_p^\circ$ ) provides information concerning, for example, hydrophobic interactions between the macromolecule and ligand. A negative value of  $\Delta C_p^\circ$  usually indicates that there is an increase in hydrophobic interactions whereas a positive value indicates a decrease in hydrophobic interactions.  $\Delta C_p^\circ$  is determined by measuring  $\Delta H^\circ$  values at two or more temperatures using the following equation.

$$\Delta C_p^\circ = d(\Delta H^\circ)/dT. \quad (1.10)$$

#### 1.4 Non-covalent forces (general)

Microcalorimetry can provide direct information on the energetics of ligand binding. However, it is important to evaluate the relative strength and importance of the various non-covalent forces which contribute to the overall binding energy.

Hydrogen bonding, hydrophobic, electrostatic and van der Waals interactions will be discussed in this and the following section with a view to outlining the types of thermodynamic effects each interaction might exert on ligand binding.

### 1.4.1 Hydrogen bonding

A hydrogen bond is formed when two electronegative atoms are linked by a hydrogen atom which is covalently bound to one of them. The hydrogen bond is the strongest of the non-covalent interactions with a typical free energy in the gas-phase of 25-79 kJmol<sup>-1</sup> (Weiner, 1984, Meot-Nir & Sieck, 1986). Hydrogen bonds are partially directional since the interaction is strongest when the three interacting atoms are co-linear; hydrogen bonds can therefore be important in determining geometric constraints between enzyme and substrate and hence specificity.

The contribution to overall binding energy of a macromolecule-ligand hydrogen bond depends on its surroundings; the effective strength is altered in the presence of water due to competition with water hydrogen bonds. In aqueous solution, a macromolecule and ligand will participate in hydrogen bonding to surrounding water molecules and, therefore, there may be no net gain in the number of hydrogen bonds formed when the two molecules associate. This is demonstrated by the usually low enthalpy and free energy values associated with hydrogen bond formation between groups in water (Klotz & Franzen, 1962). There may be, however, an increase in entropy of the system due to the release of hydrogen-bonded water molecules to the bulk phase, which may go some way to stabilizing the interaction. In general, however, hydrogen bonds may be more important in controlling specificity rather than stabilizing the complexes themselves.

### 1.4.2 Hydrophobic effects

Hydrophobic effects are a consequence of the strong interactions of water molecules with each other. When a hydrophobic molecule (such as a hydrocarbon) is transferred to an aqueous environment it is unable to participate in hydrogen bonding and therefore neighbouring water molecules compensate by forming the maximum number of hydrogen bonds with each other, thus there is an increase in local order around the solute. This leads to a slightly favourable change in enthalpy but a large unfavourable change in entropy. There is therefore a driving force to bring hydrophobic molecules together in aqueous solution since this decreases the hydrophobic surface area accessible to water and hence some of the ordered water molecules are released resulting in a large increase in entropy (Kauzmann, 1959). These effects also give rise to significant heat capacity changes.

### 1.4.3 Electrostatic forces

The energy relationship between two point charges is given by Coulomb's law:

$$\Delta E = \frac{q_1 q_2 k}{\epsilon r}, \quad (1.11)$$

where  $q_n$  = unit charge,  $k$  is a constant and  $\epsilon$  is the dielectric constant. For oppositely charged species there is an attractive force which is related to the distance,  $r$ , between the charges; this is a non-directional attraction. Polar solvents have a shielding effect on the ions and therefore reduce the attraction; the degree to which this happens depends on the dielectric constant of the solvent. Water, which is a highly polar solvent, has a large dielectric constant of 80 and consequently electrostatic interactions are weakened in aqueous solution. Electrostatic interactions

between a macromolecule and ligand are also weakened by high salt concentrations. The contribution of electrostatic bonds to complex formation is mainly an entropy effect due to the release of electrostricted water molecules.

In addition to charge-charge interactions, there are also electrostatic attractions between molecules with permanent dipoles or induced dipoles. The van der Waals or dispersion interaction is a special type of electrostatic interaction which can occur between any pair of atoms, even between apolar atoms.

#### **1.4.4 van der Waals forces**

Van der Waals interactions arise when a transient dipole in one molecule induces dipoles in surrounding molecules. These interactions are effective only over short distances since the attractive energy varies as the inverse sixth power of distance. Van der Waals interactions are, therefore, most effective when there is close packing between molecules. Although these interactions are weak individually, they are additive and when summed over the entire binding site can contribute significantly to binding.

The possible thermodynamic contributions of the various non-covalent forces to ligand binding in water can be summarised in table 1.1 (Eftink & Biltonen, 1980).

**Table 1.1** Thermodynamics of various intermolecular, non-covalent interactions

Type of interaction	$\Delta H$	$\Delta S$	$\Delta C_p$
Hydrophobic	$\approx 0$	$> 0$	$< 0$
Electrostatic	$\approx 0$	$> 0$	$> 0$
Hydrogen bond	$< 0$	$< 0$	$< 0$
van der Waals	?	?	?

There are difficulties in estimating the contribution of van der Waals interactions to overall binding energies since it is impossible to measure these quantities in isolation experimentally, however, the values estimated for the other types of non-covalent interactions probably include contributions from van der Waals interactions.

### 1.5 Non-covalent forces in biological complexes

The role of non-covalent forces in stabilising biological complexes has been the subject of many research investigations. However, few of these studies have determined all the thermodynamic variables related to binding. In particular, some of the examples discussed in this section used kinetic techniques, such as measurements of  $K_I$  or  $k_{cat}/K_M$ , to obtain free energy values: these values can only approximate to the thermodynamic free energies.

#### 1.5.1 Hydrogen Bonding

Hydrogen bonds between neutral partners stabilize binding free energies of enzyme-substrate complexes by approximately 2.1-7.5 kJmol<sup>-1</sup>, whereas hydrogen

bonds between charged partners have a contribution of 12.5-25.1 kJmol<sup>-1</sup> (Fersht, 1987). These values have been measured in several laboratories using different model systems. One such model system was based on protein engineering studies of the tyrosyl-tRNA synthetase complex (Fersht *et al.*, 1985). Enzyme side-chains believed to be participating in hydrogen bonding to substrate were identified from the crystal structure of the complex; these were then subjected to site-directed mutagenesis experiments. Each side-chain was modified and the contribution of the side-chain to the free energy of binding was evaluated. Kinetic experiments were used to determine values for  $k_{\text{cat}}$  and  $K_{\text{M}}$  for wild-type and mutant enzymes and  $\Delta\Delta G$  was calculated using equation 1.19. The values calculated were 2.1-6.3 kJmol<sup>-1</sup> for hydrogen bonding interactions between uncharged groups and 14.6-18.8 kJmol<sup>-1</sup> for interactions between charged groups.

Similar results were obtained using a model system involving the enzyme, glycogen phosphorylase, which catalyses the reversible phosphorolysis of glycogen to give glucose-1-phosphate (Street *et al.*, 1986). In this instance the carbohydrate substrate was modified to remove or alter hydrogen bonds by constructing deoxy and fluorodeoxy analogues of the natural substrate. The inhibition constants for each analogue ( $K_{\text{I}}$ ) were measured and the free energy differences between analogues,  $\Delta\Delta G^{\circ}$ , were calculated from the expression

$$\Delta\Delta G^{\circ} = RT \ln (K_{\text{I2}}/K_{\text{I1}}). \quad (1.12)$$

Values of approximately 4.2 kJmol<sup>-1</sup> for uncharged H-bonds and approximately 12.5 kJmol<sup>-1</sup> for charged H-bonds were found.

However, there are examples in which hydrogen bonding contributions have been found to have a greater stabilising effect than proposed above. A hydrogen bond in a thermolysin-inhibitor complex was found to have an energy of 16.7 kJmol<sup>-1</sup>,

although the hydrogen bonding partners are uncharged (Bartlett & Marlowe, 1987). Likewise, a higher energy (nearly 42 kJmol<sup>-1</sup>) was found for a single hydroxyl group of a transition state analogue of adenosine deaminase (Kati & Wolfenden, 1989). These examples demonstrate that the values for hydrogen bonding can vary over a wide range.

### 1.5.2 Hydrophobic effects

The energetics of hydrophobic effects have been estimated from the partitioning of solutes, such as hydrocarbons or amino acid side-chains, between aqueous and non-polar solvents (Leo *et al.*, 1971, Radzicka & Wolfenden, 1988). These type of experiments revealed that the hydrophobic free energy is proportional to the surface area of the solute. This means that if the hydrophobic surface area removed from solvent on ligand binding can be measured (using for example molecular surfacing algorithms) then this can be correlated to the hydrophobic free energy using a factor of 192-197 J/mol.A<sup>2</sup> (Sharp *et al.*, 1991). This value gives good agreement with experimental results based on mutant protein stability measurements, where the effect of removing hydrophobic amino acid residues on protein stability was measured by comparing the denaturation of wild-type and mutant proteins (Kellis *et al.*, 1989, Shortle *et al.*, 1990).

### 1.5.3 Electrostatic effects

Proteins may contain amino acid residues with functional groups that are charged under physiological conditions; these include the negatively charged aspartic or glutamic acid and the positively charged histidine, arginine or lysine amino acid residues. These residues may participate in electrostatic interactions to the substrate molecule. It is difficult to estimate the contribution of electrostatic forces to binding

energies since the dielectric constant at the enzyme active site is unknown. The internal protein dielectric constant has been estimated to be between 2-6 (Gilson & Honig, 1987, Gilson *et al.*, 1985) but this value probably increases at the protein-water interface. For example, a dielectric constant of 40-50 for the active site of subtilisin has been measured by examining the effect of mutational changes of the charge of surface residues on the  $pK_a$  of an active site histidine (Russell *et al.*, 1987). Protein engineering techniques have been used to make experimental measurements of electrostatic contributions to enzyme-substrate binding. Experiments with subtilisin as the model enzyme measured values of 7.5 and 9.6  $\text{kJmol}^{-1}$  for ion pair interactions at two positions in the active site (Wells *et al.*, 1987) and similarly, the electrostatic component for the interaction of glutamic acid with a mutant aspartate aminotransferase (R292D) has been estimated to be 6.8  $\text{kJmol}^{-1}$  (Cronin & Kirsch, 1988).

## 1.6 Methods for studying binding

Although the majority of the binding studies to be described in this thesis involved microcalorimetry, there are numerous other methods which can be used to examine ligand binding. Some of these methods are discussed in this section.

### 1.6.1 Equilibrium dialysis

Equilibrium dialysis requires a membrane which is permeable to all components of the experiment except for the protein. In a typical experiment, an enzyme solution is placed in a compartment on one side of the membrane, whilst the ligand solution is on the other side. After equilibration the concentration of ligand is measured in both compartments. The concentration,  $[L]_1$ , measured in the compartment containing only ligand is equal to the free ligand concentration ( $[L]$ ).

The concentration,  $[L]_2$ , of ligand in the compartment containing enzyme equals the free ligand concentration plus the concentration of bound ligand ( $[ML]$ ). Therefore since

$$[L] = [L]_1 \text{ and } [ML] = [L]_2 - [L]_1,$$

the concentration  $[M]$  of the unbound macromolecule is

$$[M]_{\text{initial}} - [ML] \text{ or } [M]_{\text{initial}} - [L]_2 + [L]_1.$$

The association constant for a simple 1:1 complex formation, can be calculated from equation 1.13.

$$K_a = \frac{[L]_1 - [L]_2}{[L]_1 ([M]_{\text{initial}} - [L]_2 + [L]_1)} \quad (1.13)$$

More complicated methods of analysis (e.g. Scatchard plots etc.) are required for multi-site binding processes. A Scatchard plot is a graph of  $r/[L]$  versus  $r$ , where  $r$  is the degree of binding i.e. moles of ligand bound per mole of protein. The gradient of the line gives the negative association constant and the intercept on the x-axis is the maximum number of ligand molecules bound.

### 1.6.2 Equilibrium gel-filtration

Equilibrium gel-filtration experiments can also be used to determine association constants. First a column containing a gel-filtration medium which excludes enzyme from the beads is equilibrated with ligand. The enzyme is applied to the column and as it passes through, it binds to ligand causing the ligand to elute at the same rate. The concentration of ligand is continuously monitored in the eluent and as the protein elutes a peak in ligand concentration is observed. This is later followed

by a trough where the ligand would have eluted in the absence of protein. The association constant can be calculated in a similar fashion to the equilibrium dialysis technique.

### 1.6.3 Spectroscopic techniques

Changes in spectral properties of the enzyme caused by the interaction with substrate can also be used to estimate association constants. If some property (e.g. UV absorbance) of the enzyme or ligand is proportional to the amount of complex formed then the fractional degree of association ( $f$ ) is given by

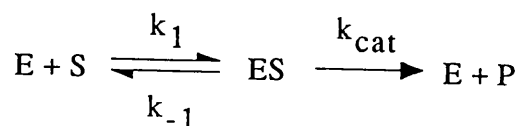
$$f = \Delta A / \Delta A_{\max} = K_a [L] / (1 + K[L]), \quad (1.14)$$

where  $\Delta A$  is the change in absorbance and  $\Delta A_{\max}$  is the total change in absorbance between the enzyme in the fully liganded state and the unliganded state.  $K_a$  is determined by analysis of  $\Delta A$  as a function of ligand concentration,  $[L]$ .

### 1.6.4 Kinetic experiments

The velocity of an enzyme catalysed reaction at a constant substrate concentration is normally directly proportional to the enzyme concentration. However a non-linear, hyperbolic relationship is usually observed when the enzyme concentration is held constant and the substrate concentration is varied. The velocity is proportional to substrate concentration only at low levels and at saturating concentrations of substrate the velocity approaches a maximum value,  $V_{\max}$ . Most rates are measured in the steady state period of the enzyme reaction, which occurs soon after the reaction has started.

Michaelis and Menten proposed the following mechanism:



The enzyme and substrate first associate to form a non-covalent complex (ES) which can then dissociate to give free substrate (S) and enzyme (E) or react to give products (P). Since initial velocities are measured, the formation of the enzyme-substrate complex from E and P can be neglected because only a small amount of product is available in the early stages of the reaction. The velocity of the enzyme catalysed reaction is expressed by the Michaelis-Menten equation.

$$V = \frac{[S] k_{\text{cat}}[E]_{\text{T}}}{K_{\text{M}} + [S]} \quad (1.15)$$

where  $V$  is the initial velocity,  $[S]$  is the substrate concentration,  $[E]_{\text{T}}$  is the total enzyme concentration and  $K_{\text{M}}$  is equal to  $(k_{\text{cat}} + k_{-1})/k_1$ .  $K_{\text{M}}$ , the Michaelis constant, is equal to the concentration of substrate at which the velocity is equal to half its maximum rate. The Michaelis constant is comparable to the dissociation constant. However, unlike the dissociation constant,  $K_{\text{M}}$  specifies the relative concentrations of E, S and ES under steady-state conditions and not at equilibrium.  $K_{\text{M}}$  approximates to  $K_{\text{d}}$  only if  $k_{\text{cat}}$  is much less than  $k_{-1}$  so that  $K_{\text{M}} = k_{-1}/k_1$ .  $k_{\text{cat}}$  is also known as the turnover number and is equal to the number of substrate molecules converted to products per second.

Michaelis constants are determined experimentally by measuring initial velocities at fixed enzyme concentration and varying substrate concentrations. The data

can then be analyzed to yield values of  $K_M$  and  $V_{max}$ .  $k_{cat}$  is determined from  $V_{max}$  and the enzyme concentration since

$$V_{max} = k_{cat}[E]_T. \quad (1.16)$$

The ratio  $k_{cat}/K_M$  can be thought of as the second order rate constant for the reaction between substrate and free enzyme since

$$V = (k_{cat}/K_M)[E][S]. \quad (1.17)$$

$k_{cat}/K_M$  is related to the total binding energy of an enzyme-substrate complex ( $\Delta G_b$ ) by equation 1.18.

$$RT \ln (k_{cat}/K_M) = RT \ln (kT/h) - \Delta G^\ddagger - \Delta G_b, \quad (1.18)$$

where  $\Delta G^\ddagger$  is the activation free energy,  $k$  is Boltzmann's constant and  $h$  is Planck's constant.

If an enzyme is mutated so that a group involved in binding a substrate is removed then, assuming that  $\Delta G^\ddagger$  is unaltered, the contribution of that group to binding in the wild-type enzyme relative to its absence in the mutant ( $\Delta G_{rel}$ ) is given by equation 1.19.

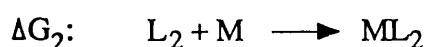
$$\Delta G_{rel} = RT \ln [(k_{cat}/K_M)_{mutant}/(k_{cat}/K_M)_{wild-type}]. \quad (1.19)$$

This equation is often used to assess the effect of mutations after site-directed mutagenesis experiments.

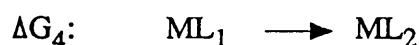
### 1.6.5 Molecular mechanics, molecular dynamics and free energy perturbation methods

Although the free energy of binding cannot yet be calculated using

computational approaches, the difference in binding free energy resulting from mutation of an enzyme or modification of a substrate can be calculated using the free energy perturbation method (McCammon & Harvey, 1987). This is achieved by computationally mutating the enzyme or substrate in a large number of small steps. At each step the molecule is allowed to adjust structurally and energetically using molecular dynamics. The free energy change and the change in enthalpy due to the mutation can be calculated. An example of this approach would be to study the binding of two ligands,  $L_1$  and  $L_2$ , to a protein. The relative binding affinity is the free energy difference  $\Delta\Delta G$ , which equals  $\Delta G_2 - \Delta G_1$  for the following processes



However it is easier to calculate  $\Delta G$  values for the hypothetical reactions



Since these reactions form a thermodynamic cycle,

$$\Delta\Delta G = \Delta G_2 - \Delta G_1 = \Delta G_4 - \Delta G_3,$$

the relative free energy can be found using the perturbation method.

A thermodynamic perturbation technique was used to measure the relative free energy of binding for the enzyme thermolysin complexed with a pair of phosphoramidate and phosphonate ester inhibitors.  $\Delta\Delta G$  was calculated to be  $17.6 \pm 2.2 \text{ kJmol}^{-1}$  (Bash *et al.*, 1987). This value was in close agreement with an experimental measurement of  $17.1 \text{ kJmol}^{-1}$ , determined kinetically (Bartlett & Marlowe, 1987).

## 1.7 Phosphoglycerate kinase

Phosphoglycerate kinase (PGK), which was chosen as a model system in this

thesis, is a key enzyme in the glycolytic pathway in which ATP is produced from the breakdown of glucose to pyruvate. ATP functions as the "energy currency" of the cell since its free energy of hydrolysis is used to drive endergonic reactions. The pathway is a ten step process, with each step catalysed by a different enzyme. PGK is the enzyme that catalyses the first ATP generating step by transferring a phosphoryl group from 1,3-diphosphoglycerate (1,3-DPG) to ADP to give 3-phosphoglycerate (3-PG) and ATP as depicted in figure 1.1. The true nucleotide substrates are the metal complexes (usually  $Mg^{2+}$ ) of ADP and ATP

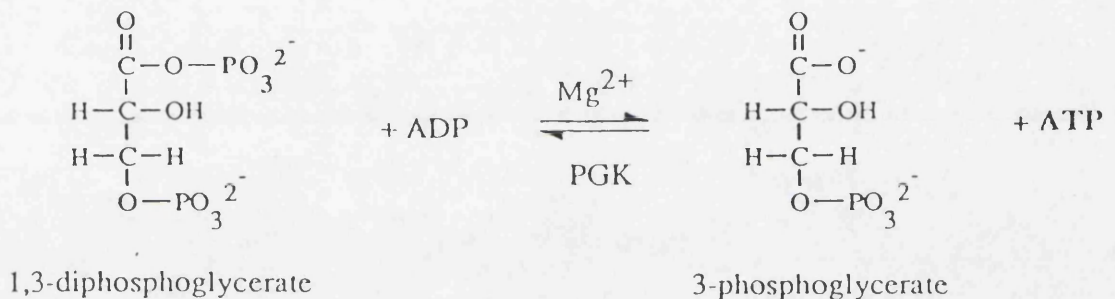


**Figure 1.1** The reaction catalysed by PGK in the glycolytic pathway

One of the most remarkable features of PGK is that in the 22 known PGK sequences from different sources, including mammalian, plant and bacterial species, there is a very high degree of conserved residues (Mori *et al.*, 1986, Watson & Littlechild, 1990). If all the sequences are aligned in such a way that the tertiary structure is taken into consideration, then there are a total of 62 completely conserved amino acid residues and approximately 30% of the remaining residues are conservative alterations (similar in size and charge). Most of the totally conserved residues line the surface of the cleft between the two domains, reflecting the

importance of this region with respect to catalytic action. An experiment which proved the conservative nature of PGK was performed by Mas *et al.* in 1986. Human and yeast hybrid PGK enzymes were constructed by joining a human C-domain to a yeast N-domain and *vice versa*. The resultant chimeras exhibited catalytic properties which were relatively unchanged.

In 1979 the X-ray structure and amino acid sequence were reported for horse-muscle PGK (Banks *et al.*, 1979). Earlier X-ray structures had been published for horse-muscle (Blake & Evans, 1974) and yeast PGK (Bryant *et al.*, 1974) however, knowledge of the sequence of amino acids allowed the side-chains to be clearly defined for the first time. Horse-muscle PGK contains 416 residues and has a molecular weight of 45 519. The main feature of the structure is that it is divided into two lobes with a deep cleft between the lobes. The polypeptide chain forms most of the N-domain before crossing to form the C-domain and then returning to complete the N-domain. The interdomain region where the polypeptide chain crosses twice, is known as the waist region.

The N- and C- domains are of approximately equal size and are each composed of a central  $\beta$ -sheet structure surrounded by helices and loops of irregular structure. The  $\beta$ -sheet cores contain 6 strands, the order of the strands in the N-domain is CDBAEF, and in the C-domain CBADEF. This arrangement found in the C-domain is common in nucleotide binding enzymes and is known as the Rossman fold (Rossman, 1974). The PGK molecule has a total of 15 helices, 12 internal  $\beta$ -strands and 5 external  $\beta$ -strands, corresponding to 25% of amino acids in  $\beta$ -structures and 42% in helices.

The analysis of the horse-muscle enzyme structure was followed in 1982 by the publication of the sequence and structure of yeast PGK (Watson *et al.*, 1982)

(figure 1.2). A high degree of structural homology was observed between yeast PGK and horse-muscle PGK and a 65% sequence homology was found. More recently, the binary complex of pig-muscle PGK and 3-phosphoglycerate was analysed by X-ray crystallography (Harlos *et al.*, 1992).

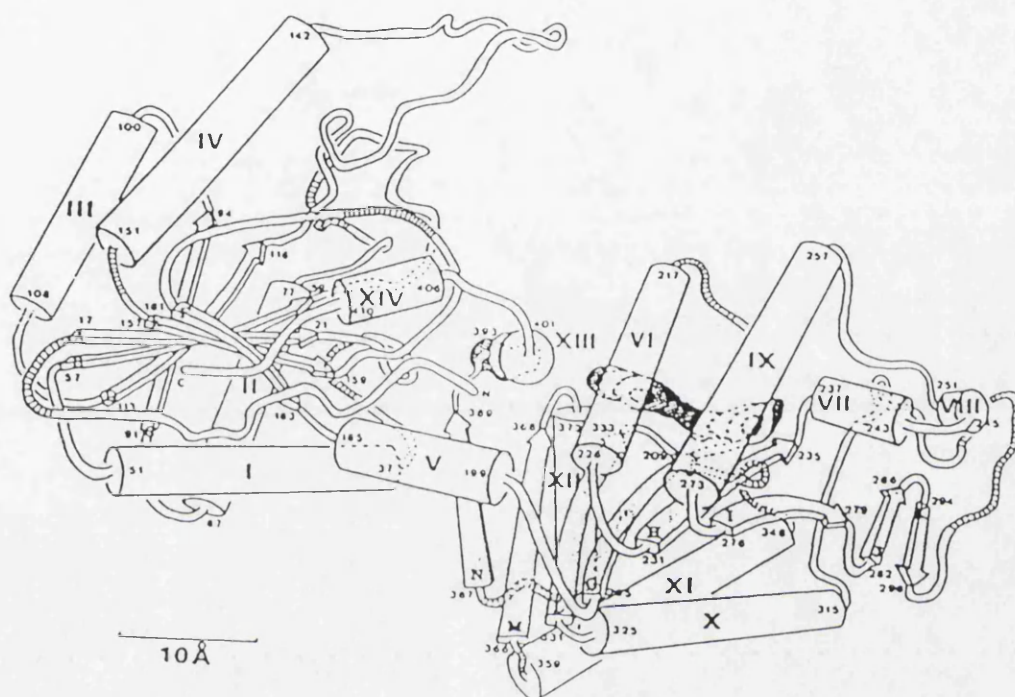


**Figure 1.2** Crystallographic structure of Yeast PGK (Watson *et al.*, 1982)

These X-ray crystallographic studies provided some information regarding the position of the substrate binding sites. The location of the Mg.ADP and Mg.ATP binding site in horse-muscle PGK was found by crystal soaking experiments. This site is located on the C-domain, on the surface of the cleft, facing the N-domain. The adenine ring of ATP fits into a hydrophobic slot in the enzyme and the ribose portion lies above the pyrrolidine ring of Pro 338. The  $\alpha$ -phosphate interacts with Lys 219 and the  $\beta$ - and  $\gamma$ - phosphates interact with the helix dipole of helix 13. Mg.ADP binds in a similar way, although the magnesium ion is differently positioned. In ADP binding,

the  $Mg^{2+}$  ion is between the  $\alpha$ - and  $\beta$ - phosphates and Asp 374, whereas, in ATP binding, it is believed to interact with either the  $\beta$ - or  $\gamma$ - phosphate or both.

The 3-phosphoglycerate molecule could not be located in the density map following crystal soaking, but the authors proposed that the most probable position would be on the N-domain at a region of basic residues. It was concluded that since the nucleotide and 3-phosphoglycerate sites were 12-15 Å apart, a large conformational change was required to bring the substrates into a position where phosphoryl transfer could take place. This would involve a "hinge-bending" motion of the enzyme.

Crystal soaking experiments were also performed with yeast PGK crystals and the binding site of an analogue of ATP, Mn-adenyl- $\beta$ - $\gamma$ -imidodiphosphate, was identified. The binding site of the nucleotide substrates is similar to that of horse-muscle PGK. The  $\gamma$ -phosphate of ATP hydrogen bonds to main chain N atoms of residues 372 and possibly 371. The metal ion is located 3 Å from the  $\gamma$ -phosphate and 5 Å from both the  $\alpha$ - and  $\beta$ - phosphates and is hydrogen bonded to the acidic group of Asp 372. Difference Fourier maps between crystals grown in ammonium sulphate and then transferred to ammonium selenate indicated the presence of a selenate ion in the position of the  $\gamma$ - phosphate of ATP.

There was no evidence of 3-phosphoglycerate binding to yeast PGK from the X-ray studies. However, an unexplained electron density peak was assigned to the 3-phosphoglycerate binding site. This site is in the interdomain region of PGK, with the substrate in a suitable position for phosphoryl transfer.

The ambiguity of the position of the 3-phosphoglycerate binding site was resolved with the publication of the structure of the binary complex of pig-muscle PGK and 3-phosphoglycerate. Crystals of the complex were grown using polyethylene

glycol as the precipitating agent instead of ammonium sulphate and therefore 3-phosphoglycerate was able to bind to the enzyme. The horse-muscle and yeast PGK crystals had both been crystallised from ammonium sulphate and it is possible that sulphate ions from the mother liquor were competing with 3-phosphoglycerate for the binding site (Blake & Rice, 1981).

The 3-phosphoglycerate molecule binds to the N-domain as suggested by Banks *et al.* for the horse-muscle enzyme. The binding interactions include hydrogen bonding and electrostatic effects between the substrate and some of the basic patch residues. The 3-phosphate group interacts with three arginine residues: Arg 170, Arg 65 and Arg 122 (horse-muscle PGK numbering). The hydroxyl group is hydrogen bonded to residues Asp 23 and Asn 25; this determines the stereospecificity at this site. The carboxyl group forms a hydrogen bond with an ordered water molecule which is situated at the N-terminal end of helix-14. A diagram of the interactions is shown in figure 1.3.

The structure of the 3-phosphoglycerate-PGK binary complex was superimposed with the structure of the substrate-free horse-muscle PGK structure and a difference in the relative positions of the N- and C- domains was found. The domains in the binary complex are rotated by 7.7Å compared to the substrate-free enzyme. This movement brings the substrate binding sites closer together, although they are still too far apart for phosphoryl transfer to occur.

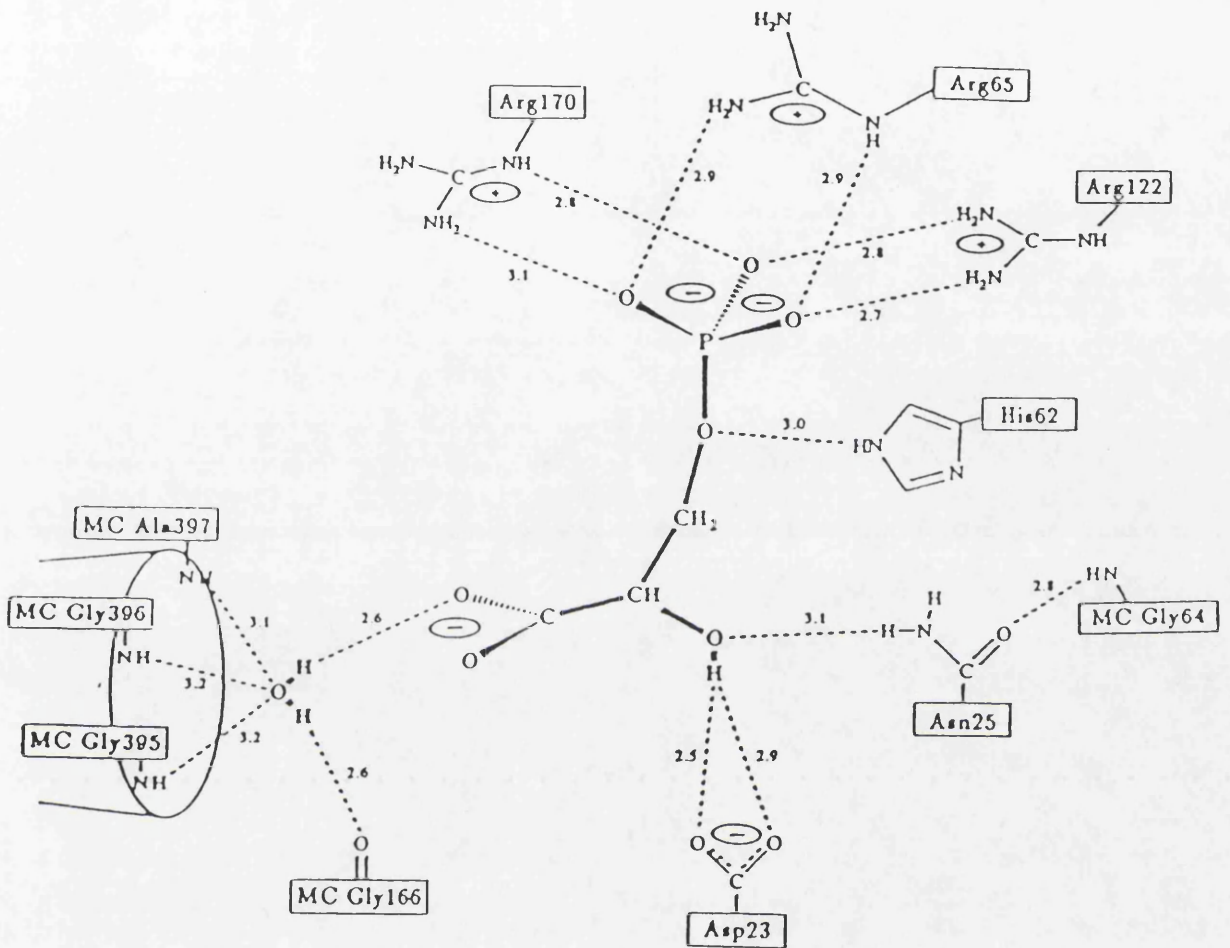


**Figure 1.3** *Diagram of the interactions between pig-muscle PGK and 3-phosphoglycerate (Harlos et al., 1992)*

There are two possible reasons why a conformational change is needed on substrate binding: the first is that by bringing the domains together, the substrate binding sites and catalytic residues will be brought into close proximity and the

second is that domain closure will expel water from the active site, thus preventing phosphate transfer to water molecules instead of between substrates.

Conformational changes have been observed or predicted for other enzymes, particularly other kinases (Anderson *et al.*, 1979). Hexokinase, an enzyme which is similar to PGK in size, shape and catalytic function, has been shown to undergo domain closure and this has proved essential for catalytic action (McDonald, 1979, Bennett, 1978). The movement is considered as a rotation about an axis in the interdomain region, which allows the domains to move relative to each other. For horse-muscle PGK, a 20° rotation of two helices in the interdomain region has been proposed and modelled (Blake *et al.*, 1986) (figure 1.4). This action brings the nucleotide binding site and the basic patch within 5Å of each other and causes few unfavourable interactions between residues within the protein. Direct evidence for domain closure has not been obtained from X-ray crystallography, since it has been impossible to crystallise the ternary complex. However, evidence using other techniques has been found.

Small angle X-ray scattering measurements of solutions of yeast PGK have revealed that the presence of substrates decreases the radius of gyration (Pickover *et al.*, 1979). Mg.ATP and 3-phosphoglycerate each individually lead to a small decrease, while the presence of both substrates causes a more substantial decrease in the radius of gyration of  $1.09 \pm 0.34\text{Å}$  indicating a large conformational change consistent with domain closure. Diffuse X-ray scattering data with pig muscle PGK show a similar decrease of 1.2Å (Sinev *et al.*, 1989).

Analytical centrifugation studies of free and liganded PGK appeared to give further evidence of domain closure (Roustan *et al.*, 1980).

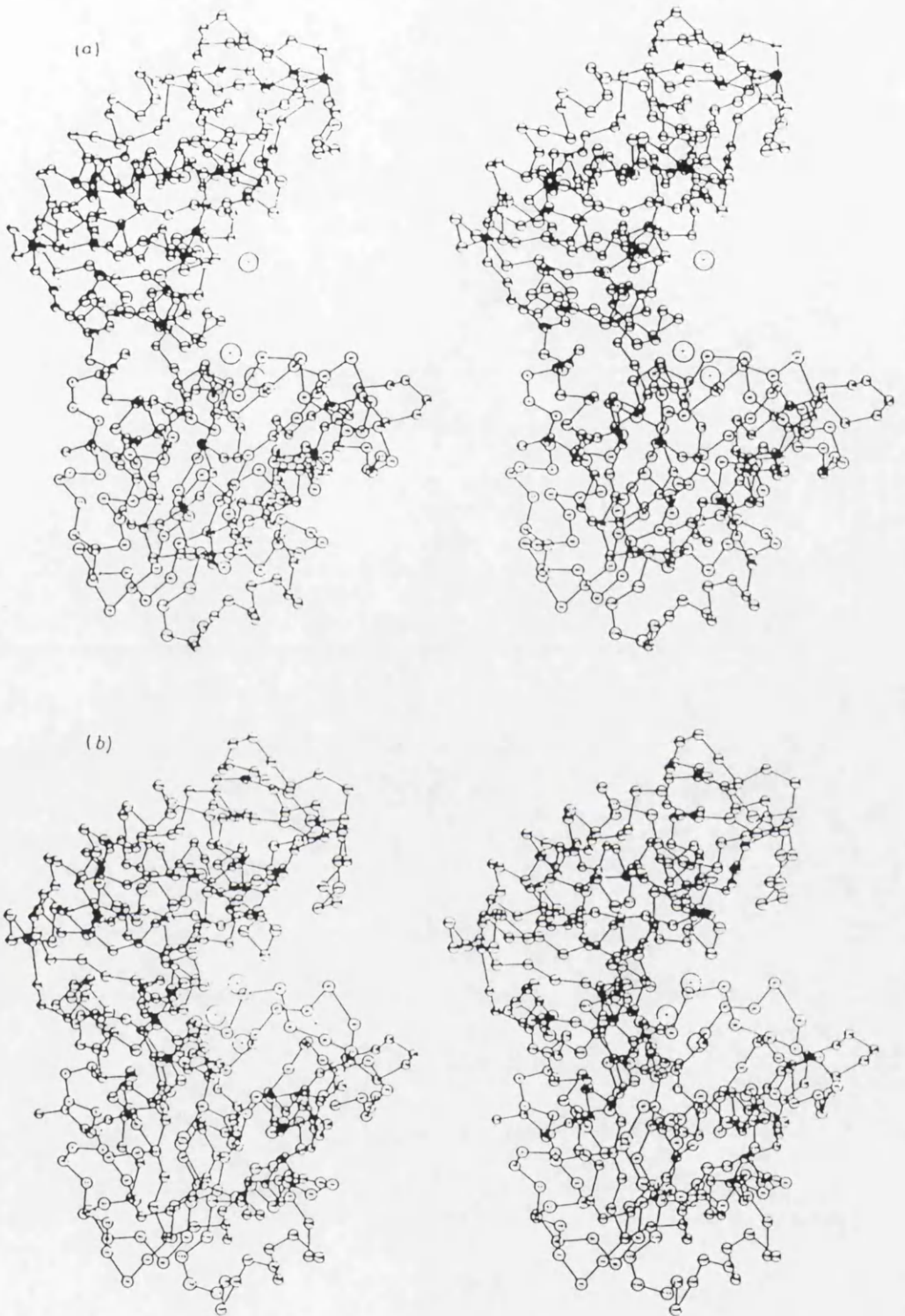


*Figure 1.4 Stereo diagram of PGK in the open, (a), and closed, (b), conformations (Blake et al., 1986)*

The sedimentation co-efficients for the ternary complex, PGK.ATP.3-PG, and the enzyme-sulphate complex were significantly higher than for free PGK or PGK with one substrate. These results could be explained by the molecule changing shape in the presence of both substrates or sulphate. However, these effects were later assigned to aggregation of the enzyme and sedimentation velocity measurements conducted in another laboratory, under similar conditions, showed that the sedimentation co-efficients were approximately the same for free and liganded PGK (Mas & Resplandor, 1988).

High resolution NMR studies reveal that the interdomain region is more mobile than the remainder of the molecule and that the enzyme fluctuates between several open and closed forms in solution (Tanswell *et al.*, 1976, Fairbrother *et al.*, 1989); this was also suggested from Rayleigh scattering experiments (Cooper *et al.*, 1989).

It is almost certain that domain closure does occur upon substrate binding to PGK and it has been proposed that substrate binding destabilises the interdomain interactions, allowing the enzyme to adopt the closed form (Adams & Pain, 1986). However the mechanism of this transition is unclear and the question of whether both substrates, 3-phosphoglycerate alone or anions initiate the conformational change has still to be answered.

Another question which has still to be resolved is whether the substrates bind at one or two sites on PGK. The evidence from the crystallographic experiments indicates that the nucleotide substrates bind on the C-domain and the triose substrate binds on the N-domain. However, equilibrium gel-filtration experiments have provided evidence for the presence of more than one binding site for the nucleotide substrates and kinetic studies have indicated that there are two sites for both substrates

(Scopes, 1978b, Larsson-Raznikiewicz, 1979, Schierbeck & Larsson-Raznikiewicz, 1979).  $^1\text{H}$  and  $^{31}\text{P}$  NMR experiments have been used to study the binding of nucleotide substrates to PGK (Nageswara Rao *et al.*, 1978, Ray *et al.*, 1990, Fairbrother *et al.*, 1990b, Graham & Williams, 1991b) and these have confirmed that there are two binding sites for the nucleotides. One of these is equivalent to the site determined by crystallography and the other site is on the N-domain. The C-domain binding site is a predominantly hydrophobic binding interaction between the enzyme and the adenosine portion of the nucleotide, whereas, binding on the N-domain is mainly an electrostatic interaction between the phosphate groups and the "basic patch" residues. Magnesium ions alter the affinity of the nucleotides for the two sites. In the absence of  $\text{Mg}^{2+}$ , the primary interaction is at the electrostatic site, but addition of  $\text{Mg}^{2+}$  reduces the affinity of the electrostatic site and increases the relative affinity for the proposed catalytic site on the C-domain.

Steady-state kinetic experiments have demonstrated that the mechanism of PGK is of the rapid equilibrium random order type and that the enzyme exhibits complex kinetic behaviour (Larsson-Raznikiewicz, 1964, 1967, 1970, Larsson-Raznikiewicz & Arvidsson, 1971). Kinetic experiments produce biphasic Eadie-Hofstee plots (Scopes, 1978a). These effects could be partially explained by the enzyme having more than one nucleotide site as discussed above, but there are other complicating factors. The concentration of  $\text{Mg}^{2+}$  ions is relevant since this alters affinity of ATP for the two sites and also because the magnesium complex with 3-phosphoglycerate is inactive as a substrate. Another relevant factor is the presence of anions in the assay buffer. Various anions have been shown to activate the enzyme activity at low anion concentrations and inhibit at higher concentrations. The effect is dependent on the anion: multivalent anions have a greater activating effect, and on the substrate concentrations. This effect is used to transform the biphasic Eadie-

Hofstee plots to linear plots; commonly used assay buffers contain 20 mM or more sulphate. This means that the Michaelis constants determined for PGK are very dependent on the composition of the assay buffer. The anions may act by binding to PGK in the active site. The X-ray studies located a selenate ion in the position of the  $\gamma$ -phosphate of ATP (Watson *et al.*, 1982). Scopes (1978b) proposed that binding of anions at this position could accelerate the rate of reaction by aiding in the dissociation of 1,3-diphosphoglycerate, which is the rate-limiting step of the reaction. Inhibition at higher anion concentrations occurred because the anions compete with both substrates. NMR experiments studying the interaction of various anions with PGK found that the anions bound preferentially not at the position determined in the crystallographic structure, but at the basic patch on the N-domain (Fairbrother *et al.*, 1990a) (figure 1.5). A secondary, very weak, binding site was observed. This site involves interaction with surface lysine residues which could possibly be Lys 213 and Lys 217 at the active site.

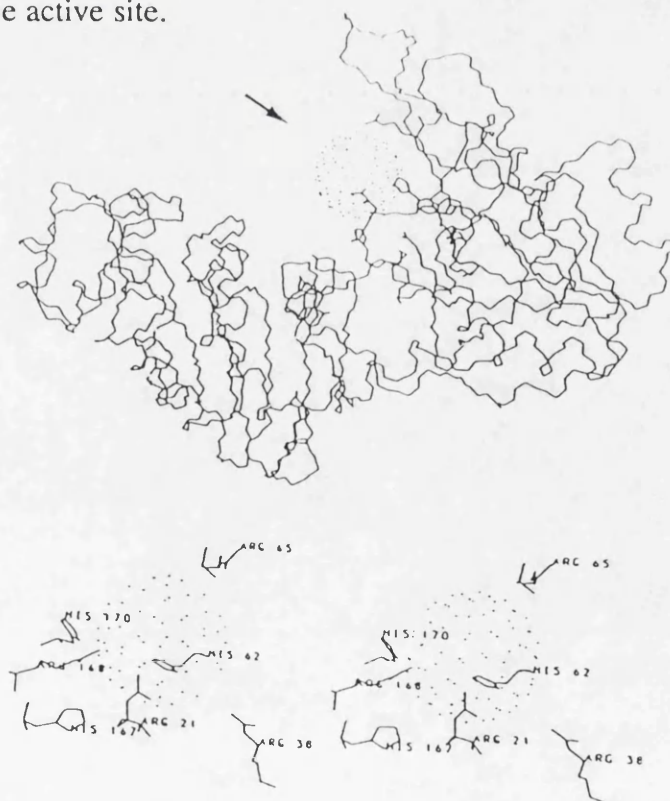


**Figure 1.5** Location of the anion binding site (adapted from Fairbrother *et al.*, 1990a)

Many mutant forms of yeast PGK have been constructed within the last few years, but the two that were used in this work involved the amino acid residues at positions 388 and 168. Histidine-388 is located in the interdomain region of the enzyme where it forms a salt link with glutamate-190. This interaction was originally believed to be vital to the hinge-bending mechanism of PGK. It was proposed that the interaction stabilised the open conformation of the enzyme and that substrate binding disrupted the salt link and allowed the enzyme to adopt the closed conformation (Banks *et al.*, 1979). To test this theory, several mutations were made at position 388 (figure 1.6).

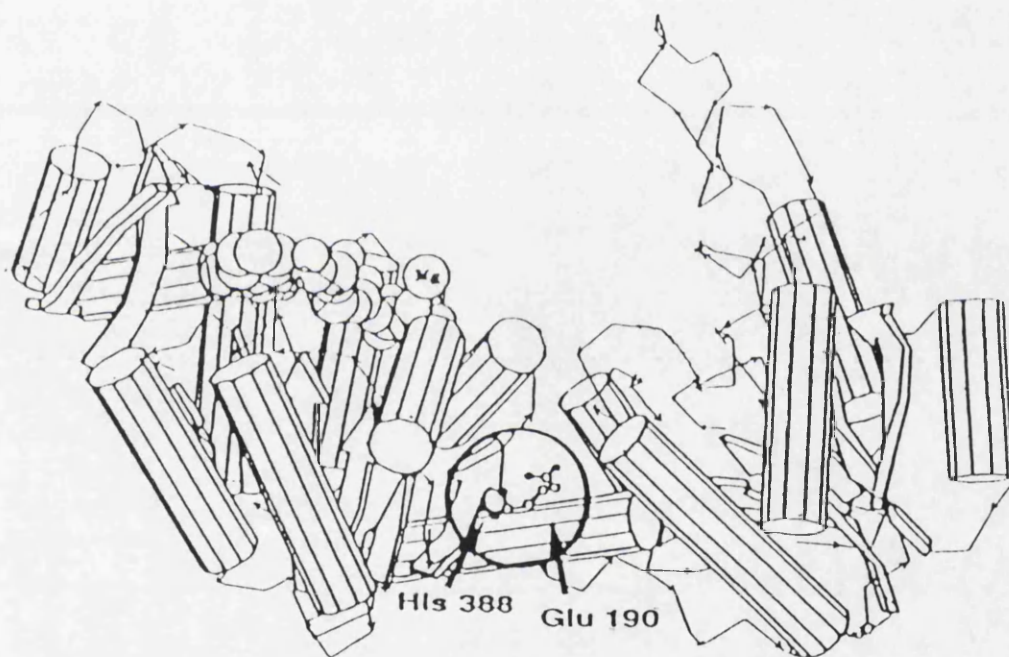


*Figure 1.6* Position of the His-388 and Glu-190 interaction (adapted from Graham *et al.*, 1991)

Substitutions of His-388 by glutamine (Wilson *et al.*, 1987), alanine or lysine (Mas *et al.*, 1988) produced enzymes that remained catalytically active although the

specific activities were decreased by factors of 5, 7 and 20 respectively. The Michaelis constants for ATP were reduced in all cases by a factor of 3, but the effects on the Michaelis constants for 3-phosphoglycerate were more varied. Since the enzyme was still catalytically active, it was deduced that the His-388/Glu-190 interaction is not responsible for controlling domain closure. The mutants exhibit large reductions in specific activity even though the Michaelis constants indicate that substrate binding is not hindered. This implies that the reduced specific activities have resulted from perturbations of the enzyme's conformational flexibility. This view is supported by depolarized Rayleigh scattering measurements (Cooper *et al.*, 1989) where the binding of 3-phosphoglycerate was observed to "loosen" the protein structure of the H388Q mutant, an effect which was not observed for the wild-type enzyme. Additionally, DSC (differential scanning calorimetry) studies which monitor the heat denaturation of proteins, found that although wild-type PGK undergoes a single cooperative transition, H388Q and H388P have two transitions, one corresponding to the N-domain and the other to the C-domain (Johnson *et al.*, 1991, Bailey *et al.*, 1990). These experiments suggest that there are interactive forces between the domains in the wild-type enzyme which are disrupted when a mutation is made at position 388.

The other mutant enzyme which was used in the microcalorimetric studies was R168K. Arginine-168 is a residue located in the basic patch region (figure 1.7). This residue was proposed to stabilise the transition state of the enzymic reaction following domain movement (Walker *et al.*, 1989). Substitution of arginine by lysine shortens the side-chain whilst retaining the charge. The specific activity of R168K is more than halved compared to wild-type enzyme (Walker *et al.*, 1989). However, since the mutant retains some activity, this positively charged residue cannot be essential to catalysis. Kinetic studies reveal that there is an increase in  $K_M$  for both substrates with this mutant, particularly for 3-phosphoglycerate.

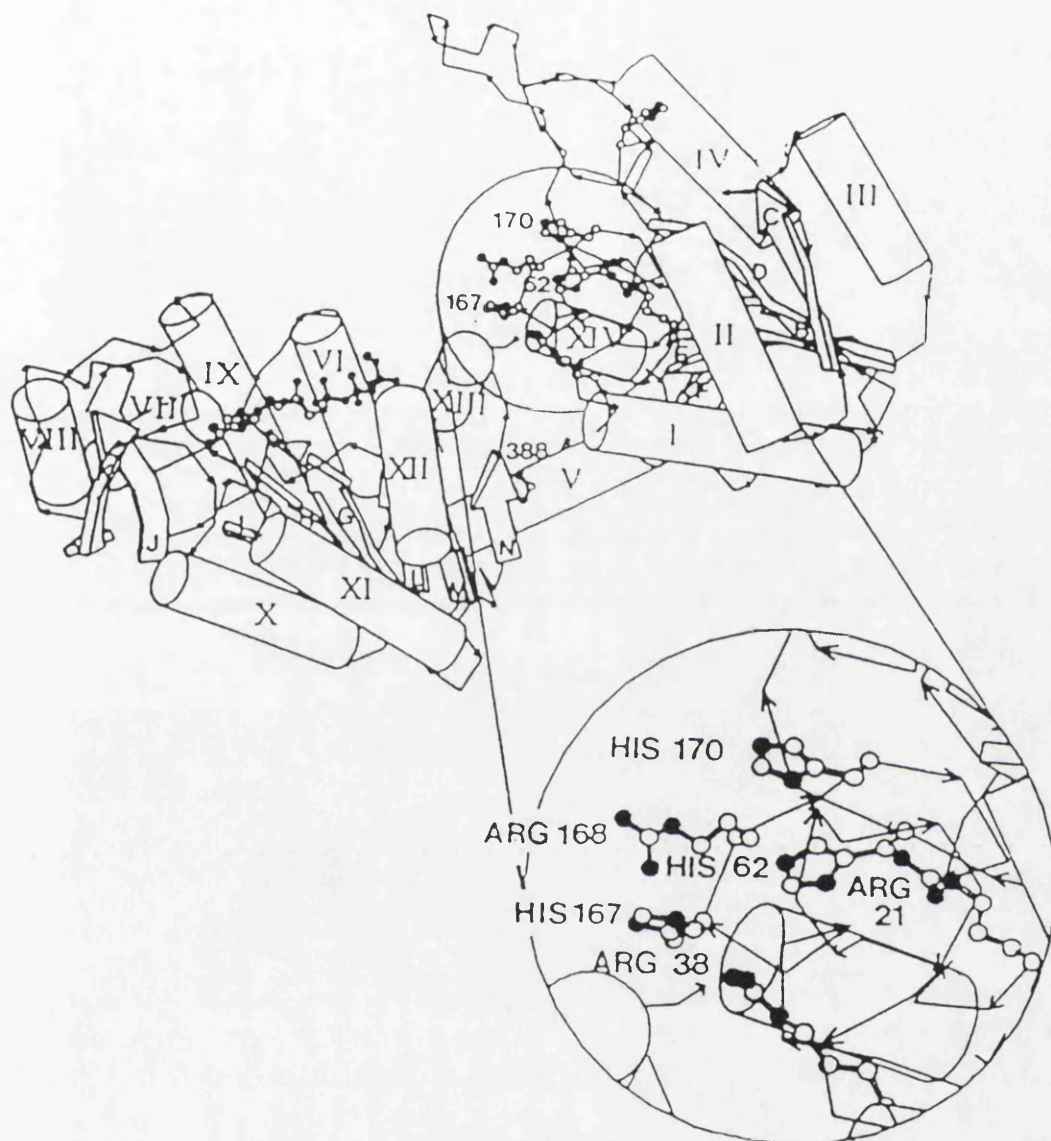


**Figure 1.7** Close-up view of the basic patch residues of the N-domain (Fairbrother *et al.*, 1989)

PGK has previously been investigated by microcalorimetry to study both the thermal denaturation of the enzyme (Johnson *et al.*, 1991) and the substrate binding parameters (Hu & Sturtevant, 1987). DSC experiments have shown that wild-type

PGK undergoes a cooperative transition giving rise to a single asymmetric peak, whereas the H388Q mutant gives rise to two transitions: one presumably corresponding to the unfolding of the C-domain and the other to the N-domain. The melting temperature ( $T_m$ ) of the lower temperature transition was increased in the presence of 3-phosphoglycerate and so this transition probably arises from the unfolding of the N-domain. The substrate binding studies by microcalorimetry (Hu & Sturtevant, 1987) have been much more limited and, as will be shown later, are of dubious validity.

### 1.8 The Vancomycin Group of Antibiotics

Antibiotics of the vancomycin group inhibit bacterial cell growth and are important in the treatment of penicillin-resistant staphylococcus infections. These antibiotics act by interfering with cell wall synthesis, resulting in eventual destruction of the bacterial cell by lysis. Vancomycin, ristocetin, actinoidin and avoparcin are some of the members of this group, although the total number of structural variants is in the region of one hundred (Williams *et al.*, 1980). Ristocetin, actinoidin and avoparcin exist in two forms, A and B, differing in their carbohydrate content.

Gram-positive bacteria have a cell wall made of a cross-linked, multilayered, polysaccharide-peptide complex called peptidoglycan. Long polysaccharide chains of alternating N-acetylglucosamine (NAG) and N-acetylmuramic acid (NAM) units are cross-linked by short peptides in a multistage biosynthetic process (Ghuysen, 1980) (figure 1.8). A peptide unit (L-ala-D-glu-L-lys-D-ala-D-ala) is joined to NAM-uridine diphosphate (stage 1) which is subsequently transferred to a carrier lipid (stage 2), then NAG and pentaglycine are added (stage 3). The disaccharide is removed from the carrier lipid to the growing polysaccharide chain (stage 4). The final step,

catalysed by a transpeptidase enzyme, is to cross-link the chains (stage 5). A peptide bond is formed between glycine and one of the D-ala residues and the terminal D-ala residue is released.

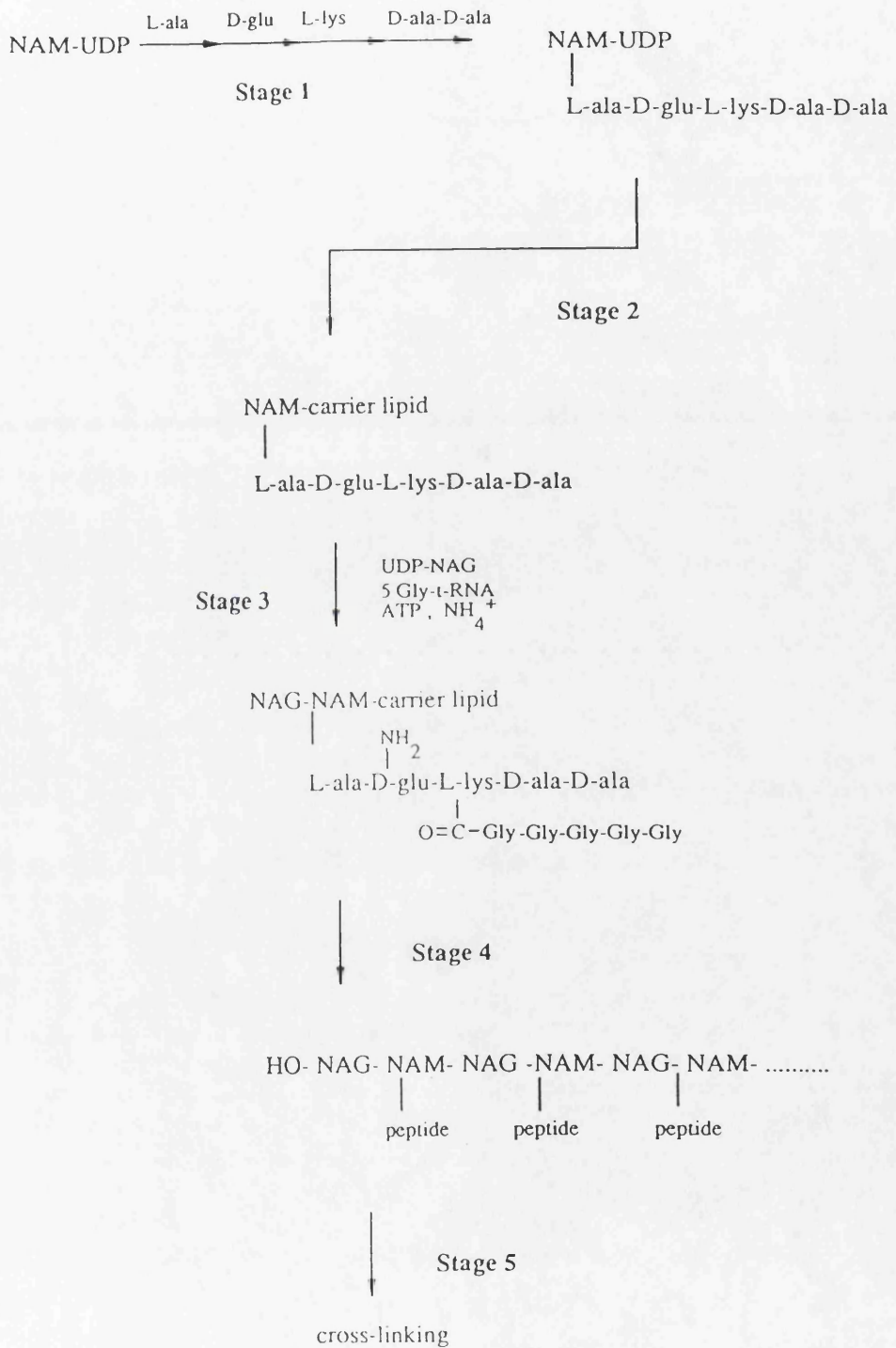


**Figure 1.8** Stages in the synthesis of the peptidoglycan

When the antibiotics inhibit cell growth there is an accumulation of UDP-N-acetylmuramylpentapeptide precursors (Reynolds, 1961, Wallas & Strominger, 1963, Chatterjee & Perkins, 1966). Perkins (1969) proposed that the antibiotic inhibited growth by binding specifically to D-ala-D-ala residues at the carboxy terminus of the cross-linking peptide. This inhibits transpeptidase activity and prevents cross-linking of the cell wall (figure 1.9).

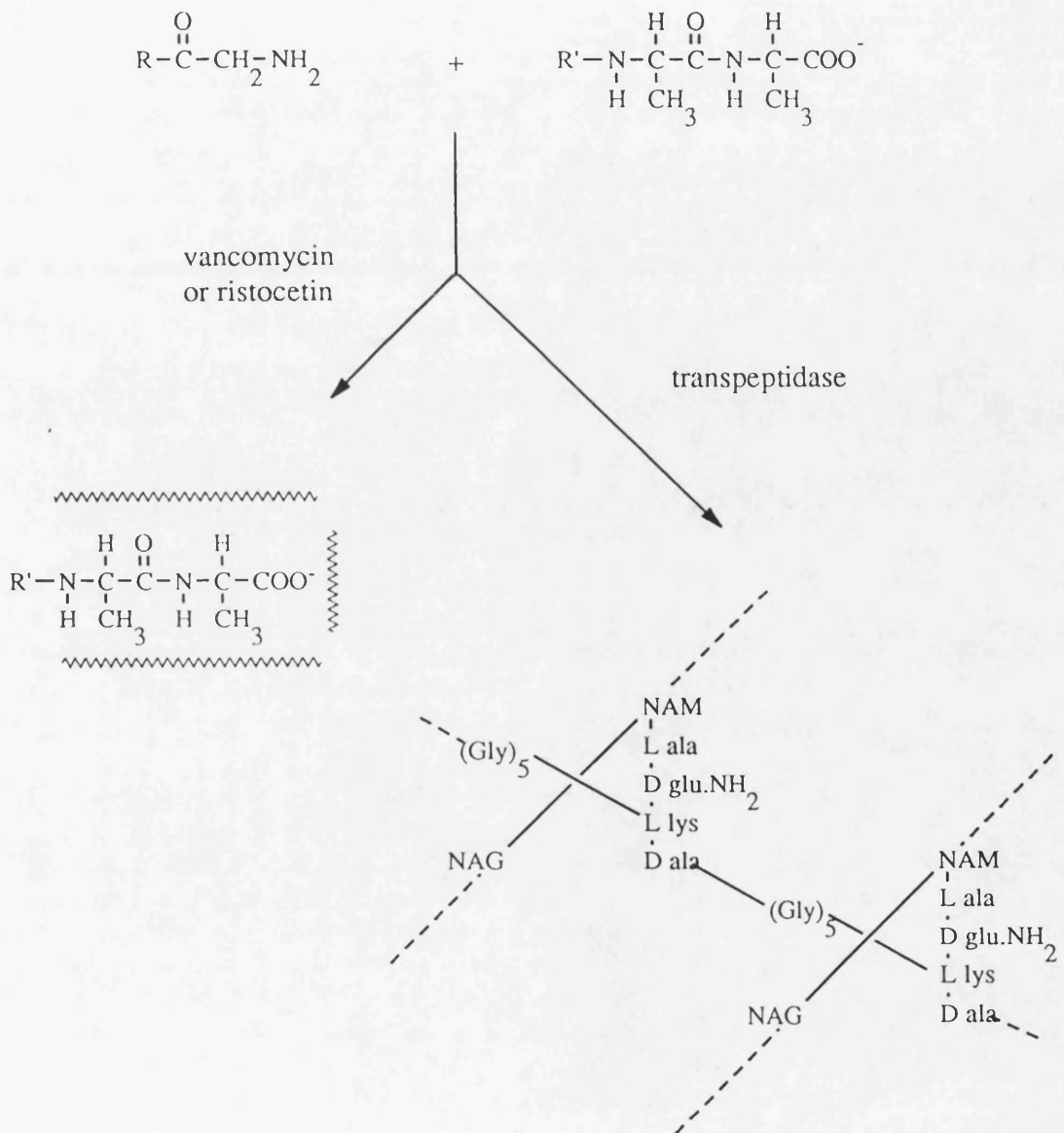


**Figure 1.9** Site of action of the vancomycin type antibiotics

These early studies using UV difference spectroscopy showed that the minimum requirement for binding was a D-ala-D-ala peptide with the C-terminus free and the N-terminus acetylated (Perkins, 1969). Further studies using tripeptides, with amino acid substitutions at each position, explored the specificity of the binding site (Nieto & Perkins, 1971b). Binding is strongest with the tripeptide most closely resembling the amino acids incorporated in the cell wall i.e. di-Ac-lys-D-ala-D-ala. The residue at the N-terminus and the middle residue are very important in determining specificity, peptides containing L-amino acids at either position are unable to bind to the antibiotic. The residue at the carboxy terminus gives the highest specificity when the residue is diacetyl-L-lys, however this position is less sterically demanding and D-amino acids can be accepted. Ristocetin is capable of binding peptides with larger side-chains than vancomycin.

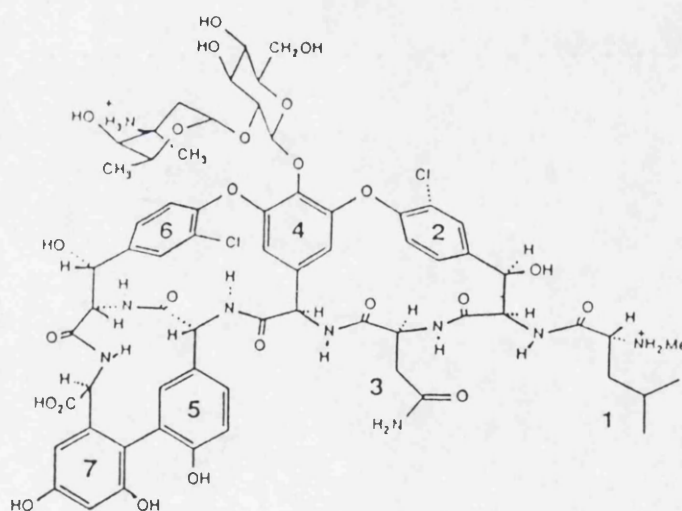


**Figure 1.10** Structure of vancomycin (Waltho & Williams, 1991)

Vancomycin is a heptapeptide containing mainly aromatic amino acid residues (figure 1.10). This unusual tricyclic structure is formed by three phenol-oxidative coupling reactions. It contains glucose and an amino sugar, vancosamine. The structure was elucidated by a combination of techniques: chemical analysis, NMR and X-ray crystallography of a derivative of vancomycin, CDP-1 (Sheldrick *et al.*, 1978). It was assumed that the only structural change that had occurred on forming CDP-1 was that a primary amide in vancomycin had been hydrolysed to a free carboxylate. However, an intramolecular rearrangement (Harris & Harris, 1982b) and a 180° flip of an aromatic ring had taken place (Williamson & Williams, 1981). This led to a revision of the structure of vancomycin in 1981.

The structural similarities between ristocetin and vancomycin allowed the structure of ristocetin to be determined almost entirely by NMR (Kalman & Williams, 1980, Harris & Harris, 1982a). Ristocetin is a heptapeptide but with a tetracyclic structure, formed by four oxidative coupling reactions (figure 1.11). Ristocetin A contains the sugars, mannose, ristosamine and a tetrasaccharide. Ristocetin B is identical to ristocetin A except that it lacks two of the sugars in the tetrasaccharide unit.

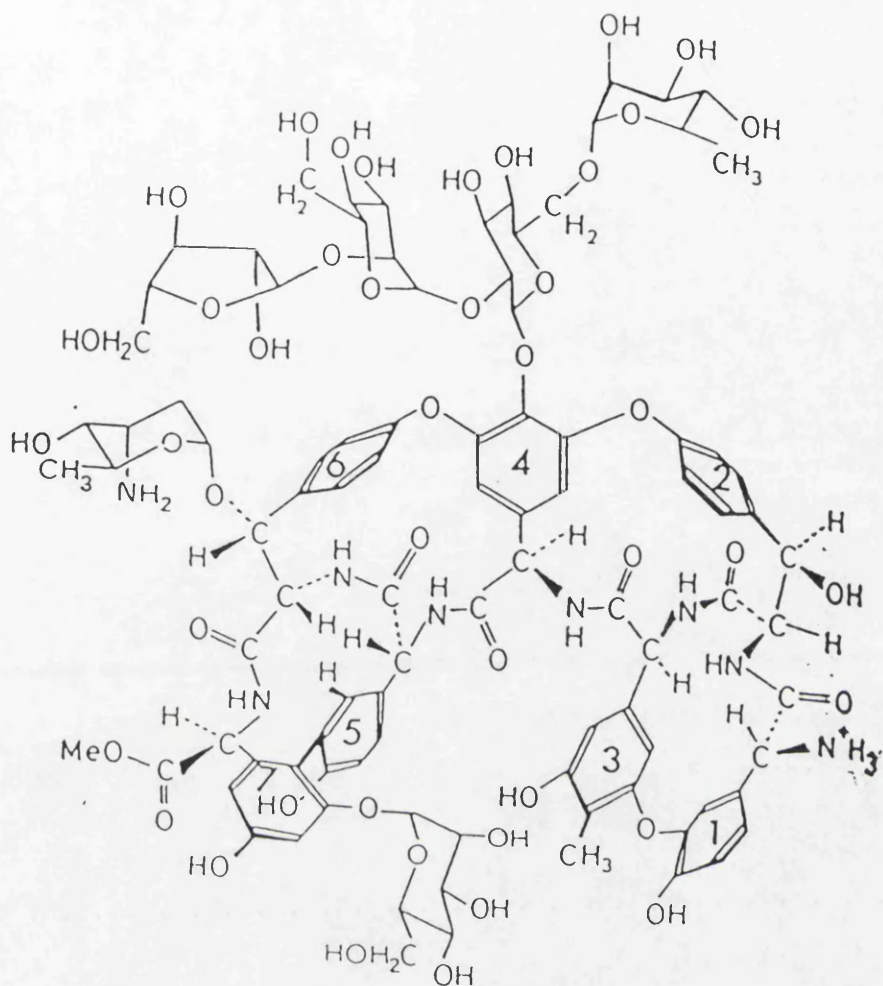


**Figure 1.11** Structure of ristocetin (Williams, 1984)

The antibiotic-peptide complexes have not been crystallised in a form suitable for X-ray studies. However, NMR studies have provided useful structural information (Williams, 1984). Space-filling models of ristocetin and peptides show an obvious binding site for a peptide ligand which has been confirmed by NMR studies (Kalman & Williams, 1980, Williams *et al.*, 1983, Williamson & Williams, 1985). The ristocetin binding site contains five amide groups, suitably positioned to form

hydrogen bonds with di-ac-lys-D-ala-D-ala. Three of these amide NH groups interact with the carboxylate ion, therefore explaining the requirement of a free carboxylate ion for binding to take place. The remaining two amide groups form hydrogen bonds to amides in the tripeptide. Hydrophobic interactions occur between the alanine methyl groups and methyl-shaped pockets on the antibiotic (figure 1.12). A conformational change takes place on binding: the benzene ring of residue 1 folds over the carboxylate ion to form a hydrophobic pocket that serves to strengthen the binding interactions (Waltho & Williams, 1989).

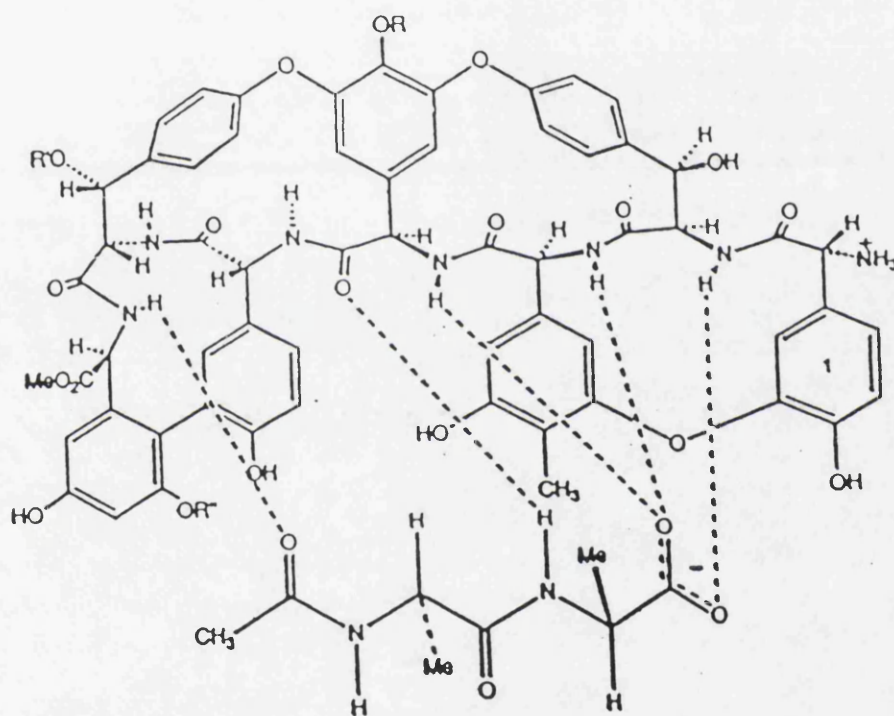


**Figure 1.12** Structure of the ristocetin-dipeptide complex (Williams et al., 1991)

Vancomycin also undergoes a conformational change on binding (Williams & Butcher, 1981). This structural change, involving a series of rotations, brings a N-methylleucine side-chain into position to form a carboxylate pocket similar to the ristocetin pocket. The rest of the binding site is also similar, the biggest difference

being the presence of a chlorine atom in vancomycin (figure 1.13). The conformational change has the effect of creating a hydrophobic environment around the carboxylate ion.

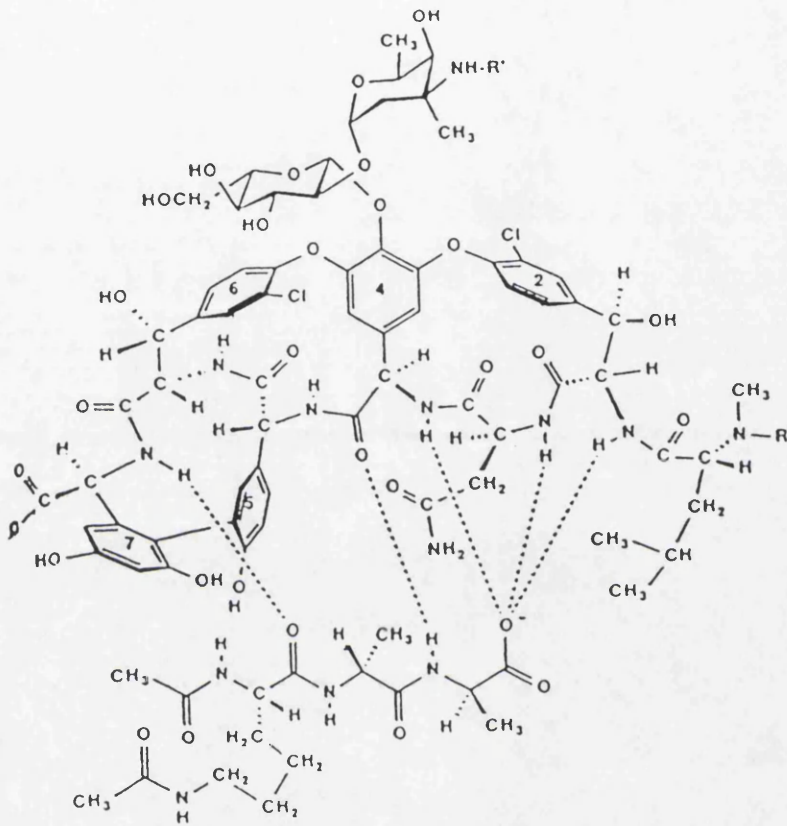


**Figure 1.13** Structure of the vancomycin-tripeptide complex (Waltho & Williams 1989)

It has been proposed that the initial interaction between the antibiotics and the peptide is between a protonated amine on the antibiotic and the peptide carboxylate (Williamson *et al.* 1984). Experiments with N-acetylated derivatives of ristocetin (Barna *et al.*, 1985, Herrin *et al.*, 1985) and vancomycin (Kannan *et al.*, 1988) have demonstrated that although the protonated amine is not essential for binding it does significantly increase the binding affinity. The interaction between the

rest of the antibiotic and the peptide determines specificity and although the aglycone portion of the antibiotic forms the main interactions with cell-wall analogues, the sugars act to increase specificity. Vancosamine sterically prevents peptides with side-chains larger than methyl at the C-terminus from binding to vancomycin. Similarly, the mannose portion of ristocetin prevents the binding of peptides with side-chains larger than methyl at the second amino acid from the C-terminus. These features prevent the antibiotics binding to intact cell walls and thus increase biological activity (Williams & Waltho, 1988).

The formation of a ristocetin dimer in solution was first observed in the  $^1\text{H}$  NMR spectrum. Several resonances of ristocetin A and the ristocetin A-tripeptide complex in water (Williams *et al.*, 1979, Williamson & Williams, 1985, Waltho & Williams, 1989) are present as two forms in slow exchange and further NMR studies confirmed the presence of an antibiotic dimer in solution. The molecules associate through the back faces, leaving the binding sites accessible to the peptide ligand. Four intermolecular hydrogen bonds are made between the ristocetin molecules (figure 1.14) (Waltho & Williams, 1989). Three forms of ristocetin were suggested by the NMR spectra. Two forms had resonances with similar chemical shifts, whilst the third form was considerably different. The ratio of the population of the three forms was approximately 5:5:1 using a 15 mM sample. Diluting the sample by a factor of 10 changed the ratios to 1:1:4. These ratios indicate an association constant of  $2 \times 10^3 \text{M}^{-1}$  for dimer formation. The two sets of dimer resonances can be explained either by the dimer existing in two different forms of equal energy which are in slow exchange or there is asymmetry within the dimer with a slow interconversion rate between the two halves.

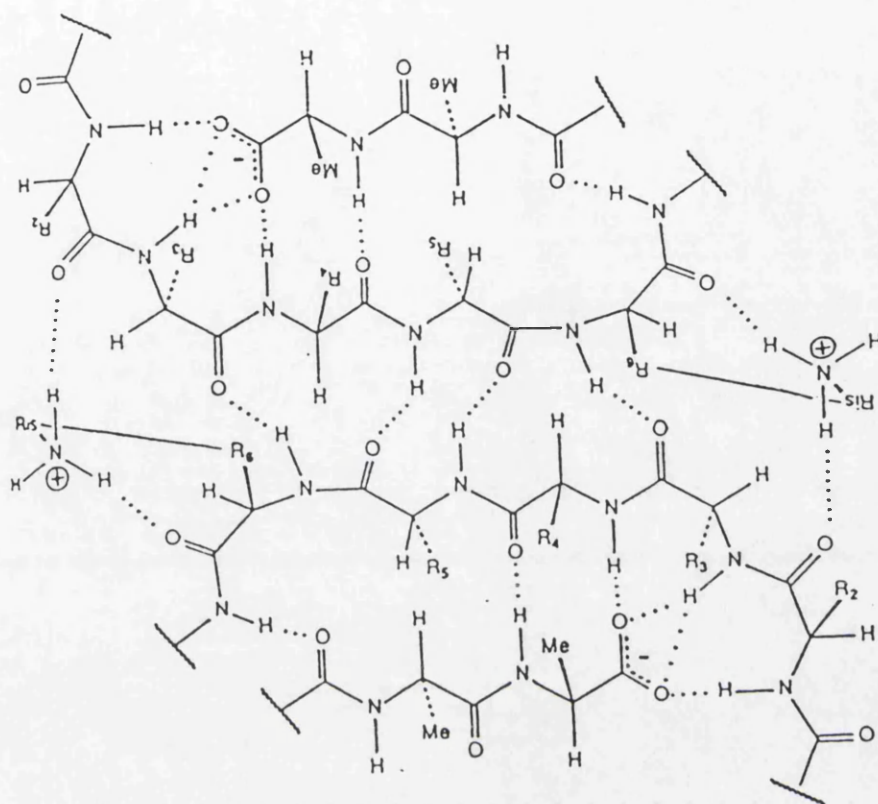


**Figure 1.14** Structure of Ristocetin Dimer (Williams & Waltho, 1988)

Dimerisation is also believed to occur with vancomycin. Studies of the specific rotation of vancomycin in 0.02M citrate buffer at pH 5 showed significant aggregation at low concentrations. The aggregation was judged to be total at an antibiotic concentration of 10 mM. Assuming dimerisation had occurred, an association constant of  $8 \times 10^2 \text{ M}^{-1}$  was calculated (Nieto & Perkins, 1971a).

Microcalorimetry previously has been used to investigate the thermodynamics of interaction between vancomycin, ristocetin and peptidoglycan analogue peptides (Rodriguez-Tebar *et al.*, 1986). These experiments studied the binding of Ac-D-ala

and three dipeptide ligands, Ac-D-ala-D-ala, Ac-Gly-D-ala and Ac-D-ala-gly, to the antibiotics. In all cases, negative values for  $\Delta G^\circ$ ,  $\Delta H^\circ$ ,  $\Delta S^\circ$  and  $\Delta C_p^\circ$  were observed. There are several reasons for repeating and extending these microcalorimetric studies. For example, if the antibiotics dimerise then altering the antibiotic concentration will lead to changes in the thermodynamic parameters relating to substrate binding. In the paper by Rodriguez *et al.* it is not clear if the experiments were carried out at one antibiotic concentration or at several concentrations and so this point needs to be clarified. The choice of ligands is also different in this study and the experiments were performed over a wider temperature range to obtain more accurate  $\Delta C_p^\circ$  values.

## 2 MICROCALORIMETRY

### 2.1 Introduction to calorimetry

Although thermodynamic parameters can be determined by measuring association constants and applying the van't Hoff equation, a more direct route to thermodynamic information is via calorimetry. Calorimeters are instruments which measure heat effects. Hence enthalpy values, in principle, can be directly determined. Enthalpy measurements can be conducted at fixed temperatures and since it is not necessary to use the van't Hoff equation higher accuracy can be attained. Most binding reactions occur with a change in temperature and so calorimetry can be used for the study of almost all associations (except when  $\Delta H^\circ = 0$ ). On the other hand, other techniques such as equilibrium dialysis and gel-filtration require specific analytical methods to determine the ligand concentrations and therefore a new assay has to be devised for each situation. Many spectroscopic techniques require the enzyme and substrate solutions to be transparent, however, this is not a requirement for calorimetry. Another advantage of calorimetry is that the starting materials can usually be recovered.

Highly sensitive microcalorimeters are required for biological applications. This is necessary since we are measuring changes in weak non-covalent forces and generally wish to use small quantities of biological materials. The types of calorimeter suited to this kind of work are called microcalorimeters. Microcalorimeters have increased in sensitivity in recent years and can now measure effective temperature

changes of the order of a millionth of a degree.

In addition to providing information on enthalpy changes, some calorimeters have been designed to study temperature induced transitions e.g. protein denaturation. These differential scanning calorimeters (DSC) measure the apparent specific heat of a system as a function of temperature (Privalov, 1974, Sturtevant, 1974). Ligand binding effects have been studied using DSC (Hu & Sturtevant, 1987, Brandts & Lin, 1990), however, isothermal titration calorimetry (ITC) is more commonly employed and gives the more direct and (usually) the less ambiguous information.

There are several types of isothermal calorimeters which may be used to study ligand binding processes, but the two most suited to biophysical applications are those from Thermometric (previously LKB) and the Omega reaction calorimeter from MicroCal Inc. The Thermometric models are based on the heat conduction principle.

The LKB heat conduction microcalorimeter was designed by Wadso in 1968 (Wadso, 1968), using earlier designs with similar principles (Calvet, 1963, Benzinger & Kitzinger, 1960). This calorimeter has sample and reference cells contained within a heat-sink as shown in figure 2.1. When a reaction occurs in the cells, heat flows between the heat sink and the cells. Thermopiles are situated between the cells and the heat sink so that all the heat passes through the thermopiles and generates a voltage (V) which is proportional to the temperature difference ( $\Delta T$ ) between the cells and heat sink, which in turn, is proportional to the rate of heat flow ( $dQ/dt$ ).

$$\frac{dQ}{dt} = k_1 \Delta T \quad \text{and} \quad V = k_2 \Delta T \quad (2.1)$$

$$\text{hence} \quad \frac{dQ}{dt} = kV$$

The total heat generated may be obtained by integration of equation 2.1, where  $k$  (equal to  $k_1/k_2$ ) is the calibration constant of the calorimeter.

$$Q = k \int V \cdot dt \quad (2.2)$$

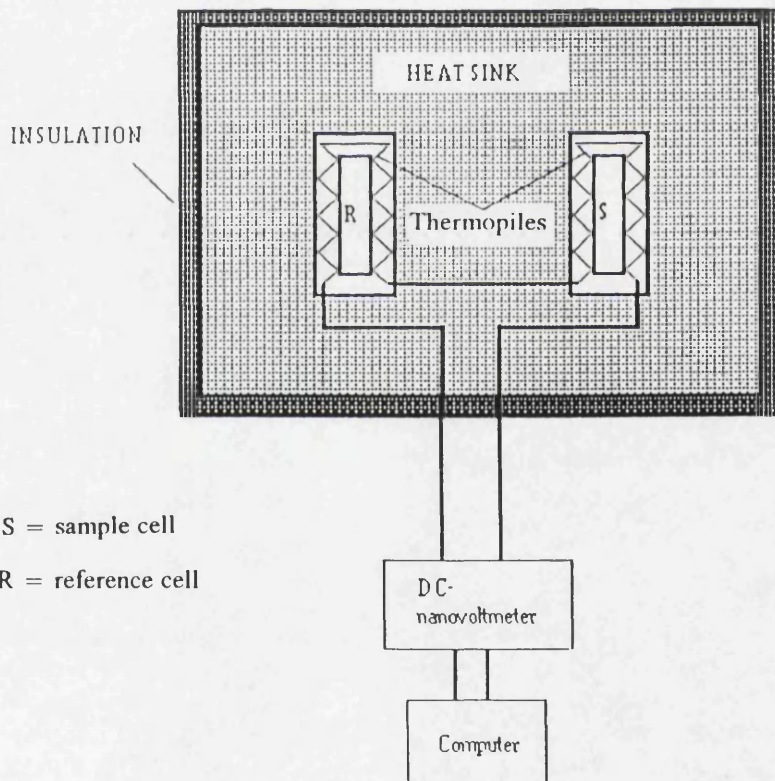


*Figure 2.1 Schematic diagram of a heat-conduction calorimeter*

The original heat conduction calorimeter designed by Wadso was a batch calorimeter. The batch calorimeter contains cells that are divided into two sections. The sample cell usually contains, for example, enzyme solution in one compartment and ligand in the other, whereas, the reference cell contains buffer. After thermal equilibration has been achieved, the calorimeter unit is rotated so that the solutions are mixed and the enzyme and ligand can combine. Batch calorimetric experiments are easy to perform. However single loadings of the system give only one measurement of the heat effect and equilibration times are long. Therefore the time required for a single experimental measurement is approximately three hours which is the main disadvantage of the batch calorimeter.

Another type of calorimeter which can be used to study ligand binding is the flow calorimeter; this is based on the same design principle as the batch calorimeter (Monk & Wadso, 1968). The reactant solutions are pumped separately through a heat exchanger before mixing, then through the reaction cell and out of the calorimeter. The heat exchanger means that equilibration times prior to the experiment can be omitted.

The batch calorimeter can be converted to a titration calorimeter by the addition of motor-driven syringes, which allow reagents to be added to the reaction cells during an experiment (Chen & Wadso, 1982). The titration calorimeter still requires an equilibration time of approximately two hours, however, a complete titration curve can be obtained from one loading of the calorimeter. Titration calorimeters may operate in a stepwise or continuous mode. Enzyme solution is equilibrated in the sample cell and then substrate is injected into the cell via a syringe. In the continuous mode the signal is a heat flux. Calculation of the heat effect can be made if the concentrations of reactant, flow rate of titrant and total volume are known. In stepwise mode, heat effects can be measured for each injection. Stepwise

calorimeters, in addition to determining  $\Delta H^\circ$  values, can also give values of the association constant from a single experiment. The cells of a batch, titration and flow calorimeter are demonstrated in figure 2.2.

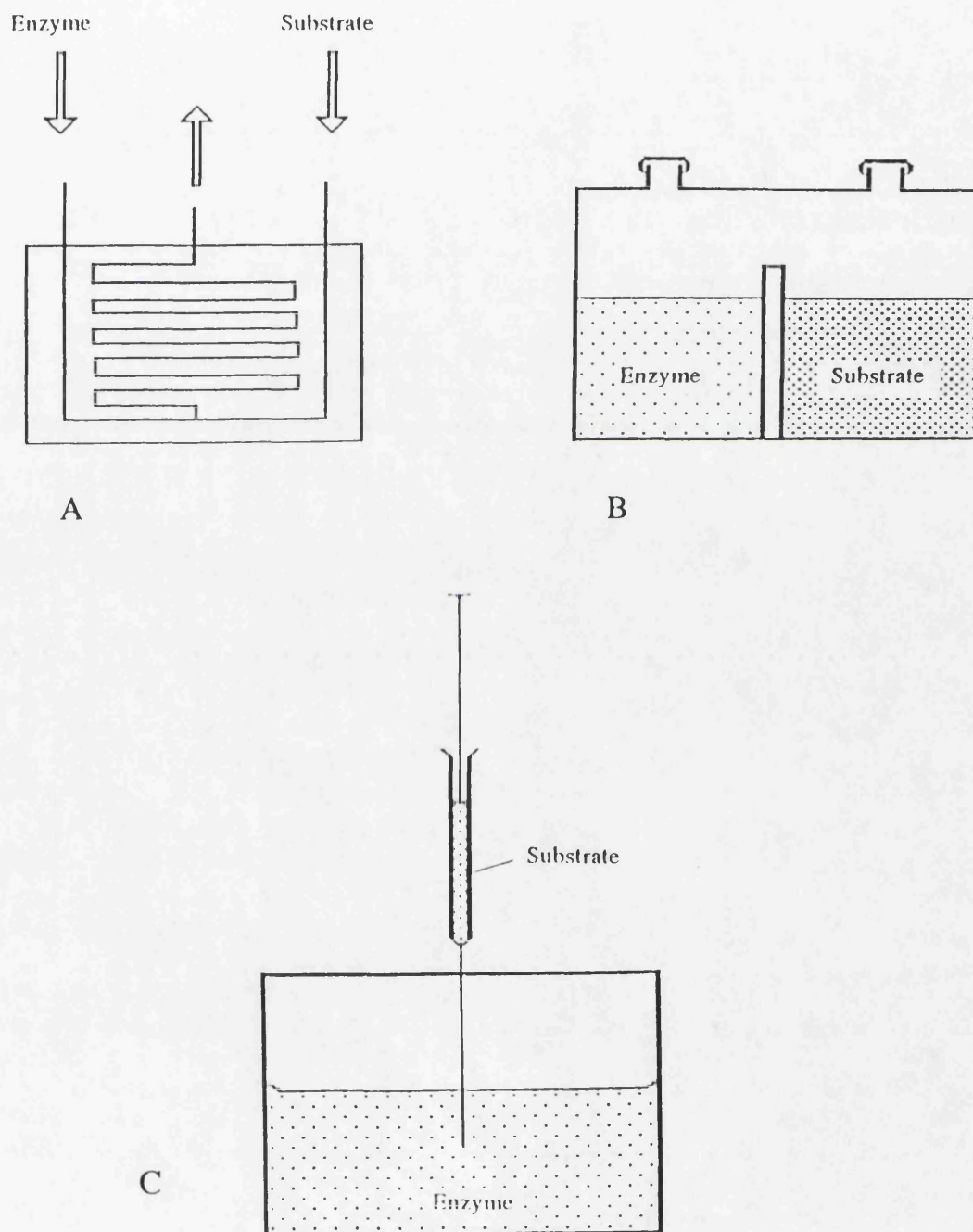


**Figure 2.2** *A. Flow cell. Arrows indicate flow of enzyme/substrate solution through cell*  
*B. Batch cell. Contents of cell are mixed by rotation of the calorimetric unit*  
*C. Titration cell. Substrate is injected by a motor-driven syringe*

The Omega Reaction Microcalorimeter was recently designed by Microcal Inc. specifically for measuring binding constants and heats of binding for biological associations (Wiseman *et al.*, 1989, Brandts *et al.*, 1990). It is very sensitive and can measure binding constants of up to  $10^8$ . The results are analyzed using the accompanying software package - Origin. A titration experiment can be achieved in a very short time using the Omega calorimeter: equilibration of samples occurs within several minutes after loading and the fast-response time of the calorimeter means that ligand can be injected at two or three minute intervals.

The calorimeter comprises two coin-shaped cells contained within an adiabatic jacket. The cells are made of Hastelloy C and have a volume of approximately 1.4 ml. Heaters are positioned on the surface of both cells. Samples are introduced into the cells via long, narrow access tubes. The injection syringe has a long needle with a stirring blade at the end; this is inserted into the sample cell as depicted in figure 2.3. The injection syringe is coupled to a motor which rotates the syringe during the experiment to mix the contents of the sample cell. The plunger of the syringe is connected to a stepping motor which controls the volume to be injected.

A thermoelectric device is located between the sample and reference cell: this measures the temperature difference between the two cells ( $\Delta T_1$ ). The temperature difference between the cells and the adiabatic jacket ( $\Delta T_2$ ) is also monitored, using a thermopile.

When a reactant is injected into the sample, heat is either released or absorbed. This heat effect is monitored by the calorimeter using a feedback system as shown in figure 2.4. The reference cell is continuously heated at a slow, constant rate which makes  $\Delta T_1$  non-zero; this activates a feedback system which supplies power to the sample cell to return  $\Delta T_1$  to zero. When an endothermic or exothermic reaction

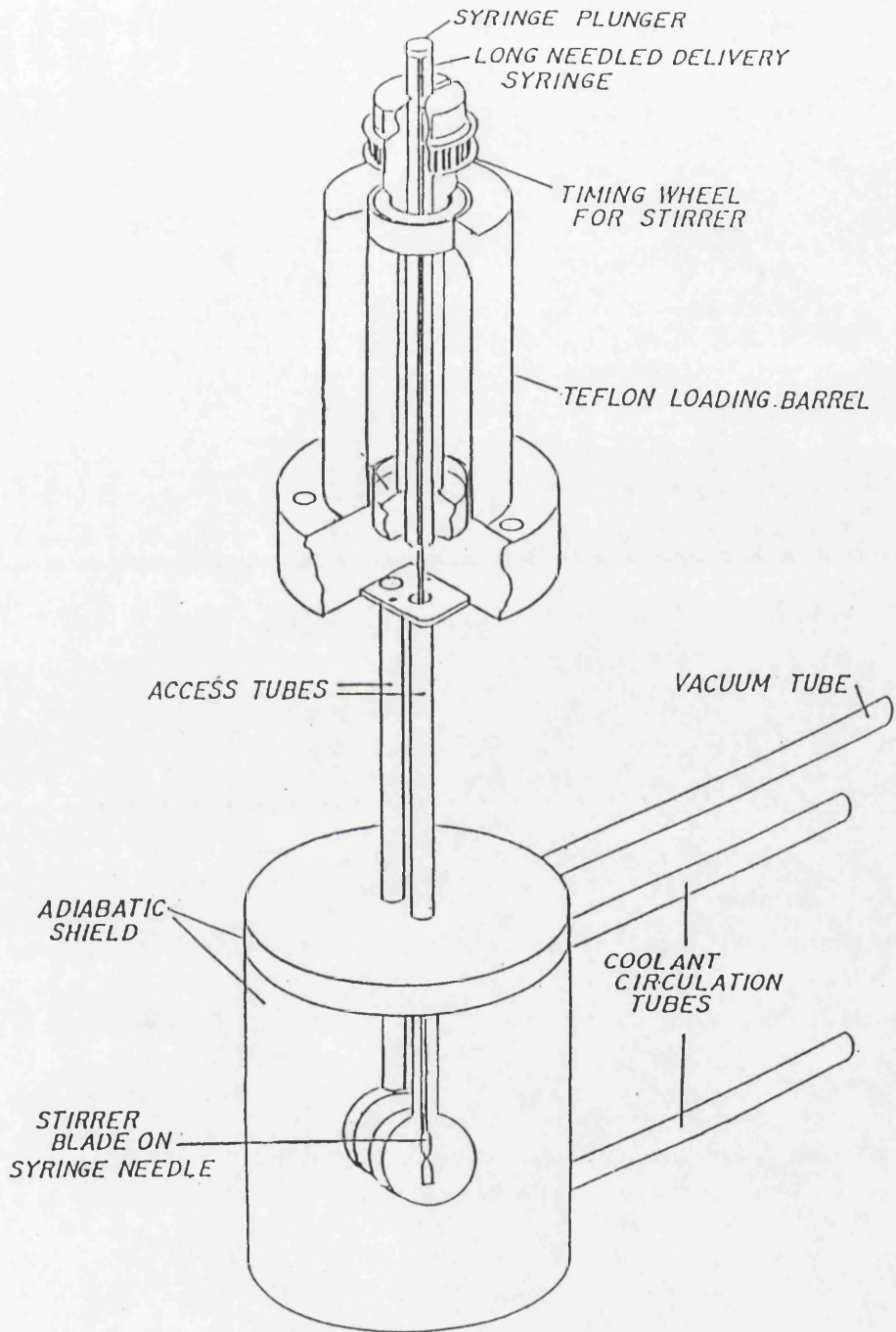
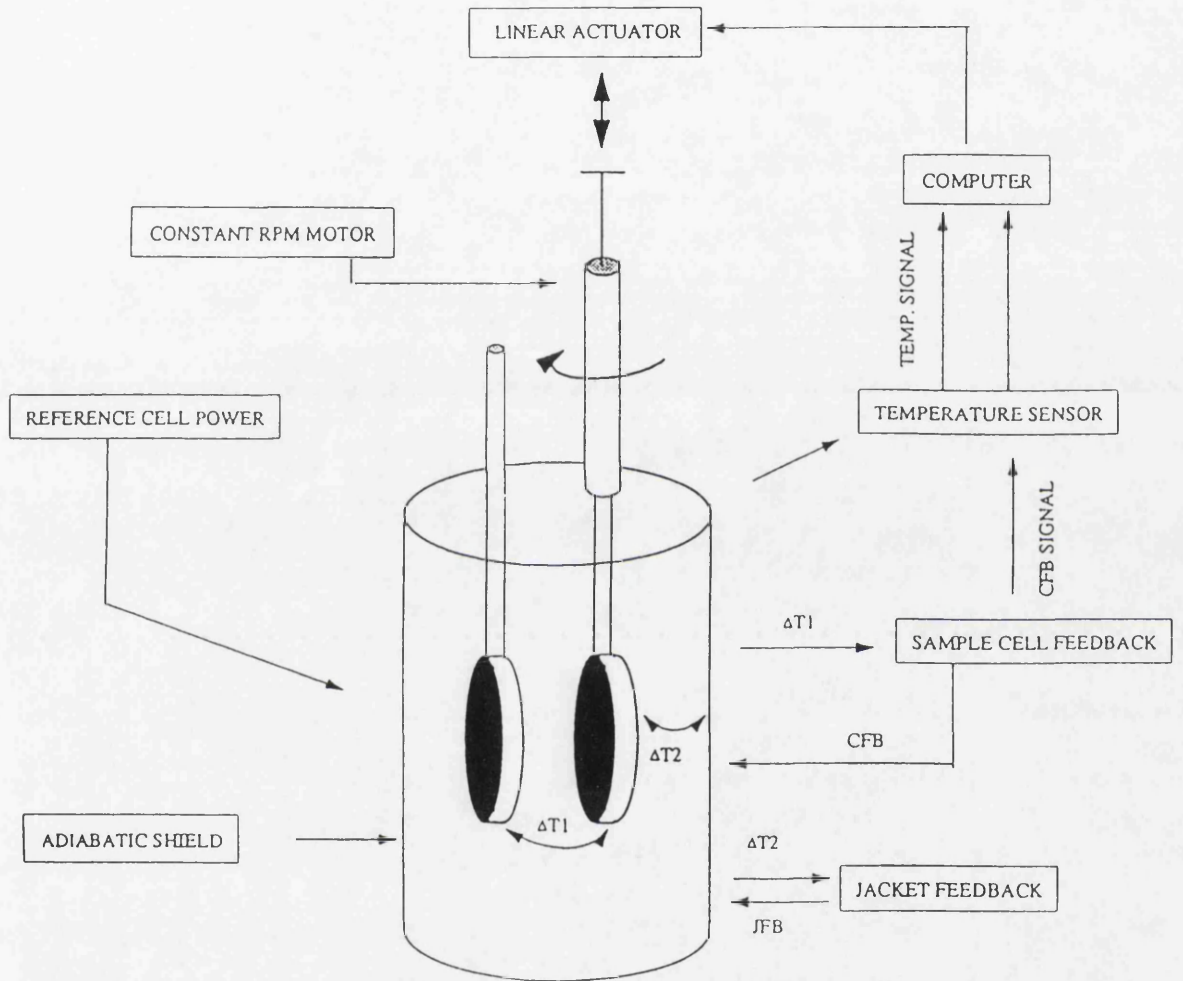


Figure 2.3 Injection syringe of the Omega microcalorimeter



*Figure 2.4 Schematic diagram of the Omega calorimeter*

occurs in the sample cell, more or less power is required to minimise  $\Delta T_1$ . The cell feedback signal is monitored by the computer and its integral over time is a measure of the total heat change resulting from an injection. The jacket feedback operates in a similar fashion to maintain the temperature of the jacket to the average cell temperature, thus preventing heat loss.

## 2.2 Calibration

Both the LKB and the Omega calorimeters require a calibration constant to convert the observed signal to a heat quantity. The calibration constant is determined experimentally using electrical and/or chemical techniques. Electrical calibration is accomplished by heating the sample cell at a chosen rate for a selected time period. The integral of the heat pulse should agree with the known applied heat; if not, then the calibration constant must be altered. Standard chemical reactions can also be used to calibrate the calorimeter, for example, the enthalpy of protonation of Tris buffer (equal to  $47.44 \text{ kJmol}^{-1}$ , Grenthe *et al.*, 1970).

## 2.3 Calculation of thermodynamic parameters from experimental data

For an association reaction, the observed heat effect is equal to the heat of binding of enzyme and substrate ( $Q_r$ ) plus the heats of dilution of the components ( $Q_{dil}$ ) and the heat of mixing ( $Q_{mix}$ ).

$$Q_{obs} = Q_r + Q_{dil} + Q_{mix} \quad (2.3)$$

$Q_{dil}$  values for all the components of the experiment have to be measured. The following experiments must be performed to obtain the corrected enthalpy of binding:

	Contents of sample cell	Contents of syringe
$Q_{\text{obs}}$	macromolecule	ligand
$Q_1$	macromolecule	buffer
$Q_2$	buffer	ligand
$Q_3$	buffer	buffer

The heat of binding  $Q_r$  is then equal to

$$Q_r = Q_{\text{obs}} - Q_1 - Q_2 + Q_3 \quad (2.4)$$

In practice, the heats of dilution may be small and can be neglected, however, this is not always the case and therefore it is important to perform all four experiments.

If an enzyme is titrated to saturation with a ligand then the enthalpy change is equal to the total reaction heat divided by the protein concentration ( $[M]$ ):

$$\Delta H^\circ = Q_r/[M] \quad (2.5)$$

A titration microcalorimeter can be used not only for enthalpy measurements but also for the determination of association constants, using heat production or uptake as a measure of the extent of the reaction:

$$Q_r = [ML] \Delta H^\circ/[M]_t \quad (2.6)$$

where  $[M]_t$  is the total concentration of macromolecule and  $[ML]$  is the concentration of the complex. This equation can be expressed in terms of the association constant and the free ligand concentration ( $[L]$ ), for simple 1:1 binding:

$$Q = \frac{K_a[L]\Delta H^\circ}{1 + K_a[L]} \quad (2.7)$$

Equation 1.16 can be rearranged to give:

$$\frac{1}{Q} = \frac{1}{\Delta H^{\circ}} + \frac{1}{K_a[L]\Delta H^{\circ}} \quad (2.8)$$

Therefore a double reciprocal plot of  $1/Q$  versus  $1/[L]$  will yield values of  $\Delta H^{\circ}$  and  $K_a$ :  $\Delta H^{\circ}$  is obtained from the intercept on the y-axis and  $K_a$  is calculated from the gradient of the line. This method of analyzing the experimental data although simple has two major flaws: first, a double reciprocal plot is biased and places more weight on the less accurate points and second, this approach requires that the free ligand concentration at equilibrium is known: this approximates to the total ligand concentration only in situations of very weak binding. A preferred method is to use the hyperbolic relationship for the observed heat as a function of total enzyme and ligand concentration:

$$Q = -\Delta H^{\circ}(N[M]_t + [L]_t + 1/K_a)\{1 - (1 - 4N[M]_t[L]_t/(N[M]_t + [L]_t + 1/K_a)^2)^{1/2}\}/2[M]_t$$

where  $N$  is the number of binding sites. (2.9)

This equation applies to simple 1:1 binding. For a system with multiple non-interacting sites, the observed heat effect will be

$$Q = \sum_{i=1}^j \frac{N_i \Delta H_i [L] K_i}{1 + K_i [L]} \quad (2.10)$$

where  $j$  is the number of sets of distinct binding sites,  $K_i$ ,  $\Delta H_i$  and  $N_i$  are the apparent association constant, enthalpy change and number for each set of sites.

The calorimetric titration curves can be analysed using a two sets of sites model, however if there are more than two sets of sites then an unique fit to the data

may not be obtained since there are three variable parameters for each set of sites.

Further complications arise when the binding sites are interactive. The binding of one ligand may enhance or decrease the binding affinity of a second ligand. The thermodynamic variables can be measured in the absence and presence of the other ligand and the changes in  $\Delta H^\circ$  values and association constants examined.

## 2.4 Data analysis

The experimental data obtained from a calorimetric titration can thus be analysed to give values of  $\Delta H^\circ$ ,  $K_a$  and the number of binding sites per mole of protein. The raw data obtained from an experiment, using the Omega calorimeter, is a record of the cell feedback signal as a function of time. The first step in analysing the data is to integrate each of the peaks (for both enzyme-substrate titration and dilution experiments). The dilution heats are subtracted from the corresponding enzyme-substrate heats to give the corrected heat values. The heats for each injection are plotted versus the injection number and then a theoretical fit to the experimental points is derived, using a least-squares approach, to yield values of  $N$ ,  $K_a$  and  $\Delta H^\circ$ . The data may be fitted assuming either one set of binding sites or two sets of binding sites. All of the data analysis steps can be performed using the Origin software.

It may be found that more than one set of  $N$ ,  $K_a$  and  $\Delta H^\circ$  values will give a good fit to the experimental data as may occur in situations of weak binding; if this is the case then it may be necessary to fix one of the parameters e.g.  $N = 1$ .

The mathematical models used in the Origin software to analyse the experimental data are given in the following sections.

### 2.4.1 Model for one set of sites

For a 1:1 binding reaction, the binding constant is related to the ligand concentration,  $[L]$ , and the fraction of sites occupied by ligand,  $\theta$ , by the equation

$$K = \frac{\theta}{(1-\theta)[L]} \quad (2.10)$$

and

$$[L]_t = [L] + N\theta[M]_t \quad (2.11)$$

where  $[L]_t$  and  $[M]_t$  are, respectively, the bulk ligand and bulk macromolecule concentrations. Combining equations 2.10 and 2.11 gives the quadratic equation

$$\theta^2 - \theta \left[ 1 + \frac{[L]_t}{N[M]_t} + \frac{1}{NK[M]_t} \right] + \frac{[L]_t}{N[M]_t} = 0 \quad (2.12)$$

The total heat content of the solution,  $Q$ , is equal to

$$Q = N\theta[M]_t \Delta H V_0 \quad (2.13)$$

where  $\Delta H$  is the enthalpy of binding and  $V_0$  is the active cell volume. Solving equation 2.12 for  $\theta$  and substituting into equation 2.13 gives

$$Q = \frac{N[M]_t \Delta H V_0}{2} \left[ 1 + \frac{[L]_t}{N[M]_t} + \frac{1}{NK[M]_t} - \sqrt{\left[ 1 + \frac{[L]_t}{N[M]_t} + \frac{1}{NK[M]_t} \right]^2 - \frac{4[L]_t}{N[M]_t}} \right] \quad (2.14)$$

This equation can be solved for  $Q_i$  given values of  $N$ ,  $K$  and  $\Delta H$  at the end of the  $i$ th

injection. The calorimeter actually measures the difference in heat,  $\Delta Q_i$ , between the  $i$  and  $i-1$  injections, which approximates to

$$\Delta Q_i = Q_i - Q_{(i-1)} \quad (2.15)$$

Some corrections are made in the calculations to account for the volume of liquid which is displaced from the cell on injection.

Initial guesses of the fitting parameters  $n$ ,  $K$ , and  $\Delta H$ , are made automatically and are substituted into equation 2.14 to find values for  $\Delta Q_i$  for each injection. These calculated values of  $\Delta Q_i$  are compared with the corresponding experimental values of  $\Delta Q_i$  and new values of the fitting parameters are found using statistical methods until there is an optimum fit between experimental and calculated  $\Delta Q_i$  values.

#### 2.4.2 Model for two sets of independent sites

This model is used when the ligand is assumed to bind at two non-interacting binding sites. Values of  $N$ ,  $K_a$  and  $\Delta H^\circ$  are derived for each site.

The fractional saturation for each type of site ( $\theta_1, \theta_2$ ) is used as the progress variable during saturation

$$K_1 = \frac{\theta_1}{(1 - \theta_1) [L]} \quad K_2 = \frac{\theta_2}{(1 - \theta_2) [L]} \quad (2.16)$$

$$[L]_t = [L] + [M]_t(n_1\theta_1 + n_2\theta_2) \quad (2.17)$$

where  $[L]$  and  $[L]_t$  are the free and bulk concentration of ligand and  $[M]_t$  is the bulk concentration of macromolecule. Combining equations 2.16 and 2.17 and rearranging yields a cubic equation of the form

(2.18)

$$[L]^3 + p[L]^2 + q[L] + r = 0$$

where

$$p = 1/K_1 + 1/K_2 + (n_1 + n_2)[M]_t - [L]_t$$

$$q = (n_1/K_2 + n_2/K_1)[M]_t - (1/K_1 + 1/K_2)[L]_t + 1/(K_1K_2)$$

$$r = - [L]_t/(K_1K_2)$$

(2.19)

Equations 2.18 and 2.19 can be solved for  $[L]$  numerically once  $[L]_t$ ,  $[M]_t$ ,  $n_1$ ,  $n_2$ ,  $K_1$  and  $K_2$  are assigned. Substitution of  $[L]$  into equation 2.16 then gives values for  $\theta_1$  and  $\theta_2$ .

The heat content of the solution after the  $i$ th injection,  $Q_i$ , will in general be

$$Q_i = [M]_t V_0 (n_1 \theta_1 \Delta H_1 + n_2 \theta_2 \Delta H_2). \quad (2.20)$$

Initial guesses of the fitting parameters  $n_1$ ,  $n_2$ ,  $K_1$ ,  $K_2$ ,  $\Delta H_1$  and  $\Delta H_2$ , are made and are substituted into equations 2.18 and 2.19 to find a value for  $[L]$  and then  $\theta_1$  and  $\theta_2$  using equation 2.16. Values for  $\Delta Q_i$  are then found using equation 2.20. The parameters are optimised using statistical techniques as described before.

## 2.5 Associated heat effects

Heat effects are not specific to association reactions, and any other heat changes that take place during the experiment will be detected by the calorimeter. These additional heat effects may lead to erroneous interpretation of the experimental data unless appropriate corrections are made to the data. Some of these heat effects have already been mentioned i.e.  $\Delta H_{dil}$  and  $\Delta H_{mix}$ . Less obvious heat effects can be

caused by contamination of the protein sample. For example, a calorimetric titration of glycogen phosphorylase b with AMP produced biphasic titration curves: this was found to be a result of small amounts of AMP amino hydrolase. Removal of this contaminating enzyme resulted in monophasic titration curves (Cortijo *et al.*, 1982). Measuring the thermodynamic parameters associated with substrate binding to an enzyme can be complicated since the heat of reaction will obscure the much smaller heat of binding. This problem is usually overcome by examining the binding of an inhibitor to the enzyme or by using an enzyme which requires two or more substrates to bind before the catalytic reaction occurs; in this case each substrate can be investigated individually. Other heat effects may arise from the release or uptake of protons by the enzyme or substrate during the binding process, or from changes in the state of aggregation of the species involved or even from conformational changes in the structure of the macromolecule associated with binding. Calorimetry if interpreted with caution can therefore provide information in addition to ligand binding thermodynamics.

It is common practice to buffer solutions containing protein in order that the pH of the solution remains constant. Consider an association process in which protons are released, these protons are picked up by the buffer and will produce a heat effect, the size of which depends on the heat of protonation of the buffer. If calorimetric experiments of this association are repeated in buffers of different heats of protonation then the observed enthalpies of binding will vary. The parameters obtained can be used to calculate the number of moles of protons being released to the buffer. The observed enthalpy ( $\Delta H_{\text{obs}}^{\circ}$ ) will equal the enthalpy of the association reaction plus an additional heat contribution from the association of the protons and buffer molecules.

$$\Delta H_{\text{obs}}^{\circ} = \Delta H_0^{\circ} + \Delta N \Delta H_{\text{b}}^{\circ}, \quad (2.21)$$

where  $\Delta H_0^{\circ}$  is the enthalpy change in the absence of buffer effects and  $\Delta H_{\text{b}}^{\circ}$

is the heat of protonation of the buffer. Plotting  $\Delta H^{\circ}_{\text{obs}}$  versus  $\Delta H^{\circ}_{\text{b}}$  should give a straight line with a slope equal to  $\Delta N$  and an ordinate intercept equal to  $\Delta H^{\circ}$ .

## 2.6 Recent uses of the Omega calorimeter

In the past few years, several uses of the Omega calorimeter have appeared in the literature. Some of these have concentrated on macromolecule-ligand associations, but other uses have included small molecule associations and kinetic studies. A few examples will be mentioned here.

A thermodynamic study of the binding of  $\alpha$ - and  $\omega$ - amino acids to the isolated kringle 4 (K4) region of human plasminogen was achieved using the Omega calorimeter (Sehl & Castellino, 1990). The thermodynamic parameters for binding of  $\epsilon$ -amino caproic acid (EACA) to K4 were found to be approximately constant over a range of pH values (5.5-8.2); suggesting that titratable groups on K4 do not affect the binding interaction. Further experiments with structural analogues of EACA explored the relationship between binding affinity and structure of ligand; the spacing between the functional groups of EACA was found to be important.

The Omega calorimeter has also been applied to the study of the binding of cations to ATP (Wilson & Chin, 1991). The cations which were investigated by calorimetry were  $\text{Mg}^{2+}$ ,  $\text{Ca}^{2+}$  and  $\text{Sr}^{2+}$ . In all cases the binding occurred with a positive enthalpy change and an increase in entropy.  $\text{Mg}^{2+}$  was found to have the highest association constant followed by  $\text{Ca}^{2+}$  and then  $\text{Sr}^{2+}$ . Monovalent cations such as  $\text{Na}^{+}$ ,  $\text{Li}^{+}$  and  $\text{K}^{+}$  were found to compete with  $\text{Mg}^{2+}$  for complexation with ATP.

A detailed investigation into the binding of ferric ions to ovotransferrin also employed the Omega calorimeter (Lin *et al.*, 1991). Ovotransferrin is a two-domain

protein which binds ferric ion to two binding sites: one on each domain. The binding of ferric ion to ovotransferrin and to the N- and C- half molecules of ovotransferrin was studied by titration microcalorimetry. The half molecules demonstrated similar binding parameters to those of the corresponding site in the intact ovotransferrin. Although these binding sites are approximately 40Å apart, they were found to interact via ligand-dependent changes in the heats and free energies of domain-domain interactions.

The kinetics and thermodynamics of an enzyme reaction has been investigated. The system under study was the reaction catalysed by yeast cytochrome c oxidase (Morin & Freire, 1991). Calorimetry offered an easy method of determining information about the thermodynamics, kinetics and protonation changes associated with the oxidation of cytochrome c by the enzyme. Injection of catalytic quantities of cytochrome c into a solution of yeast cytochrome c oxidase produced a calorimetric trace which was analysed to give the reaction enthalpy and the kinetic constant (figure 2.5).

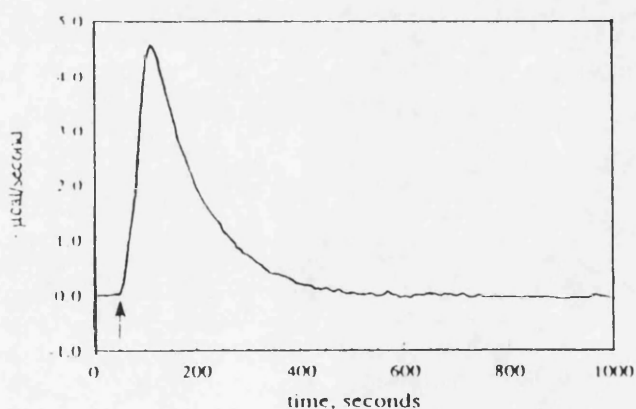


**Figure 2.5** *Calorimetric trace from Morin and Freire, 1991*

The area under the curve equals the total heat produced by the reaction, therefore, the reaction enthalpy can be determined by dividing the total heat by the

amount of cytochrome c oxidized. The shape of the curve is defined by the kinetic behaviour of the reaction. For a 1st order rate reaction, the heat flow ( $dQ/dt$ ) measured by the calorimeter is represented by equation 2.22.

$$dQ/dt = \Delta H V k[S]_0 \exp(-kt) \quad (2.22)$$

where  $[S]_0$  = initial substrate concentration,  $V$  = volume,  $k$  = rate constant

Rate constants determined by this method were found to be within 3% of values determined using spectral methods.

Enthalpy values measured in phosphate, MOPS, Tricine and Tris buffers at pH 7.0 had different values; from which the number of protons being released during the reaction could be calculated. This was found to be approximately one proton per cytochrome c oxidised.

### 3 MATERIALS AND METHODS

The PGK studies required considerable preparative and purification effort, mainly involving over-producing yeast strains, since the relatively large quantities of wild-type enzyme required for calorimetric studies were not available at an economic price and since mutant enzymes are not commercially available. Materials for the antibiotic-peptide binding experiments were supplied from Cambridge University or were commercially available. This chapter gives details of the basic experimental procedures involved.

#### 3.1 Yeast cultures

Yeast cultures transformed with plasmids pMA27 and pMA40b, containing wild-type and H388Q genes, respectively, were supplied by Dr. L. Gilmore, University of Edinburgh. Yeast cultures containing plasmids encoding for R168K mutant were supplied by Dr. J. Littlechild and Dr. H.C. Watson, University of Bristol.

#### 3.2 Proteins

PGK was isolated from over-producing yeast strains as described later in this chapter. Glyceraldehyde 3-phosphate dehydrogenase (GAPDH) from baker's yeast was obtained from Sigma Chemical Co. as a lyophilized and sulphate free powder. Bovine serum albumin (BSA) and Dalton Mark VII-L SDS-PAGE molecular weight marker

set, containing  $\alpha$ -lactalbumin, trypsin inhibitor, trypsinogen, carbonic anhydrase, GAPDH, egg albumin and bovine albumin were obtained from Sigma Chemical Co.

### **3.3 Substrates and Ligands**

Sigma Chemical Co. supplied the following substrates: adenosine as free base, adenosine 5'-diphosphate as di(monocyclohexylammonium) salt (ADP), adenosine 5'-triphosphate as disodium salt (ATP), D(-)3-phosphoglyceric acid as disodium salt (3-PG) and tripolyphosphate as pentasodium salt.

### **3.4 SDS-PAGE Chemicals**

Ammonium persulphate, N,N,N',N'-tetramethylene-diamine (TEMED) and bromophenol blue were supplied by Shandon Ltd. Acrylamide, N,N'-methylene-bis-acrylamide and  $\beta$ -mercaptoethanol were supplied by Sigma Chemical Co.

### **3.5 Fermentation and purification reagents**

Bacto-peptone, yeast extract, bacto-agar and yeast nitrogen base without amino acids were obtained from DIFCO. Protamine sulphate, benzamidine, phenylmethylsulphonyl fluoride (PMSF), Sephacryl S-200 and DEAE-sephadex A-25 were from Sigma Chemical Co.

### **3.6 Antibiotics and cell wall analogues**

Vancomycin HCl, Ristocetin A, N-acetyl-D-alanine, N-acetyl-D-alanyl-D-alanine, N $\alpha$ ,N $\gamma$ -diacetyl-lys-D-ala-D-ala, D-alanyl-D-alanine were supplied by Dr.

D.H. Williams, Cambridge University and members of his group. Additional supplies of Vancomycin HCl and N-acetyl-D-alanine were obtained from Sigma Chemical Co.

### **3.7 General Chemicals**

All other chemicals used were of A.R grade.

### **3.8 Preparation of PGK, substrate and ligand samples for calorimetry**

PGK samples were stored at 4°C as ammonium sulphate precipitates. Before use, the enzyme samples were centrifuged to obtain a pellet, the supernatant was discarded and the pellet redissolved in a small volume of buffer. The enzyme solution was then dialysed for about 20 hours against 2 x 1 litre (or more) dialysis buffer, at 4°C, with stirring. The enzyme solution was centrifuged after dialysis to remove any precipitated material and diluted with dialysis buffer to give a suitable concentration, which was measured from the absorbance at 280 nm (see section 3.13.1), assuming a molecular weight for PGK of 44 500 dalton. The experimental protein concentrations were usually in the region of 0.1 mM. Samples were degassed under vacuum with stirring for 2-3 minutes to remove dissolved air and to prevent the formation of bubbles in the sample cell of the calorimeter, which are a major source of baseline instability.

ATP, ADP, 3-phosphoglycerate and other ligand solutions were made up with final, equilibrated dialysis buffer. Typical concentrations were 20 mM for ADP and ATP, and 10 mM for 3-phosphoglycerate. The dialysis buffer contained magnesium at usually 4 mM concentration so that the magnesium complexes of ADP and ATP were formed. These samples were degassed as before.

### 3.9 Preparation of antibiotic samples for calorimetry

Antibiotic solutions were prepared by weight in 0.1 M sodium phosphate buffer at pH 7.0, containing 0.05% sodium azide (molecular weights are vancomycin = 1448, ristocetin = 2063, N-acetyl D-alanine = 131, N-acetyl D-alanyl-D-alanine = 202, D-alanyl-D-alanine = 160, and di-N-acetyl-L-lys-D-ala-D-ala = 372).

### 3.10 Procedure for microcalorimetry using the LKB calorimeter

This calorimeter had previously been modified from a standard batch calorimeter to a titration version and upgraded so that data collection, ligand injection and mixing schedules are fully computerized. Microlitre quantities of samples can be injected into the reaction cells using motor-driven, Hamilton MicroLab P injector syringes.

In a typical experiment, 7 ml of enzyme solution and 7 ml of buffer were added to the sample cell and reference cell, respectively. The syringes were rinsed and filled with substrate solution and the tubing connecting the syringes to the reaction cells was also charged with substrate solution. The calorimeter was allowed to equilibrate for approximately two hours, until a steady baseline reading was obtained. A typical experimental sequence consisted of 10 to 20 injections of 10-15  $\mu$ l substrate solution over a period of several hours. The data were integrated and analysed using as described in chapter 2.

### 3.11 Procedure using Omega titration microcalorimeter

The unstirred reference cell was filled with degassed distilled water containing 0.05% sodium azide (this acts as a reference only and rarely needs re-filling). The

sample cell was filled to the top of the inlet tube with sample (enzyme) solution, using a syringe with tubing attachment. Care was taken to avoid air bubbles being trapped in the cell. After loading, the temperature of the cells was raised to the experimental temperature (usually 25 °C) and the system was allowed to reach thermal equilibrium (usually a few minutes). The injection syringe was rinsed and filled with substrate solution, mounted in the calorimeter and stirred at a constant 400 rpm.

Experiments were started as soon as the baseline was sufficiently stable (RMS noise 0.04  $\mu\text{J}/\text{sec}$  or less). An injection schedule, usually 20 injections of 5  $\mu\text{l}$  volume at 3 minute intervals, was set up and executed under computer control. Appropriate dilution experiments were done under identical conditions. The data from the experiments were stored on disk for later evaluation.

The sample cell was cleaned daily with detergent (5% SDS, 1 mM Na.EDTA, pH 8.3) and all buffers contained sodium azide to prevent bacterial contamination.

The experimental data were corrected by subtracting the heats of dilution of the substrates; PGK dilutions and buffer/buffer dilutions were small and usually negligible. The data were analyzed using the Origin software, usually using the one set of sites model to give values of  $\Delta H^{\circ}$  and  $K_a$ , from which  $\Delta G^{\circ}$  and  $\Delta S^{\circ}$  were calculated. Enthalpy values ( $\Delta H_{\text{add}}$ ) were also calculated by summing the individual heat effects for each injection and dividing by the amount of protein present in the cell; this approach is model free but could only be used in cases where enzyme saturation had been attained. Both values of  $\Delta H^{\circ}$  are given in the PGK results section.

### 3.12 PGK enzyme activity measurements

Two methods were used to determine PGK activity: method A was used for routine assays whilst method B was used for more detailed kinetic studies. In both cases PGK activity was assayed (as is conventional) in the direction of 1,3-diphosphoglycerate formation by coupling the PGK reaction to the reaction catalysed by glyceraldehyde-3-phosphate dehydrogenase (GAPDH) as displayed in figure 3.1. The rate of reaction was followed by monitoring the decrease in absorbance at 340nm as a result of oxidation of NADH.

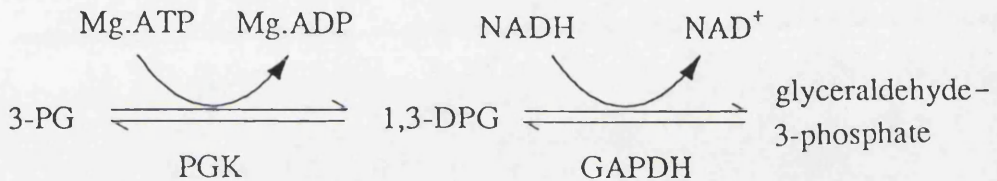


*Figure 3.1 Reaction scheme for PGK assay*

#### 3.12.1 Method A (Scopes, 1975)

The stock assay buffer contained the components listed in table 3.1, and was adjusted to pH 7.5 with HCl. This buffer could be stored for several weeks at 4 °C.

*Table 3.1 Components of stock assay buffer*

<u>Component</u>	<u>Concentration mM</u>
Triethanolamine (TEA).....	30
3-PG .....	10
KCl.....	50
MgSO <sub>4</sub> .....	5
Na <sub>2</sub> EDTA .....	0.2

The assay mix was prepared from the stock assay buffer by adding BSA and NADH to give concentrations of 0.2 mgml<sup>-1</sup> and 0.1 mM respectively. This mixture was prepared daily and was stable for several hours at 4 °C. ATP and GAPDH solutions were prepared in 30 mM TEA at pH 7.5 at concentrations of 50 mM and 1 mgml<sup>-1</sup> respectively; these solutions could be stored frozen at -20 °C for several months.

The following reagents were added to a microcuvette of 1cm path length: 0.88 ml assay mix, 40 µl stock GAPDH solution and 80 µl stock ATP solution. The microcuvette was placed in the thermostat block of a spectrophotometer (Pye Unicam SP 8-200 or Shimadzu UV-160A) and allowed to warm to 25 °C. A baseline was measured at 340 nm to check for contaminating enzyme, then 20-25 µl of a dilute PGK solution was added and the decrease in absorbance as a function of time was measured. PGK activity was calculated using a molar extinction coefficient of 6.22 x 10<sup>3</sup> for NADH at 340nm as follows:

$$\text{No. of enzyme units added to cuvette} = \Delta A_{340}/6.22,$$

where  $\Delta A_{340}$  is the change in absorbance at 340 nm per minute (initial rate of reaction) and 1 unit of enzyme activity causes conversion of 1 µmol NADH to NAD per minute at 25 °C. The approximate specific activity is equal to the number of enzyme units per milligram of enzyme.

### 3.12.2 Method B (Scopes, 1978a)

In this method solutions are chosen such that the concentration of free magnesium ions is fixed at 1 mM. The stock assay buffer contained the components given in table 3.2 and was adjusted to pH 7.5 with glacial acetic acid. This buffer could be stored for several weeks at 4 °C.

**Table 3.2 Components of stock assay buffer for method B**

<u>Component</u>	<u>Concentration mM</u>
Triethanolamine .....	30
Ammonium sulphate .....	40
Magnesium acetate.....	1

The assay mix was prepared as before by adding BSA and NADH to the stock assay buffer to give concentrations of 0.2 mgml<sup>-1</sup> and 0.1 mM. The ATP and 3-phosphoglycerate solutions were prepared in the stock assay buffer, with the addition of more magnesium acetate: 0.98 mol magnesium acetate/mol ATP and 0.09 mol magnesium acetate/mol 3-phosphoglycerate. PGK was dialysed overnight against 30 mM TEA pH 7.5 and diluted so that addition of 25 µl to the assay cuvette resulted in a maximum rate of  $\Delta A_{340} = 0.3 \text{ min}^{-1}$ .

The assay procedure was performed as described before but the microcuvette contained: 0.76 ml assay mix, 40 µl GAPDH, 100 µl ATP and 100 µl 3-phosphoglycerate.

### **3.12.3 Determination of Michaelis constants**

The Michaelis constants for Mg.ATP binding were determined from initial velocity measurements at several ATP concentrations using method B. The 3-phosphoglycerate concentration was held constant at 10 mM, whilst the ATP concentration was varied from 0.1 to 4 mM for wild-type PGK, from 0.05 to 2 mM for H388Q mutant and from 0.4 to 4 mM for R168K mutant.

The Michaelis constants for 3-phosphoglycerate binding were measured with a constant ATP concentration of 5 mM and different 3-phosphoglycerate concentration ranges: from 0.1 to 5 mM for wild-type, 0.05 to 5 mM for H388Q and 0.5 to 10 mM for R168K.

#### **3.12.4 Sulphate activation measurements**

The role of sulphate ions in the activation of wild-type PGK was investigated by measuring the specific activity of PGK at different concentrations of ammonium sulphate. In one experiment, the 3-phosphoglycerate and ATP concentrations were held constant at 0.1 mM and in another experiment the concentration of ATP and 3-phosphoglycerate was 0.5 mM. The assay mix and dialysis buffer were prepared as described in section 3.12.2, except that ammonium sulphate was omitted from the assay mix. A stock solution of 100 mM ammonium sulphate was prepared and aliquots of this solution were added to the cuvette to give the desired concentration of sulphate.

#### **3.13 Determination of protein concentration**

It is important to be able to determine the concentration of PGK with some accuracy, since this is an important parameter in the analysis of the microcalorimetric data. The standard method of determining the concentration of enzyme samples uses the UV absorbance at 280 nm, but an assay employing a Coomassie blue dye can also be used, since both methods produce similar values.

### 3.13.1 Estimation of protein concentration by UV absorption

All proteins containing the aromatic residues, tyrosine and tryptophan, absorb at about 280 nm (Creighton, 1984). From the knowledge of the absorbance at 280 nm and the corresponding extinction coefficient, the protein concentration can be calculated according to the Lambert-Beer law. The extinction coefficient of a 1 mgml<sup>-1</sup> PGK solution was taken to be 0.495, which is an average of extinction coefficients reported by Spragg *et al.*, 1976 and Bucher, 1955. This value was used for both wild-type and mutant PGK enzymes, since neither of the mutations involved changes in aromatic residues. Protein concentrations measured using this value accord with concentrations measured using the Coomassie blue technique.

### 3.13.2 Estimation of protein concentration by the Coomassie blue technique

This technique relies on the change in colour of a dye solution when the dye anion forms a non-covalent complex with a protein (Sedmak & Grossberg, 1977). The free dye has a brownish orange colour and absorbs at 465nm, whilst the bound dye is intense blue absorbing at 620 nm. The absorbance ratio  $A_{620}/A_{465}$  is measured and plotted against standard protein solutions of known concentration to form a calibration graph. The standard protein used was bovine serum albumin (BSA).

The dye solution contained 0.06% Coomassie G250 in 3% perchloric acid. The solution was stirred overnight at room temperature and then the undissolved material was removed by filtration and the solution diluted to give an  $A_{465}$  reading of 1.3-1.5. The following reagents were added to the cuvette to make a total volume of 2 ml: 1 ml dye stock, 925-995  $\mu$ l H<sub>2</sub>O and 5-75  $\mu$ l BSA (1 mg/ml). The absorbance ratio of a control solution (1ml dye + 1ml H<sub>2</sub>O) was measured and subtracted from values

obtained for protein samples. A new calibration graph was constructed for each batch of dye prepared.

The concentrations of PGK samples were determined by measuring the  $A_{620}/A_{465}$  ratio of several dilutions and then reading the protein concentrations from the calibration graph. These results confirmed the choice of 0.495 for the extinction coefficient at 280 nm.

### 3.14 SDS polyacrylamide gel electrophoresis

Protein homogeneity was verified by gel electrophoresis under denaturing conditions using a modified Laemmli gel system (Laemmli, 1970). A vertical slab electrophoresis apparatus (Shandon Ltd.) was used. The composition of various buffers and solutions used in the electrophoresis experiments are described in table 3.3.

The separating gel was prepared as follows: 7.5 ml of separating buffer, 10.5 ml H<sub>2</sub>O and 12 ml acrylamide stock solution were mixed and polymerization was initiated by the addition of 25 µl TEMED and 100 µl of a 10% ammonium persulphate solution. The solution was quickly poured between the glass plates of the electrophoresis apparatus to give a gel of 1.2 mm thickness. The gel was allowed to set for approximately 20 minutes. Once the gel had set, the stacking gel was prepared and poured onto the separating gel. 3.75 ml stacking gel buffer, 9.15 ml H<sub>2</sub>O and 1.34 ml acrylamide stock solution were mixed, and followed by addition of 15 µl TEMED and 75 µl ammonium persulphate. A plastic comb was inserted into the stacking gel to act as a mould to form wells for the samples.

The protein samples were diluted to give a concentration of approximately 1 mgml<sup>-1</sup> using 10 mM Tris buffer at pH 7.0. An equal volume of double-strength

**Table 3.3** Electrophoresis buffers

<b>Separating gel buffer</b>	<b>Stacking gel buffer</b>	<b>Sample buffer</b>
0.5 M Tris	0.5 M Tris	30 ml of 10% SDS solution
0.4% SDS adjusted to pH 8.7 with HCl	0.4% SDS adjusted to pH 6.8 with HCl	12.5 ml stacking gel buffer 10 ml glycerol adjusted to pH 6.8 with HCl
<b>Reservoir buffer</b>	<b>Acrylamide stock solution</b>	<b>Staining solution</b>
0.125 M Tris	30% acrylamide	0.1% Coomassie blue R250
0.96 M glycine 0.5% SDS adjusted to pH 8.3 and diluted 5X before use	0.8% bis-acrylamide	400 ml glacial acetic acid 1000 ml methanol 1000 ml H <sub>2</sub> O
<b>Destaining solution</b>	<b>Tracking dye</b>	
10% glacial acetic acid	1% bromophenol blue	

sample buffer containing 2% v/v  $\beta$ -mercaptoethanol was added and the sample tubes were placed in boiling water for 2 minutes. Tracking dye was prepared by mixing equal volumes of  $\beta$ -mercaptoethanol and 1% w/v bromophenol blue and then 5  $\mu$ l of this dye was added to each 100  $\mu$ l of protein sample. Between 10 and 60  $\mu$ l of sample per lane was applied to the gel. Standard protein markers were run in adjacent lanes for molecular weight calculations.

Electrophoresis in the gel was performed at a current of 8-10mA (or 150-200V) for approximately 16 hours, until the tracking dye had run almost to the bottom of separating gel. The gel was then removed from the apparatus and stained with Coomassie blue staining solution for 1 hour, with occasional shaking, and then destained with 10% acetic acid.

The molecular weight of protein bands could be determined from the relative migration of bands with respect to a standard protein set: Sigma Dalton Mark VII-L containing:  $\alpha$ -lactalbumin (14200), soybean trypsin inhibitor (20100), trypsinogen (24000), carbonic anhydrase (29000), rabbit muscle GAPDH (36000), egg albumin (45000) and bovine albumin (66000). The position of PGK bands were easily identified since they were very strong and occurred at the about the same position as egg albumin.

### **3.15 Wild-type and mutant PGK plasmids**

Although it is possible to extract PGK from ordinary baker's yeast, the yield is improved by using genetically engineered yeast strains which have been designed to over-produce PGK. The yeast strains used in this project were supplied already transformed with the required plasmids. The plasmids containing the wild-type and H388Q mutant PGK genes were received from Dr L. Gilmore and the plasmid

containing the R168K mutant gene was donated by Dr. J. Littlechild and Dr. H.C. Watson. These plasmids are described below.

### pMA27

pMA27 contains the gene encoding for yeast PGK, which was isolated from chromosome III on a 2.95 kbp *Hind*III fragment. pMA27 is derived from plasmid pBR322 and a fragment from the yeast 2 $\mu$  plasmid. pMA27 is a yeast/*E.coli* shuttle vector which may be propagated in *E.coli* strain trpC 117 using ampicillin selection or in *Saccharomyces cerevisiae* strain MD40-4C (*ura2*, *trp1*, *leu2-3*, *his3-11*, *his3-15*) using leucine selection (Wilson *et al.*, 1984)(figure 3.2).

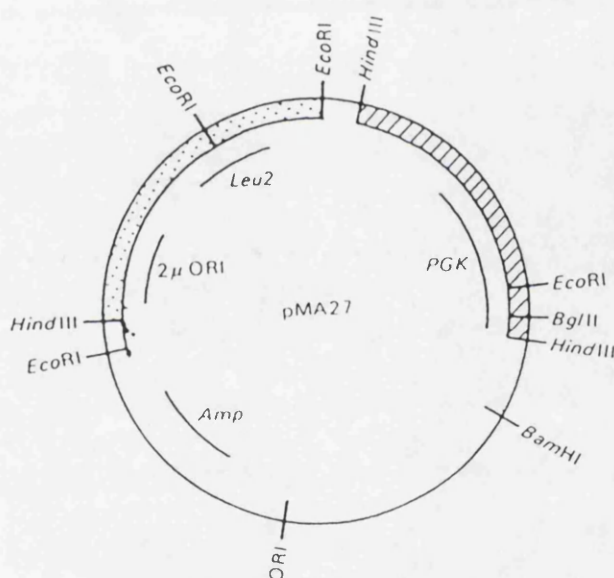


**Figure 3.2** pMA27

### H3880 mutant

The 2.95 kbp fragment containing the PGK gene was excised from pMA27 with *Hind*III, inserted into phage M13 mp9 and used to transfect *E.coli* JM01. Single-stranded DNA was prepared and a gapped-duplex was formed by annealing a linear fragment of M13-mp9 to the single-stranded M13-mp9-PGK.

An oligonucleotide specifying a T - A replacement was added and after extension and ligation, was used to transfect *E.coli*. Single-stranded DNA containing the mutant PGK gene was prepared, the mutant gene was isolated and purified before inserting into plasmid pMA40b (Wilson *et al.*, 1987). pMA40b is very similar to pMA27 but with the *EcoRI* fragment in the opposite orientation (figure 3.3).

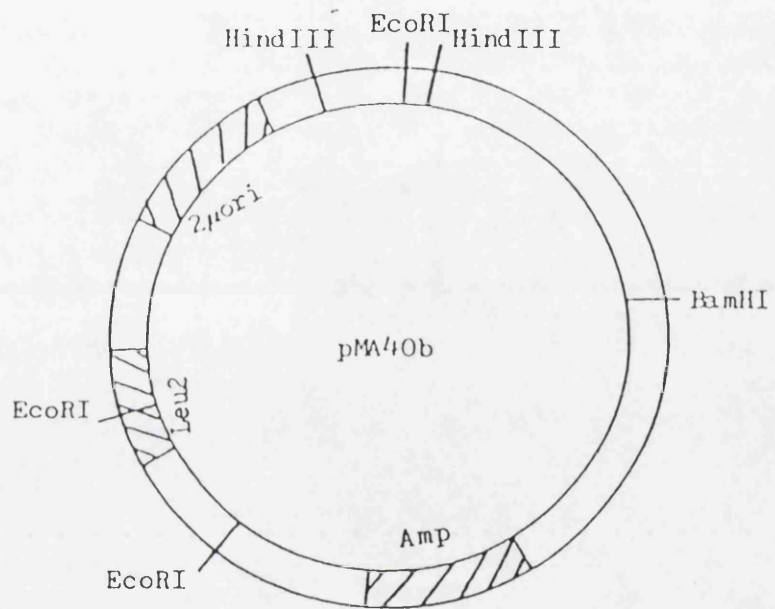


**Figure 3.3** pMA40b

#### R168K mutant

In this case, a new expression vector, pYE-PGK was used to transform yeast cells, strain MD40/4C (Minard *et al.*, 1989). A *HindIII* fragment containing the yeast PGK gene was excised from pMA27, the sticky ends were filled in by DNA polymerase and *BamHI* linkers were ligated onto the blunt ends. A new shuttle vector pYE-PGK was formed from the double *EcoRI* fragment of plasmid pAT153 and pMA27. The PGK gene with *BamHI* linkers was ligated into the *BamHI* site of pYE-vec to produce pYE-PGK (figure 3.4). This vector has the advantage over pMA27 of having the PGK

gene at a unique restriction site within the vector. The R168K mutant was formed by oligonucleotide-directed mutagenesis (Minard *et al.*, 1990)

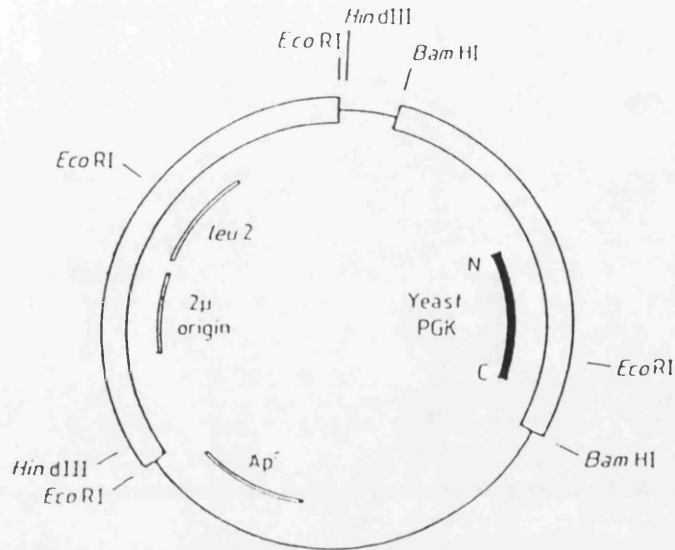


**Figure 3.4** pYE-PGK

### 3.16 Maintenance of yeast cultures

After initial transfer to Glasgow, the yeast cultures had to be carefully maintained to ensure that they remained viable over long storage periods and to ensure that contamination did not occur. This involved taking small amounts of a yeast culture and streaking onto a fresh agar plate to start a new subculture. Yeast grows quickly at 30 °C, but very slowly at 4 °C therefore, after an initial growth period of approximately 48 hours, the subcultures were stored in a cold room at approximately 4 °C.

Most of the yeast strains required various supplements to be able to grow however, although all the yeast strains are leu<sup>-</sup>, the leu gene is carried by plasmids and therefore leucine does not need to be added to the growth medium. Each yeast strain

requires different amino acid or base supplements. Table 3.4 lists the type of plasmid, the host yeast strain, and the supplement requirements of that yeast strain.

**Table 3.4** *Plasmids, host yeast strains and supplements*

<b>Plasmids</b>	<b>Host Yeast</b>	<b>Agar/Medium supplement</b>
pMA27,pMA40b	Y22	Ade, His, Met, Ura, Trp
pYE-PGK	MD40-4C	His, Ura, Trp
pMA27, pMA40b	MC40-10D	none

The supplement stock solutions were prepared as 10 mg/ml solutions in distilled water, sterilised by autoclaving at a pressure of 15lb/in<sup>2</sup> for 10 minutes and stored at 4 °C until required. The yeast cultures were grown on GYNB agar plates which had been supplemented with the required amino acid and base (adenine or uracil) stock solutions: 1 ml supplement stock solution was added to 100 ml molten agar prior to pouring in the plates. The composition of the GYNB agar and several other types of media are given in table 3.5.

**Table 3.5** *Composition of media and agar*

<b>GYNB</b>	<b>GYNB agar</b>	<b>YPG</b>
20 g/l Glucose	20 g/l Glucose	20 g/l Glucose
6.5 g/l Yeast nitrogen base (without amino acids)	6.5 g/l Yeast nitrogen base (without amino acids)	20 g/l Yeast extract
	20 g/l Bacto agar	10 g/l Bacto peptone

Yeast cultures were checked periodically using marker plates (these plates contained all but one of the essential supplements) and subcultures were plated every 2 months. Subcultures were incubated at 30 °C for 48 hours and stored at 4 °C. An improved method of storing yeast cultures was on agar slants in screw-capped universal bottles: these cultures could be stored for up to 6 months without contamination.

### **3.17 Yeast Fermentation**

3 x 5ml of GYNB media were inoculated with a single yeast colony and grown with agitation at 30 °C for 48 hours. These cultures were used to inoculate 3 x 500ml GYNB media and were grown at 30 °C for 48 hours. A Life-Sciences LM-15 fermentor was sterilised, filled with 12 litres of YPG medium, prewarmed and inoculated with two of the 500ml cultures; the third culture was added on the third day of fermentation. The contents of the fermentor were stirred at 100 rpm, aerated and maintained at 30 °C. Approximately 10 litres of medium were removed from the fermentor every 36 hours, centrifuged at 1000rpm for 30 minutes in an Heraeus M-7000 centrifuge to obtain a yeast pellet. The fermentor was refilled with freshly autoclaved and cooled medium and the fermentation continued until 5 or 6 harvests had been collected. Yeast pellets were stored frozen at -70 °C until required.

### **3.18 Purification of Yeast PGK**

PGK was isolated by modification of the method devised by Minard *et al*, 1990. The procedure contains five main stages:

1. Lysis of yeast cells
2. Selective ammonium sulphate precipitation
3. Precipitation by lowering pH

4. Ion-exchange chromatography

5. Gel-filtration chromatography

All centrifugations were performed at 12000 rpm for 30 minutes in a MSE high-speed 18 refrigerator centrifuge at 4 °C. The progress of purification was monitored after each stage by gel electrophoresis and by measuring specific activities.

### Stage 1. Cell lysis

Yeast pellets containing either wild-type or mutant PGK were removed from the freezer and allowed to warm to room temperature. 500 ml of extraction buffer (containing 10 mM Tris, 0.1 mM Na.EDTA, 6 mM  $\beta$ -mercaptoethanol,  $10^{-3}$  mM PMSF and  $20^{-3}$  mM benzamidine, adjusted to pH 7.5) was added to the pellet, and the pH was slowly adjusted to 10.6 with concentrated ammonia solution. It was then stirred overnight at 4 °C to minimise the action of protease enzymes, and in addition, the buffer contained PMSF and benzamidine to inhibit these enzymes. After this overnight lysis, the slurry was adjusted to pH 7.5 with 5 M lactic acid (previously adjusted to pH 3.5 with ammonia), the cell debris was removed by centrifugation and discarded. The supernatant was treated with protamine sulphate (1ml of a 10% solution/100ml extract) to precipitate most of the nucleic acid, and stirred at 4 °C for 30 minutes before centrifugation.

### Stage 2. Ammonium sulphate fractionation

Ammonium sulphate (300g/litre extract) was added over 20 minutes, with stirring, to the supernatant. Stirring was continued for a further 30 minutes. After centrifugation, the pellet containing precipitated protein (non-PGK), was discarded and further 170g/litre extract ammonium sulphate was added to supernatant. This solution

was stirred and centrifuged as before. Both supernatant and pellet were retained. The pellet was re-suspended in 10 mM Tris pH 7.0.

### Stage 3. Lowering of pH

The supernatant from stage 2 was slowly acidified to pH 4.3 with 5M lactic acid buffer (pH 3.5 with ammonia). The precipitated protein, containing the majority of PGK, was collected by centrifugation and the supernatant was discarded. The pellet was redissolved in 10 mM Tris pH 7.0.

### Stage 4. Anion-exchange chromatography

The protein solutions obtained in stages 2 and 3 were further purified using identical procedures, but the samples were not mixed.

The samples were dialysed overnight against 10 mM Tris pH 7.0, centrifuged to remove any precipitated material and then applied to a DEAE-sephadex A-25 anion exchange column (20 x 2.3cm) and eluted with the same buffer at a flow rate of roughly 1 ml/min. Fractions of approximately 10 ml were collected manually, starting as soon as the protein sample had been applied. Fractions which absorbed strongly at 280 nm were combined and stored as ammonium sulphate precipitates (0.65g ammonium sulphate/ml).

### Stage 5. Gel-filtration chromatography

The partially purified PGK ammonium sulphate precipitate was dialysed overnight against 10 mM Tris pH 7.5 containing 5% saturated ammonium sulphate,

0.05% sodium azide, and then applied to a Sephacryl S-200 gel-filtration column (100 x 3 cm). Fractions, containing 60 drops each, were collected using a LKB 7000 Ultrorac fraction collector, starting 6 hours after sample loading. Fractions were tested for PGK activity (Method A), and only fractions with specific activities greater than 500 units/mg were combined and used without further purification. Samples were stored at 4 °C as ammonium sulphate precipitates (0.65g ammonium sulphate/ml). These samples retained most of their activity even over long storage periods.

## 4 PGK RESULTS

The basic questions to be examined in this thesis are: can isothermal titration microcalorimetry be used to probe molecular recognition problems of current interest and if so, how do the results obtained compare to alternative techniques? What additional information might calorimetry yield and to what extent might the thermodynamic data be interpreted in relation to structural information?

In this section (chapter 4) I present the basic results of a range of experiments on PGK, followed by a discussion and interpretation (chapter 5). Data for antibiotic studies and their interpretation are presented in subsequent chapters (chapters 6 and 7).

### 4.1 PGK preparation

The specific activities of the wild-type, H388Q and R168K mutant enzymes, when purified by the methods described in chapter 3, were in the ranges of 500-680 units/mg, 100-180 units/mg and 130-220 units/mg, respectively, using the GAPDH-coupled activity assay. The overall percentage yields, calculated from equation 4.1,

$$\frac{\text{total number of enzyme units after purification}}{\text{total number of enzyme units after cell lysis}} \times 100 \quad (4.1)$$

varied over a wide range i.e. 20-65% for wild-type, 15-40% for R168K mutant, and 20-40% for H388Q mutant. Part of the reason for the large variation in yields was poor

long-term plasmid stability in the yeast cells. For example, the purification procedure for wild-type PGK was initially very successful in terms of yield. However over a period of approximately 18 months, the yields decreased from 400000 units of PGK activity per yeast pellet to less than 60000 units per pellet. This decrease in the percentage protein being expressed as PGK led to difficulties in obtaining pure PGK samples and low yields. This problem was resolved by transforming a new yeast strain, MC40-10D, with plasmids pMA27 and pMA40b. Yields improved dramatically and approximately 500 mg-1g purified wild-type PGK could be obtained from one yeast pellet. A typical set of purification results for wild-type PGK is shown in table 4.1.

**Table 4.1** Purification of wild-type PGK

Stage	Total Activity (units)	Yield (%)	Specific Activity (units/mg)
1	235 320	100	not measured
2	235 600	100	not measured
3	190 960	81	288
4	107 338	46	59
5	98 990	42	416
6	73 070	31	585

Stage 1: sample taken after removal of cell debris

Stage 2: sample taken after treatment with protamine sulphate

Stage 3: sample of supernatant after 1st ammonium sulphate fractionation

Stage 4: sample taken from redissolved ammonium sulphate precipitate following second fractionation step

Stage 5: sample taken from redissolved pellet following pH crash

Stage 6: sample 5 after ion-exchange and gel-filtration chromatography

The PGK preparations were shown to be free of contaminating proteins differing in molecular weight by the presence of a single band in SDS polyacrylamide gel electrophoresis experiments as shown in figure 4.1.

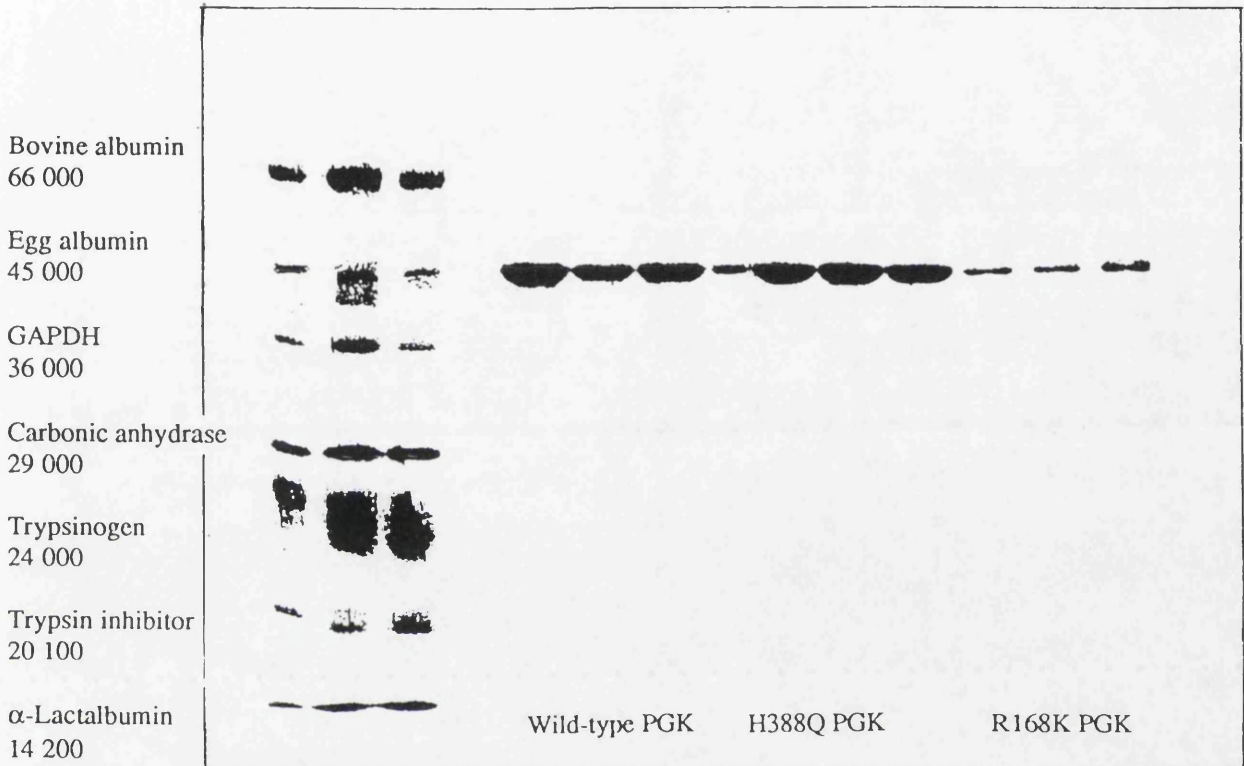


**Figure 4.1** SDS-gel showing marker protein bands, wild-type PGK, H388Q PGK and R168K PGK

#### 4.2 Kinetic studies of PGK

Kinetic experiments were performed as described in chapter 3, using the GAPDH coupled assay system, with the free magnesium concentration fixed at 1 mM (Method B).

Steady-state kinetic experiments were performed to determine Michaelis constants for substrate binding to wild-type, R168K and H388Q mutant PGK. The results from these experiments (table 4.2) were used to assess purity of PGK samples and for comparison with previous kinetic experiments (table 4.3). The raw data obtained were transformed to linear plots using Lineweaver-Burk, Eadie-Hofstee and Hanes methods (Appendix B) and average values of  $K_M$  and  $V_{max}$  were taken. Kinetic data for wild-type PGK and 3-phosphoglycerate are shown in figure 4.2.

**Table 4.2** Kinetic parameters for wild-type and mutant PGK at 25 °C

Enzyme	Substrate	$K_M$ (mM)	$V_{max}$ (units/mg)
Wild-type	ATP	0.29 (0.03)	595 (67)
	3-PG	0.52 (0.04)	651 (55)
H388Q	ATP	0.12 (0.02)	132 (33)
	3-PG	0.19 (0.03)	145 (27)
R168K	ATP	0.79 (0.04)	176 (39)
	3-PG	1.79 (0.05)	184 (44)

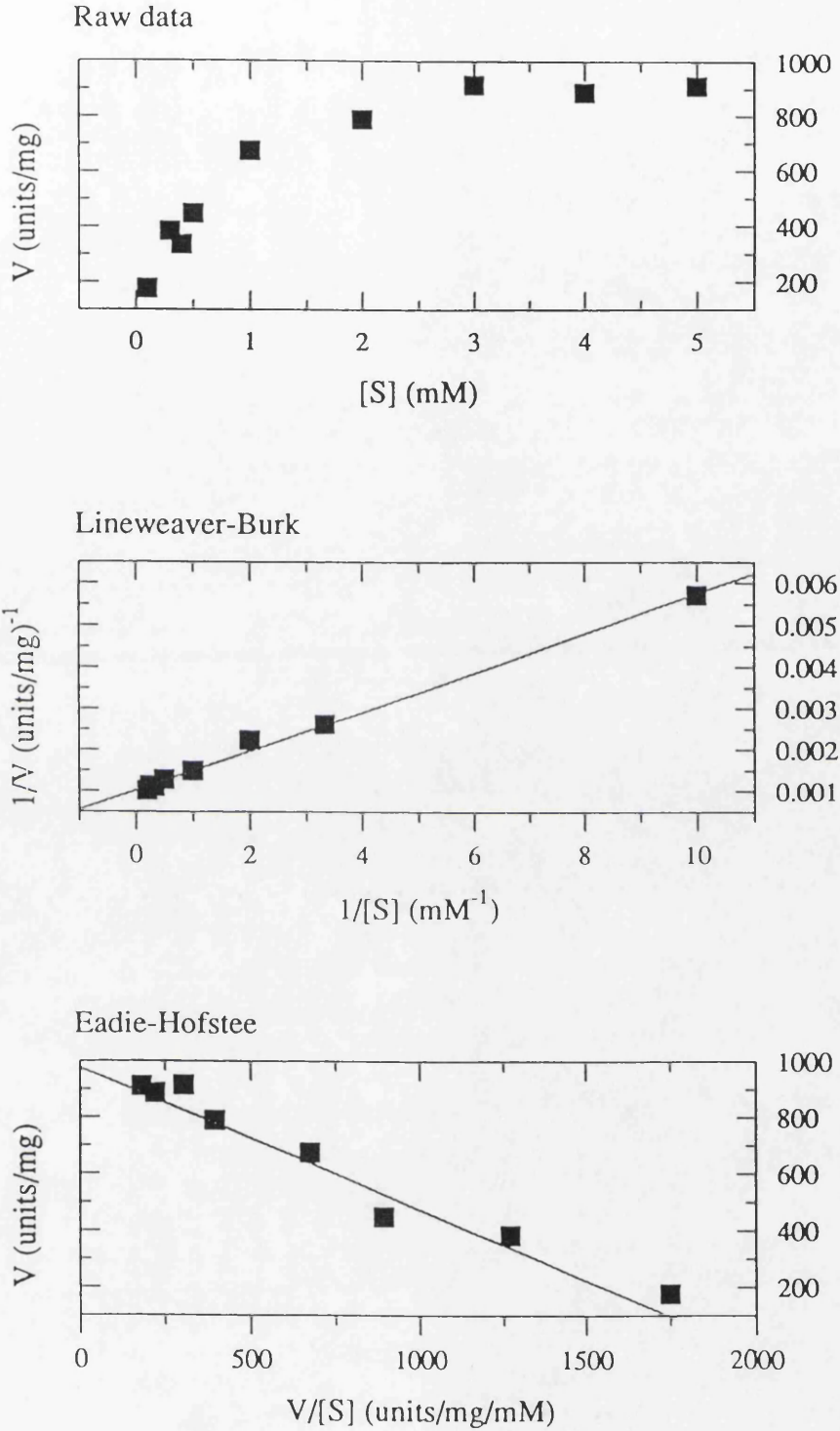


Figure 4.2 Kinetic data for 3-phosphoglycerate binding to wild-type PGK

**Table 4.3** Literature values for  $K_M$  and  $V_{max}$

ref.	Wild-type PGK			H388Q			R168K		
	$K_M$ (mM)		$V_{max}$ h	$K_M$ (mM)		$V_{max}$ h	$K_M$ (mM)		$V_{max}$ h
	ATP	3-PG		ATP	3-PG		ATP	3-PG	
a	0.30	0.50	826						
b	0.32	-	-	0.11	f	g			
c	0.33	0.78	500				0.90	2.11	
d	0.29	0.40	517						
e	0.33	0.60	510	0.07	0.15	165			

a = Mas *et al.* 1987, 1988

b = Wilson *et al.*, 1987

c = Walker *et al.*, 1989

d = Sherman *et al.*, 1991

e = Johnson *et al.*, 1991

f = "unchanged from wild-type" Wilson *et al.*, 1987

g = "fivefold reduction from wild-type" Wilson *et al.*, 1987

h = units/mg

The effect of sulphate on the activity of wild-type PGK is shown in figure 4.3. The sulphate concentration was varied from 0 to 50 mM, whilst the 3-phosphoglycerate and ADP concentrations were fixed at either 0.5 mM or 0.1 mM. The results are expressed as percentage activity with respect to the activity in the absence of sulphate. The activation pattern is dependent on substrate concentration. When both ADP and 3-phosphoglycerate are present at 0.5 mM, the enzyme activity reaches a maximum value of about 400% at a sulphate concentration of approximately 20 mM. The activating effect is less marked at low concentrations of substrate (0.1 mM), reaching a maximum

value of 225% at a sulphate concentration of 14 mM. Inhibition is observed above 35 mM sulphate, for example the percentage activity at a 50 mM concentration of sulphate is only 47%.

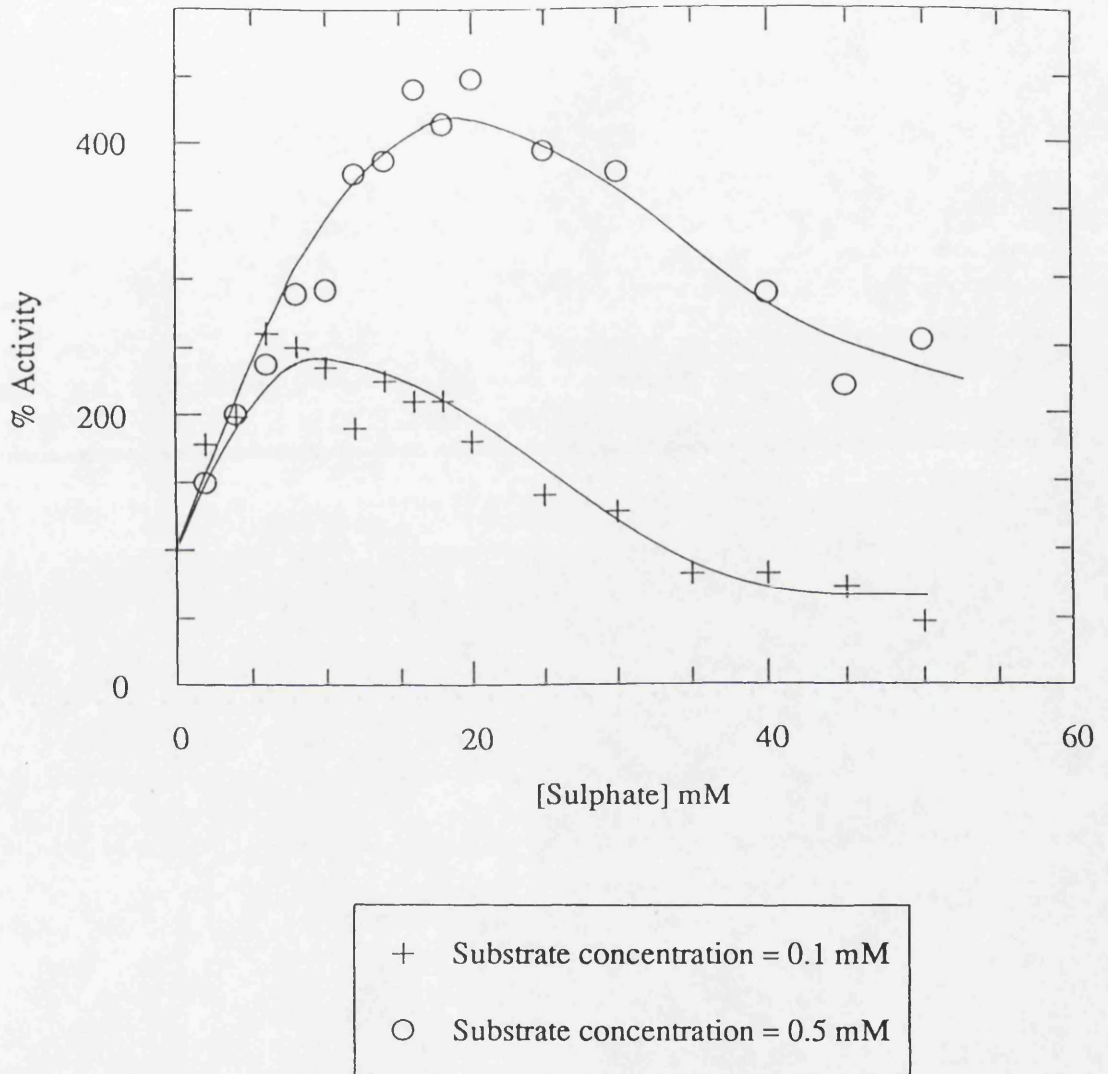


**Figure 4.3** Sulphate activation patterns for two concentrations of substrate, 0.1 mM and 0.5 mM.

### **4.3 Microcalorimetry of substrate/ligand binding to PGK**

Kinetic experiments can give an indication of the relative binding affinities of substrates to PGK, but a more detailed study is required to determine the nature of the forces between the enzyme and the substrate. Microcalorimetry is useful for these studies since the heat effects which occur when the substrates or ligands bind to PGK are measured and, since no catalysis occurs with single substrates, the observed heat effects arise mainly from the heat of binding. Therefore microcalorimetry provides a convenient technique to obtain enthalpies of binding and also binding affinities. The comparison of the results obtained for the wild-type and mutant enzymes can give information regarding the effect that the mutation has on enzyme binding activity. In addition, since PGK has been found to undergo complicated substrate/anion activation or inhibition effects, these processes can also be studied using microcalorimetry by comparing the binding parameters of the substrates in the absence and presence of other ligands. These experiments can possibly give an insight into the control mechanisms which are used to modify substrate binding to enzymes and hence activity.

#### **4.3.1 The LKB titration calorimeter experiments**

Early experiments of substrate binding to PGK used an LKB microcalorimeter modified for titration, as described earlier. Several problems were associated with these measurements: the LKB calorimeter requires a long equilibration time of roughly 2 hours or more and the time interval required to regain baseline levels between injections was approximately 20-30 minutes. This means that an experiment designed to attain enzyme saturation in 10 injections would require about 7 hours of experimental time. The second problem was that the calorimeter was sensitive to changes in room temperature: the baseline would drift throughout the day. Air conditioning did not alleviate this problem but rather resulted in a cyclic fluctuation of the baseline. The

large cell volumes (7ml) and relatively low sensitivity required a substantial quantity (approximately 30-50mg) of protein for each titration curve. For these reasons, although reasonable titration data could sometimes be obtained, the experiments using the LKB calorimeter were abandoned in favour of the Omega microcalorimeter. An example of the raw data and a titration curve obtained with the LKB calorimeter are shown in figures 4.4 and 4.5. The data have been corrected by subtracting the heat of mixing and the formation of a 1:1 enzyme-substrate complex has been assumed.

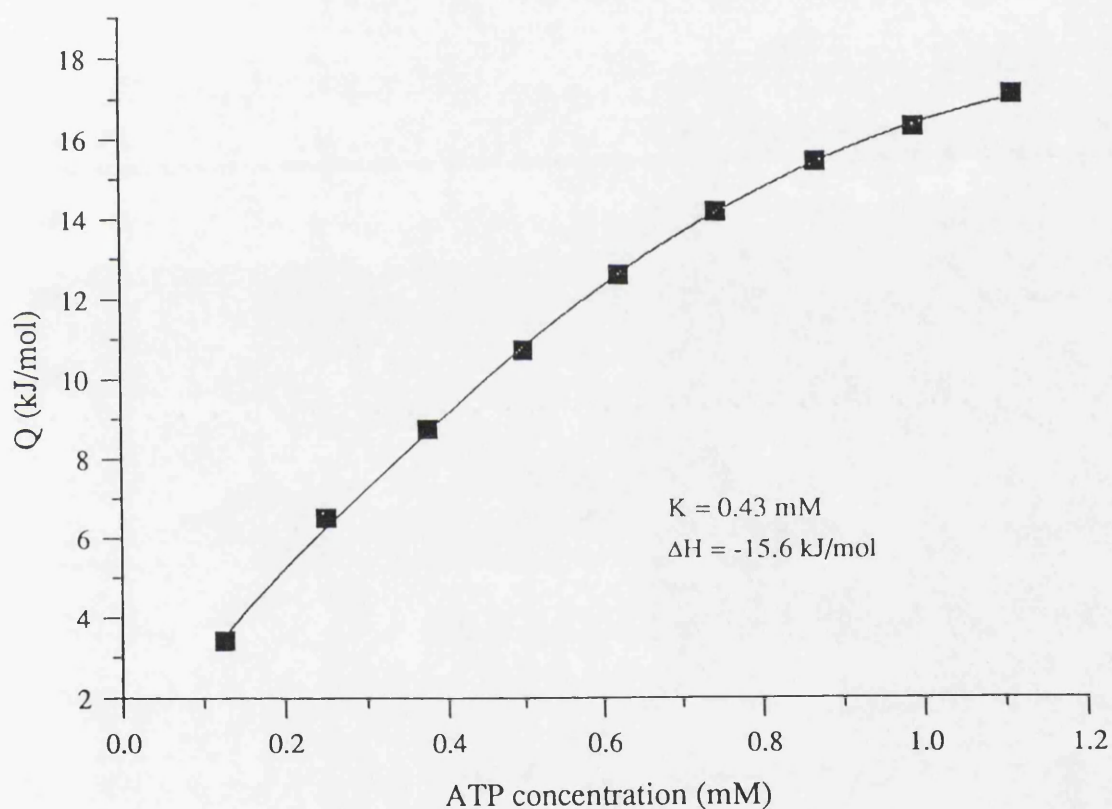


**Figure 4.4** *Binding isotherm for ATP binding to wild-type PGK, data collected with LKB calorimeter*

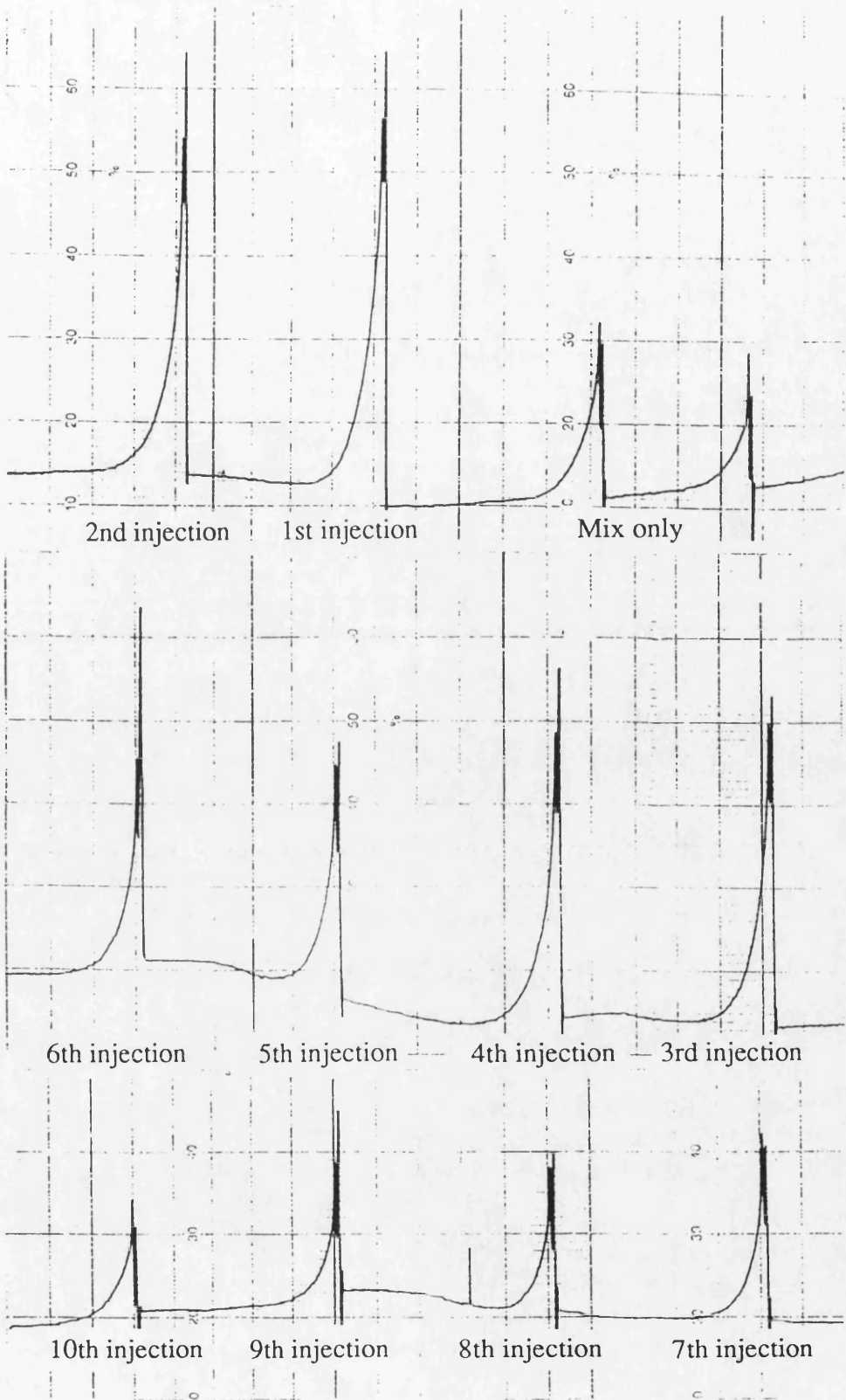


**Figure 4.5** Raw data for ATP binding to wild-type PGK using LKB calorimeter

### 4.3.2 The Omega Calorimeter experiments

The experiments were performed at 25 °C, with an injection schedule usually of 20 injections of 5 µl at 3 minute intervals. In general, injection of substrate into the PGK enzyme solution results in exothermic heat effects which decrease in size during the titration until the enzyme becomes saturated. At this point, heat effects are still observed but these are similar in magnitude to the heat effects observed on titration of buffer with substrate. A typical dataset from a titration of PGK with substrate is shown in figure 4.6. Comparison of figure 4.5 and figure 4.6 demonstrates the advantages of the Omega calorimeter over the LKB calorimeter; in the latter experiment, 20 injections were obtained in 60 minutes, whereas, 10 injections required about 7 hours with the LKB calorimeter. Also, the baseline drift is insignificant using the Omega calorimeter.

The experimental data in figure 4.6 and subsequent data in this chapter have been corrected for substrate dilution effects and have been analysed using the one set of sites model with N fixed as 1, unless otherwise stated. The Omega calorimeter is calibrated in calories and hence the data analysis programs also use calories rather than the S.I units, joules. This means that the figures generated by Origin are in calories, whereas, the data given in the tables have been converted to joules.

### 4.3.3 Wild-type PGK

The initial microcalorimetric experiments were concerned with measuring the thermodynamic parameters for substrate binding to wild-type PGK under various experimental conditions (different buffers, pH, magnesium concentrations) to investigate the effects of these factors on the association constants and enthalpies of binding. The thermodynamics of binding of Mg.ATP, Mg.ADP and 3-phosphoglycerate

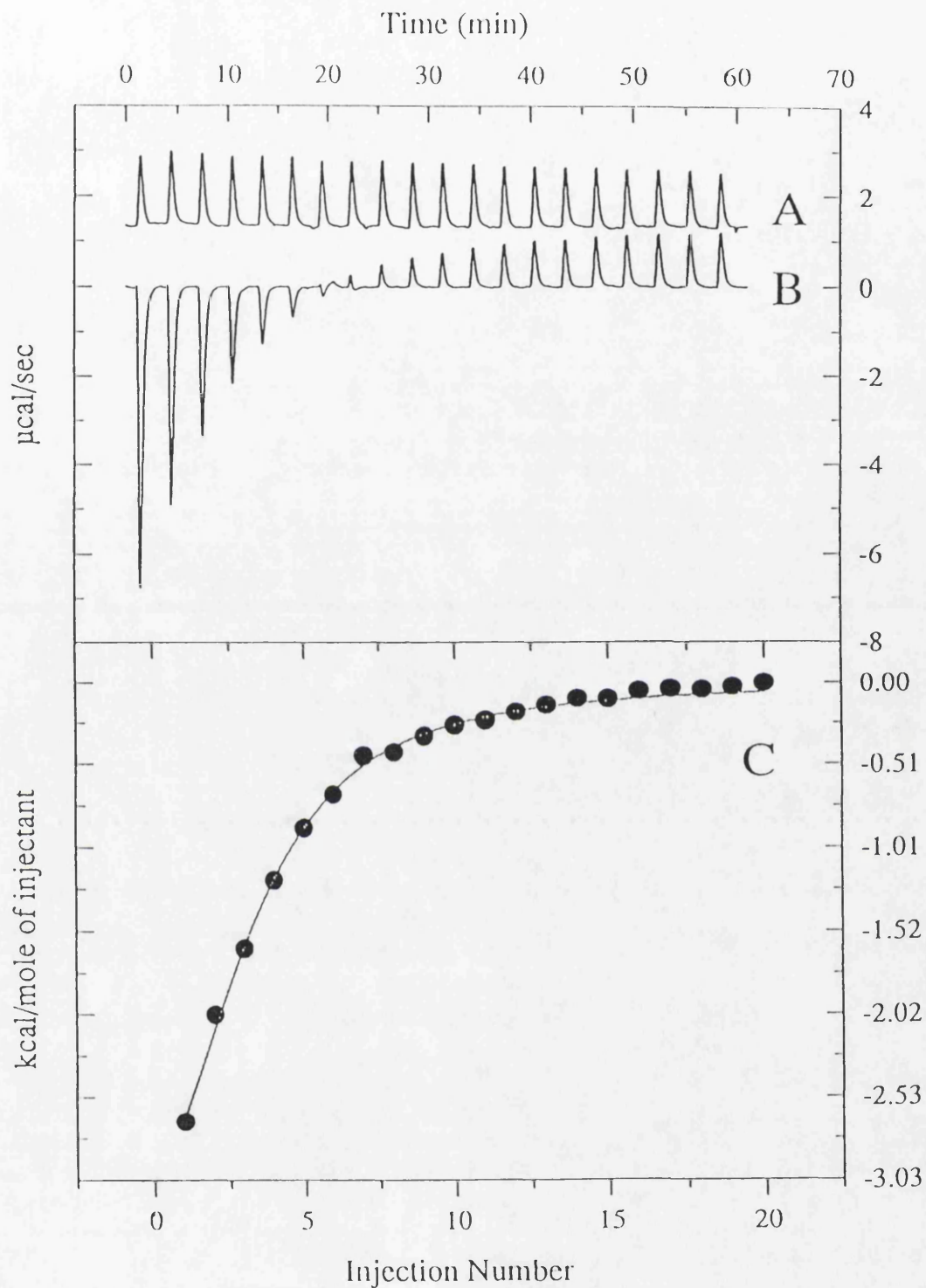


**Figure 4.6** A. Raw data for ADP dilution experiment  
 B. Raw data for titration of wild-type PGK with ADP  
 C. Integrated and corrected (B-A) data. The solid line through the experimental points represents the theoretical fit to the data

to PGK could be examined. However the fourth substrate, 1,3-diphosphoglycerate, is not readily available and is too unstable in solution to be studied by microcalorimetry.

The binding parameters of substrate binding to wild-type PGK were measured in two different buffer systems, one at pH 7 (tris/MOPS buffer) and the other at pH 6 (MES buffer). The results obtained in tris/MOPS buffer are presented in table 4.4, with the raw data and binding isotherms presented in figures 4.7 to 4.9. The binding of ADP to PGK in tris/MOPS buffer is strongly exothermic, whilst the highest binding affinity occurs with 3-phosphoglycerate. The theoretical fitting curves agree well with the experimental data for the ADP and 3-phosphoglycerate experiments, but slight deviations can be noticed with the ATP data.

*Table 4.4 Thermodynamic parameters for binding of Mg.ADP, Mg.ATP and 3-phosphoglycerate to wild-type PGK in Tris/MOPS at pH 7.0, 4mM magnesium acetate, 0.1mM DTT and 0.05% w/v sodium azide*

Parameters	Mg.ADP	Mg.ATP	3-PG
$K_a$ ( $M^{-1}$ )	3550 (480)	6855 (560)	180000 (30000)
$\Delta H^\circ$ ( $kJmol^{-1}$ )	-57.5 (4.9)	-34.3 (1.5)	-15.5 (0.7)
$\Delta G^\circ$ ( $kJmol^{-1}$ )	-20.2 (0.3)	-21.9 (0.2)	-30.0 (0.4)
$\Delta S^\circ$ ( $Jmol^{-1}K^{-1}$ )	-125 (16)	-44 (5)	+49 (3)
$\Delta H^\circ_{add}$ ( $kJmol^{-1}$ )	-45.5 (1.0)	-28.9 (0.5)	-14.7 (2.2)

The calorimetric experiments were repeated in MES buffer at pH 6.0 and the results are listed in table 4.5 with the raw data and binding isotherms in figures 4.10 to 4.12. The results obtained in MES buffer are roughly similar to those obtained in

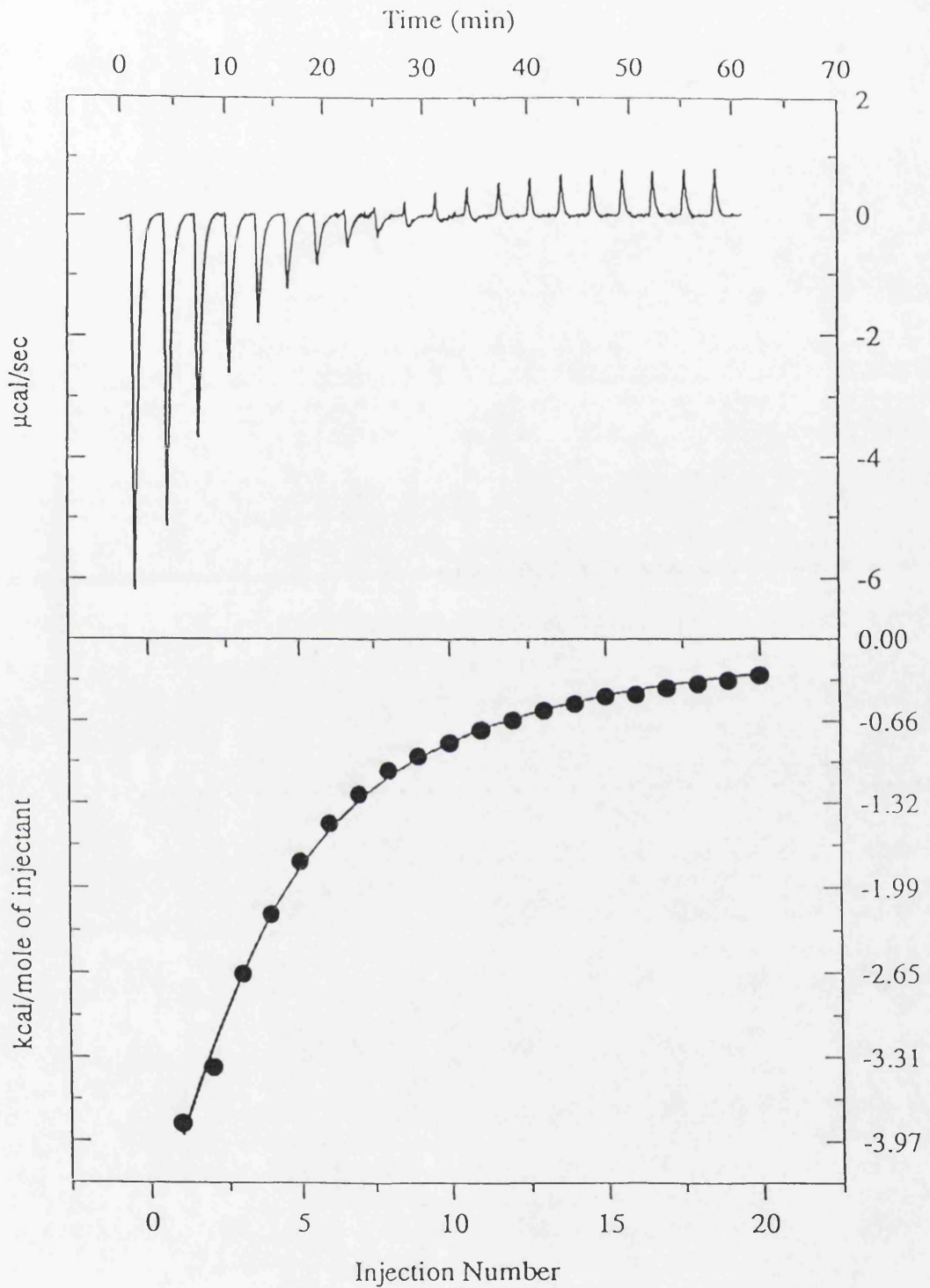


**Figure 4.7** Wild-type PGK and ADP. 50 mM tris/MOPS pH 7.0, 4 mM Mg acetate, 0.1 mM DTT and 0.05% w/v sodium azide.

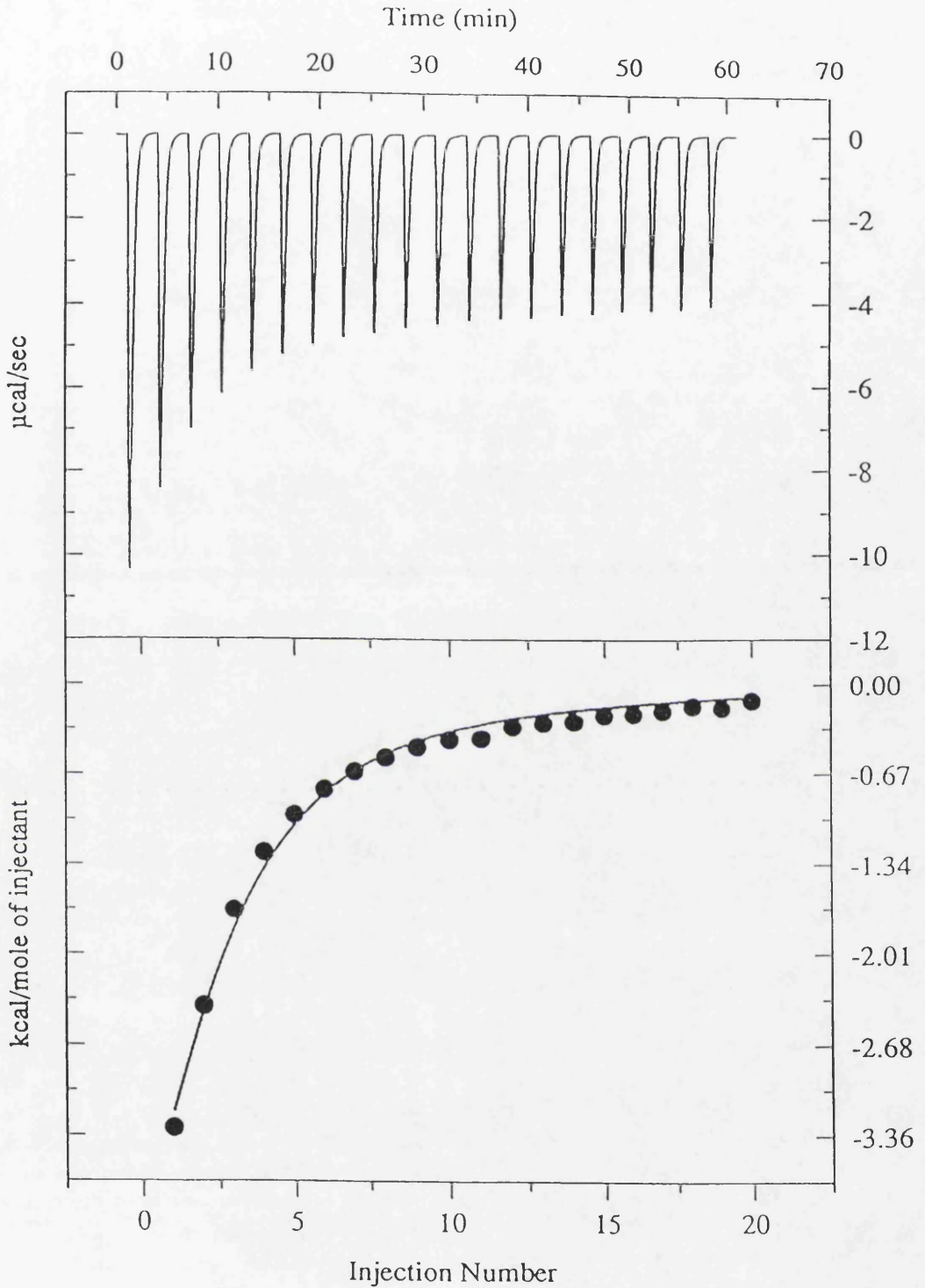


**Figure 4.8** Wild-type PGK and ATP. 50 mM tris/MOPS pH 7.0, 4 mM Mg acetate, 0.1 mM DTT and 0.05% w/v sodium azide.

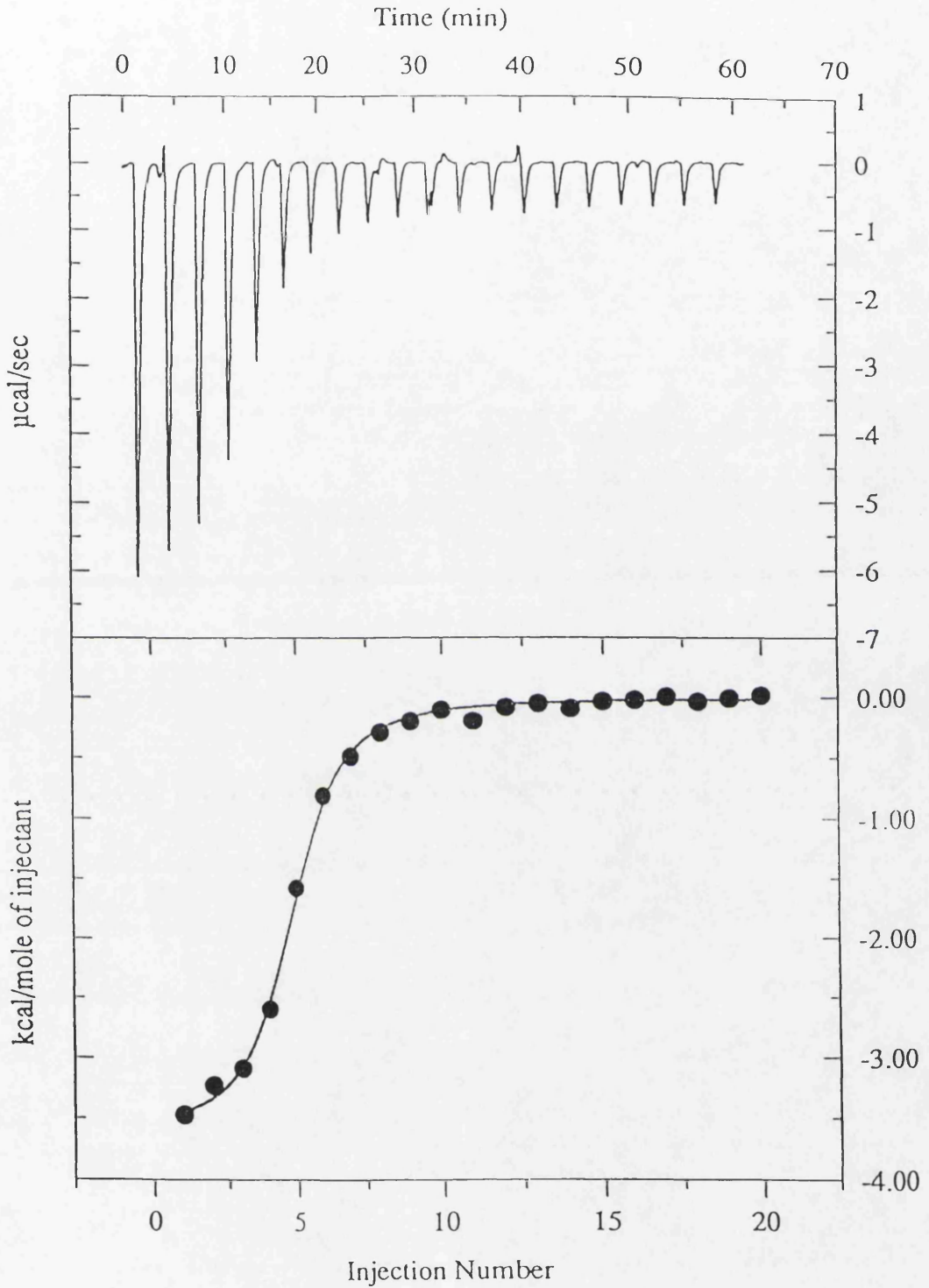


**Figure 4.9** Wild-type PGK and 3-phosphoglycerate. 50 mM tris/MOPS pH 7.0, 4 mM Mg acetate, 0.1 mM DTT and 0.05% w/v sodium azide.

tris/MOPS buffer, except the binding of ADP to PGK is somewhat less exothermic. Differences in binding parameters for the association of 3-phosphoglycerate with PGK are also noticed.

*Table 4.5 Thermodynamic parameters for binding of Mg.ADP, Mg.ATP and 3-phosphoglycerate to wild-type PGK in MES at pH 6.0, 4mM magnesium Acetate, 0.1mM DTT and 0.05% sodium azide*

Parameters	Mg.ADP	Mg.ATP	3-PG
$K_a$ ( $M^{-1}$ )	5940 (790)	6610 (500)	113000 (6000)
$\Delta H^\circ$ ( $kJmol^{-1}$ )	-34.8 (0.8)	-34.8 (0.7)	-19.1 (0.6)
$\Delta G^\circ$ ( $kJmol^{-1}$ )	-21.5 (0.3)	-21.8 (0.2)	-28.8 (0.1)
$\Delta S^\circ$ ( $Jmol^{-1}K^{-1}$ )	-34 (4)	-44 (2)	+33 (2)
$\Delta H^\circ_{add}$ ( $kJmol^{-1}$ )	-34 (4)	-35 (6)	-17.5 (1.4)

Microcalorimetry was also used to investigate the binding of other ligands (sulphate, adenosine and tripolyphosphate) to PGK (table 4.6). The data are shown in figures 4.13 to 4.15. Both anions were observed to bind to PGK, in particular, the multivalent triphosphate binds with high affinity. In contrast, adenosine did not appear to bind to PGK. Figure 4.14 depicts the raw data for the titration of PGK with adenosine and, for comparison, the raw data for the injection of adenosine into buffer. Both experiments give rise to similar heat effects.

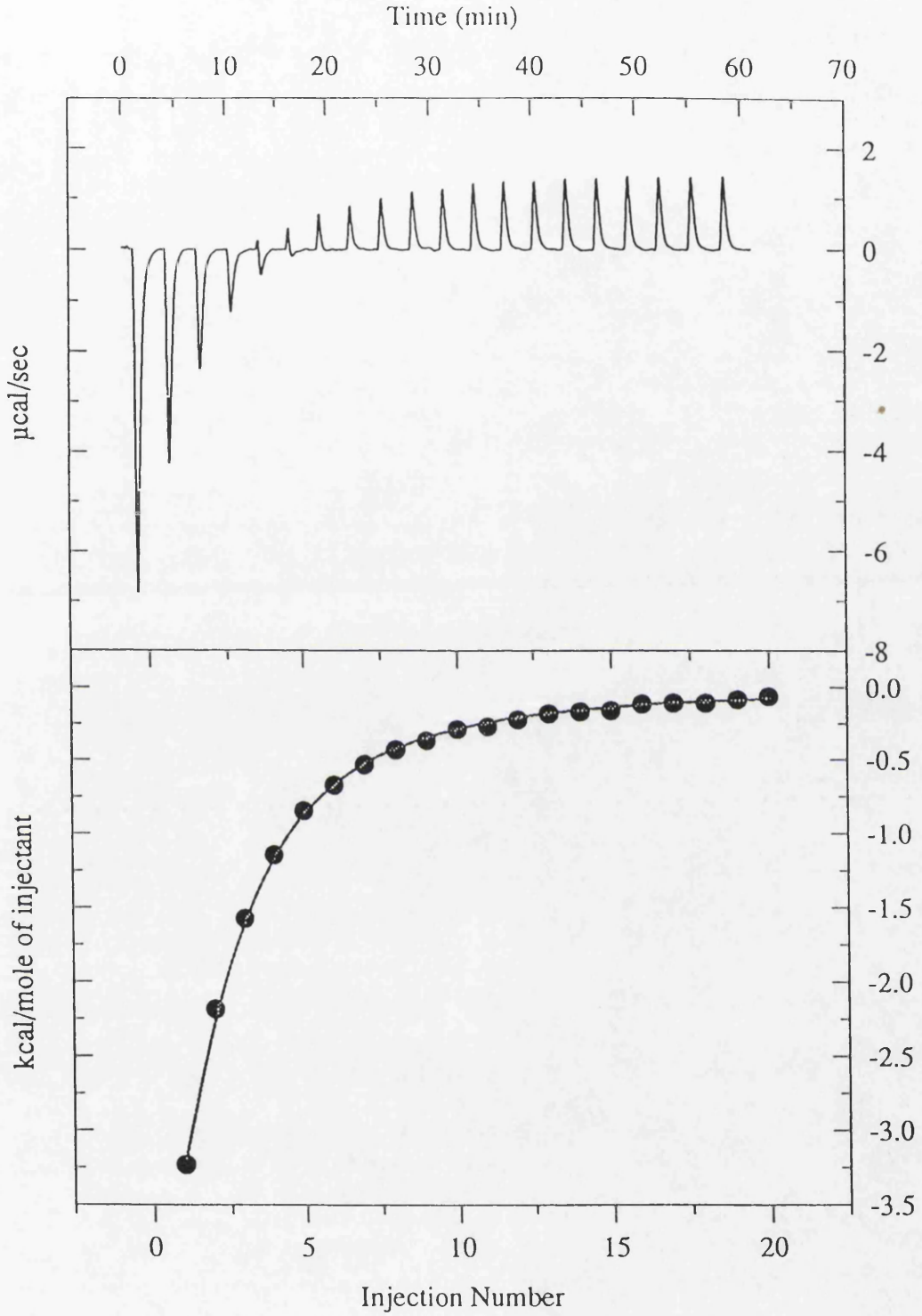


**Figure 4.10** Wild-type PGK and ADP. 50 mM MES pH 6.0, 4 mM Mg acetate, 0.1 mM DTT and 0.05% w/v sodium azide.

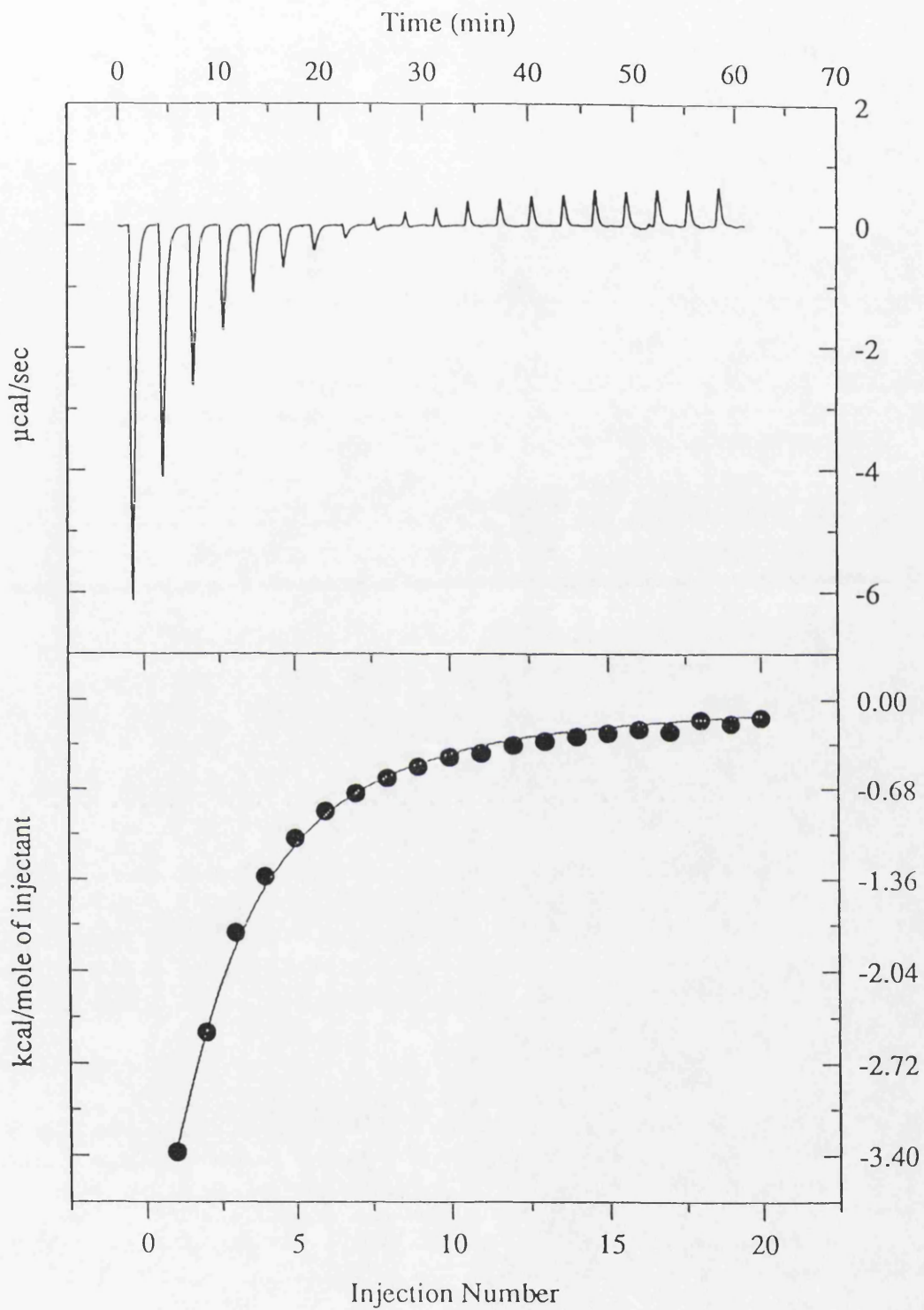


*Figure 4.11 Wild-type PGK and ATP. 50 mM MES pH 6.0, 4 mM Mg acetate, 0.1 mM DTT and 0.05% w/v sodium azide.*

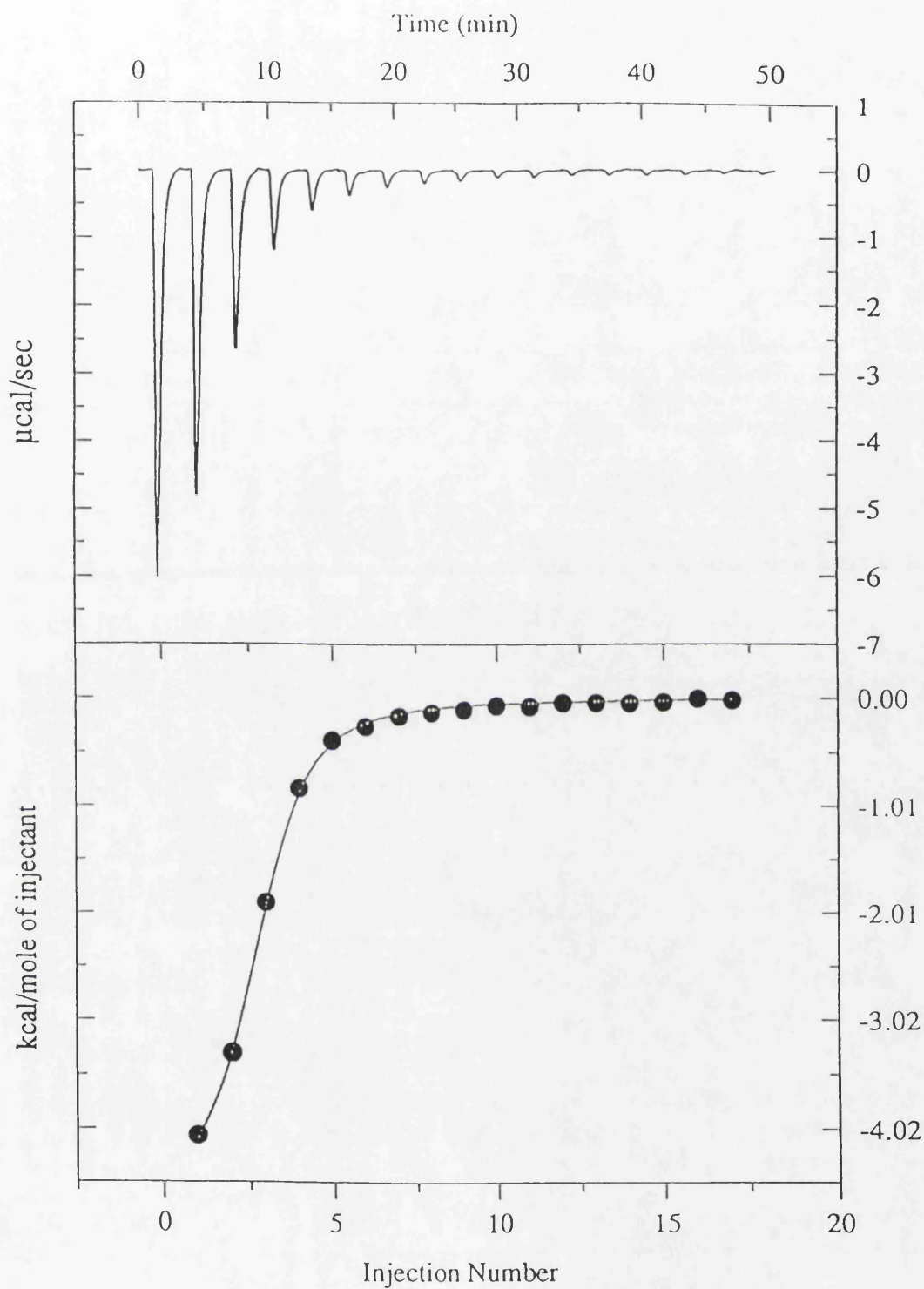


**Figure 4.12** Wild-type PGK and 3-phosphoglycerate. 50 mM MES pH 6.0, 4 mM Mg acetate, 0.1 mM DTT and 0.05% w/v sodium azide.

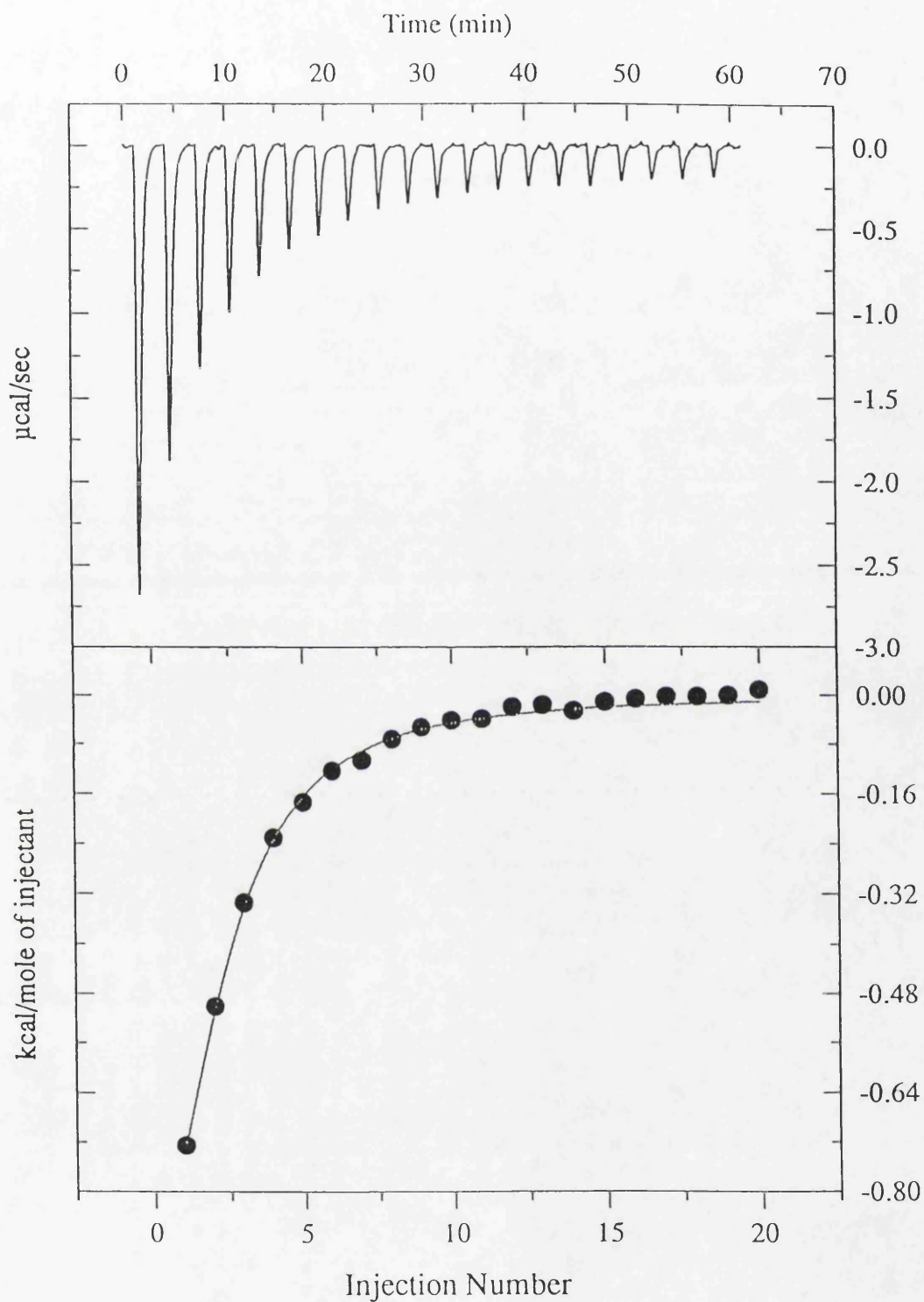


**Figure 4.13** Wild-type PGK and ammonium sulphate. 50 mM MES pH 6.0, 4 mM Mg acetate, 0.1 mM DTT and 0.05% w/v sodium azide.

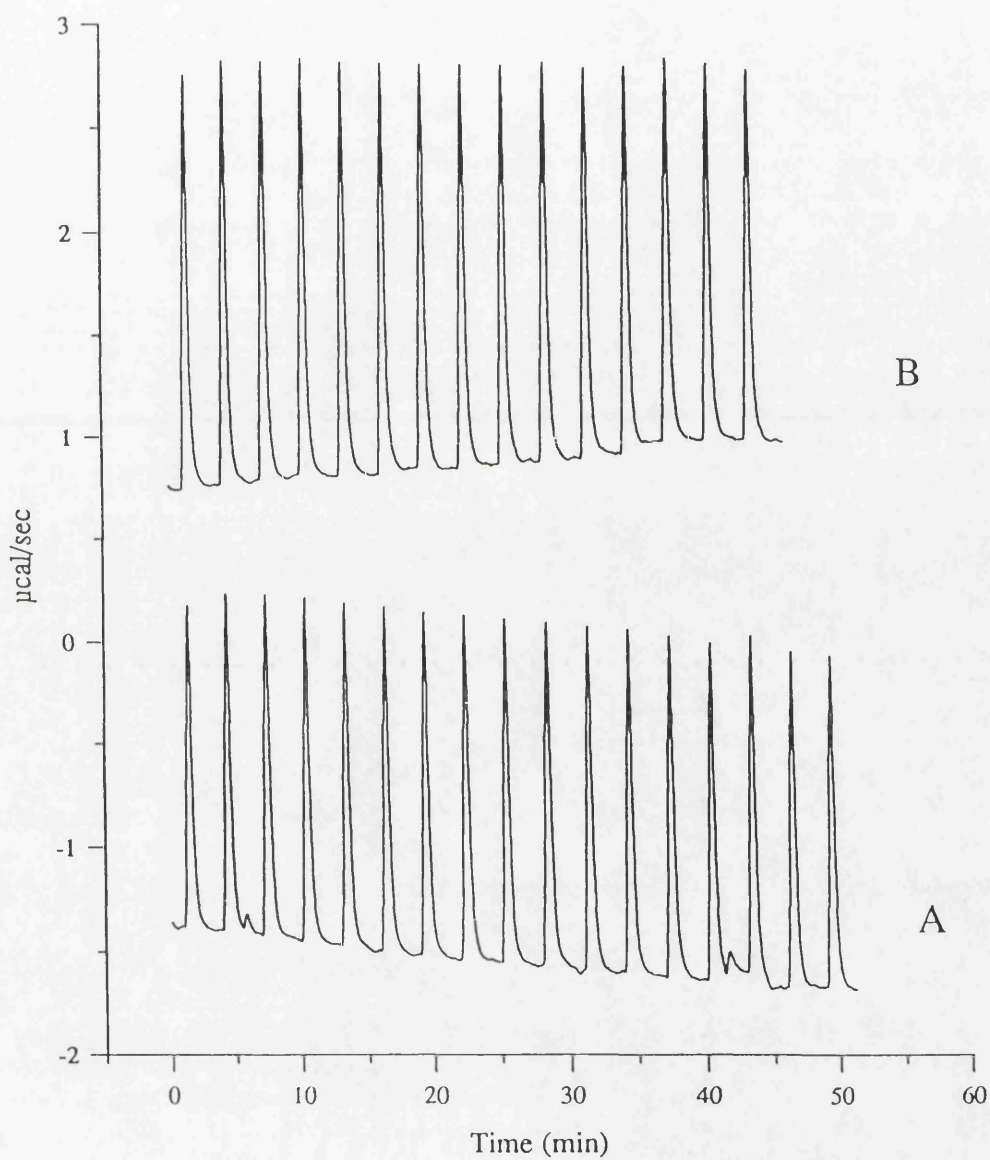


**Figure 4.14** A. Wild-type PGK and adenosine. 50 mM MES pH 6.0, 4 mM Mg acetate, 0.1 mM DTT and 0.05% w/v sodium azide.

B. Adenosine dilution experiment

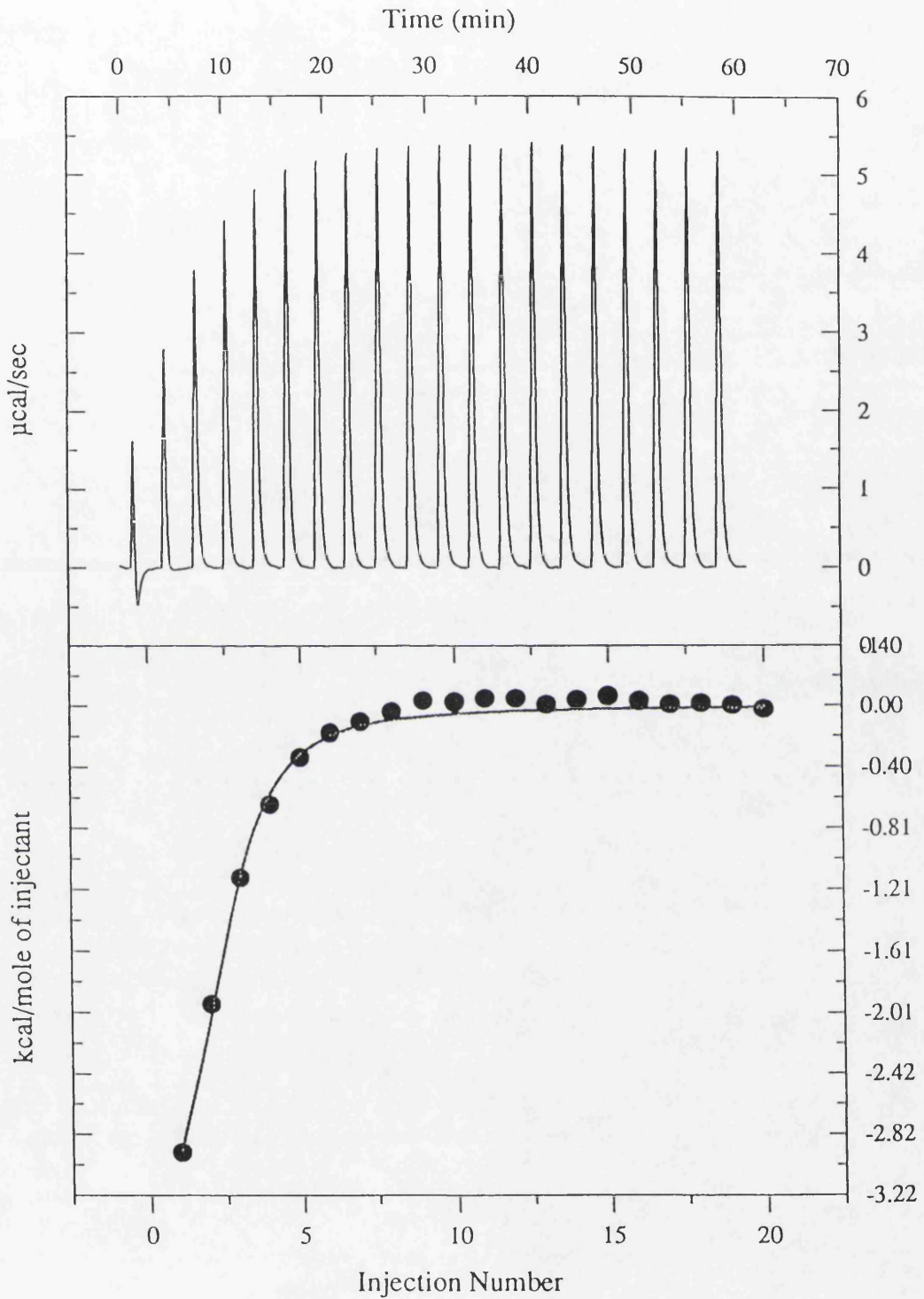


**Figure 4.15** Wild-type PGK and tripolyphosphate. 50 mM MES pH 6.0, 4 mM Mg acetate, 0.1 mM DTT and 0.05% w/v sodium azide.

**Table 4.6** Thermodynamic parameters of ligand binding to wild-type PGK in MES at pH 6.0, 4mM magnesium acetate, 0.1mM DTT, 0.05% sodium azide.

Parameters	sulphate	adenosine	triphosphate
$K_a$ ( $M^{-1}$ )	3850 (275)		60880 (9000)
$\Delta H^\circ$ ( $kJmol^{-1}$ )	-6.8 (0.4)		-16.6 (1.0)
$\Delta G^\circ$ ( $kJmol^{-1}$ )	-20.4 (0.2)	weak /no binding	-27.3 (0.4)
$\Delta S^\circ$ ( $Jmol^{-1}K^{-1}$ )	+46 (2)		+36 (4)
$\Delta H^\circ_{add}$ ( $kJmol^{-1}$ )	-6.0 (0.9)		-15.9 (1.5)

#### 4.3.4 Mutant PGK

The substrate titration experiments were repeated with mutant enzyme under conditions which were as close as possible to the experiments with wild-type PGK in MES buffer. These experiments were required to demonstrate the effects of a mutation at the active site of PGK and the effects of a mutation at a more distant position. Two mutant forms of PGK were investigated, H388Q and R168K, the results from the experiments with H388Q enzyme are given in table 4.7, and the results for R168K are in table 4.8. The raw data and calorimetric isotherms of substrate binding to H388Q are illustrated in figures 4.16 to 4.18. The binding parameters obtained for H388Q are very similar to the values obtained for wild-type PGK, except that the binding of 3-phosphoglycerate is more exothermic.

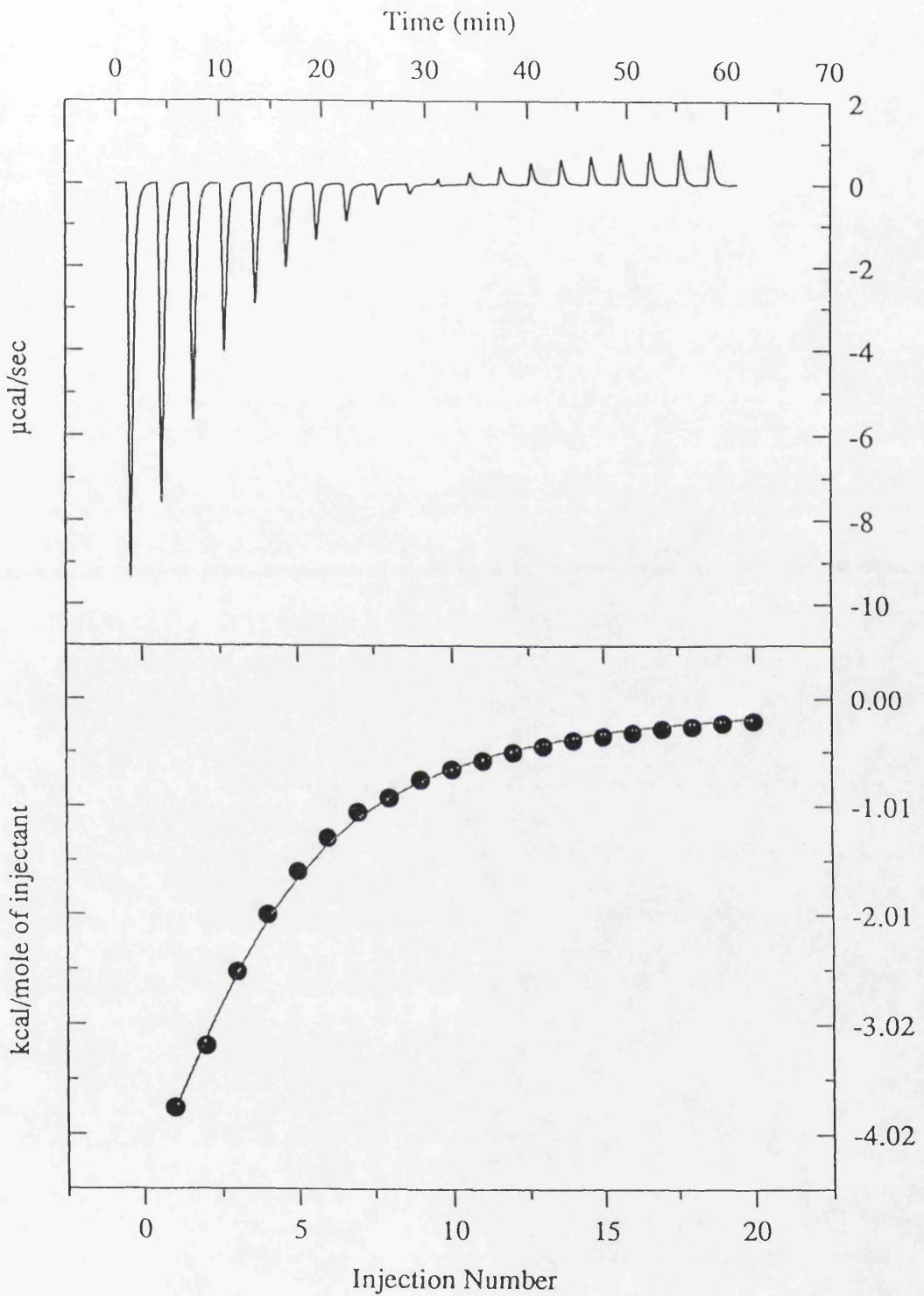


**Figure 4.16** *H388Q PGK and ADP. 50 mM MES pH 6.0, 4 mM Mg acetate, 0.1 mM DTT and 0.05% w/v sodium azide.*

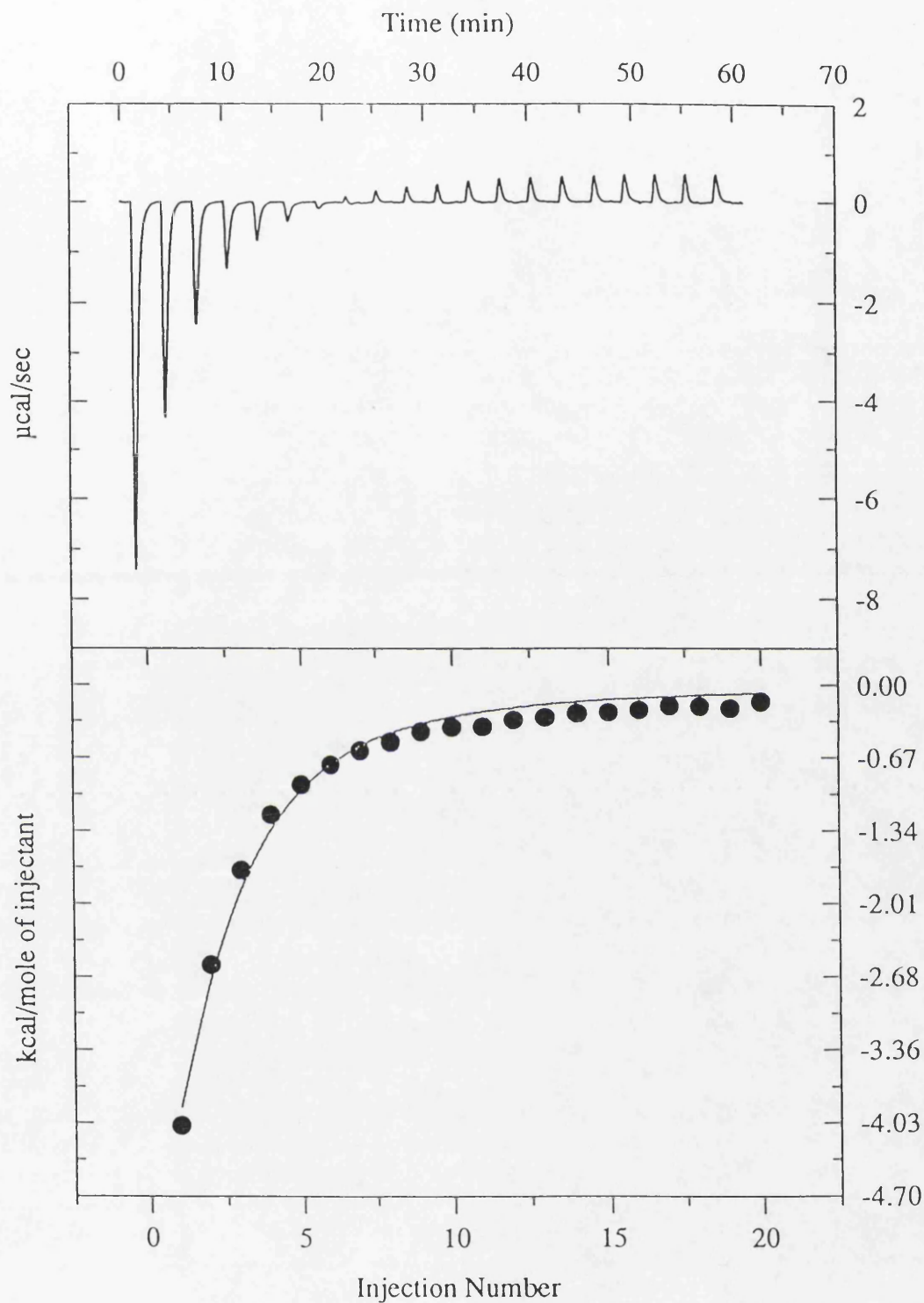


Figure 4.17 H388Q PGK and ATP. 50 mM MES pH 6.0, 4 mM Mg acetate, 0.1 mM DTT and 0.05% w/v sodium azide.

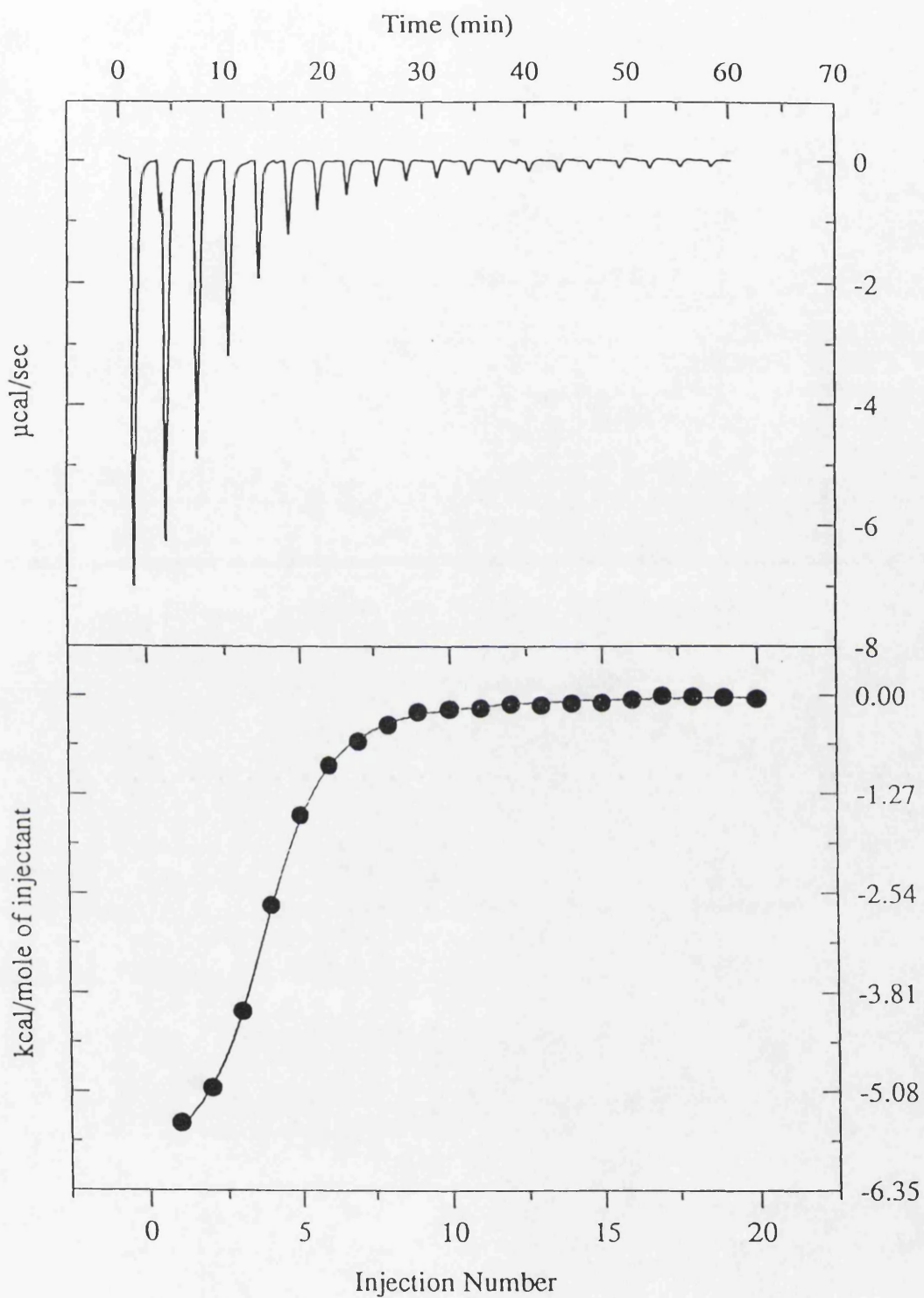


Figure 4.18 *H388Q PGK and 3-phosphoglycerate. 50 mM MES pH 6.0, 4 mM Mg acetate, 0.1 mM DTT and 0.05% w/v sodium azide.*

**Table 4.7** Thermodynamic parameters for binding of Mg.ADP, Mg.ATP and 3-phosphoglycerate to H388Q PGK in MES pH 6.0, 4mM magnesium acetate, 0.1mM DTT, 0.05% w/v sodium azide

Parameters	Mg.ADP	Mg.ATP	3-PG
$K_a$ ( $M^{-1}$ )	8372 (327)	7845 (225)	118000 (1700)
$\Delta H^\circ$ ( $kJmol^{-1}$ )	-33.2 (3.5)	-34.7 (0.5)	-25.8 (2.6)
$\Delta G^\circ$ ( $kJmol^{-1}$ )	-22.4 (3.5)	-22.2 (0.2)	-28.9 (2.6)
$\Delta S^\circ$ ( $Jmol^{-1}K^{-1}$ )	-36 (11)	-41 (1)	+10 (3)
$\Delta H^\circ_{add}$ ( $kJmol^{-1}$ )	-28 (3)	-31 (2)	-18.9 (3)

The experiments with R168K PGK indicated that alterations in substrate binding had occurred. ADP binding appears to be least affected by the mutation and could be analysed using the one set of sites model to give good agreement between the experimental data and the theoretical fitting curve. This model does not appear to be satisfactory for the titrations with ATP and 3-phosphoglycerate, however, the values obtained from the analyses are given below. The raw data for substrate binding to R168K are shown in figures 4.19 to 4.21.

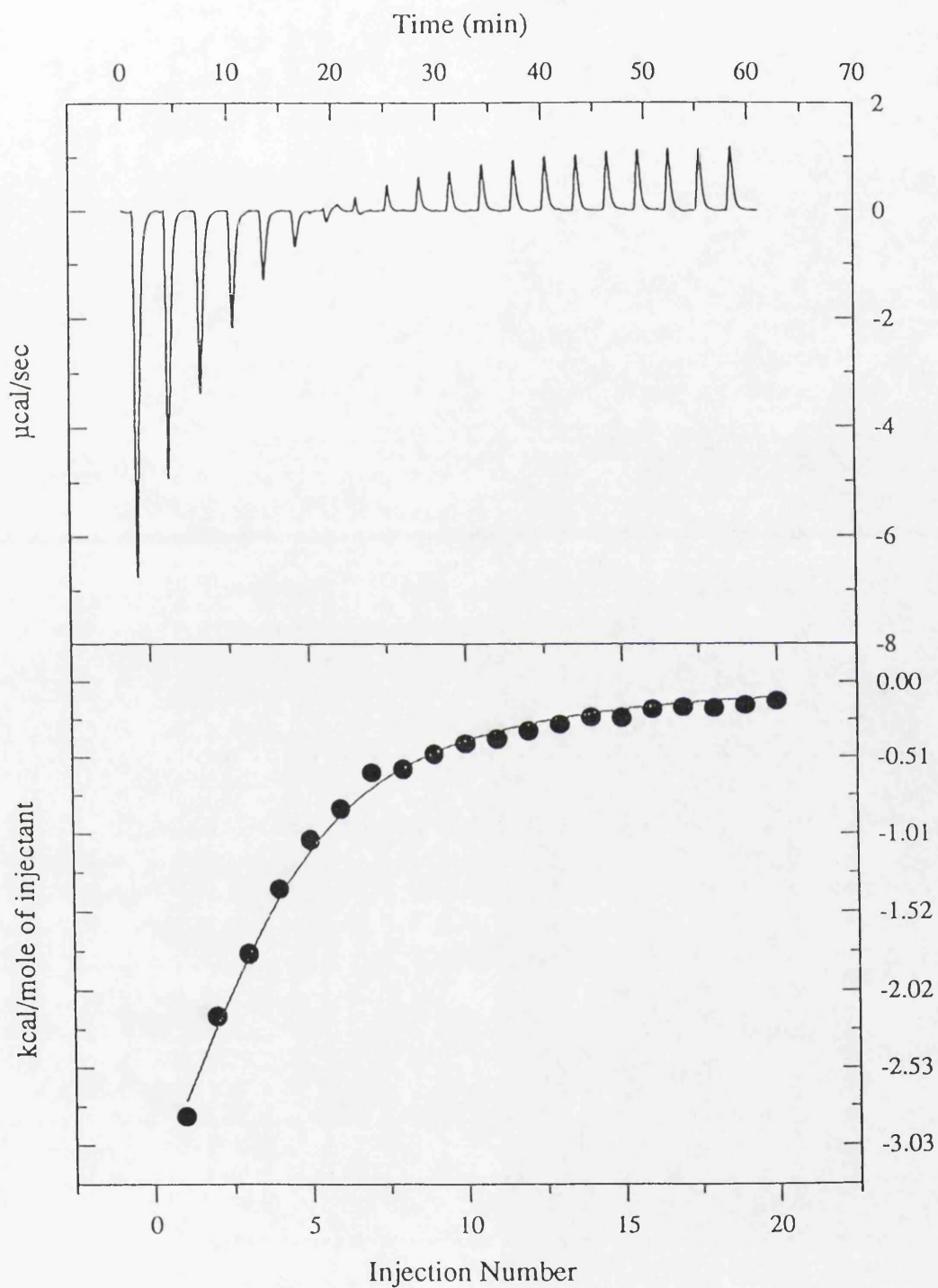
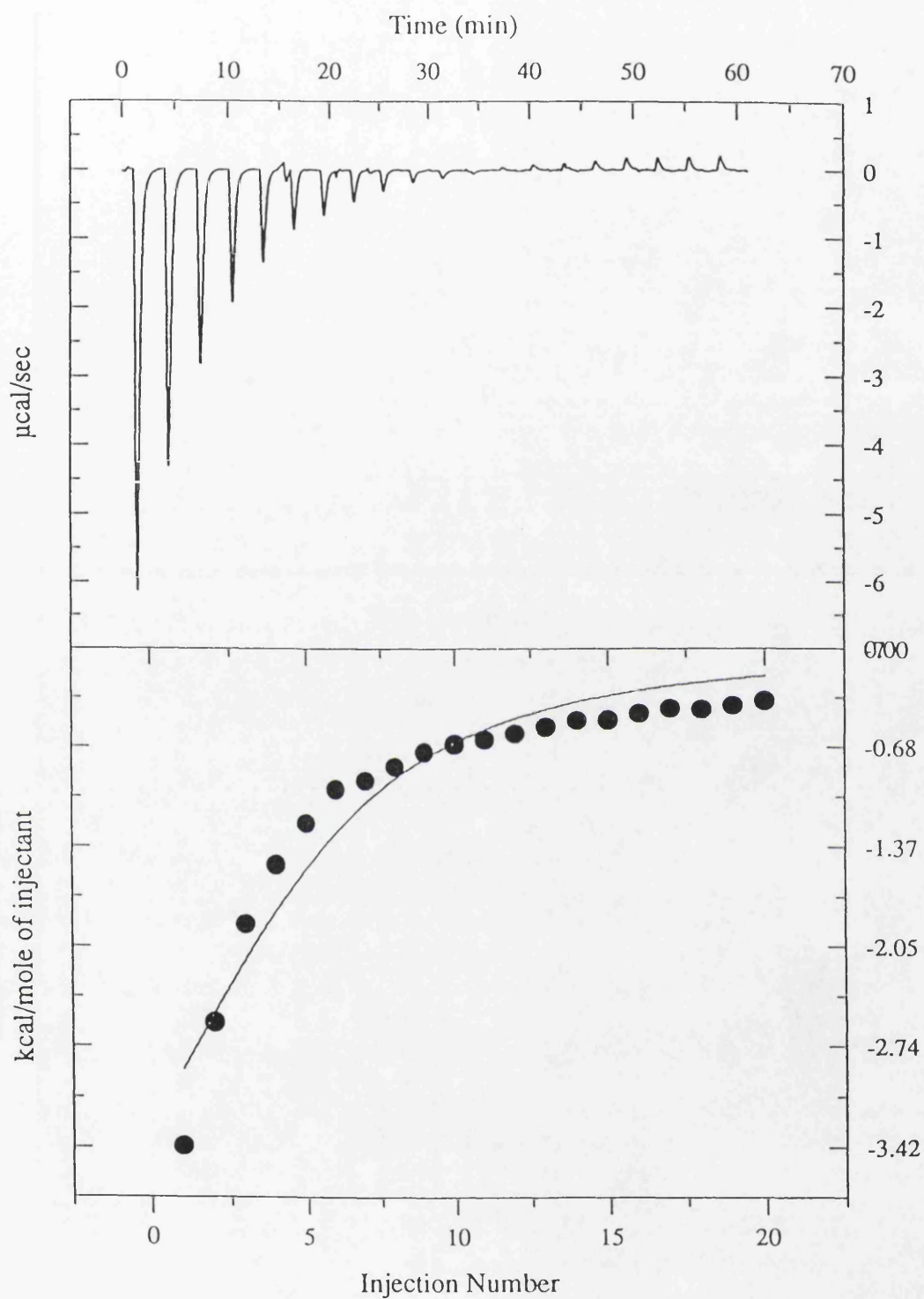
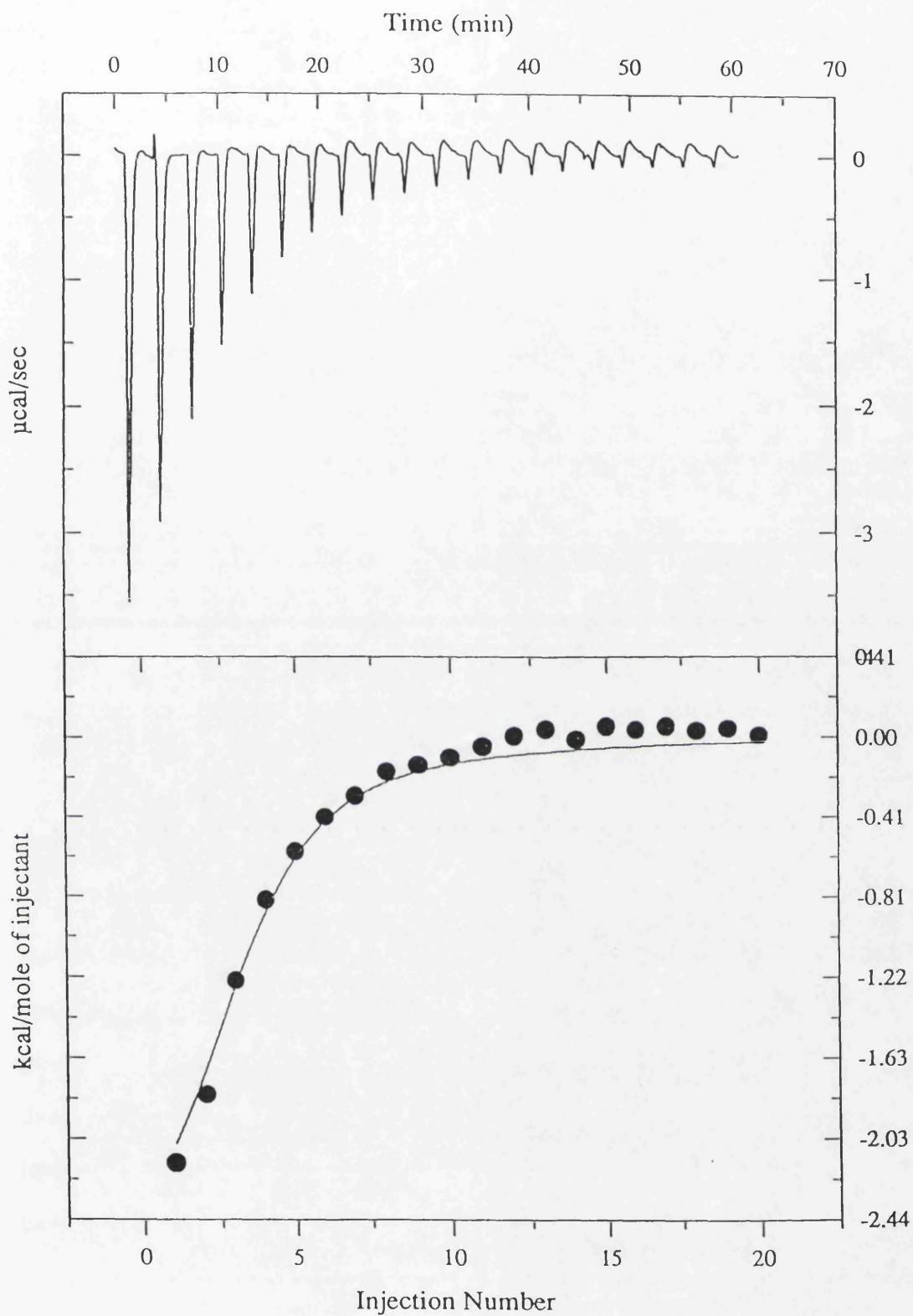


Figure 4.19 R168K PGK and ADP. 50 mM MES pH 6.0, 4 mM Mg acetate, 0.1 mM DTT and 0.05% w/v sodium azide.



**Figure 4.20** *R168K PGK and ATP. 50 mM MES pH 6.0, 4 mM Mg acetate, 0.1 mM DTT and 0.05% w/v sodium azide.*



*Figure 4.21 R168K PGK and 3-phosphoglycerate. 50 mM MES pH 6.0, 4 mM Mg acetate, 0.1 mM DTT and 0.05% w/v sodium azide.*

**Table 4.8** Thermodynamic parameters for binding of Mg.ADP, Mg.ATP and 3-phosphoglycerate to R168K in MES pH 6.0, 4mM magnesium acetate, 0.1mM DTT, 0.05% w/v sodium azide

Parameters	Mg.ADP	Mg.ATP	3-PG
$K_a$ ( $M^{-1}$ )	5300	5000	28000
$\Delta H^{\circ}$ ( $kJmol^{-1}$ )	-23.6	-33.1	-13.8
$\Delta G^{\circ}$ ( $kJmol^{-1}$ )	-21.2	-21.1	-25.4
$\Delta S^{\circ}$ ( $Jmol^{-1}K^{-1}$ )	-8.3	-40.3	+38.9
$\Delta H^{\circ}_{add}$ ( $kJmol^{-1}$ )	-20.6	-20.2	-4.7

#### 4.3.5 Buffer effects on the binding of 3-phosphoglycerate to wild-type PGK

There is evidence in the literature that the binding of 3-phosphoglycerate to PGK results in a change in  $pK_a$  of the substrate carboxylate group (Wilson *et al.*, 1988). This effect was studied here by performing experiments of 3-phosphoglycerate binding to PGK in buffers with different heats of ionization and/or pH. Table 4.9 contains the results from these experiments and the raw data obtained in tricine, PIPES, and piperazine buffers are given in figures 4.22 to 4.24. The binding curves obtained were different for each buffer: binding of 3-phosphoglycerate to PGK in tricine gave rise to a low exothermic  $\Delta H^{\circ}$  value, whereas at lower pH values, the binding was more exothermic.

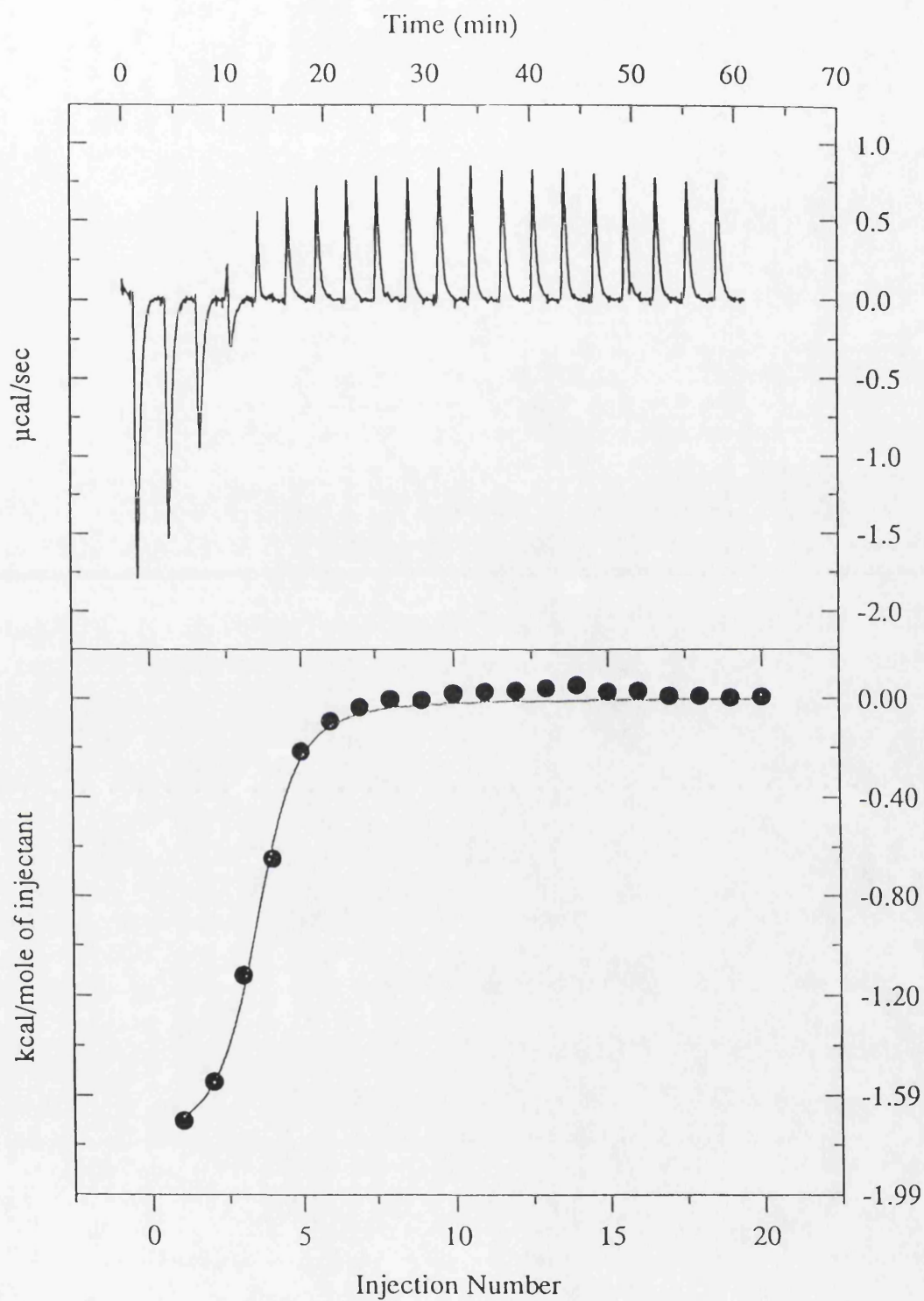


*Figure 4.22 Wild-type PGK and 3-phosphoglycerate. 50 mM tricine pH 8.0, 0.1 mM DTT and 0.05% w/v sodium azide.*

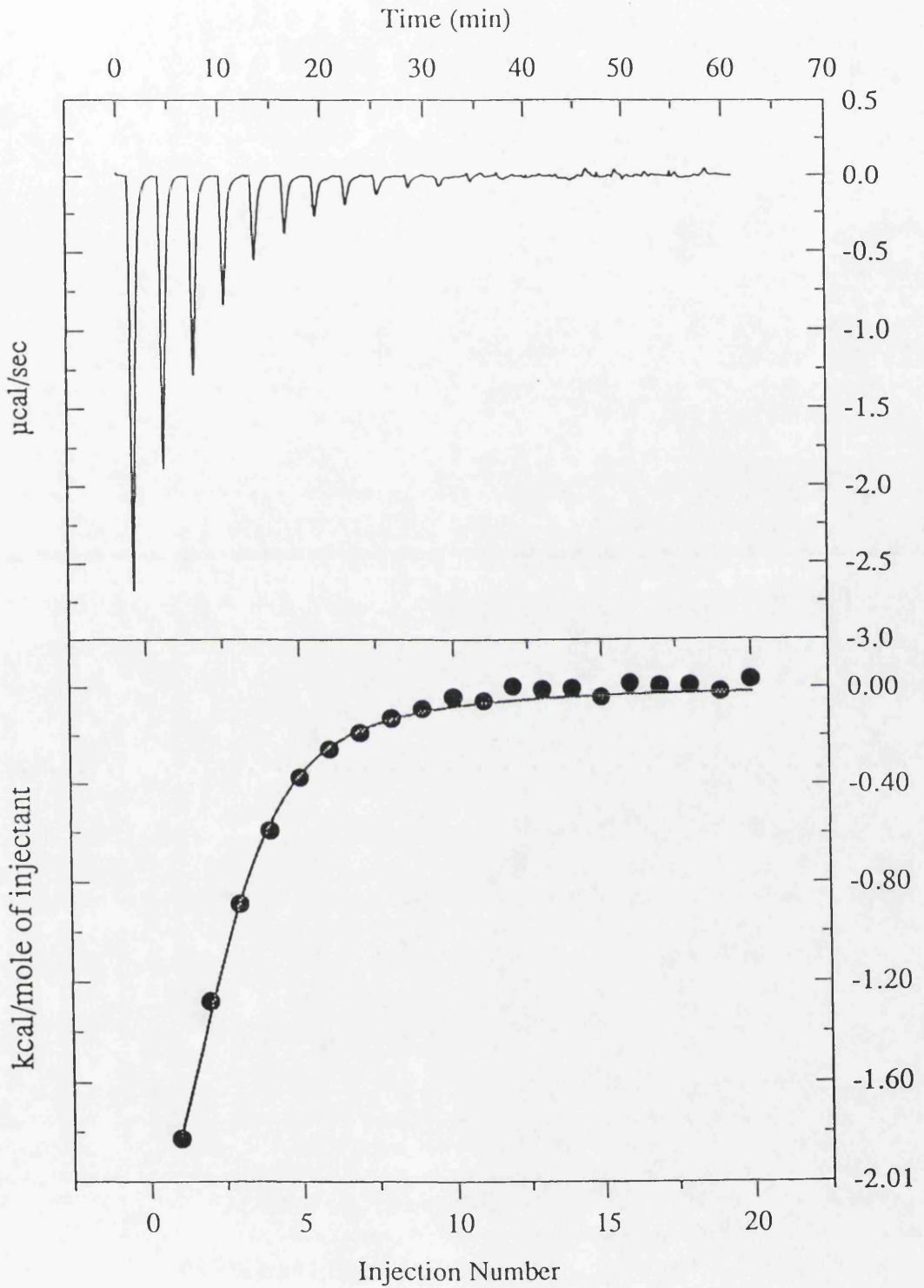
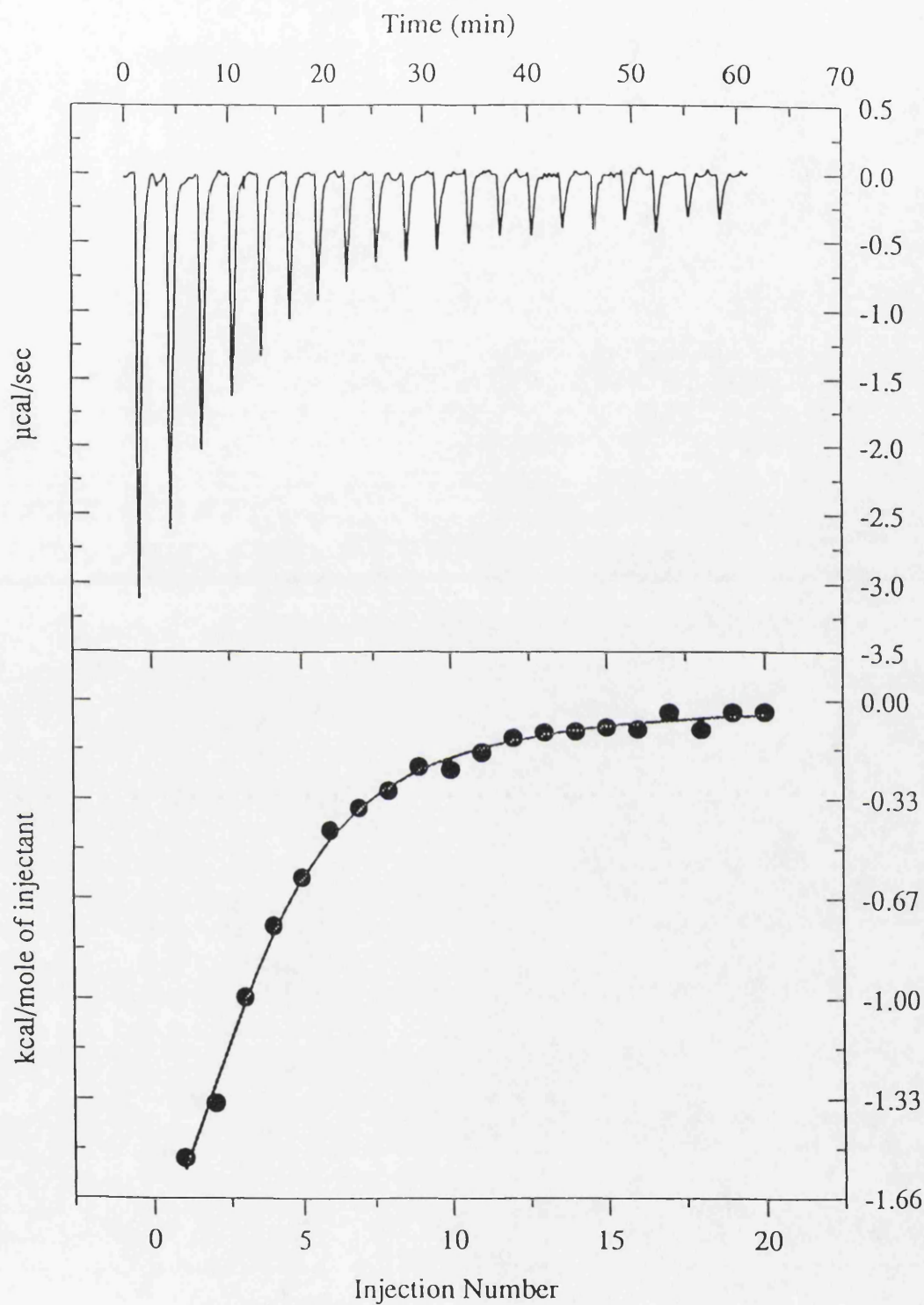


Figure 4.23 Wild-type PGK and 3-phosphoglycerate. 50 mM PIPES pH 7.0, 0.1 mM DTT and 0.05% w/v sodium azide.



**Figure 4.24** Wild-type PGK and 3-phosphoglycerate. 50 mM piperazine pH 6.0, 0.1 mM DTT and 0.05% w/v sodium azide.

**Table 4.9** 3-phosphoglycerate binding parameters in 50 mM buffer, 0.1 mM DTT, 0.05% w/v sodium azide

Buffer	pH	$\Delta H^{\circ}_I$ (kJmol <sup>-1</sup> )	$\Delta H^{\circ}_{obs}$ (kJmol <sup>-1</sup> )	$\Delta H^{\circ}_{add}$ (kJmol <sup>-1</sup> )	$K_a$ (M <sup>-1</sup> )
Tricine	8	31.2	-8.4	-9.6	2.1 x 10 <sup>5</sup>
Tris/MOPS	7	23.5	-15.5	-14.7	1.8 x 10 <sup>5</sup>
PIPES	7	11.3	-10.9	-10.2	4.1 x 10 <sup>4</sup>
MES	6	14.6	-19.1	-20.9	1.1 x 10 <sup>5</sup>
Piperazine	6	29.3	-12.1	-12.3	1.7 x 10 <sup>4</sup>

#### 4.3.6 Effect of anions on binding of 3-phosphoglycerate

The binding parameters given in table 4.10 refer to the binding of 3-phosphoglycerate in the presence of the anions noted. It has already been shown that sulphate and tripolyphosphate bind to PGK (section 4.3.3) and these experiments aim to study the effect that this binding has on 3-phosphoglycerate binding parameters. Chloride and acetate ions were present as the magnesium salt at a concentration of 60mM in 50 mM tris/MOPS, pH 7.0, 0.1 mM DTT and 0.05% w/v sodium azide. Tripolyphosphate was present at a concentration of 0.7 mM in 50 mM MES, pH 6.0, 4 mM magnesium acetate, 0.1 mM DTT and 0.05% w/v sodium azide. The raw data and binding isotherm for 3-phosphoglycerate binding in buffer containing 60 mM magnesium acetate are given in figure 4.25. 3-phosphoglycerate did not appear to bind to PGK in the presence of either a high concentration of magnesium chloride or at a relatively low concentration of tripolyphosphate. Although binding was observed in buffer containing 60 mM magnesium acetate, the binding was much weaker than usual.

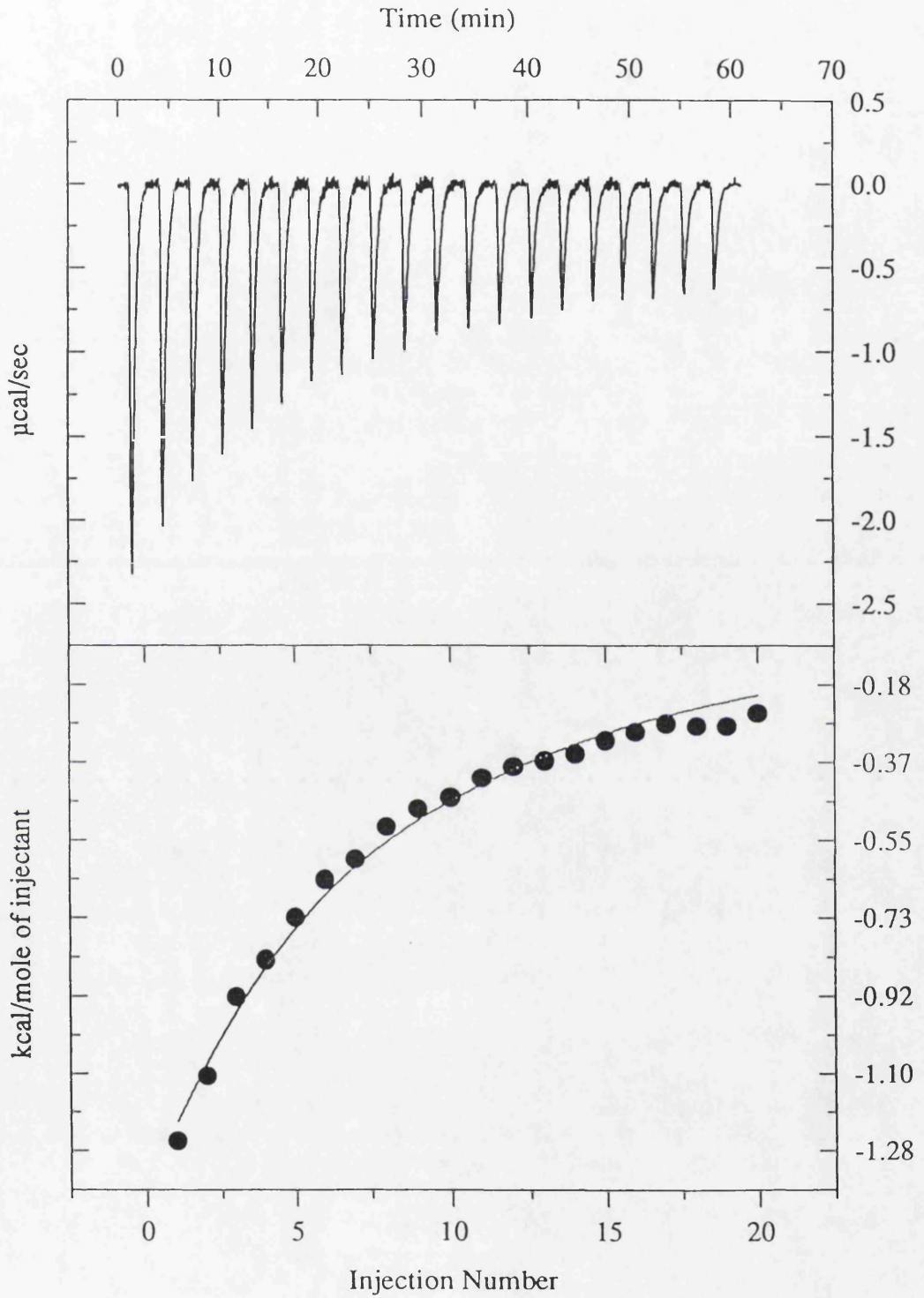


*Figure 4.25 Wild-type PGK and 3-phosphoglycerate. 50 mM tris/MOPS pH 7.0, 60 mM Mg acetate, 0.1 mM DTT and 0.05% w/v sodium azide.*

**Table 4.10** 3-phosphoglycerate binding parameters in presence of anions

Parameters	60 mM MgCl <sub>2</sub>	60 mM Mg acetate	0.7 mM tripolyphosphate
K <sub>a</sub> (M <sup>-1</sup> )		3112	
ΔH <sup>o</sup> (kJmol <sup>-1</sup> )	no binding	-22.0	no binding
ΔG <sup>o</sup> (kJmol <sup>-1</sup> )		-19.9	
ΔS <sup>o</sup> (Jmol <sup>-1</sup> K <sup>-1</sup> )		-7.0	

#### 4.3.7 Sulphate effects on ligand binding

Sulphate is another anion which is known to bind to PGK and which has a dual activating/inhibiting effect on the enzyme activity (Scopes, 1978a). The mechanism of this action is not clear, but it would be interesting to know how the presence of sulphate affects the binding parameters for the natural substrates of PGK. Therefore, the binding of Mg.ADP, Mg.ATP and 3-phosphoglycerate to PGK in the presence of a low concentration of sulphate was studied (table 4.11). The effect of sulphate on substrate binding is illustrated in figures 4.26 to 4.28. The binding of ATP is strongly affected by ammonium sulphate, the binding affinity is decreased significantly. A significant decrease in binding affinity is also observed with 3-phosphoglycerate binding.

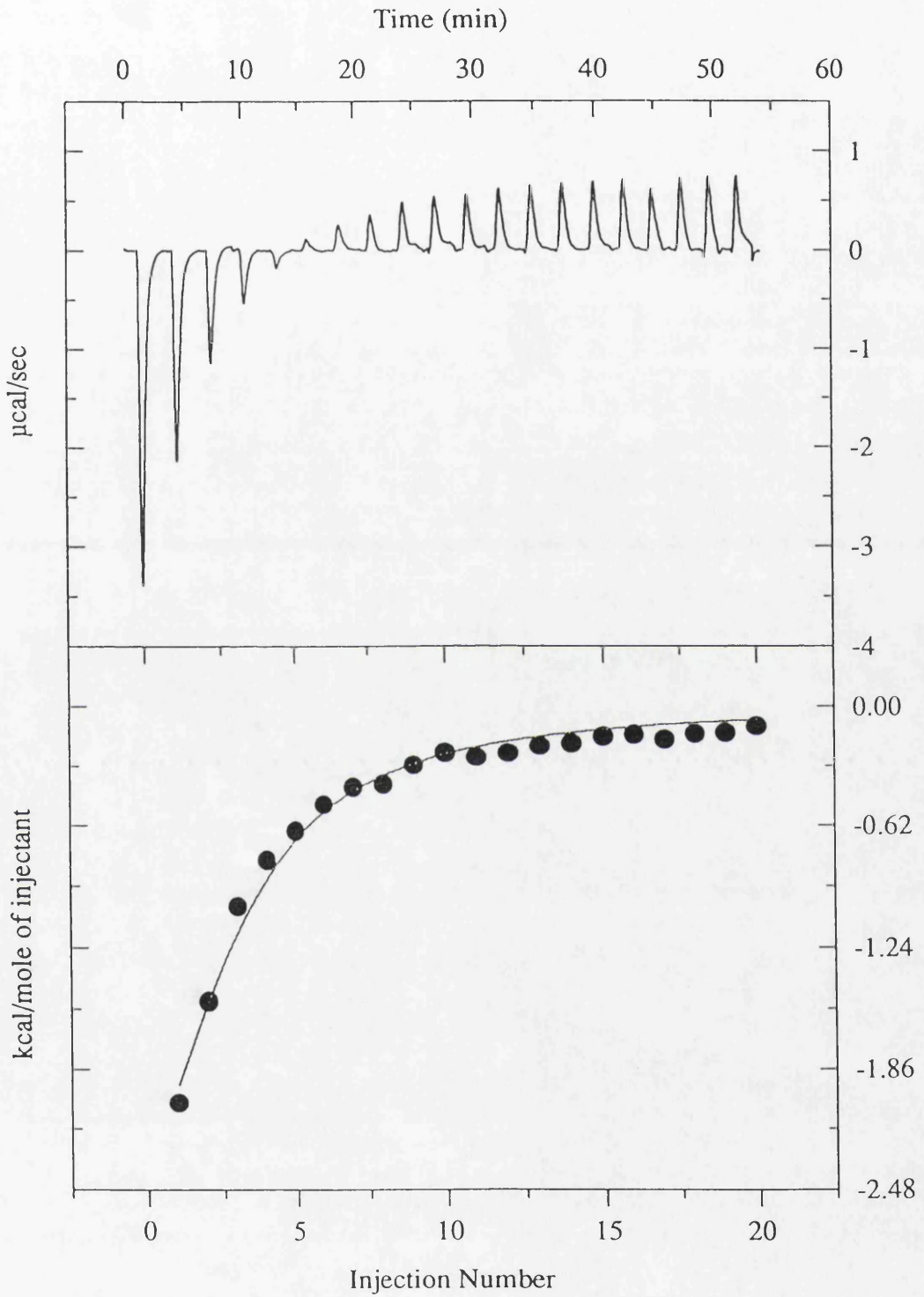


**Figure 4.26** Wild-type PGK and ADP. 50 mM MES pH 6.0, 4 mM Mg acetate, 1.1 mM ammonium sulphate, 0.1 mM DTT and 0.05% w/v sodium azide.

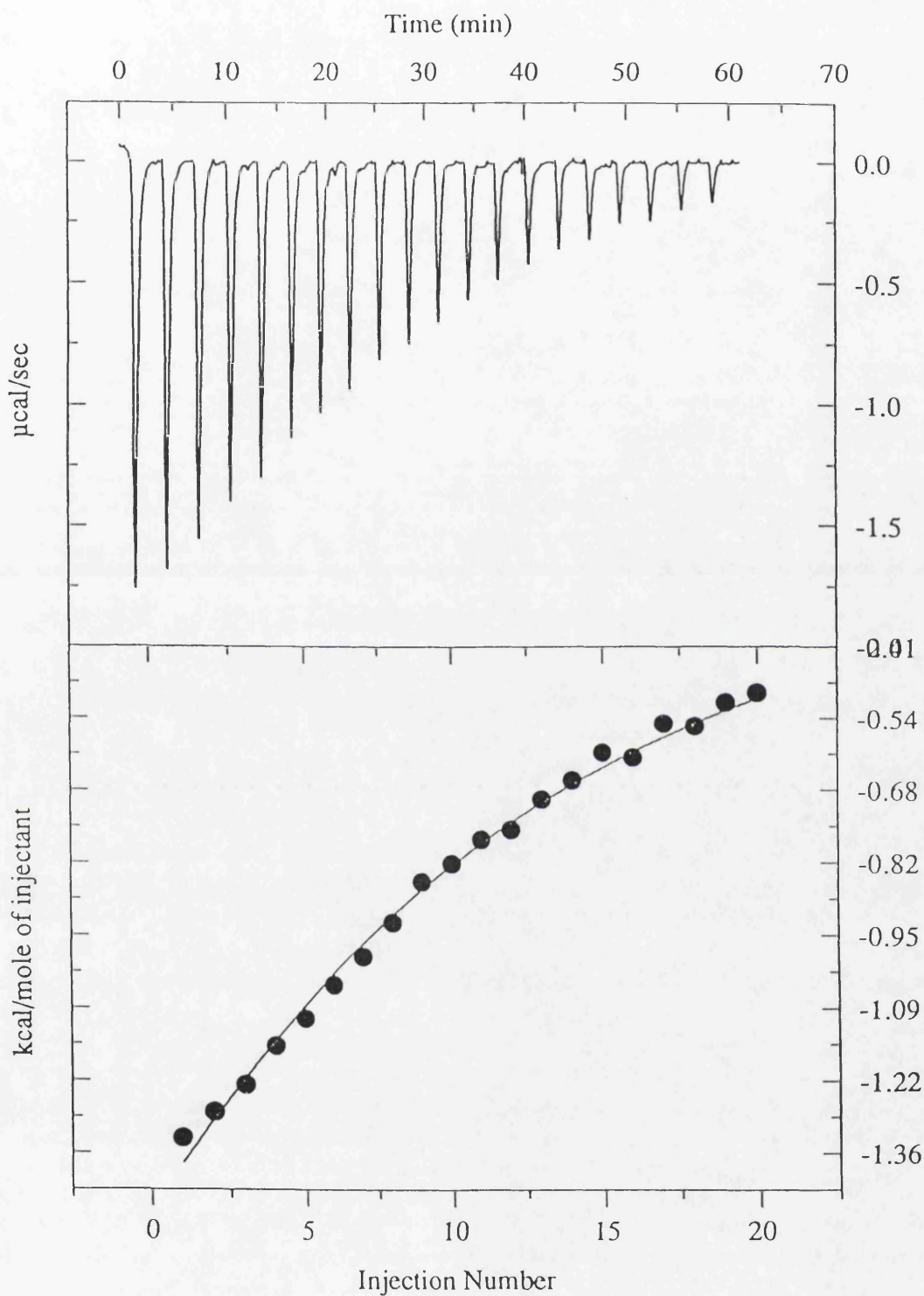


**Figure 4.27** Wild-type PGK and ATP. 50 mM MES pH 6.0, 4 mM Mg acetate, 1.6 mM ammonium sulphate, 0.1 mM DTT and 0.05% w/v sodium azide.

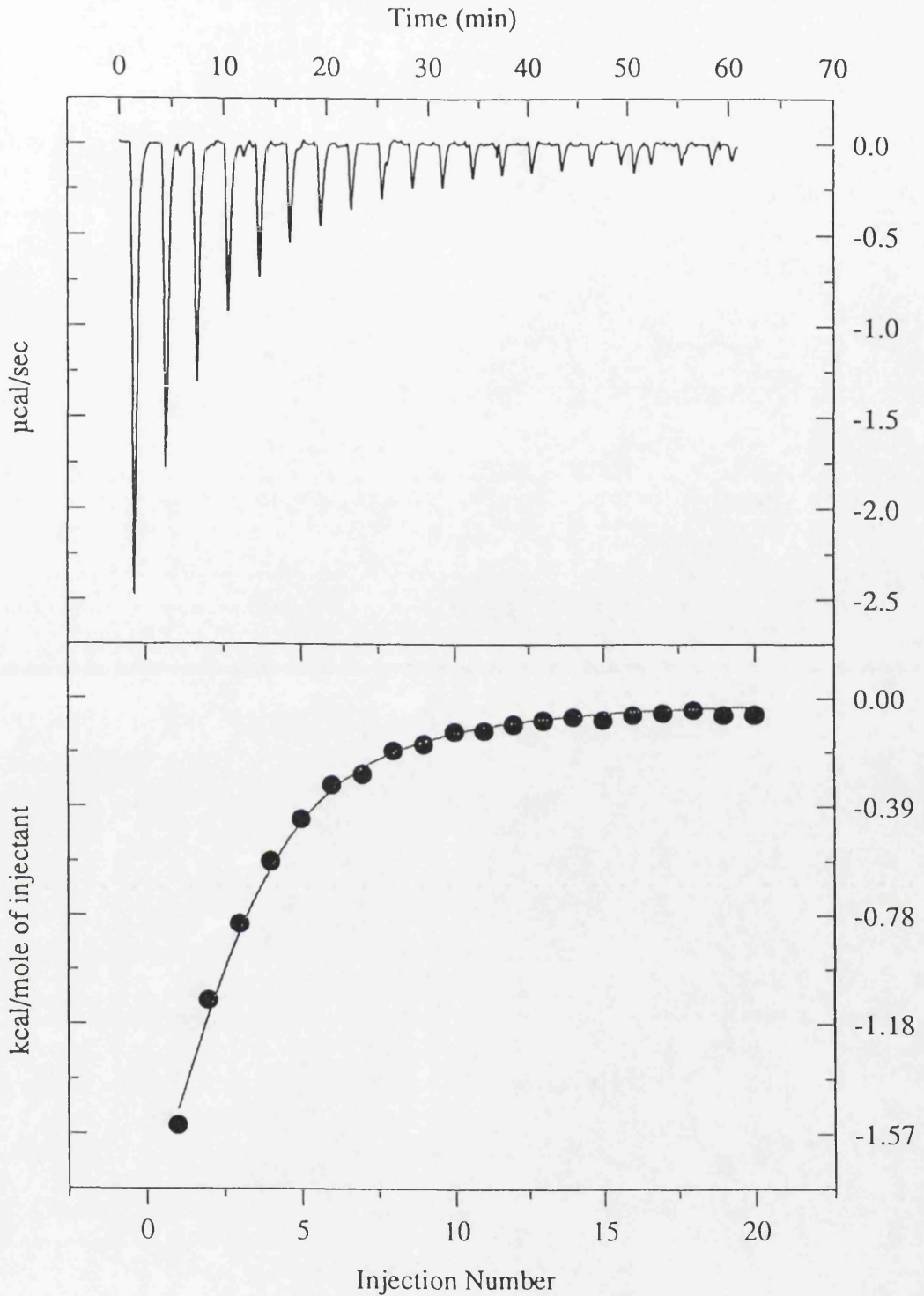


*Figure 4.28 Wild-type PGK and 3-phosphoglycerate. 50 mM MES pH 6.0, 4 mM Mg acetate, 1.1 mM ammonium sulphate, 0.1 mM DTT and 0.05% w/v sodium azide.*

**Table 4.11** Binding parameters for Mg.ADP Mg.ATP and 3-phosphoglycerate in presence of 1.1-1.6 mM ammonium sulphate

Parameters	Mg.ADP	Mg.ATP	3-PG
$K_a$ ( $M^{-1}$ )	5292	653	24760
$\Delta H^\circ$ ( $kJmol^{-1}$ )	-22.6	-68.0	-9.8
$\Delta G^\circ$ ( $kJmol^{-1}$ )	-21.1	-16.1	-25.1
$\Delta S^\circ$ ( $Jmol^{-1}K^{-1}$ )	-5	-174	+51
$\Delta H^\circ_{add}$ ( $kJmol^{-1}$ )	-19.3	not saturated	-9.1

#### 4.3.8 Studies of nucleotide binding to wild-type PGK

It is most likely that ADP and ATP bind to the same site on PGK, but to confirm that this does occur, a sample of PGK was titrated with ADP followed by titration with ATP. Similarly, a second PGK sample was titrated first with ATP and then with ADP. No binding effects were apparent in the second titrations.

The mode of binding of nucleotides to PGK is dependent on magnesium ions (e.g. Fairbrother *et al.*, 1990b, Graham & Williams, 1991b). Therefore experiments involving the binding of ATP and ADP to PGK were conducted at several magnesium concentrations. Table 4.12 contains nucleotide binding parameters which were measured at various magnesium ion concentrations in tris/MOPS and MES buffers. Some of the experimental data contained in this table are illustrated in figures 4.29 to 4.32. In the absence of magnesium, the binding affinities for ADP and ATP are increased although the enthalpy values remain roughly constant.

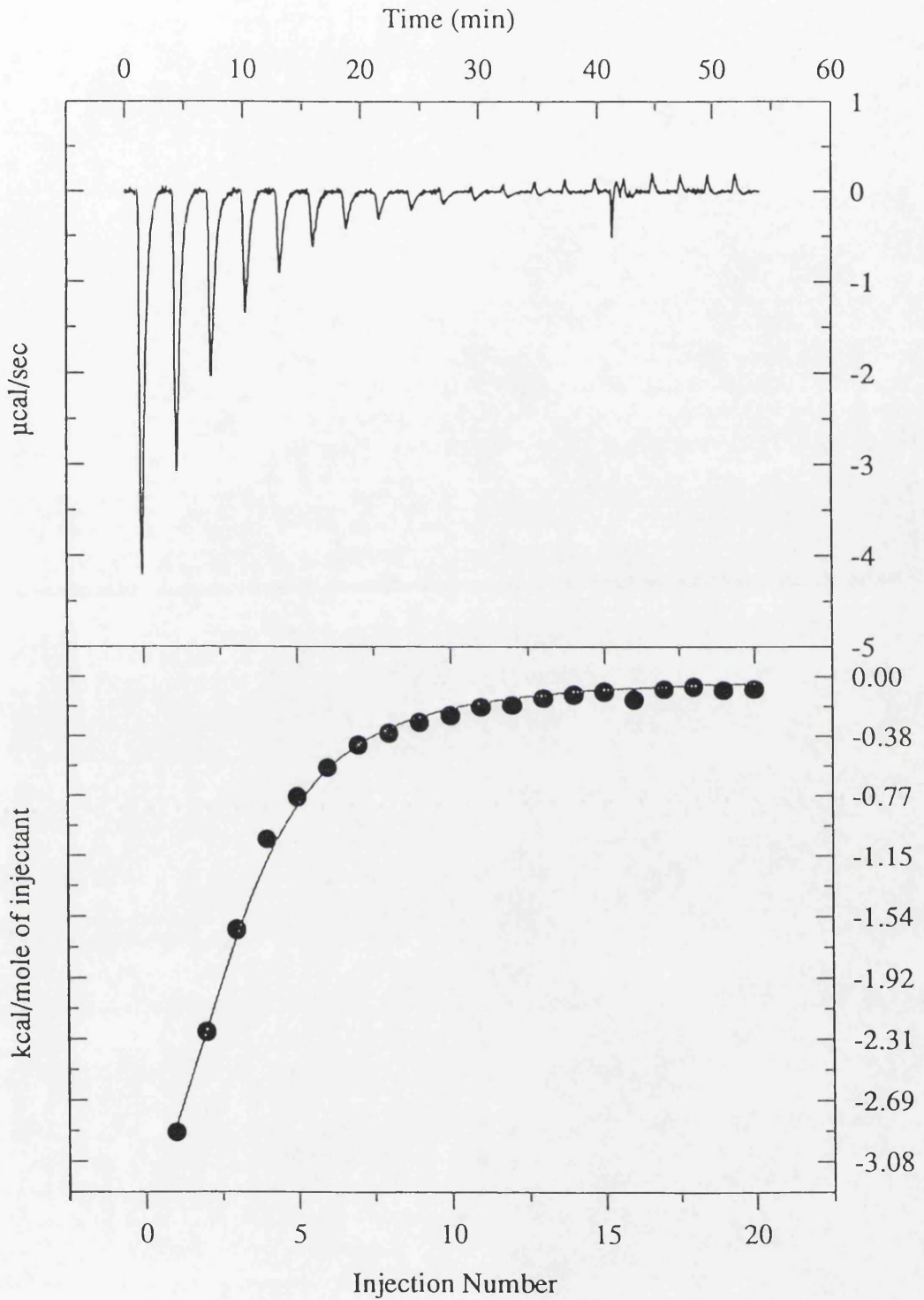


**Figure 4.29** Wild-type PGK and ADP. 50 mM tris/MOPS pH 7.0, 60mM Mg acetate, 0.1 mM DTT and 0.05% w/v sodium azide.

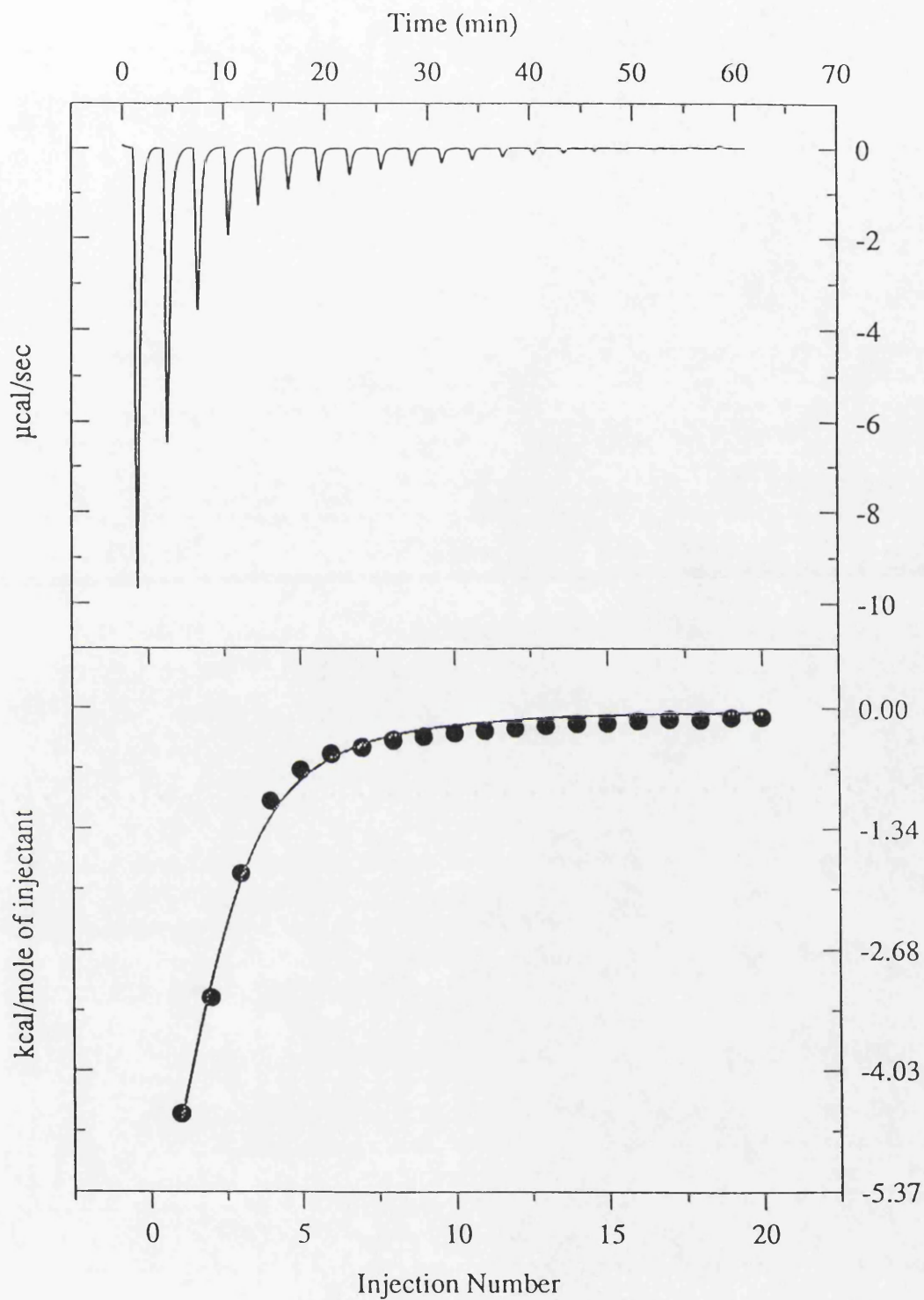
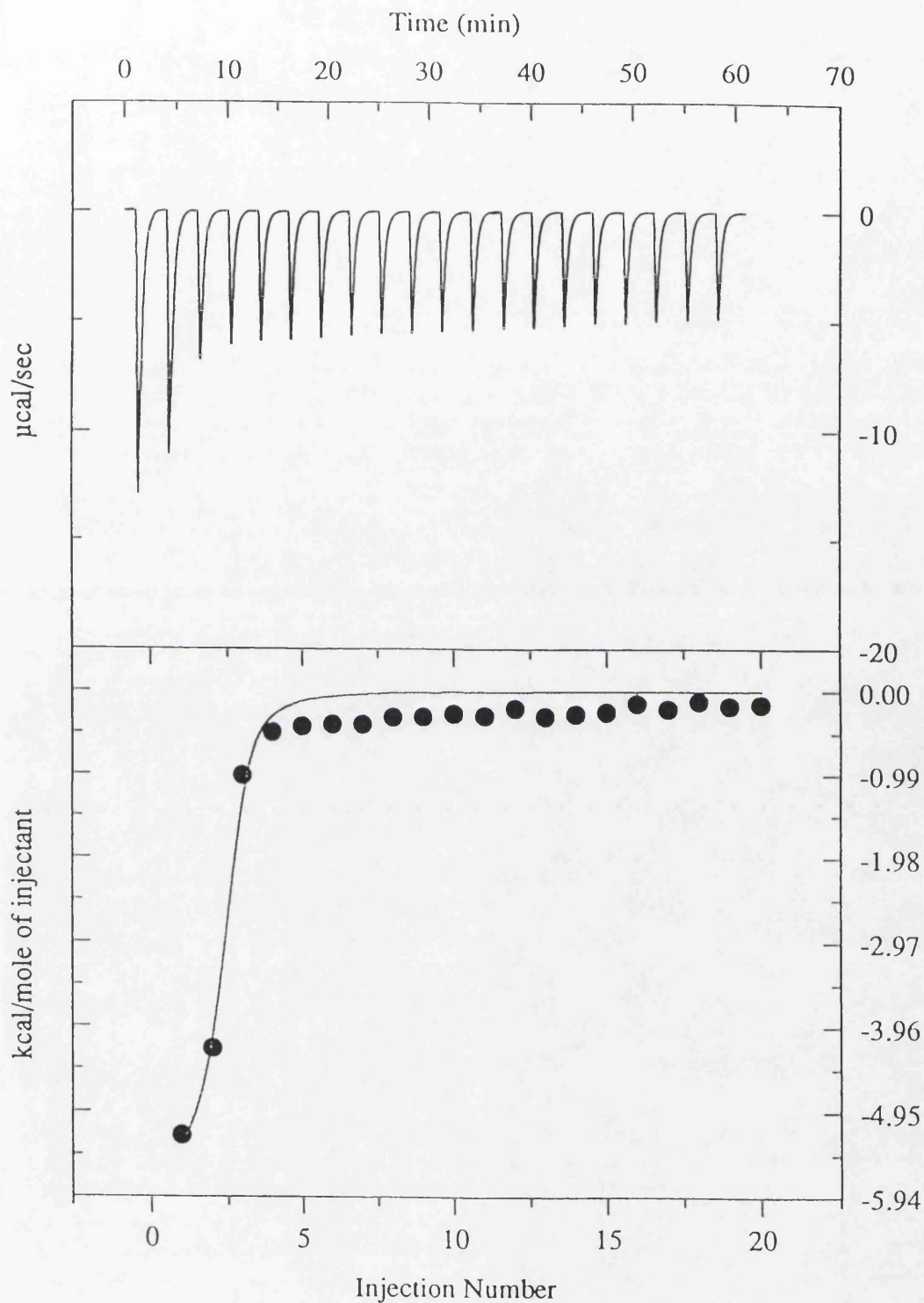


Figure 4.30 Wild-type PGK and ADP. 50 mM MES pH 6.0, 0.1 mM DTT and 0.05% w/v sodium azide.



**Figure 4.31** Wild-type PGK and ATP. 50 mM tris/MOPS pH 7.0, 0.1 mM DTT and 0.05% w/v sodium azide.

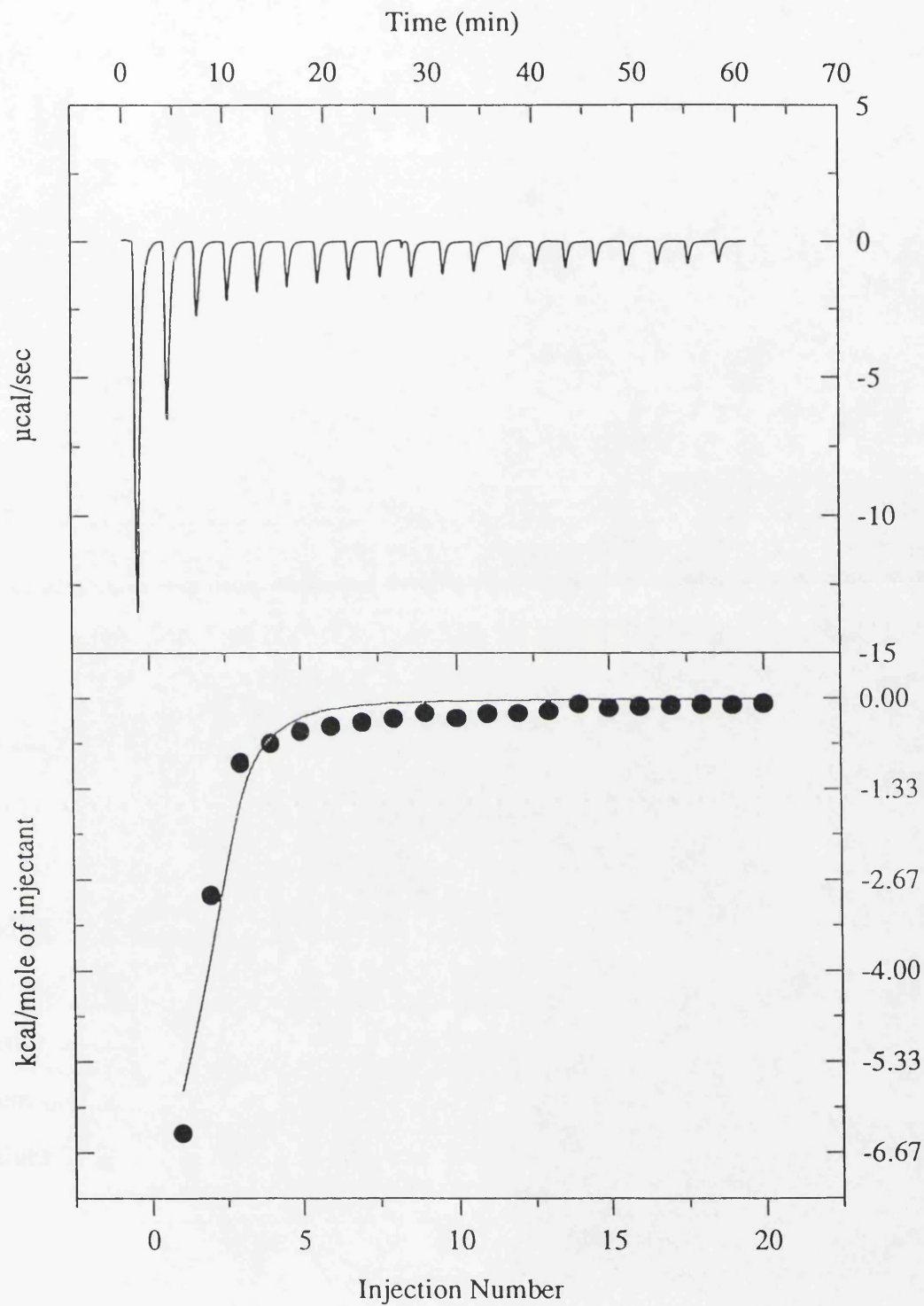
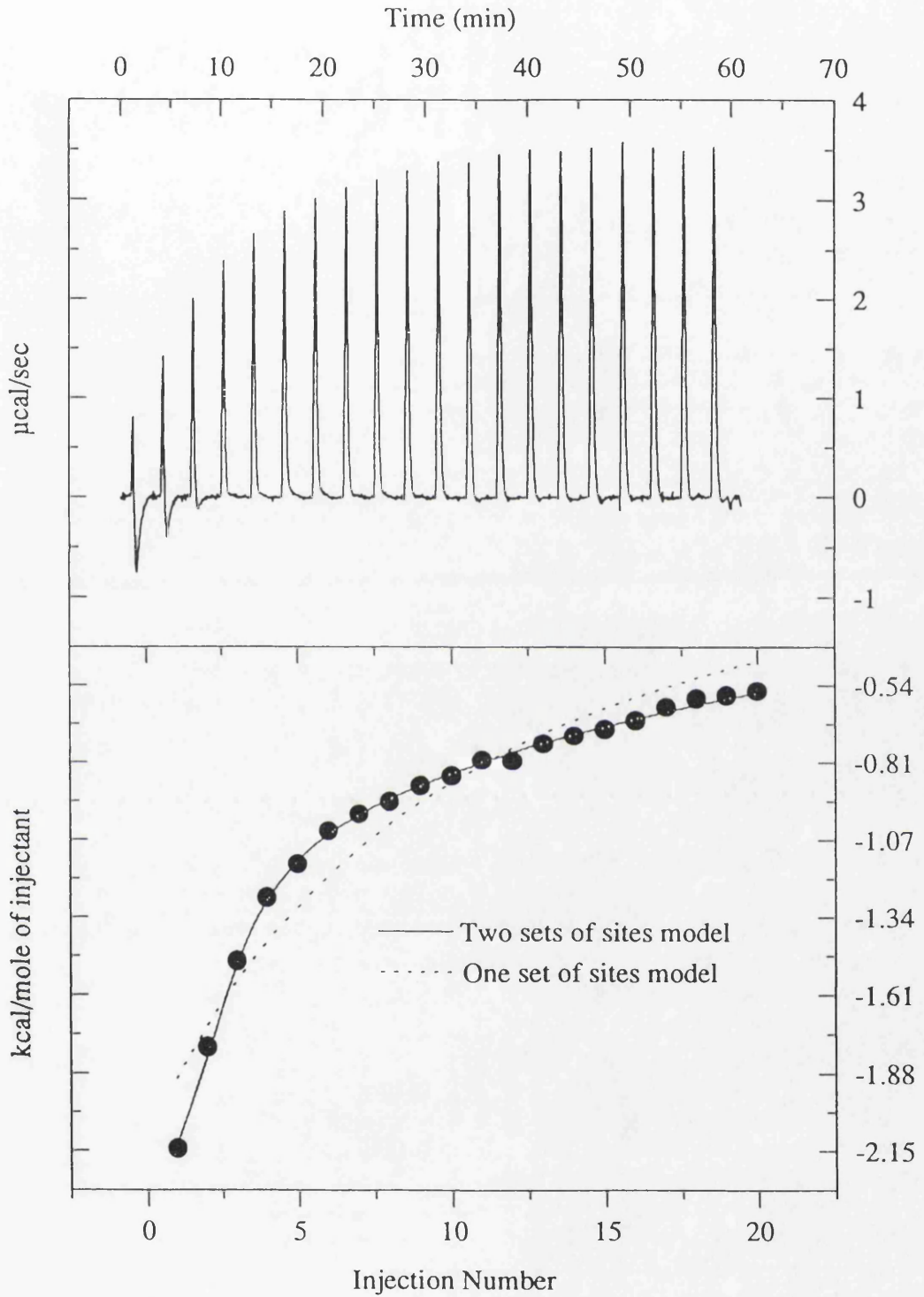


Figure 4.32 Wild-type PGK and ATP. 50 mM MES pH 6.0, 0.1 mM DTT, 0.05% w/v sodium azide

**Table 4.12** Effects of magnesium concentrations on binding parameters for nucleotide substrates

	Buffer	pH	[Mg <sup>2+</sup> ] (mM)	K <sub>a</sub> (M <sup>-1</sup> )	ΔH <sup>0</sup> (kJmol <sup>-1</sup> )	ΔG <sup>0</sup> (kJmol <sup>-1</sup> )	ΔS <sup>0</sup> (kJmol <sup>-1</sup> )
ADP	Tris/MOPS	7	60	21090	-19.1	-24.7	+19
	Tris/MOPS	7	4	3550	-57.5	-20.2	-125
	MES	6	4	5940	-34.8	-21.5	-45
	MES	6	0	17400	-36.2	-24.2	-40
ATP	Tris/MOPS	7	60	no binding			
	Tris/MOPS	7	4	6855	-34.3	-21.9	-44
	Tris/MOPS	7	0	420000	-23.8	-32.1	+28
	MES	6	4	6610	-34.8	-21.8	-44
	MES	6	0	94000	-28.7	-28.4	-1.0

Although ATP and ADP appear to bind to only one site on PGK in tris/MOPS and MES buffers, experiments conducted in other buffers indicate that the substrates are actually binding at two sites. The data obtained in PIPES buffer can be analysed more easily using the two sets of sites model as shown in figures 4.33 and 4.34. The results from these titrations in PIPES buffer are given in table 4.13. During this analysis the N values were fixed at 1.



**Figure 4.33** Wild-type PGK and ADP. 50 mM PIPES pH 7.0, 4mM Mg acetate, 0.1 mM DTT and 0.05% w/v sodium azide

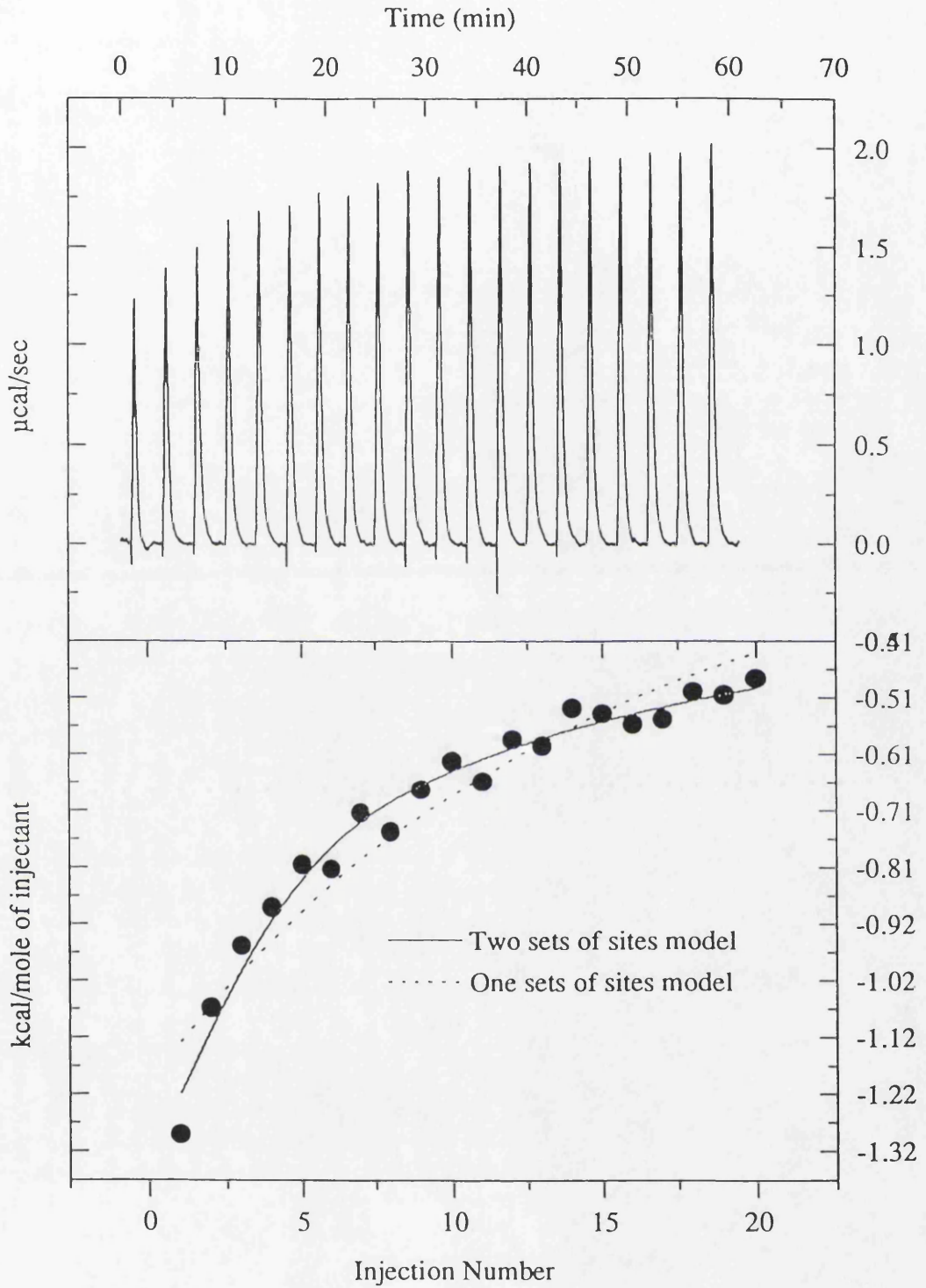


**Figure 4.34** Wild-type PGK and ATP. 50 mM PIPES pH 7.0, 0.1 mM DTT and 0.05% w/v sodium azide.

**Table 4.13** Results of a two sets of sites analysis of the binding of ATP and ADP to wild-type PGK in 50 mM PIPES, 4 mM magnesium acetate, 0.1 mM DTT and 0.05% azide at pH 7.0.

		ADP	ATP
1st binding site	$K_1$ ( $M^{-1}$ )	26300 (11150)	13600 (9000)
	$\Delta H^{\circ}_1$ ( $kJmol^{-1}$ )	-9.9 (1.1)	-7.1 (2.9)
2nd binding site	$K_2$ ( $M^{-1}$ )	818 (580)	375 (177)
	$\Delta H^{\circ}_2$ ( $kJmol^{-1}$ )	-84.9 (33)	-77.4 (8.9)

The binding sites for the nucleotide and triose substrates are located on different domains. However, it is still possible that the sites may be cooperative i.e. the binding of one substrate could alter the binding affinity for the second substrate. It is also possible that domain closure is triggered by the formation of the ternary substrate/enzyme complex. Therefore the ternary PGK/ADP/3-PG complex was studied by titrating a PGK sample with one substrate and then titrating the binary PGK/substrate complex with the second substrate. The PGK sample was left in the reaction cell following the first titration, the injection syringe was removed, rinsed and filled with new substrate and then a second titration was initiated. The ternary complex could also be formed by titrating a PGK sample with a mixture of ADP and 3-

phosphoglycerate. The results are given in tables 4.14 and 4.15, where the first, second, third and fourth columns in the table refer to titrations of PGK with ADP, PGK.ADP with 3-phosphoglycerate, PGK with 3-phosphoglycerate and PGK.3-PG with ADP, respectively.

When 3-phosphoglycerate binds to the binary PGK/ADP complex the association is endothermic, in contrast to the exothermic binding of 3-phosphoglycerate to PGK alone. The binding affinity is also decreased. There are also differences between the binding of ADP to PGK.3-PG and to PGK alone: the binding affinity is increased in the former association and the enthalpy change is less exothermic. These effects are observed in both MES and tris/MOPS buffers.

The titration of PGK with an ADP/3-phosphoglycerate mixture gave rise to a measured enthalpy change ( $\Delta H_{\text{add}}$ ) of  $-36 \text{ kJmol}^{-1}$ . The raw data and calorimetric isotherms for these experiments in MES buffer are given in figures 4.35 to 4.36 and the results in tris/MOPS buffer are presented in figures 4.37 to 4.38.

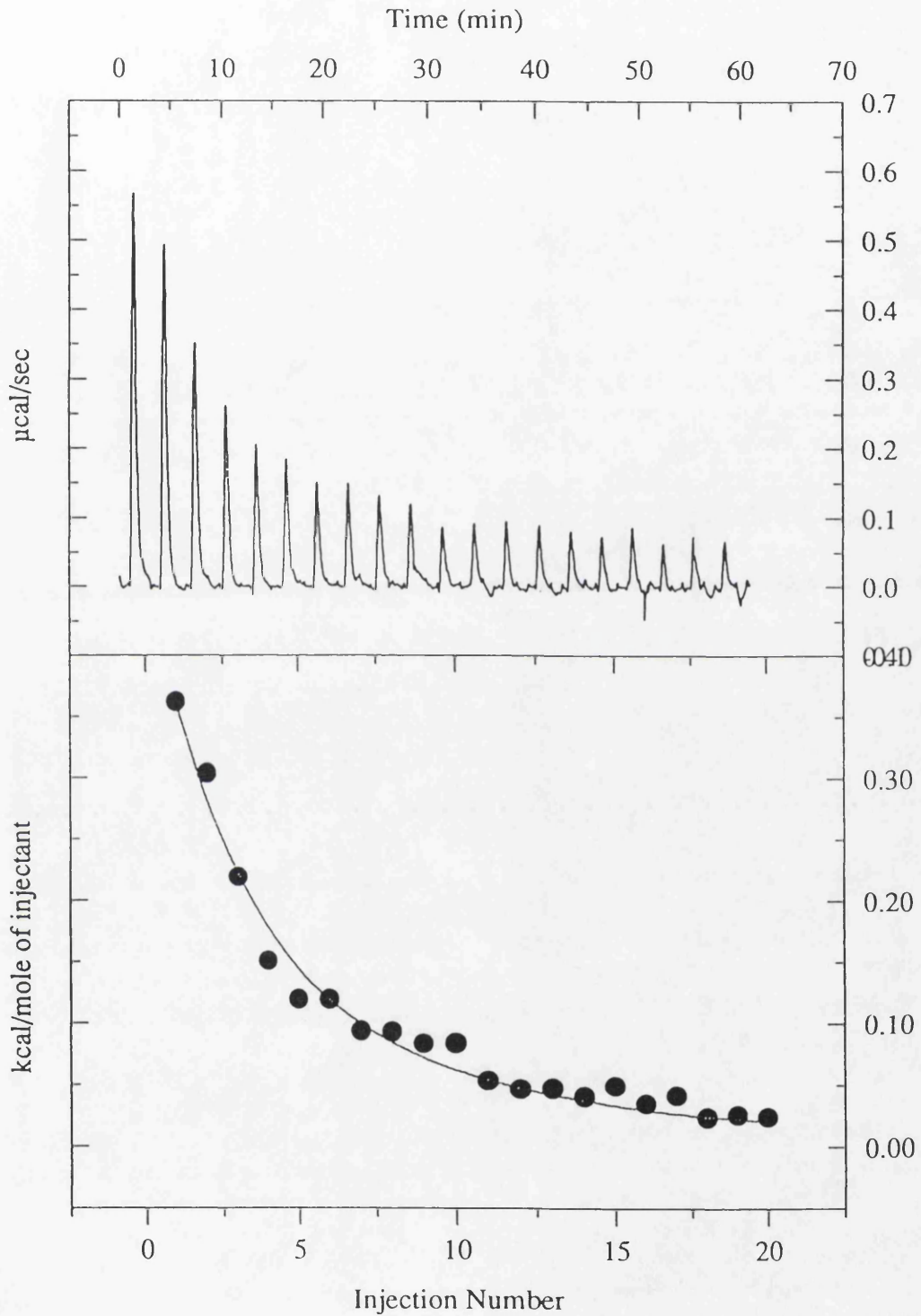


**Figure 4.35** Binary wild-type PGK.ADP complex and 3-phosphoglycerate. 50 mM MES pH 6.0, 4 mM Mg acetate, 0.1 mM DTT and 0.05% w/v sodium azide

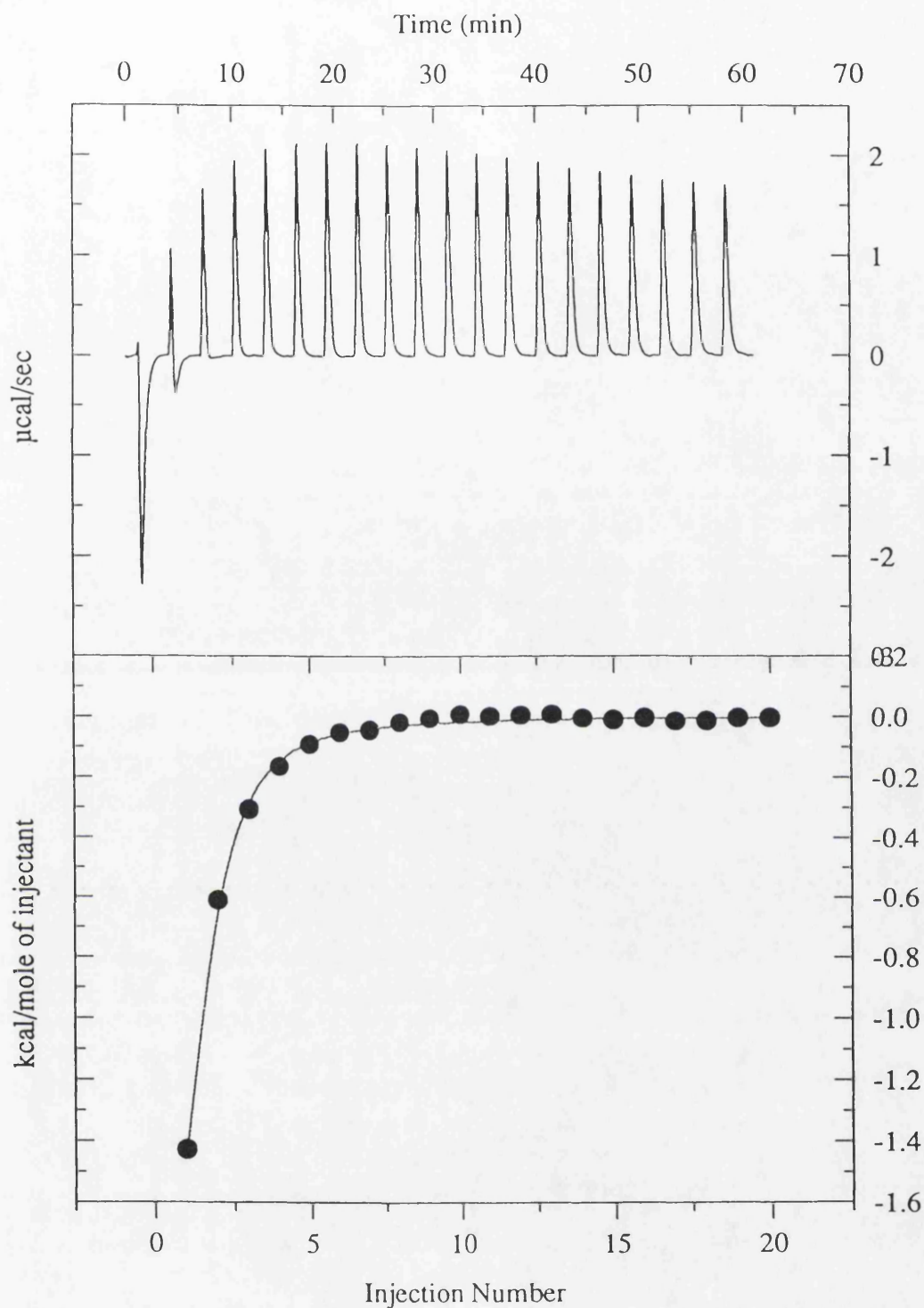


**Figure 4.36** Binary wild-type PGK.3-PG complex and ADP. 50 mM MES pH 6.0, 4 mM Mg acetate, 0.1 mM DTT and 0.05% w/v sodium azide.

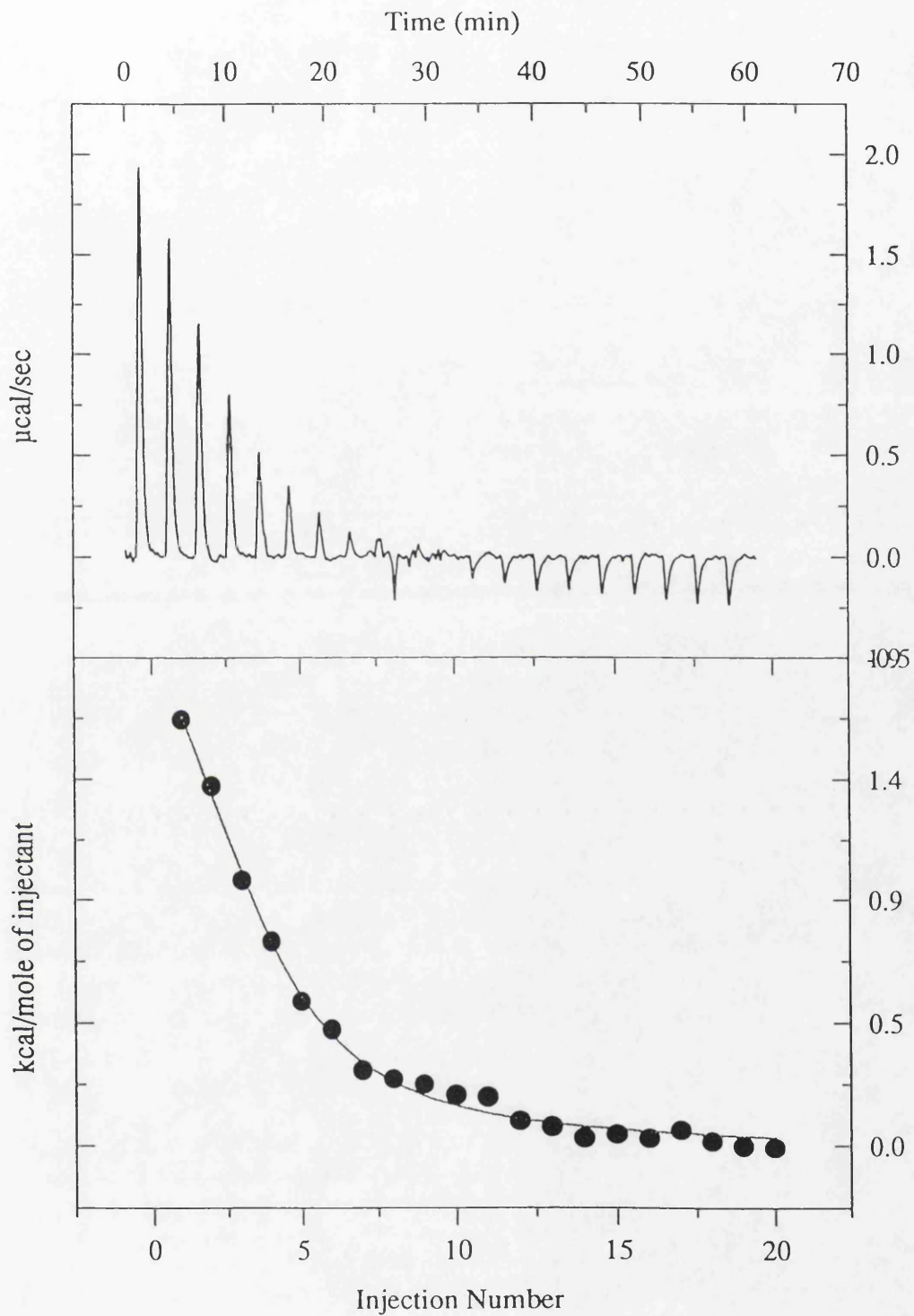


**Figure 4.35** *Binary wild-type PGK.ADP complex and 3-phosphoglycerate. 50 mM tris/MOPS pH 7.0, 4 mM Mg acetate, 0.1 mM DTT and 0.05% w/v sodium azide*

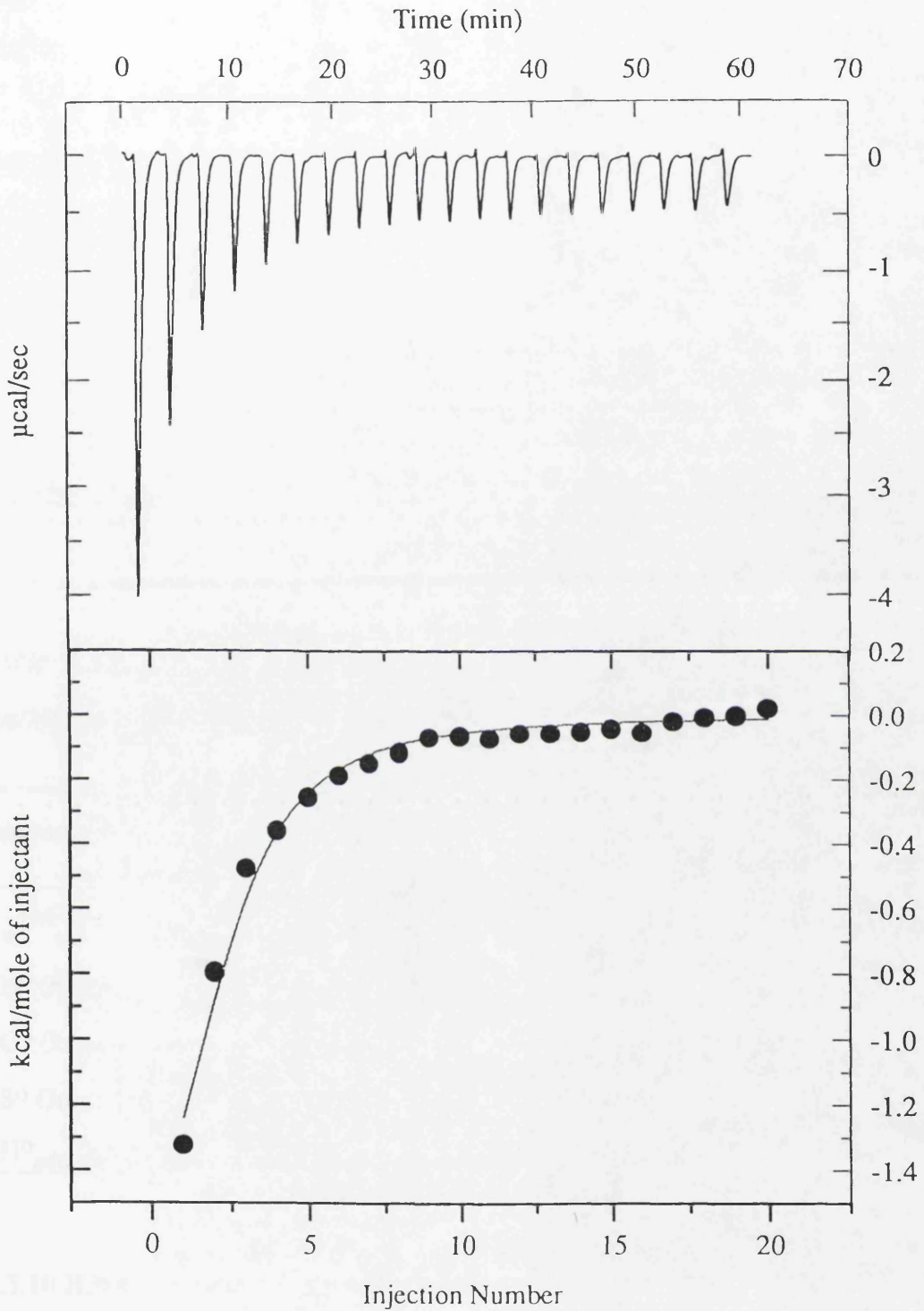


**Figure 4.32** Binary wild-type PGK.3-PG complex and ADP. 50 mM tris/MOPS pH 7.0, 4 mM Mg acetate, 0.1 mM DTT, 0.05% w/v sodium azide

**Table 4.14** Parameters for formation of ternary complex with wild-type PGK in MES buffer, pH 6

Parameters	PGK + Mg.ADP (1)	PGK.ADP + 3-PG (2)	PGK + 3-PG (3)	PGK.3-PG + Mg.ADP (4)
$K_a$ ( $M^{-1}$ )	5940	18200	111300	19000
$\Delta H^{\circ}$ ( $kJmol^{-1}$ )	-34.8	+2.8	-19.1	-13.9
$\Delta G^{\circ}$ ( $kJmol^{-1}$ )	-21.5	-24.3	-28.8	-24.4
$\Delta S^{\circ}$ ( $Jmol^{-1}K^{-1}$ )	-45	+91	+33	+35
$\Delta H^{\circ}_{add}$ ( $kJmol^{-1}$ )	-33.7	+2.7	-17.5	-12.4

**Table 4.15** Parameters for formation of ternary complex with wild-type PGK in tris/MOPS buffer, pH 7

Parameters	PGK + Mg.ADP (1)	PGK.ADP + 3-PG (2)	PGK + 3-PG (3)	PGK.3-PG + Mg.ADP (4)
$K_a$ ( $M^{-1}$ )	3550	27000	180000	11500
$\Delta H^{\circ}$ ( $kJmol^{-1}$ )	-57.5	+9.4	-15.5	-10.1
$\Delta G^{\circ}$ ( $kJmol^{-1}$ )	-20.2	-25.3	-30.0	-23.2
$\Delta S^{\circ}$ ( $Jmol^{-1}K^{-1}$ )	-125	116	49	44
$\Delta H^{\circ}_{add}$ ( $kJmol^{-1}$ )	-45.5	+8.7	-14.7	-9.2

#### 4.3.10 H388Q ternary complex

The interesting feature of this mutant enzyme is that the site of mutation is located within the hinge region of the enzyme. If there is an interaction between

substrate binding sites then this mutant could demonstrate altered interaction effects. The enthalpy change for the titration of PGK with ADP/3-phosphoglycerate mixture was found to be  $-41 \text{ kJmol}^{-1}$ . The results for these experiments are presented in table 4.16 and figures 4.39 to 4.40.

The binding of 3-phosphoglycerate to the binary mutant enzyme complex is not endothermic, however, it is less exothermic and the binding affinity is decreased. The binding of ADP occurs with a higher affinity than to PGK alone and the  $\Delta H^{\circ}$  value is less exothermic.

**Table 4.16** Parameters for formation of ternary complex for H388Q mutant PGK

Parameters	PGK + Mg.ADP (1)	PGK.ADP + 3-PG (2)	PGK + 3-PG (3)	PGK.3-PG + Mg.ADP (4)
$K_a (M^{-1})$	8372	67500	118000	38000
$\Delta H^{\circ} (\text{kJmol}^{-1})$	-33.2	-9.8	-25.8	-21.3
$\Delta G^{\circ} (\text{kJmol}^{-1})$	-22.4	-27.5	-28.9	-26.1
$\Delta S^{\circ} (\text{Jmol}^{-1}\text{K}^{-1})$	-36	+59	+10	+16
$\Delta H^{\circ}_{\text{add}} (\text{kJmol}^{-1})$	-28.2	-4.6	-18.9	-14.9

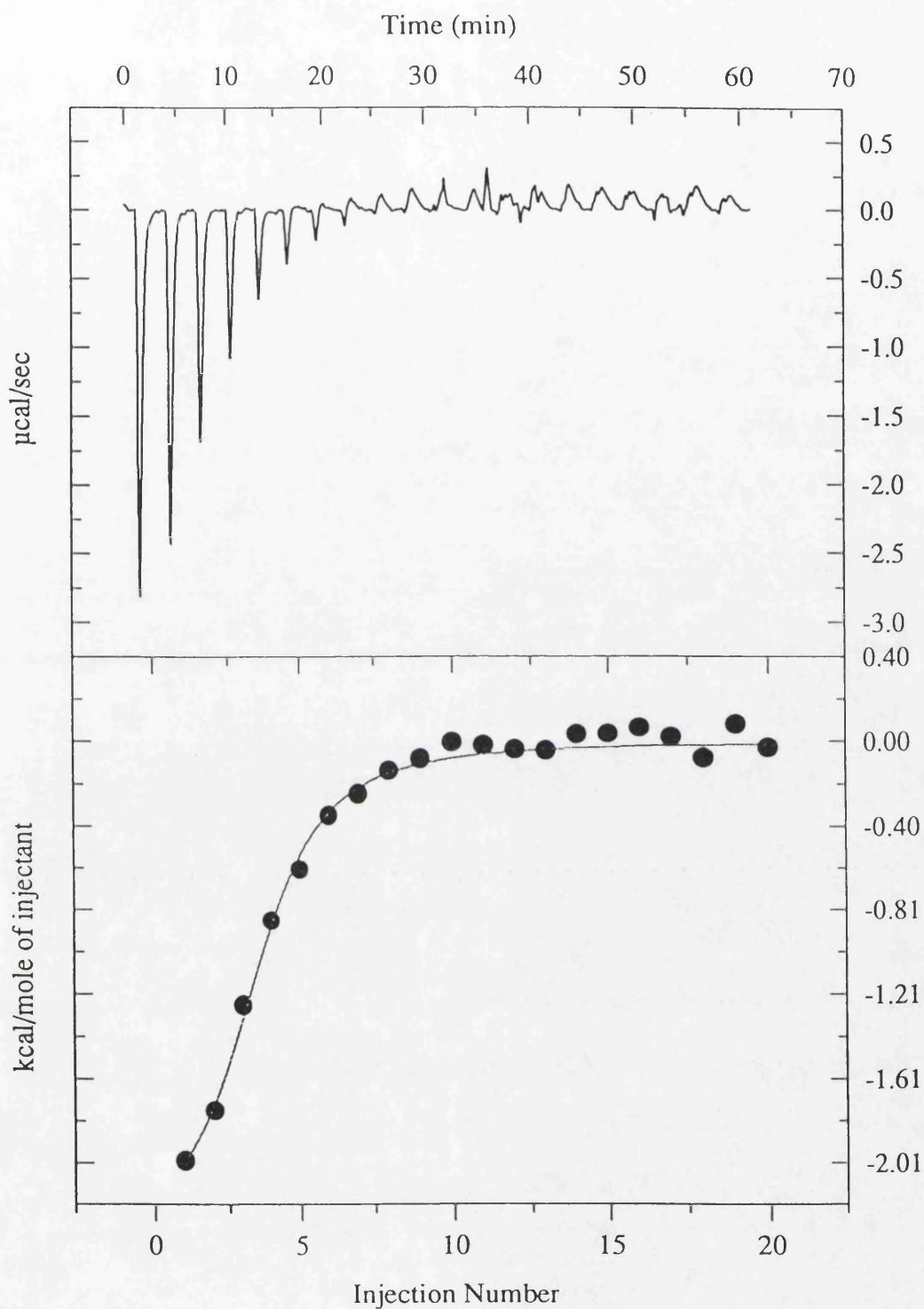


**Figure 4.39** Binary H388Q PGK.ADP complex and 3-phosphoglycerate. 50 mM MES pH 6.0, 4 mM Mg acetate, 0.1 mM DTT and 0.05% w/v sodium azide.

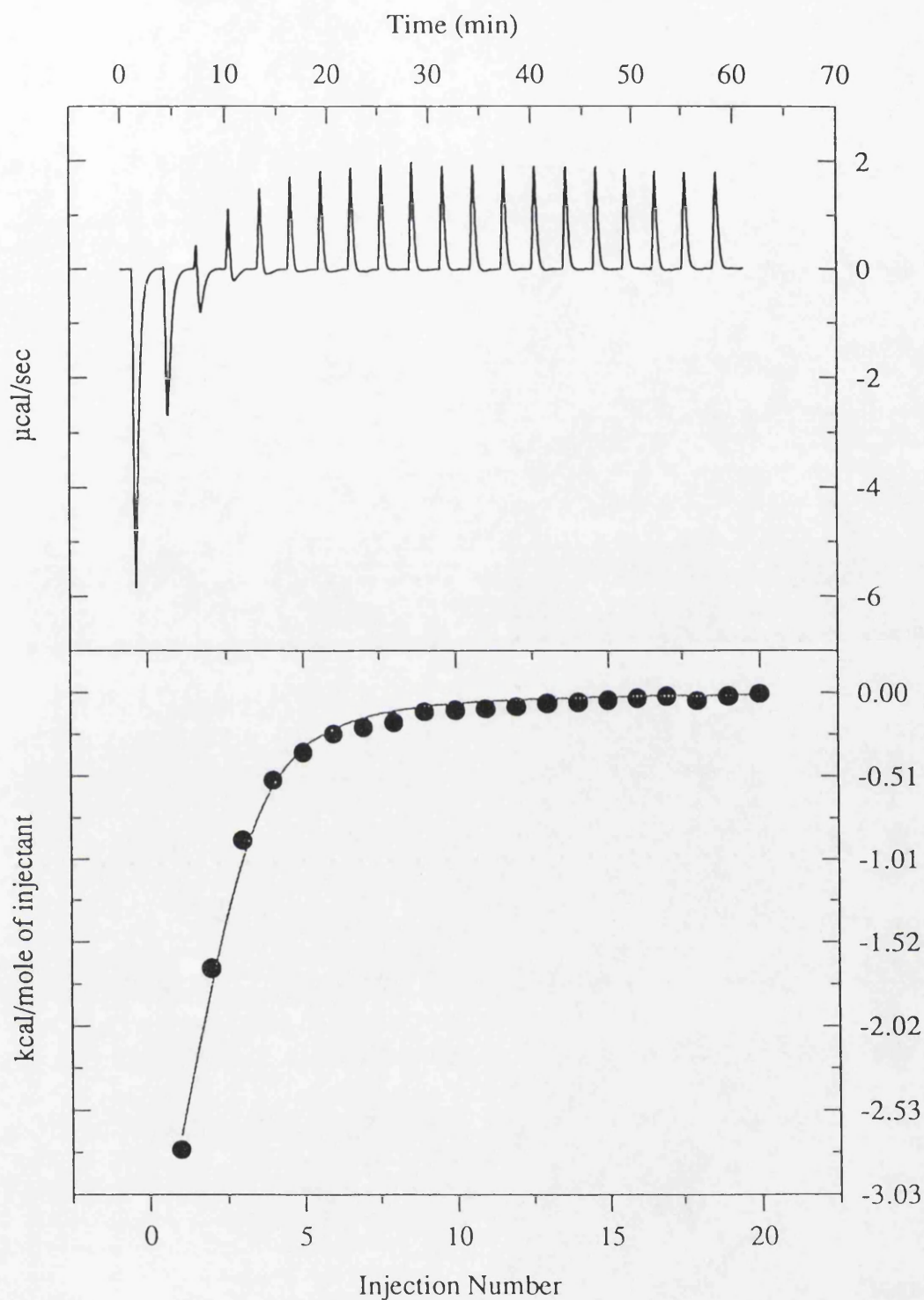


**Figure 4.40** Binary H388Q PGK.3-PG complex and ADP. 50 mM MES pH 6.0, 4 mM Mg acetate, 0.1 mM DTT and 0.05% w/v sodium azide.

## 5 DISCUSSION (PGK EXPERIMENTS)

The results given in chapter 4 fall into two main categories: the kinetic experiments which were used to investigate the binding of Mg.ATP and 3-phosphoglycerate to PGK, and the microcalorimetric experiments which involved the binding of substrates and ligands to PGK and also the effects of anion, pH etc. on the binding parameters.

The kinetic studies are relatively quick and straightforward to perform, requiring small amounts of enzyme. They were used to check the purity of enzyme samples and to compare the activities of the wild-type and mutant enzymes. The  $K_M$  values and specific activities of wild-type and mutant PGK (given in table 4.1) are similar to literature values described in table 4.2 and give confidence that the over-producing yeast strains and purification methods are satisfactory.

Both mutant enzymes exhibit a three to fourfold reduction in specific activity compared to wild-type PGK. Although the mutation at residue 388 is distant from the substrate binding sites it affects the  $K_M$  values, probably via long-range conformational or dynamic changes in the enzyme (Cooper *et al.*, 1989, Johnson *et al.*, 1991, Graham, *et al.*, 1991). The Michaelis constants for Mg.ATP and 3-phosphoglycerate with H388Q are decreased to 0.12 and 0.19 mM respectively. The R168K mutant enzyme, which contains a mutation in the active site region, has higher  $K_M$  values for both substrates ( $K_M = 0.79$  for ATP and  $K_M = 1.79$  for 3-PG): implying weaker binding compared to wild-type.

Although the kinetic experiments are easy to perform they give only limited information about substrate binding; to obtain the enthalpy of binding a van't Hoff approach would be necessary but the accuracy of this technique is low and also of dubious validity. Also, in the direction of the assay (from 3-phosphoglycerate and ATP to ADP and 1,3-DPG), it is impossible to study the binding of ADP to PGK, or to look at the binding of each substrate individually. The remainder of this chapter will be concerned with microcalorimetric results and will demonstrate the much greater amount of information that can be achieved from a calorimetric approach.

Although flow calorimetry has previously been used in limited studies of PGK-substrate associations (Hu & Sturtevant, 1987), the results presented in this thesis are the first obtained using titration calorimetry. The first titrations of wild-type PGK with substrate solution demonstrated that it was feasible to use microcalorimetry to study binding: reasonable titration curves were obtained and these could be analysed to give values of  $N$ ,  $K$ , and  $\Delta H^\circ$ . To test the accuracy of these experiments, the microcalorimetric dissociation constants were compared with dissociation constants found in the literature (table 5.1). The calorimetric data for substrate binding to wild-type PGK in Tris/MOPS and MES buffer are given in tables 4.4 and 4.5 and data from the earlier flow calorimetric measurements are given in table 5.2.

**Table 5.1** Dissociation constants for wild-type PGK

The numbers in the table are  $K_d$  values, expressed in millimolar units.

Reference	Method	Mg.ADP	Mg.ATP	3-PG
Scopes, 1978 (Ionic strength = 0.01M)	Equilibrium gel-filtration	0.01	0.009	0.011
Scopes, 1978 (Ionic strength = 0.1M)	as above	0.04	0.105	0.032
Tompa <i>et al.</i> , 1986	inhibition and thiol reactivity studies	0.04	0.15	---
Wrobel & Stinson, 1978	thiol reactivity studies	---	2.7	---
Vas & Batke, 1984	fluorimetric titrations	0.15	0.15	0.03
present work (Tris/MOPS buffer)	calorimetry	0.28	0.15	0.006
present work (MES buffer)	calorimetry	0.17	0.15	0.009

The dissociation constants quoted in table 5.1 were measured using several techniques, including thiol reactivity studies (Wrobel & Stinson, 1978) and equilibrium gel-filtration (Scopes, 1978b) etc. The dissociation constants vary over a wide range and the calorimetric dissociation constants are similar in magnitude to some of the previously measured values. All the dissociation constants are significantly lower than the Michaelis constants even though they should be equal for an enzyme following a simple Michaelis-Menten mechanism. However, kinetic experiments with PGK have

indicated that this enzyme does not follow simple Michaelis-Menten kinetics since the Eadie-Hofstee plots are biphasic in the absence of ammonium sulphate, thus 40 mM ammonium sulphate is usually included in the assay buffer. This alone could be responsible for the differences between  $K_M$  and  $K_d$  since anions compete with the natural substrates for the binding sites. Other explanations are possible: experiments have shown that adenine nucleotides weaken the binding of 3-phosphoglycerate (Vas & Batke, 1984) and there is also a strong possibility that the nucleotides bind at more than one site on the enzyme (Fairbrother *et al.*, 1990, Graham & Williams, 1991). Also, the Michaelis-Menten approach assumes that the dissociation of the enzyme-product complex is fast and so the concentration of EP can be ignored in the forward reaction (Fersht, 1985), however, it is believed that the very high affinity of 1,3-diphosphoglycerate for PGK means that the dissociation of the PGK:1,3-DPG complex is the rate-determining step in the PGK reaction (Scopes, 1978b). In this case,  $K_M$  is equal to  $K_d + k_{-1}/k_1$ . It is not surprising therefore that there are differences between  $K_M$  and  $K_d$  values for PGK.

The  $\Delta H^\circ$  values measured here can be compared with the values determined by flow calorimetry (Hu & Sturtevant, 1987).

**Table 5.2** Binding enthalpies determined by flow calorimetry

Buffer composition	Mg.ADP $\Delta H^\circ$ (kJ mol <sup>-1</sup> )	Mg.ATP $\Delta H^\circ$ (kJ mol <sup>-1</sup> )	3-PG $\Delta H^\circ$ (kJ mol <sup>-1</sup> )
50 mM PIPES pH 7.0 4 mM Mg Cl <sub>2</sub> 10 <sup>-4</sup> mM DTE	-39 (3)	-31.6 (0.07)	+15.6 (0.3)

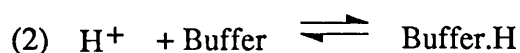
The enthalpy values for Mg.ATP and Mg.ADP binding are similar to the values obtained in MES buffer in this thesis. However, there is a major discrepancy in the enthalpy values of 3-phosphoglycerate binding. Hu & Sturtevant observed endothermic binding of 3-phosphoglycerate, whereas, measurements conducted in this laboratory give unambiguous exothermic binding (table 4.9 present work, Sanders, 1989). The slight changes in buffer composition (DTE instead of DTT and the absence of sodium azide) would not be expected to affect the enthalpy of binding to such an extent.

The main aim of this thesis was to compare the thermodynamics of substrate binding to wild-type and mutant enzymes in order to assess the effects of the mutations on substrate binding. The kinetic studies demonstrated that the  $K_M$  values for substrate binding to H388Q were lower than those observed for the wild-type enzyme. Hence, the calorimetric association constants for H388Q should be higher than the association constants measured for wild-type PGK. From table 4.7, it can be seen that the association constants are higher than for wild-type PGK, but not significantly. The enthalpy changes are unaltered for ATP and ADP binding to the mutant enzyme. However the enthalpy of binding for 3-phosphoglycerate is somewhat more exothermic. We see from these results that the mutation at position 388 does not affect substrate binding to a great extent as might be expected for a mutation distant from the active site.

The more interesting mutant for molecular recognition studies is R168K, which contains a mutation in the active site. The study of R168K is of interest since this residue is on the N-domain close to the 3-phosphoglycerate binding site (Walker *et al.*, 1989). Unfortunately, the plasmids coding for this mutant enzyme appeared to be less stable than the plasmids for wild-type and H388Q mutant enzymes: leading to difficulties in obtaining suitably large quantities of pure enzyme and therefore only a

few calorimetric experiments could be conducted. This mutation, as expected, affects the substrate binding parameters (table 4.8). The calorimetric binding isotherms when fitted with the one set of sites model do not agree well with the calculated curve. The difficulties in analysing the titration curves and the difficulties in obtaining large quantities of pure enzyme meant that no other experiments were performed with this mutant enzyme.

Since no further mutant enzymes were available for study, more detailed experiments were conducted with the wild-type enzyme. The 3-phosphoglycerate binding experiments were repeated in several other buffer systems and the binding parameters were found to vary depending on the buffer system in use, as shown in table 4.9. The changes in  $\Delta H^0$  values can be accounted for by protonation effects. The  $pK_a$  for free 3-phosphoglycerate in solution is 6.84, therefore at pH 7, approximately 50% of 3-phosphoglycerate is dissociated. However, 3-phosphoglycerate binds to the enzyme predominantly in the ionized form: the  $pK_a$  changes from 6.84 in solution to 4.95 when bound to PGK (Wilson *et al.*, 1988). This means that as the substrate binds to the enzyme protons are released and taken up by the buffer, producing an additional heat effect. This additional heat effect will vary from buffer to buffer depending on the heats of ionization of the buffer. A two-step reaction scheme can be written as follows:



The enthalpy change in the absence of protonation effects,  $\Delta H^0_o$ , can be calculated using equation 2.21, assuming the  $pK_a$  of free 3-phosphoglycerate is 6.84 and that the substrate binds to the enzyme in the fully ionized form. The results are shown in table 5.3.

**Table 5.3**  $\Delta H^{\circ}_o$  and  $\Delta N$  values for binding of 3-phosphoglycerate to wild-type PGK in different buffer systems

Buffer	$\Delta H^{\circ}_o$ (kJmol <sup>-1</sup> )	$\Delta N$
Tricine, pH 8	-6.4	0.065
Tris/MOPS, pH 7	-5.9	0.41
PIPES, pH 7	-6.3	0.41
MES, pH 6	-6.3	0.87

In the absence of protonation changes, 3-phosphoglycerate binding to PGK has a small exothermic enthalpy change which is, in effect, amplified by the uptake of protons by the buffer. Because of the importance of the protonation effects the  $\Delta H^{\circ}$  value measured in piperazine buffer at pH 6 should be the most exothermic, since this buffer has a large heat of ionization and 87% of 3-phosphoglycerate molecules are protonated at this pH. However, this is not the case. A possible explanation for the low enthalpy change measured in piperazine buffer, is that this buffer is adjusted to pH 6 with HCl, whereas, the other buffers have been adjusted to the correct pH with NaOH. The chloride ions are present at a high enough concentration that inhibition effects are apparent.

Although the enthalpy changes are consistent with the proposed protonation changes, the values of the association constant at a given pH should be equal and there should be a downwards trend in association constants from pH 8 to pH 6, since a greater proportion of 3-phosphoglycerate molecules are already ionized at pH 8. The

observed association constants do not follow this trend either because of experimental error or because components of the buffer system (such as the chloride ions in piperazine buffer) are also binding to PGK and affecting the association constants.

3-phosphoglycerate is competitively inhibited by various anions which also bind to the N-domain of PGK. Experiments were performed to determine the effects of anions on 3-phosphoglycerate binding parameters. 3-phosphoglycerate titrations were conducted in the presence of 1.1 mM ammonium sulphate (table 4.11). Under these conditions the affinity constant of 3-phosphoglycerate is reduced to  $24800 \text{ M}^{-1}$ . For competitive inhibition (both substrate and inhibitor binding at the same site) the following relation holds,

$$K_a' = \frac{K_a}{1 + K_I[I]} \quad (5.1)$$

where [I] represents the concentration of inhibitor,  $K_a'$  denotes the apparent association constant and  $K_I$  is the inhibition constant. Using this equation, a  $K_I$  value of  $3200 \text{ M}^{-1}$  can be calculated for the sulphate ion, which is similar to the  $K_d$  value of  $3850 \text{ M}^{-1}$  determined directly by calorimetric titration of PGK with ammonium sulphate (table 4.6)

Some experiments were performed in the presence of 60 mM magnesium acetate and 60 mM magnesium chloride (table 4.10) 3-phosphoglycerate did not bind to PGK when the buffer contained 60 mM magnesium chloride. However, binding was observed in the presence of 60 mM magnesium acetate. Using equation 5.1, an inhibition constant of  $950 \text{ M}^{-1}$  for the acetate ion was calculated from the 3-phosphoglycerate parameters. Since binding of 3-phosphoglycerate appears to be

completely inhibited by chloride ions it is reasonable to assume that the association constant for chloride ions is greater than  $950 \text{ M}^{-1}$ .

In summary, sulphate, chloride and acetate decrease the values of the association constant and  $\Delta H^\circ$  for 3-phosphoglycerate binding to PGK, consistent with competitive binding of anions and 3-phosphoglycerate.

The nucleotide substrates, ADP and ATP, bind to the same site on the enzyme. This was observed by titrating PGK with ADP in the presence of saturating concentrations of ATP and *vice versa*. No heat effects from binding (only dilution effects) were apparent during these titrations and it would therefore appear that the binding of these substrates is mutually competitive.

ADP and ATP titrations were also performed in 50 mM PIPES buffer at pH 7.0 to determine if protonation changes take place on binding nucleotide substrates. In this buffer it was impossible to obtain a theoretical fit to the data assuming that the substrate was binding at one site. This problem arose because of the large difference between the heats of dilution of substrate and the heat effects at enzyme saturation. After enzyme saturation has occurred, the observed heat effects resulting from injection of more substrate into the enzyme should be roughly equal in magnitude to the heat effects observed from injection of substrate into buffer. However, although the enzyme appeared to be saturated, the heat effects were more exothermic than the dilution heats. These effects suggested that the nucleotide substrates are binding at more than one site on the enzyme, even though the experiments in MES and Tris/MOPS buffer could be analysed assuming 1:1 complex formation.

The true substrates in the PGK catalytic reaction are the magnesium complexes of ADP and ATP and so the effect of magnesium ions on nucleotide binding was

investigated by performing experiments in buffers containing 0, 4, and 60mM magnesium acetate and the results are shown in table 4.12.

In the absence of magnesium the binding affinities for ADP and ATP are increased. This can be explained if the nucleotide binding is dominated by electrostatic interactions between the phosphate groups and positively charged residues in the enzyme active site (either the basic patch residues or the lysine residues near the hydrophobic binding site): the presence of magnesium reduces the charge of the nucleotide and thus decreases the binding affinity.

ATP does not appear to bind to PGK at high concentrations of magnesium acetate; probably as a result of anion competition since, at high concentrations, anions may bind to the lysine residues near the  $\gamma$ -phosphate of ATP, this could have the effect of inhibiting the binding of ATP but not the binding of ADP.

The choice of buffer system may also influence nucleotide binding since some buffers complex magnesium ions: this would alter the concentration of free magnesium ions and hence the binding parameters for the nucleotide substrates.

The titration of PGK with ADP in the presence of 1.1 mM ammonium sulphate results in altered binding parameters as shown in table 4.11. The association constant is similar in magnitude but the enthalpy change is less exothermic. A more substantial effect is observed with ATP. The binding is strongly weakened in the presence of 1.6 mM sulphate, with a decrease in association constant from  $6610 \text{ M}^{-1}$  to approximately  $650 \text{ M}^{-1}$ . The poor fit to the experimental data in this case means that the fitting parameters are not quantitative and large errors in the thermodynamic values, especially for  $\Delta H^0$ , must be expected. These calorimetric results may reflect the observations by Scopes, 1978b, where sulphate was found to competitively inhibit the binding of ATP but not ADP.

The formation of the dead-end ternary complex, PGK.ADP.3-PG, was studied to determine if there is an interaction between the nucleotide and triose binding sites. (The ternary complex, PGK.ATP.3-PG, could not be studied since the heat of reaction would obscure the heat of binding). There are three ways of forming the ternary complex:

- A.  $\text{PGK} + \text{ADP} \longrightarrow \text{PGK.ADP} + 3\text{-PG} \longrightarrow \text{PGK.ADP.3-PG}$  (two titrations)
- B.  $\text{PGK} + 3\text{-PG} \longrightarrow \text{PGK.3-PG} + \text{ADP} \longrightarrow \text{PGK.ADP.3-PG}$  (two titrations)
- C.  $\text{PGK} + \text{ADP} + 3\text{-PG} \longrightarrow \text{PGK.ADP.3-PG}$  (one titration)

In experiments A and B, the enzyme is titrated to saturation with the first substrate and then the binary enzyme-substrate complex is titrated with the second substrate. These reactions can be written in a thermodynamic cycle as shown in figure 5.1.

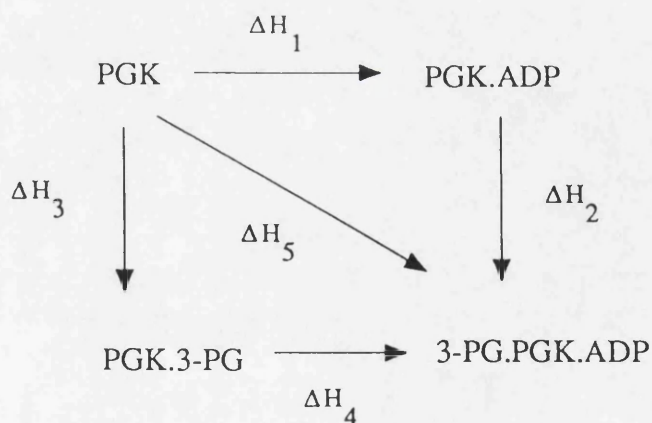


*Figure 5.1 Thermodynamic cycle for the formation of the PGK ternary complex*

According to Hess's law, the sum of  $\Delta H^0_1$  and  $\Delta H^0_2$  is equal to the sum of  $\Delta H^0_3$  and  $\Delta H^0_4$ , which in turn is equal to  $\Delta H^0_5$ .

The results for the experiments with wild-type PGK are given in tables 4.14 and 4.15 and are visualized in figures 5.2 and 5.3. The experiments were also repeated with the H388Q mutant enzyme to determine whether the mutation in the hinge region affects substrate interactions (table 4.16 and figure 5.4). It is obvious from these results that the substrate binding parameters are altered in the presence of the other substrate; this applies to both the wild-type and the mutant enzyme. ADP weakens the binding of 3-phosphoglycerate, whereas, 3-phosphoglycerate appears to enhance the binding of ADP.

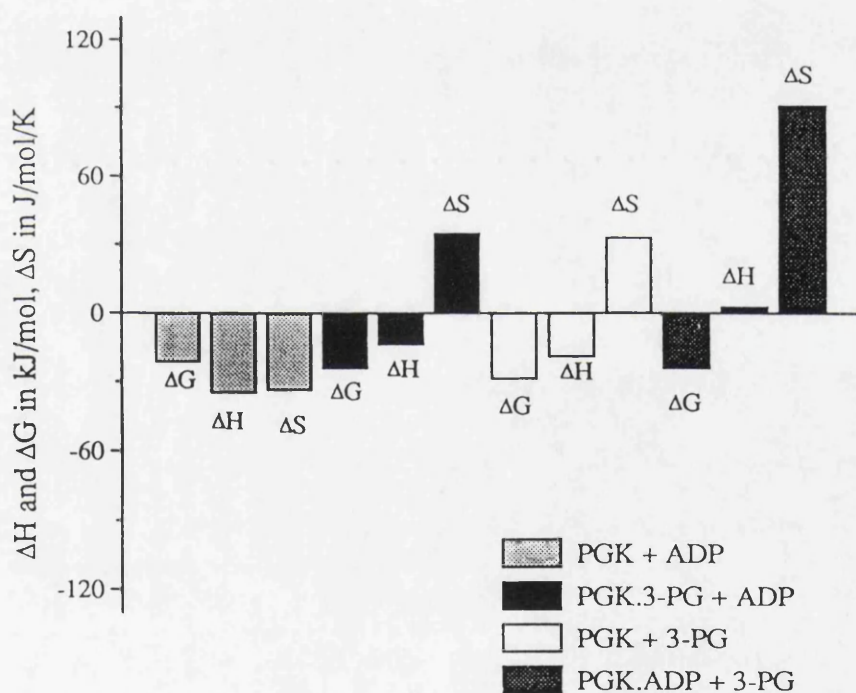


Figure 5.2 Wild-type PGK in MES buffer at pH 6.0

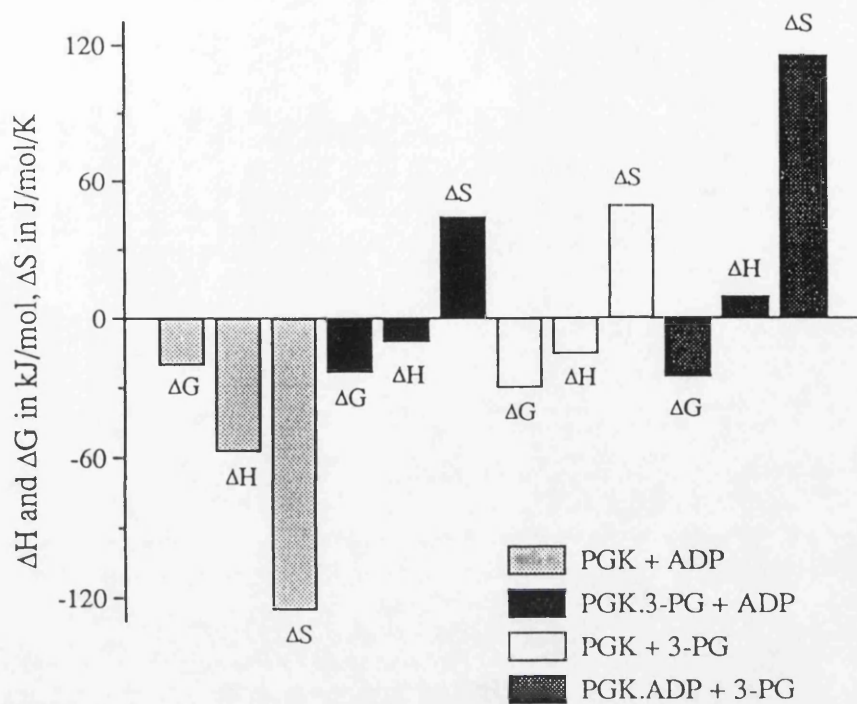


Figure 5.3 Wild-type PGK in tris/MOPS buffer at pH 7.0

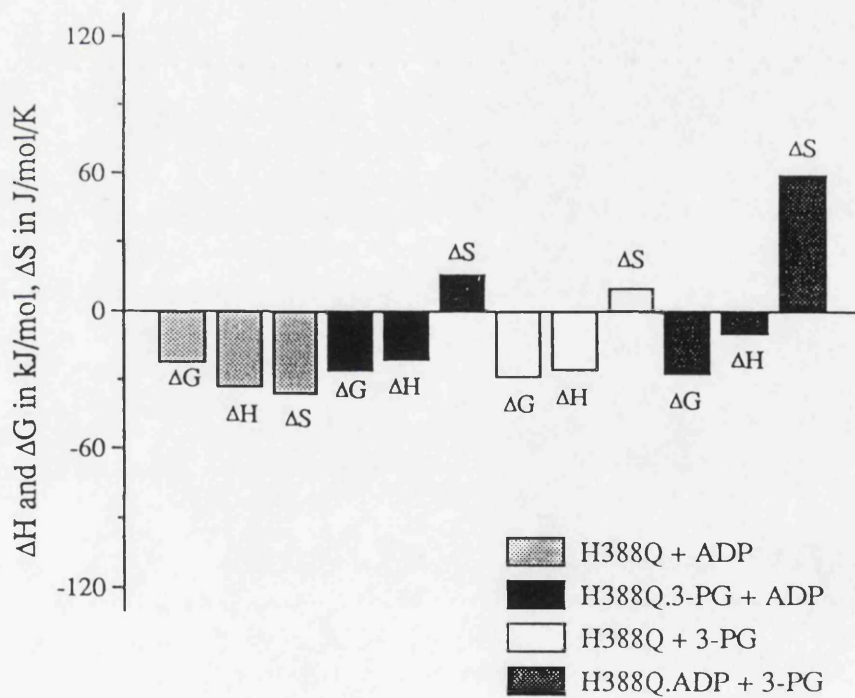


Figure 5.4 H388Q PGK in MES buffer at pH 6.0

The sums of  $\Delta H_1 + \Delta H_2$ ,  $\Delta H_3 + \Delta H_4$  and  $\Delta H_5$  for the wild-type and H388Q mutant enzyme are shown in table 5.4. These results are roughly consistent with the thermodynamic cycle proposed in figure 5.1 for the experiments in MES buffer but not for the experiments in tris/MOPS buffer.

*Table 5.4 Sums of  $\Delta H_1 + \Delta H_2$ ,  $\Delta H_3 + \Delta H_4$  and  $\Delta H_5$  for wild-type and H388Q mutant enzyme*

Enzyme	$\Delta H_1 + \Delta H_2$ (kJmol <sup>-1</sup> )	$\Delta H_3 + \Delta H_4$ (kJmol <sup>-1</sup> )	$\Delta H_5$ (kJmol <sup>-1</sup> )
Wild-type (MES)	-32 (0.9)	-33 (1.3)	-36 (2)
Wild-type (tris/MOPS)	-48 (5)	-26 (6)	not measured
H388Q	-43 (4)	-47 (6)	-41 (4)

There should also be a relationship between the corresponding association constants for these reactions i.e,

$$K_1 K_2 = K_3 K_4 = [P.PGK.A]/\{[P][PGK][A]\}$$

since the association constants are defined by

$$K_1 = [PGK.A]/\{[PGK][A]\}, K_2 = [P.PGK.A]/\{[PGK.A][P]\}$$

$$K_3 = [P.PGK]/\{[PGK][P]\}, K_4 = [P.PGK.A]/\{[P.PGK][A]\}$$

where [P], [A], [PGK], [P.PGK], [PGK.A] and [P.PGK.A] denote the concentrations of 3-phosphoglycerate, ADP, the binary complex of PGK with 3-phosphoglycerate, the binary complex of PGK with ADP and the ternary complex of PGK with both 3-phosphoglycerate and ADP, respectively.

The products  $K_1K_2$  and  $K_3K_4$  for wild-type and H388Q PGK are given in table 5.5.

**Table 5.5**  $K_1K_2$  and  $K_3K_4$  for wild-type and H388Q PGK

Enzyme	$K_1K_2$ ( $M^{-1}$ )	$K_3K_4$ ( $M^{-1}$ )
Wild-type (MES)	$1.1 (0.4) \times 10^8$	$2.1 (0.2) \times 10^9$
Wild-type (tris/MOPS)	$9.3 (2.0) \times 10^7$	$2.1 (0.5) \times 10^9$
H388Q	$5.6 (1.2) \times 10^8$	$4.5 (2.5) \times 10^9$

From the results shown in table 5.5, it is evident that there is a large discrepancy between  $K_1K_2$  and  $K_3K_4$  for both the wild-type and mutant enzymes. This means that the thermodynamic cycle proposed for the formation of the ternary complex cannot be correct. The binding of 3-phosphoglycerate is weakened by the presence of ADP but the reciprocal effect is not observed, in fact, the binding of ADP is apparently enhanced by 3-phosphoglycerate. The most probable explanation for this is that ADP is binding at two sites on the enzyme; both ADP and ATP have been observed to bind at two sites on the enzyme in previous studies (Fairbrother *et al.*, 1990, Graham & Williams, 1991). This introduces an additional step (or several different steps) in the thermodynamic cycle and means that the observed association constants for the binding of ADP are actually composite values for two or more sites. Although the calorimetric data in MES and tris/MOPS buffers are consistent with ADP binding at a single site on the enzyme, it is possible that there is a second, weak binding site as suggested for the binding of nucleotides in PIPES buffer.

These results can be compared with experiments reported by Vas & Batke in 1984, in which the dissociation constants for the binding of substrates to pig-muscle PGK were determined by measuring the change in fluorescence of a PGK-ANS (1-anilino-8-naphthalenesulphonate) complex on titration with the substrate. The  $K_d$  values for each substrate are listed in table 5.2. Adenine nucleotides were found to weaken the binding of 3-phosphoglycerate by a factor of about 6.7. This effect is also observed in the present work where the association constant for 3-phosphoglycerate is decreased by a factor of 5.9 by Mg.ADP. In the study by Vas & Batke, the binding of nucleotide substrates was unaffected by 3-phosphoglycerate.

The two possible binding sites for ADP are the hydrophobic site on the C-domain and the electrostatic site on the N-domain. There are two ways in which 3-phosphoglycerate binding can be weakened: the presence of the nucleotide could be displacing the carboxylate group of 3-phosphoglycerate, as proposed by Vas & Batke (1984), or there could be competitive inhibition between ADP and 3-phosphoglycerate at the N-domain binding site. There is still the possibility that the binding sites may be interactive and so the situation is difficult to analyse successfully. However, when the nucleotide titrations were re-analysed using the two sets of sites binding model (table 5.6), there was some evidence for two binding sites: a high affinity site (probably the catalytic site identified by crystallography) and a low affinity binding site (probably at the basic patch).

**Table 5.6** Results of a two sets of sites analysis of the binding of ATP and ADP to wild-type PGK in 50 mM tris/MOPS, 4 mM magnesium acetate, 0.1 mM DTT and 0.05% azide at pH 7.0.

		ADP	ATP
1st binding site	$K_1$ ( $M^{-1}$ )	44000 (46000)	29000 (22000)
	$\Delta H^{\circ}_1$ ( $kJmol^{-1}$ )	-15.9 (1.7)	-19.1 (3.0)
2nd binding site	$K_2$ ( $M^{-1}$ )	2400 (550)	1020 (650)
	$\Delta H^{\circ}_2$ ( $kJmol^{-1}$ )	-41.1 (3.0)	-23.8 (9.9)

**Table 5.7** Results of a two sets of sites analysis of the binding of ATP and ADP to wild-type PGK in 50 mM MES, 4 mM magnesium acetate, 0.1 mM DTT and 0.05% azide at pH 6.0.

		ADP	ATP
1st binding site	$K_1$ ( $M^{-1}$ )	35000 (13000)	25000 (3000)
	$\Delta H^{\circ}_1$ ( $kJmol^{-1}$ )	-15.8 (1.3)	-19.5 (1.9)
2nd binding site	$K_2$ ( $M^{-1}$ )	2600 (800)	1500 (700)
	$\Delta H^{\circ}_2$ ( $kJmol^{-1}$ )	-24.8 (1.0)	-28.9 (2.8)

This means that at high concentrations of ADP, the binding of 3-phosphoglycerate is competitively inhibited by the ADP already bound on the N-domain. The endothermic displacement of ADP at this site by 3-phosphoglycerate would explain the endothermic binding of 3-phosphoglycerate to the binary PGK-ADP complex. If, however, the order of titrations is reversed so that the PGK-3-PG complex is formed in the first instance, then the binding of ADP to the low affinity site may not be observed and the resulting binding isotherm would be mainly from binding to the high affinity site.

This theory could be substantiated by finding a nucleotide analogue which would bind to just one binding site, either the C-domain or the N-domain. Therefore, the binding of adenosine and triphosphate to PGK was studied. If this approach was successful then it would be possible to determine if the binding of 3-phosphoglycerate is weakened by the binding of a molecule at the C-domain binding site or by direct competition with the nucleotide on the N-domain.

If binding on the N-domain is mainly electrostatic then adenosine will be unlikely to bind on this domain; it should however bind in the hydrophobic site on the C-domain. When the experiment was performed, adenosine was found to bind either very weakly to PGK or not at all. It was difficult to achieve a sufficiently high adenosine concentration because of the low solubility of adenosine in MES buffer; it was therefore impossible to reach enzyme saturation. After titrating the enzyme with adenosine to give a final concentration of 1.4 mM, further titrations with 3-phosphoglycerate and ADP were performed. In both cases, the thermodynamic parameters were essentially unchanged and so it appears that adenosine did not bind to the enzyme.

Tripolyphosphate was used as a nucleotide "tail" mimic. Tripolyphosphate is unlikely to bind at the hydrophobic site, but since it is negatively charged, it should bind on the N-domain, at the general anion binding site. This ligand exhibited high affinity binding (table 4.6), significantly higher than other anions studied (sulphate, acetate) and there was no evidence of 3-phosphoglycerate binding in the presence of tripolyphosphate. Tripolyphosphate (at a concentration of about 0.7 mM) was observed to increase the binding affinity of ADP to PGK. The association constant was increased to about  $10900 \text{ M}^{-1}$  and the enthalpy change was  $-6.2 \text{ kJmol}^{-1}$  i.e. tripolyphosphate has similar effects on the binding of ADP as 3-phosphoglycerate.

It has been shown earlier that magnesium increases the binding affinity of nucleotide substrates, if this is the case then in the absence of magnesium more ADP may bind to the N-domain and further inhibit the binding of 3-phosphoglycerate. This was demonstrated experimentally and gives further evidence that the binding of 3-phosphoglycerate is weakened by competitive inhibition with ADP at the N-domain binding site.

In summary, the thermodynamics of substrate binding to PGK has been studied in some detail by microcalorimetry. Interpretation of these results has not been straightforward since the substrate binding studies were often complicated by competition effects involving anions or other substrates. However, some patterns have emerged: anions, such as chloride, acetate and sulphate, decrease the affinity of the substrates. The inhibition effects by anions and the activation/inhibition effects by magnesium ions may be important in the regulation of enzyme activity *in vivo*.

The bindings of Mg.ADP and 3-phosphoglycerate are not independent: Mg.ADP binds with an apparently higher affinity in the presence of 3-phosphoglycerate, whereas, the binding of 3-phosphoglycerate is weakened by Mg.ADP. The association constant of 3-phosphoglycerate to PGK in the presence of Mg.ADP ( $K_a = 18200$ ,  $K_d = 0.05\text{mM}$ ) is brought closer to the  $K_M$  value for 3-phosphoglycerate measured in the kinetic experiments (0.5 mM). It is possible that in the true ternary complex, ATP.PGK.3-PG, the association constant would be further decreased and may equal the value of the Michaelis constant. The loosening of 3-phosphoglycerate binding might be of significance in the enzyme catalysis process. However, loosening of 1,3-diphosphoglycerate binding is probably of more importance, since this substrate has a very high association constant of  $>2 \times 10^7 \text{ M}^{-1}$  (Scopes, 1978b) and in fact the release of 1,3-diphosphoglycerate is the rate-determining step in the enzymic reaction. Unfortunately, this cannot easily be studied by microcalorimetry due to the low stability of 1,3-diphosphoglycerate in solution.

## 6 VANCOMYCIN AND RISTOCETIN RESULTS

The binding of peptidoglycan precursor peptides and their analogues to the antibiotics, vancomycin and ristocetin A was studied by isothermal titration microcalorimetry using the Omega system. Solutions of the antibiotics were titrated with N-ac-D-ala, N-ac-D-ala-D-ala, di-N-ac-L-lys-D-ala-D-ala and D-ala-D-ala and the enthalpy change and association constant for binding were measured. The experiments were performed at different temperatures, over a 25 °C temperature span, to allow the determination of  $\Delta C_p^\circ$  values. Since both antibiotics are known to either dimerise or aggregate in solution, the experiments were performed with two concentrations of antibiotic ( $0.1 \text{ mgml}^{-1}$  and  $0.5 \text{ mgml}^{-1}$ ). All the experiments were conducted in 0.1 M sodium phosphate buffer at pH 7.0. In some cases the thermodynamic parameters were dependent on antibiotic concentration, indicating possible dimerization effects.

### 6.1 N-acetyl D-ala

N-acetyl D-ala forms only weak complexes with vancomycin and ristocetin. Increasing temperature weakens binding further, therefore, since antibiotic saturation is not achieved under our accessible experimental conditions, there is a higher error in  $\Delta H^\circ$  values at high temperatures. The binding parameters at 25 °C for vancomycin and N-acetyl D-ala appear to be independent of antibiotic concentration, and titration data fit consistently to a simple 1:1 model. The results from the titrations of vancomycin and

ristocetin with N-acetyl D-ala are given in tables 6.1 and 6.2, with the raw data in figures 6.1 and 6.2.

**Table 6.1** Thermodynamic parameters of N-acetyl D-ala binding to vancomycin

<sup>a</sup> [vancomycin] = 0.5 mgml<sup>-1</sup>

<sup>b</sup> [vancomycin] = 0.1 mgml<sup>-1</sup>

Peptide	Temp (°C)	K <sub>a</sub> (M <sup>-1</sup> )	-ΔH <sup>o</sup> (kJmol <sup>-1</sup> )	-ΔG <sup>o</sup> (kJmol <sup>-1</sup> )	-ΔS <sup>o</sup> (Jmol <sup>-1</sup> K <sup>-1</sup> )	-ΔC <sub>p</sub> <sup>o</sup> (Jmol <sup>-1</sup> K <sup>-1</sup> )
Ac-D-ala <sup>a</sup>	20	369 (16)	32.3 (0.5)	14.4 (0.1)	61 (2)	
	25	296 (12)	35.8 (0.5)	14.1 (0.1)	73 (2)	
	30	221 (18)	36.7 (0.3)	13.6 (0.2)	76 (1)	525 (3)
	35	187 (8)	38.6 (1.1)	13.4 (0.1)	82 (4)	
	45	105 (8)	46.2 (2.5)	12.3 (0.2)	107 (8)	
Ac-D-ala <sup>b</sup>	25	272 (12)	34.2 (1.1)	13.9 (0.1)	68 (4)	

**Table 6.2** Thermodynamic parameters of N-acetyl D-ala binding to ristocetin

Peptide	Temp (°C)	K <sub>a</sub> (M <sup>-1</sup> )	-ΔH <sup>o</sup> (kJmol <sup>-1</sup> )	-ΔG <sup>o</sup> (kJmol <sup>-1</sup> )	-ΔS <sup>o</sup> (Jmol <sup>-1</sup> K <sup>-1</sup> )	-ΔC <sub>p</sub> <sup>o</sup> (Jmol <sup>-1</sup> K <sup>-1</sup> )
Ac-D-ala <sup>a</sup>	20	1214 (51)	29.9 (0.4)	17.3 (0.1)	43 (2)	
	25	955 (19)	32.5 (0.5)	17.0 (0.1)	52 (2)	
	30	620 (26)	35.8 (0.8)	16.2 (0.1)	65 (3)	653 (21)
	35	478 (19)	38.7 (1.9)	15.8 (0.1)	82 (6)	
	45	260 (5)	46.2 (1.5)	14.7 (0.1)	99 (5)	

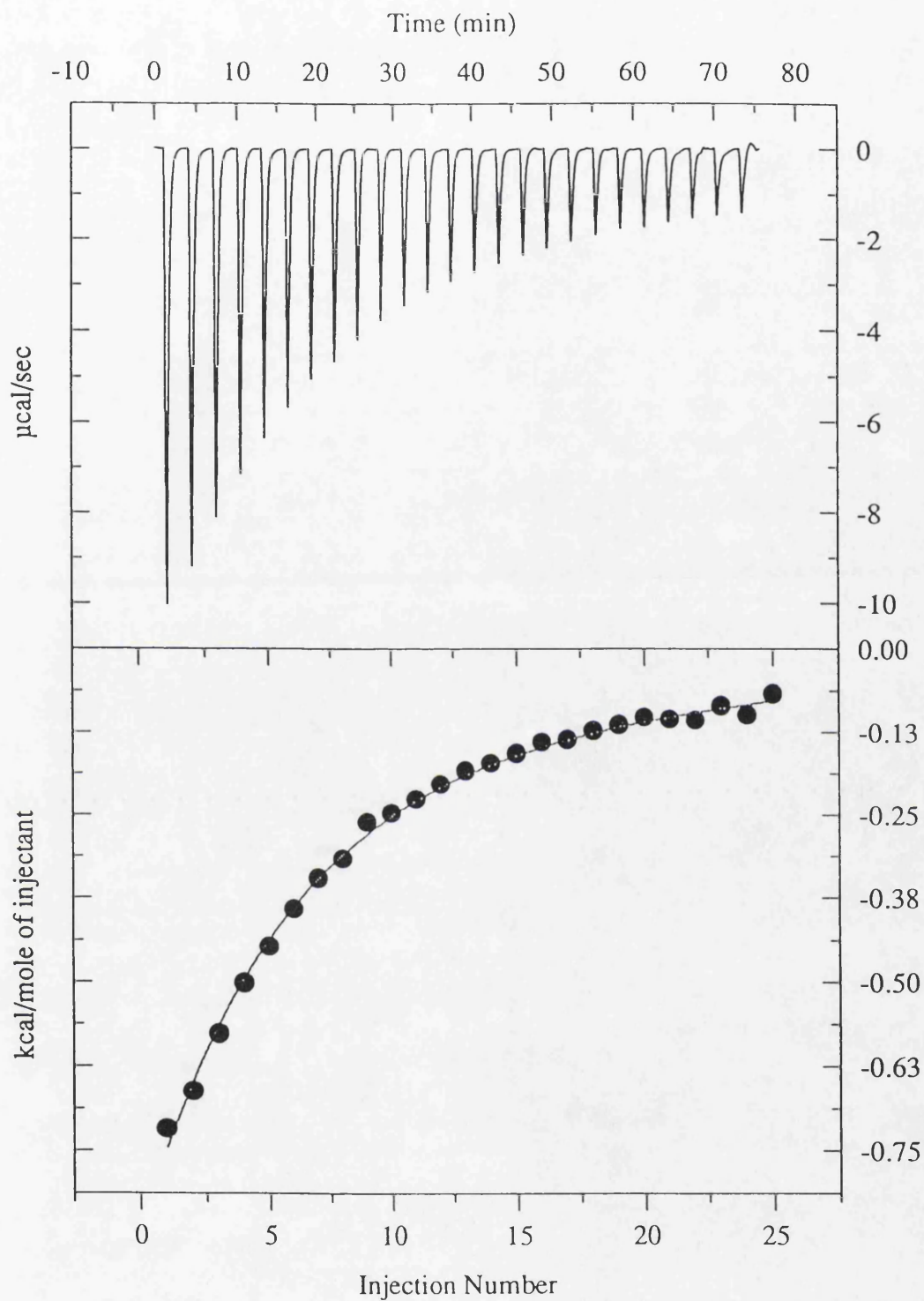


Figure 6.1 Vancomycin ( $0.5 \text{ mgml}^{-1}$ ) and *N-ac-D-alanine* at  $25^\circ\text{C}$

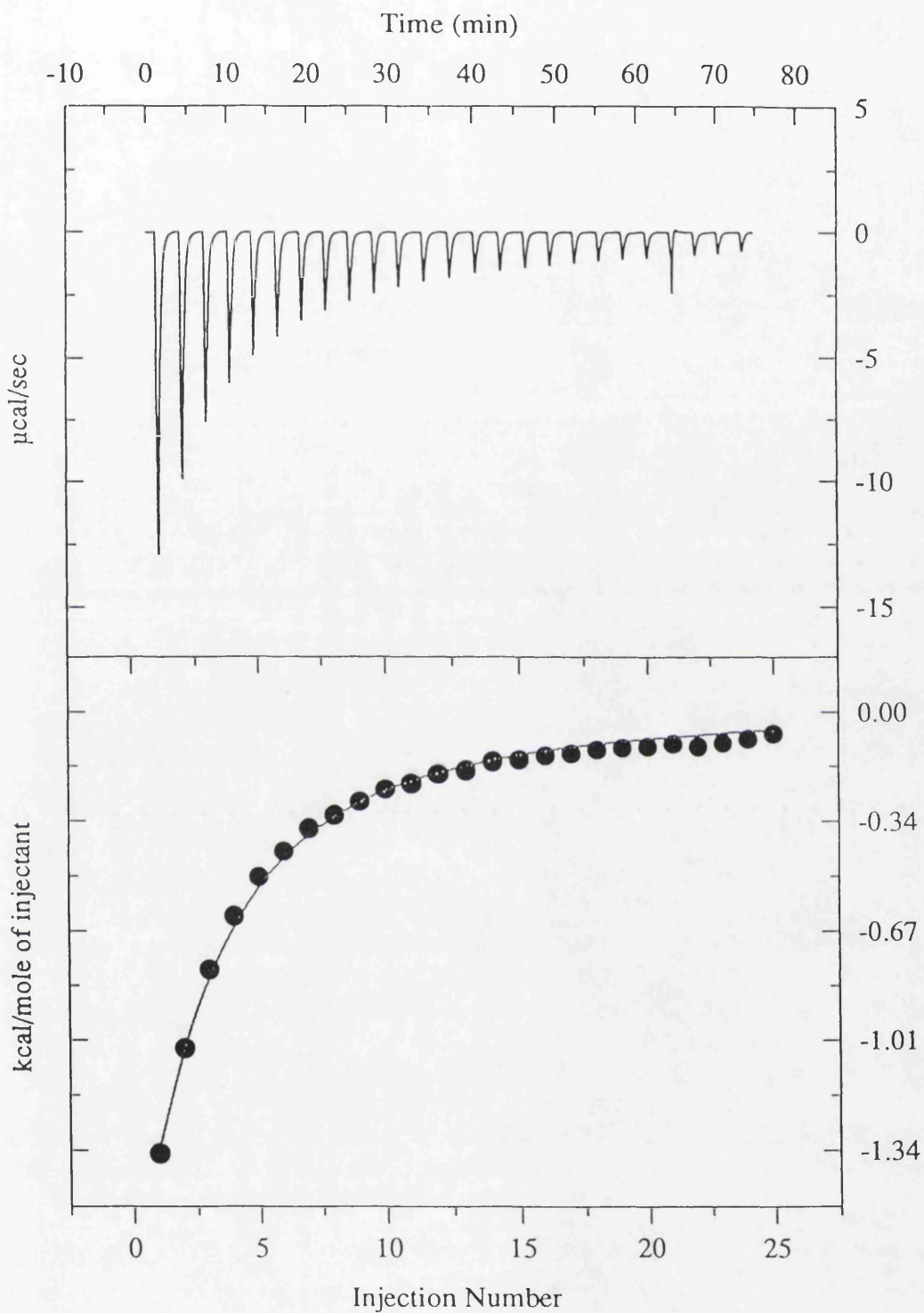


Figure 6.2 Ristocetin ( $0.5 \text{ mgml}^{-1}$ ) and *N-ac-D-alanine* at  $25^\circ\text{C}$

## 6.2 N-acetyl D-ala-D-ala

N-acetyl D-ala-D-ala forms a 1:1 complex with ristocetin at both concentrations of antibiotic (see figures 6.3 and 6.4). However, the titration of a  $0.5 \text{ mgml}^{-1}$  vancomycin solution with this peptide results in an unusual binding isotherm (figure 6.5). The first few injections are increasingly exothermic and then, as the titration progresses, the injections become less exothermic. This is not consistent with simple 1:1 complex formation. Reducing the antibiotic concentration to  $0.1 \text{ mgml}^{-1}$ , gave experimental data that could apparently be fitted to a 1:1 model (figure 6.6). The thermodynamic parameters for the binding of this ligand to vancomycin are given in table 6.3 and in table 6.4 for binding to ristocetin.

**Table 6.3** Thermodynamic parameters of N-acetyl D-ala-D-ala binding to vancomycin

Peptide	Temp (°C)	$K_a$ ( $M^{-1}$ )	$-\Delta H^\circ$ ( $\text{kJmol}^{-1}$ )	$-\Delta G^\circ$ ( $\text{kJmol}^{-1}$ )	$-\Delta S^\circ$ ( $\text{Jmol}^{-1}\text{K}^{-1}$ )	$-\Delta C_p^\circ$ ( $\text{Jmol}^{-1}\text{K}^{-1}$ )
dipeptide <sup>b</sup>	20	7701	33.5 (0.4)	21.8 (0.1)	40 (2)	
	25	6628	35.6 (0.6)	21.8 (0.1)	46 (2)	
	30	5294	37.7 (0.2)	21.6 (0.1)	53 (1)	331 (21)
	35	4260	39.2 (0.2)	21.4 (0.1)	58 (1)	
	45	2924	41.8 (0.3)	21.1 (0.1)	65 (1)	

<sup>b</sup> [vancomycin] =  $0.1 \text{ mgml}^{-1}$

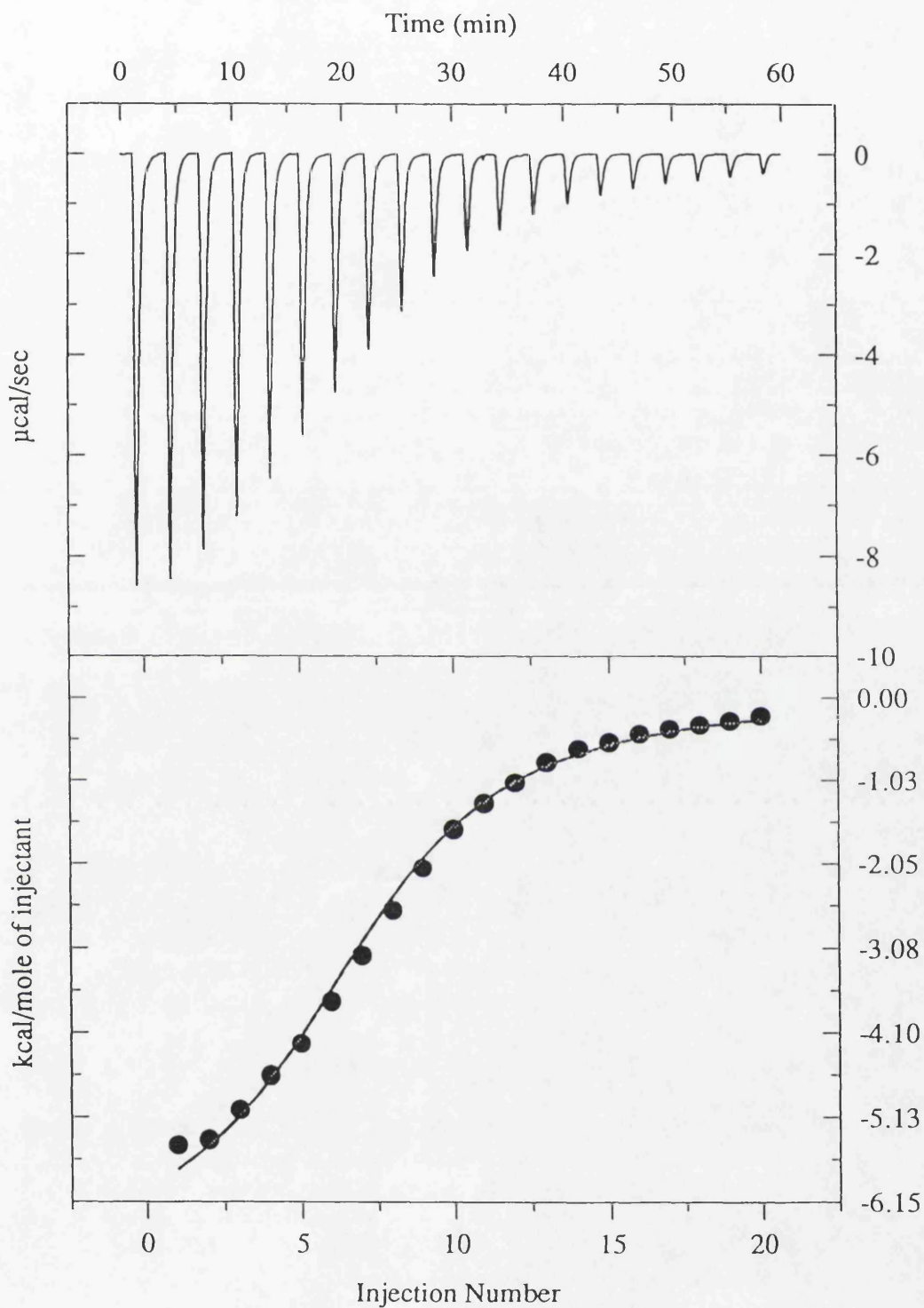


Figure 6.3 Ristocetin ( $0.5\text{mgml}^{-1}$ ) and *N-ac-D-ala-D-ala* at  $25\text{ }^{\circ}\text{C}$

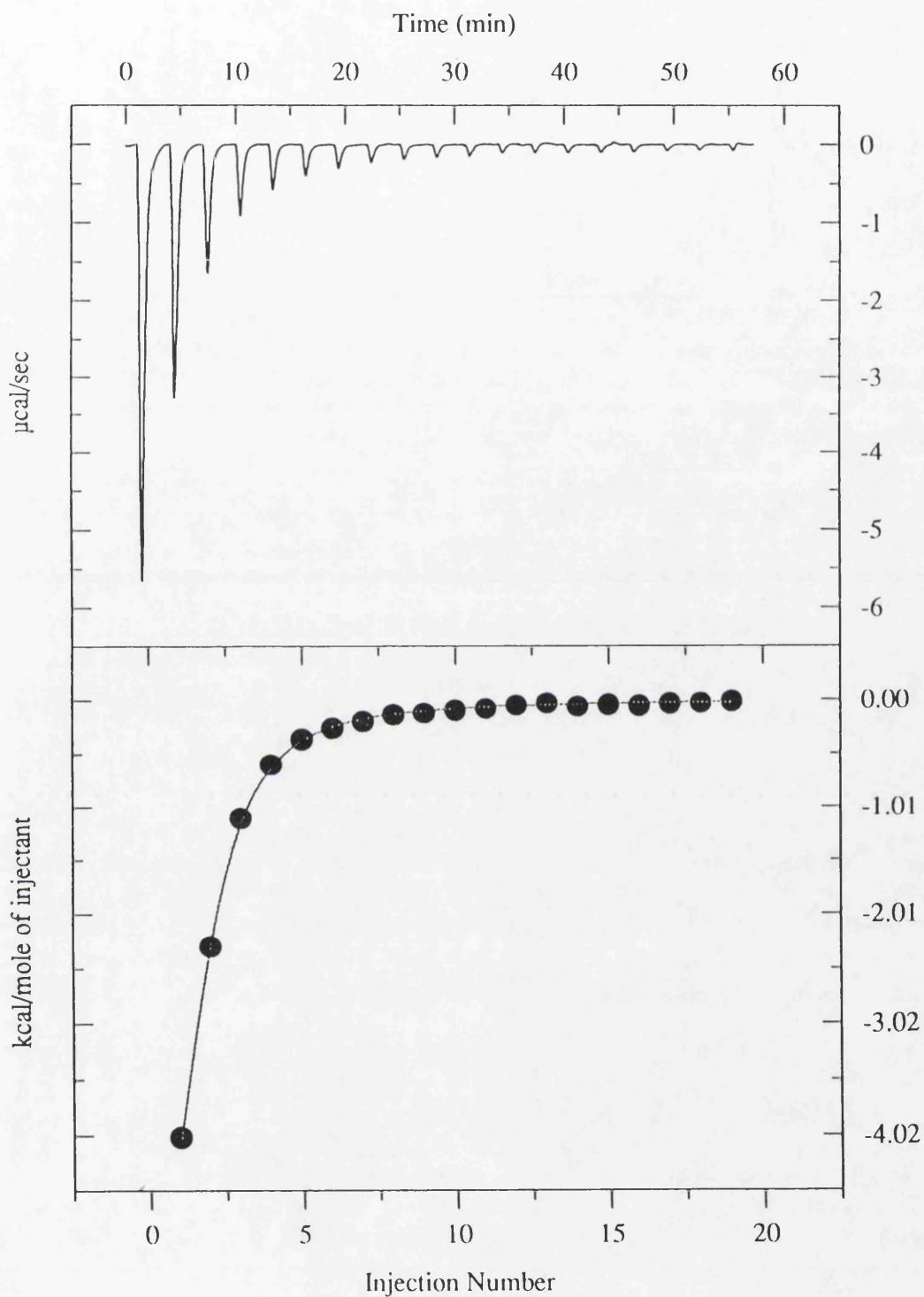


Figure 6.4 Ristocetin ( $0.1 \text{ mgml}^{-1}$ ) and *N-ac-D-ala-D-ala* at  $25^\circ\text{C}$

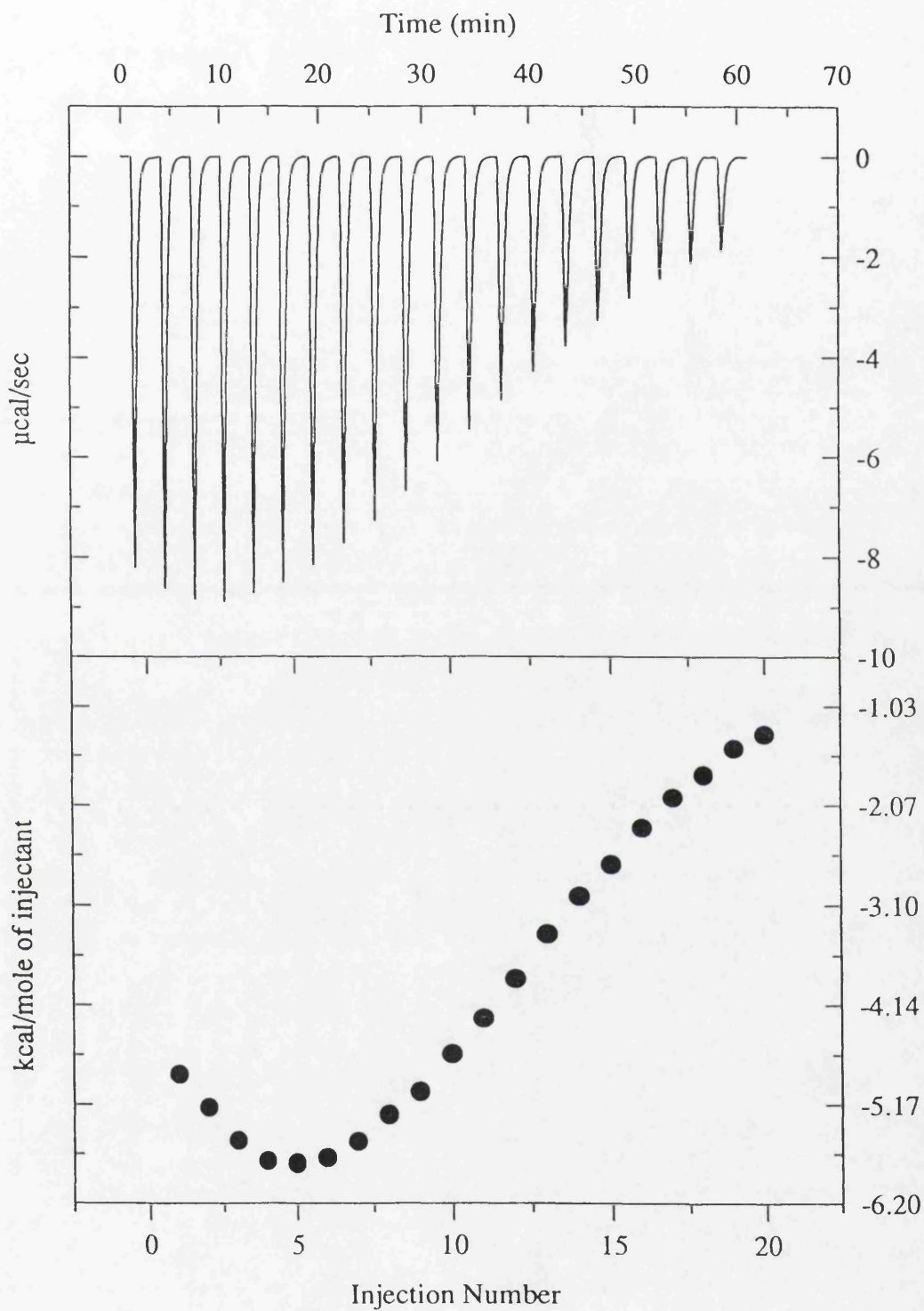


Figure 6.5 Vancomycin ( $0.5 \text{ mgml}^{-1}$ ) and *N-ac-D-ala-D-ala* at  $25^\circ\text{C}$

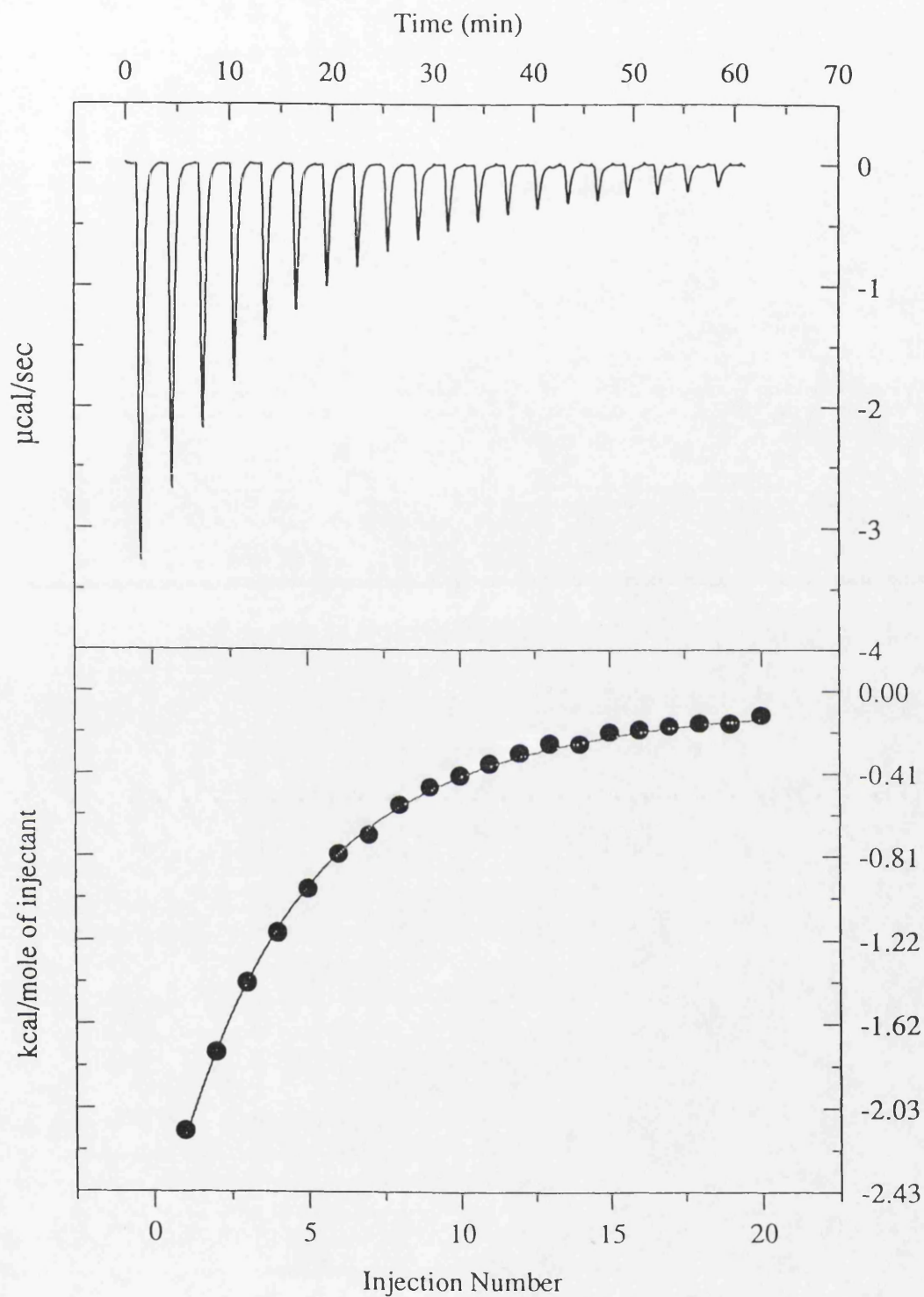


Figure 6.6 Vancomycin ( $0.1 \text{ mgml}^{-1}$ ) and *N-ac-D-ala-D-ala* at  $25^\circ\text{C}$

**Table 6.4** Thermodynamic parameters of *N*-acetyl *D*-ala-*D*-ala binding to ristocetin

Peptide	Temp (°C)	$K_a$ ( $M^{-1}$ )	$-\Delta H^\circ$ ( $kJmol^{-1}$ )	$-\Delta G^\circ$ ( $kJmol^{-1}$ )	$-\Delta S^\circ$ ( $Jmol^{-1}K^{-1}$ )	$-\Delta C_p^\circ$ ( $Jmol^{-1}K^{-1}$ )
dipeptide <sup>a</sup>	20	33759	31.7 (0.5)	25.4 (0.1)	21 (20)	
	25	29508	34.8 (0.8)	25.5 (0.3)	31 (3)	
	30	22998	38.0 (0.9)	25.3 (0.3)	42 (3)	502 (40)
	35	19538	40.6 (0.2)	25.3 (0.1)	50 (1)	
	45	13789	44.2 (0.6)	25.2 (0.2)	60 (2)	
dipeptide <sup>b</sup>	25	40754	33.8 (1.5)	26.3 (0.1)	25 (5)	
	30	35590	36.0 (0.2)	26.4 (0.1)	31 (1)	400 (23)
	35	30083	37.8 (0.3)	26.4 (0.1)	37 (1)	

### 6.3 *D*-ala-*D*-ala

*D*-ala-*D*-ala did not appear to bind to vancomycin or ristocetin. The heat effects observed in these experiments were very small and equivalent to the heats of dilution of the ligand.

### 6.4 Di-*N*-acetyl *L*-lys-*D*-ala-*D*-ala

The binding isotherm for the titration of tripeptide and  $0.5 \text{ mgml}^{-1}$  vancomycin is not consistent with simple 1:1 binding (figure 6.7) and is similar in shape to the binding isotherm of  $0.5 \text{ mgml}^{-1}$  vancomycin and *N*-acetyl *D*-ala-*D*-ala. All the experiments with the tripeptide result in *N* values less than 1, hence the values for  $\Delta G^\circ$ ,  $\Delta H^\circ$  and  $\Delta S^\circ$  (tables 6.5 and 6.6) are merely statistical fitting parameters, although they give an approximate indication of the high affinity of this ligand for the antibiotics.

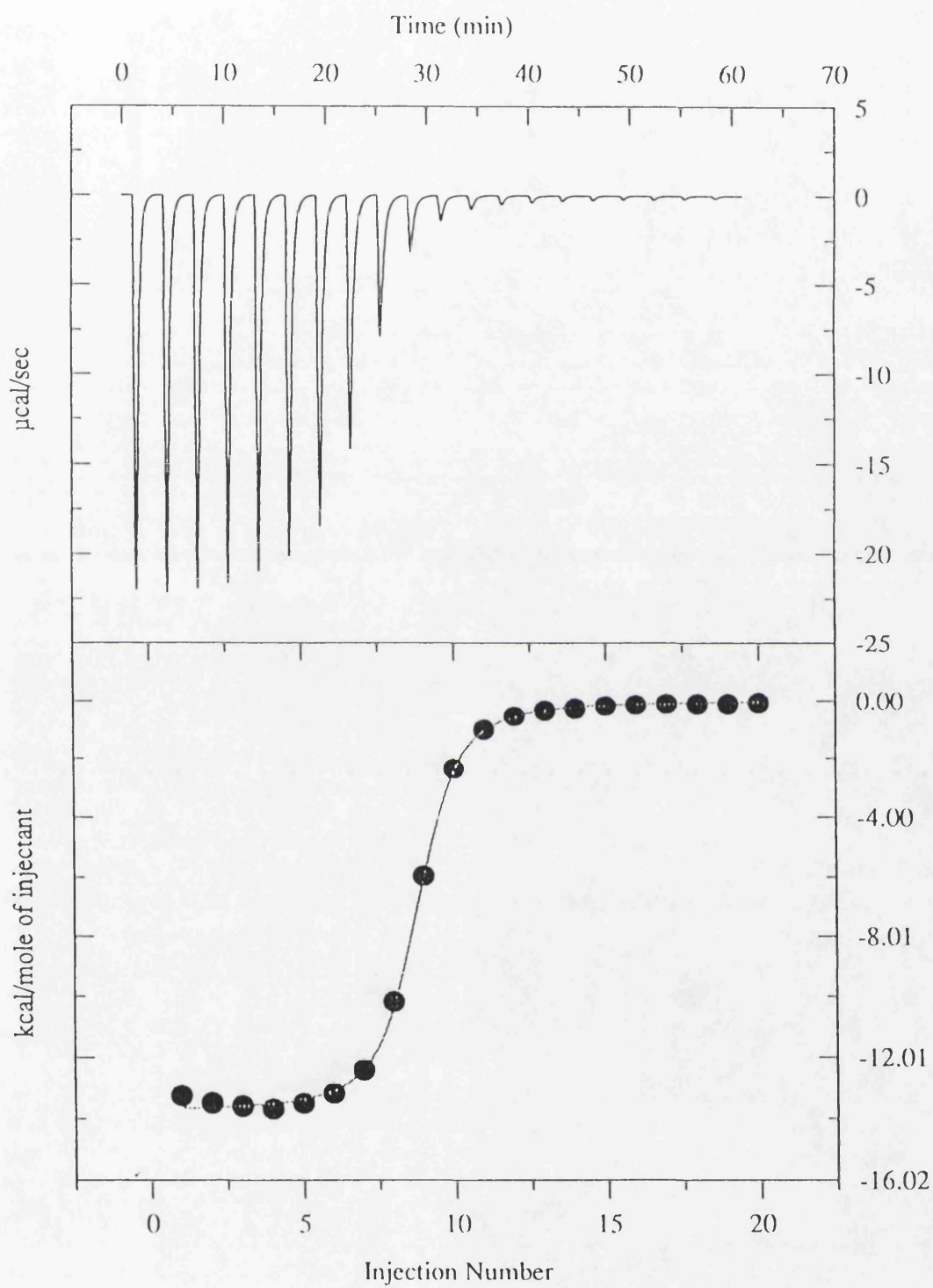


Figure 6.7 Vancomycin ( $0.5 \text{ mgml}^{-1}$ ) and di-N-ac-lys-D-ala-D-ala at  $25^\circ\text{C}$

The increased affinity for the tripeptide ligand to vancomycin appears to arise from a substantial increase in enthalpy change. Examples of titration experiments with this ligand are given in figures 6.8 to 6.10.

**Table 6.5** Thermodynamic parameters of diacetyl-L-lys-D-ala-D-ala binding to vancomycin at 25 °C

	$K_a$ ( $M^{-1}$ )	$\Delta H^\circ$ ( $kJmol^{-1}$ )	$-\Delta G^\circ$ ( $kJmol^{-1}$ )	$\Delta S^\circ$ ( $Jmol^{-1}K^{-1}$ )	N
tripeptide <sup>a</sup>	$6.6 \times 10^5$	57.6 (0.1)	33.2 (0.7)	82 (2)	0.89 (0.01)
tripeptide <sup>b</sup>	$5.2 \times 10^5$	53.3 (1.1)	32.6 (0.1)	69 (4)	0.86 (0.05)

<sup>a</sup> [vancomycin] = 0.5 mgml<sup>-1</sup>

<sup>b</sup> [vancomycin] = 0.1 mgml<sup>-1</sup>

**Table 6.6** Thermodynamic parameters of diacetyl-L-lys-D-ala-D-ala binding to ristocetin at 25 °C.

<sup>a</sup> [ristocetin] = 0.5 mgml<sup>-1</sup>

<sup>b</sup> [ristocetin] = 0.1 mgml<sup>-1</sup>

	$K_a$ ( $M^{-1}$ )	$\Delta H^\circ$ ( $kJmol^{-1}$ )	$-\Delta G^\circ$ ( $kJmol^{-1}$ )	$\Delta S^\circ$ ( $Jmol^{-1}K^{-1}$ )	N
tripeptide <sup>a</sup>	$8.1 \times 10^4$	39.5 (0.5)	28.0 (0.2)	34 (2)	0.89 (0.01)
tripeptide <sup>b</sup>	$1.4 \times 10^5$	38.4 (0.6)	29.4 (0.1)	30 (2)	0.84 (0.01)

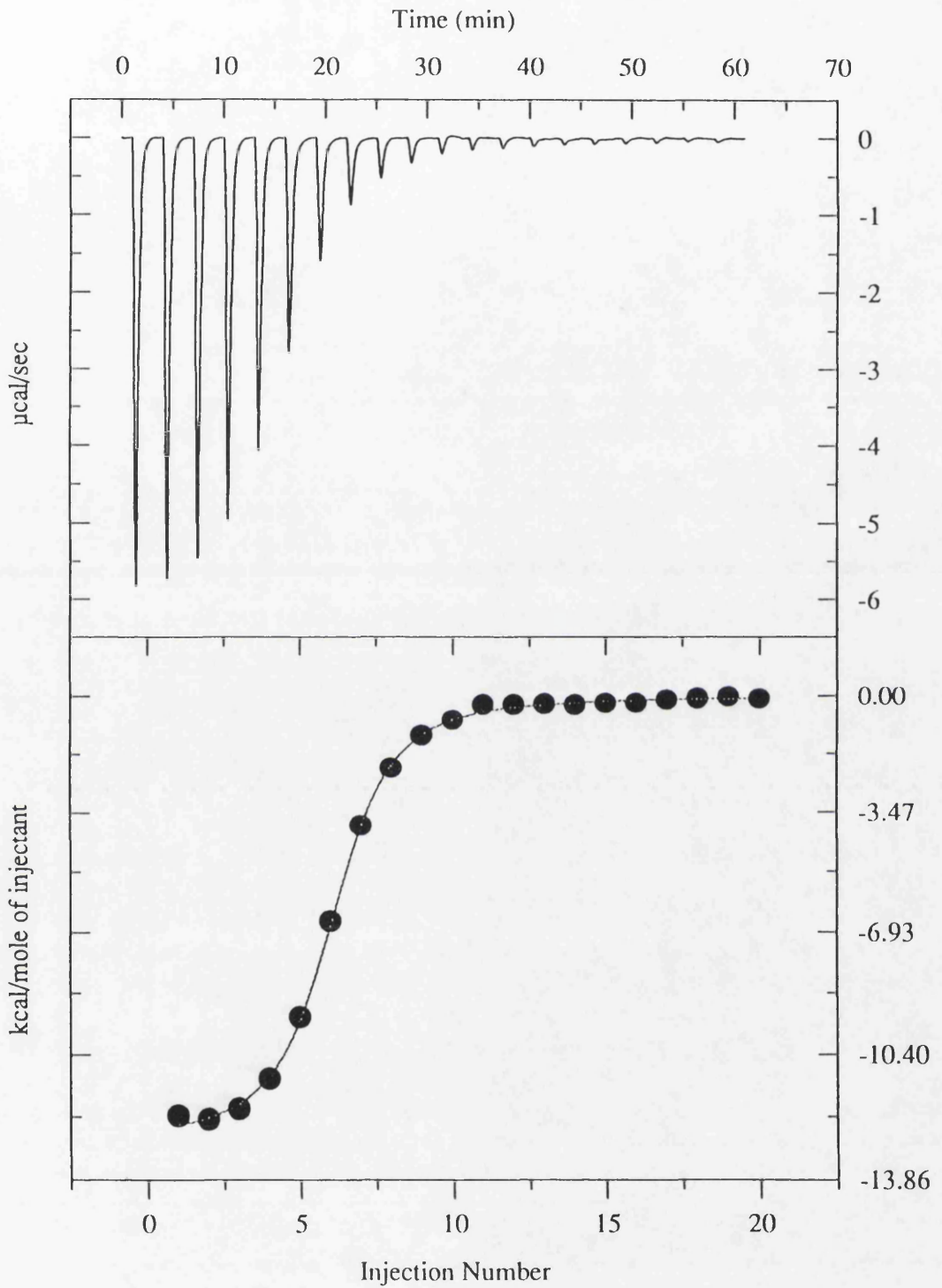


Figure 6.8 Vancomycin ( $0.1 \text{ mgml}^{-1}$ ) and di-N-ac-lys-D-ala-D-ala at  $25^\circ\text{C}$

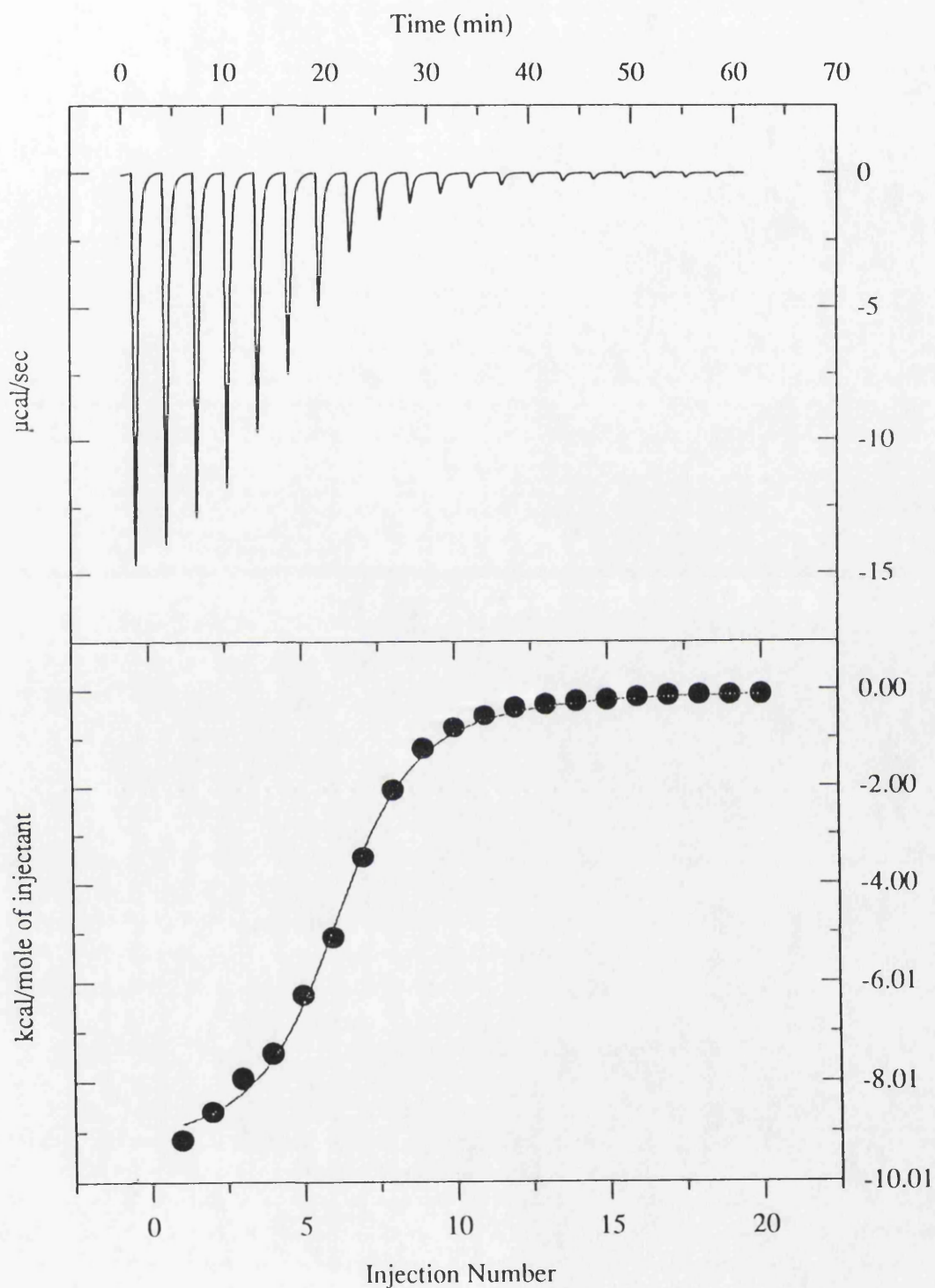


Figure 6.9 Ristocetin ( $0.5 \text{ mgml}^{-1}$ ) and di-N-ac-lys-D-ala-D-ala at  $25^\circ\text{C}$

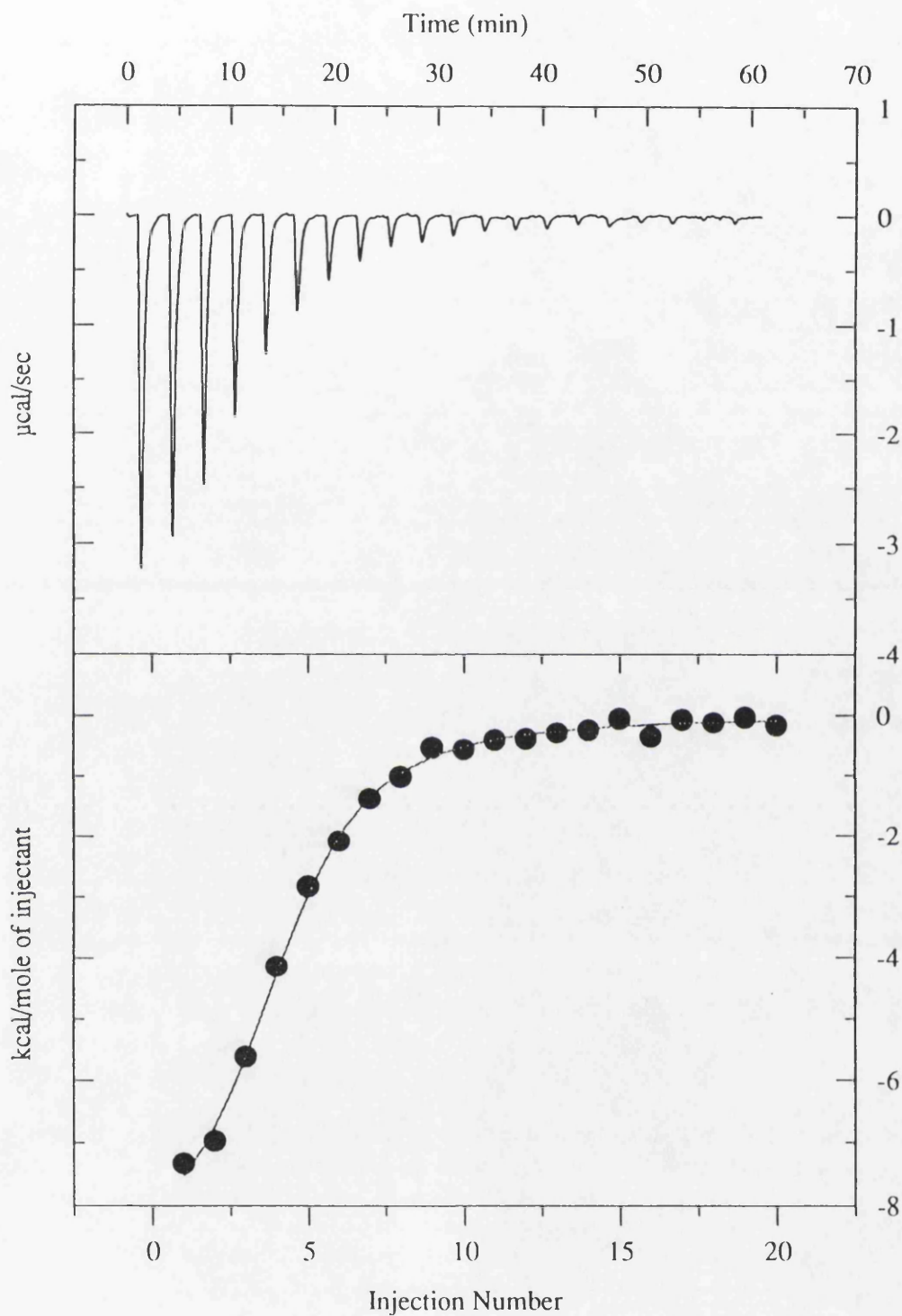
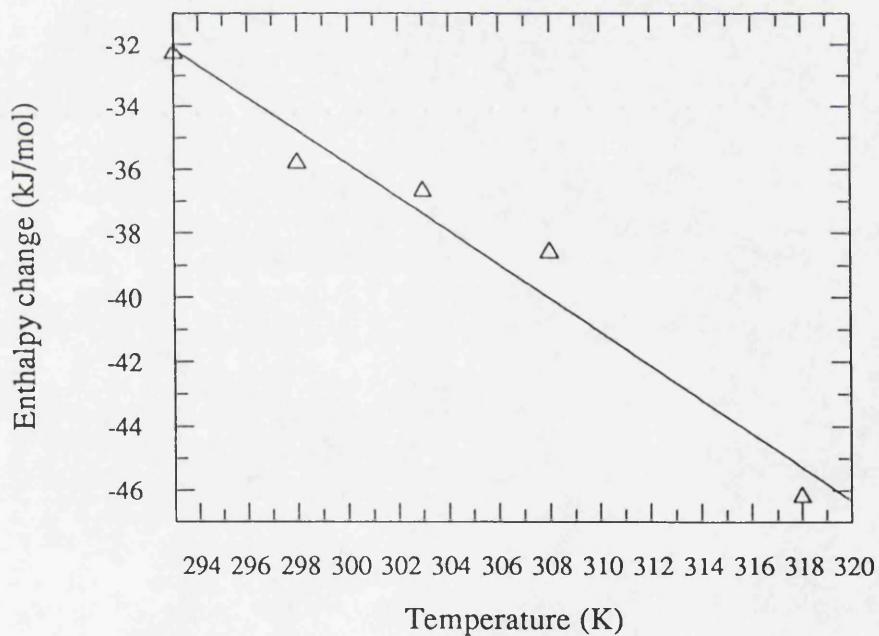


Figure 6.10 Ristocetin ( $0.1 \text{ mgml}^{-1}$ ) and di-N-ac-lys-D-ala-D-ala at  $25^\circ\text{C}$

## 6.5 Heat capacities

The heat capacities quoted in the previous tables were calculated from the gradients of best-fit straight lines through the experimental data of the variation of  $\Delta H^\circ$  with temperature as shown in figures 6.11 to 6.15.



*Figure 6.11* Enthalpy change versus temperature for vancomycin (0.5 mgml<sup>-1</sup>) and *N*-acetyl-*D*-alanine

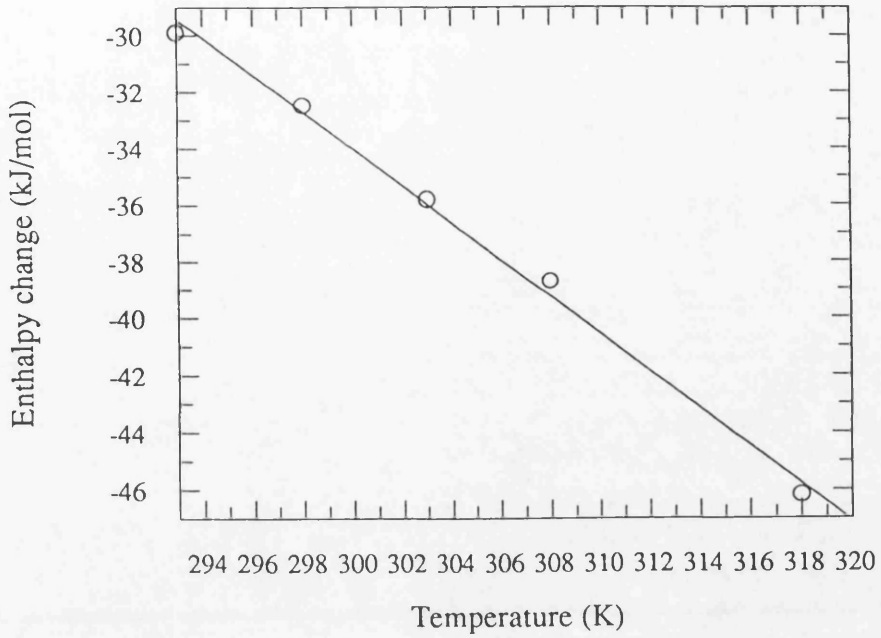


**Figure 6.12** *Enthalpy change versus temperature for ristocetin (0.5 mgml<sup>-1</sup>) and N-acetyl D-alanine*

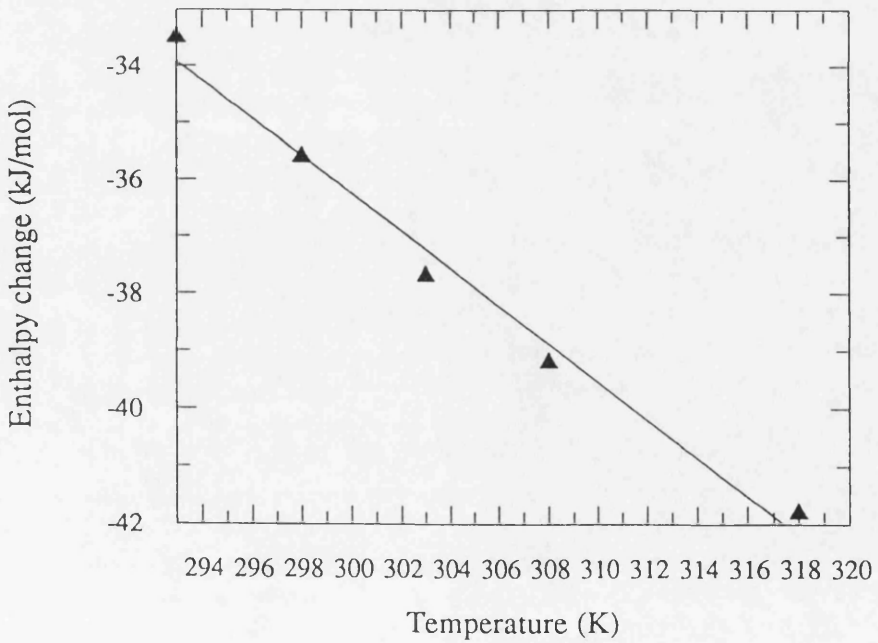


**Figure 6.13** *Enthalpy change versus temperature for vancomycin (0.1 mgml<sup>-1</sup>) and N-acetyl-D-ala-D-ala*

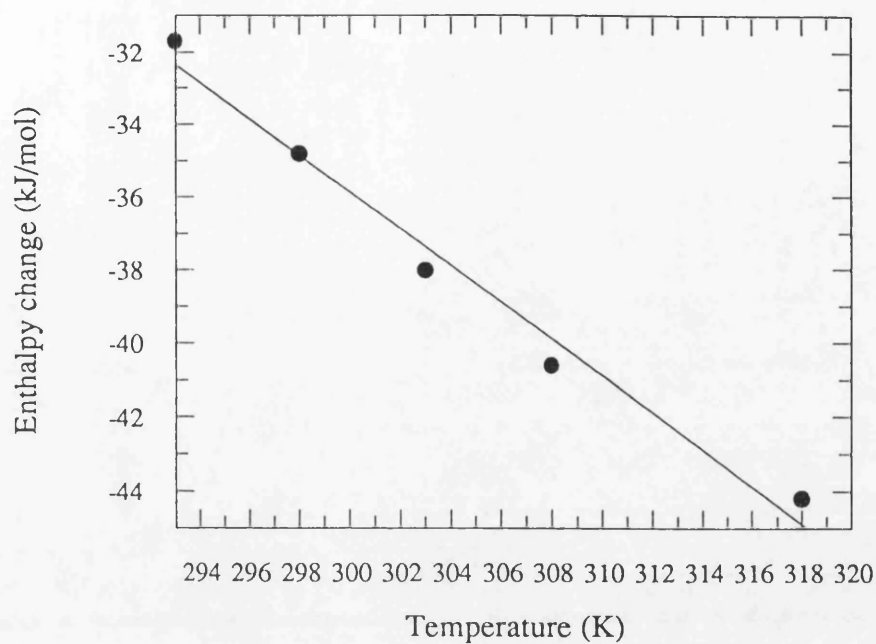


**Figure 6.14** *Enthalpy change versus temperature for ristocetin (0.5 mgml<sup>-1</sup>) and N-acetyl-D-ala-D-ala*

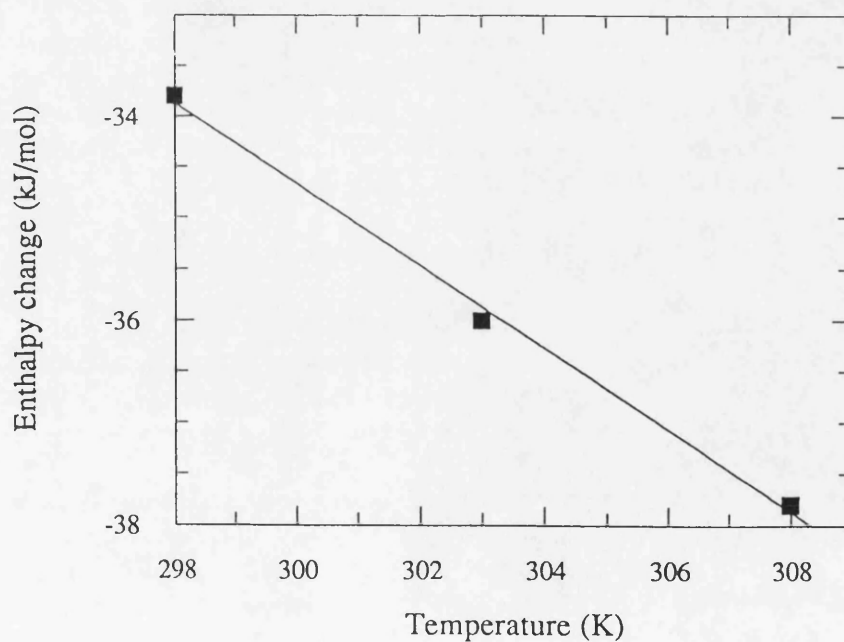


**Figure 6.15** *Enthalpy change versus temperature for ristocetin (0.1 mgml<sup>-1</sup>) and N-acetyl-D-ala-D-ala*

## 6.6 van't Hoff enthalpies

Van't Hoff enthalpies were calculated from the association constants, measured in the calorimetric experiments, by determining the gradients of graphs of  $\ln K$  versus  $1/T$  (figures 6.16 to 6.19). The enthalpy values obtained from these calculations are given in table 6.7.

*Table 6.7 van't Hoff enthalpies*

Experiment	van't Hoff enthalpy
vancomycin <sup>a</sup> + N-ac D-ala	-38.7 kJmol <sup>-1</sup>
vancomycin <sup>b</sup> + N-ac D-ala-D-ala	-48.7 kJmol <sup>-1</sup>
ristocetin <sup>a</sup> + N-ac D-ala	-30.7 kJmol <sup>-1</sup>
ristocetin <sup>a</sup> + N-ac D-ala-D-ala	-28.9 kJmol <sup>-1</sup>

<sup>a</sup> [vancomycin or ristocetin] = 0.5 mgml<sup>-1</sup>

<sup>b</sup> [vancomycin or ristocetin] = 0.1 mgml<sup>-1</sup>

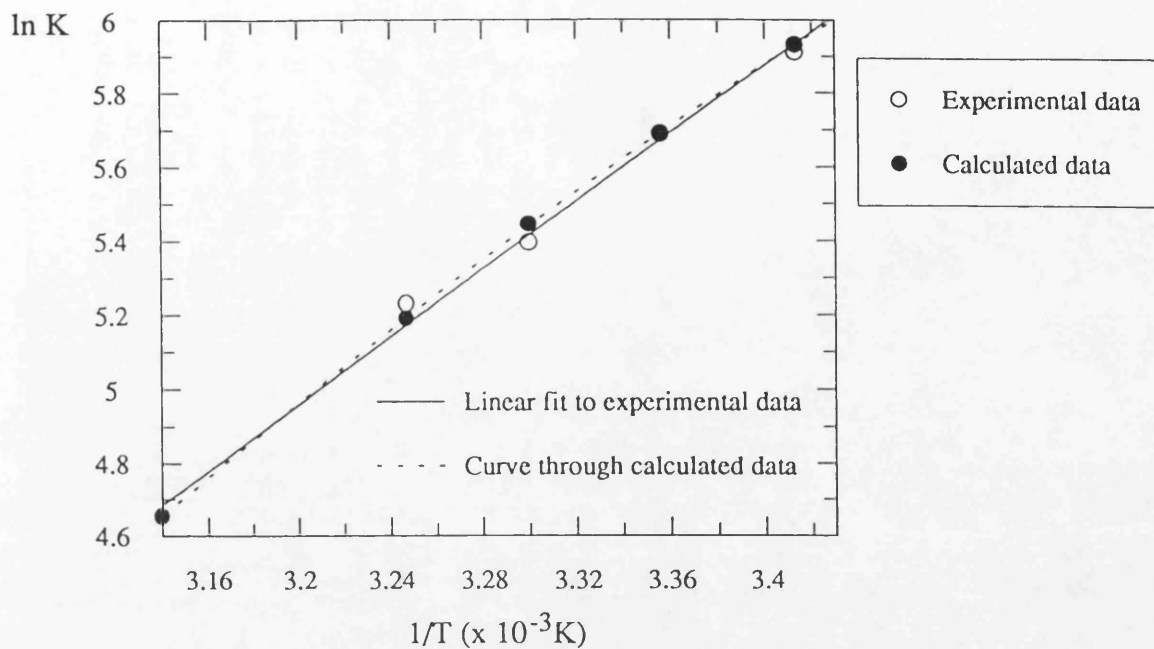


Figure 6.16 van't Hoff plot for vancomycin ( $0.5 \text{ mgml}^{-1}$ ) and N-acetyl D-alanine

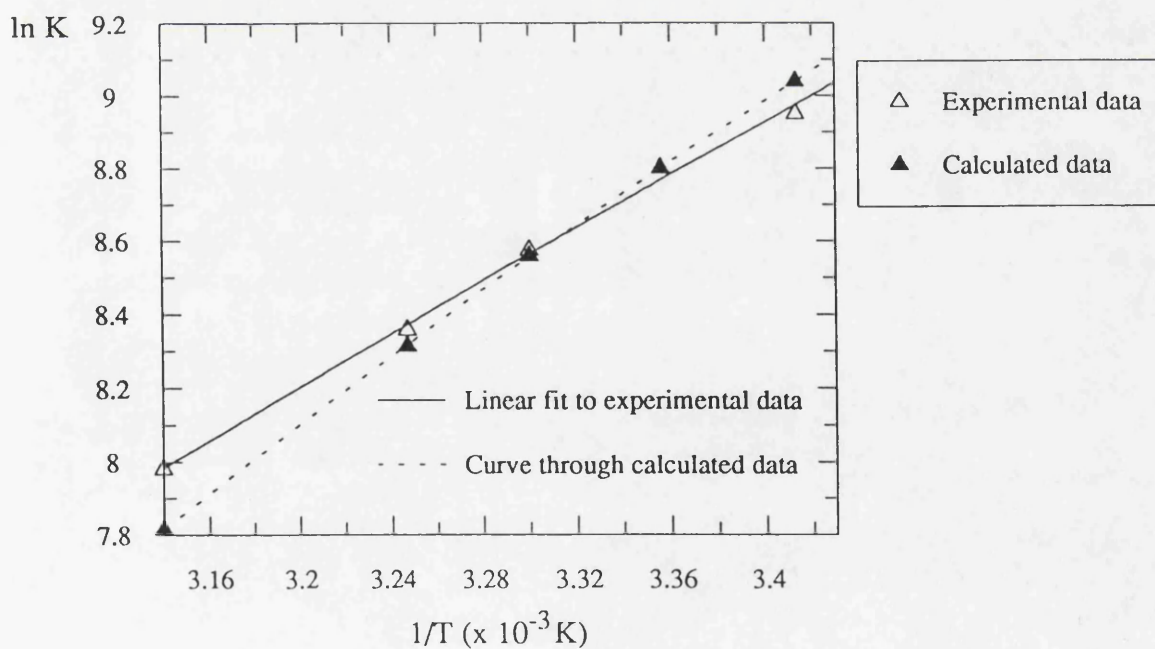


Figure 6.17 van't Hoff plot for vancomycin ( $0.1 \text{ mgml}^{-1}$ ) and N-acetyl-D-ala-D-ala

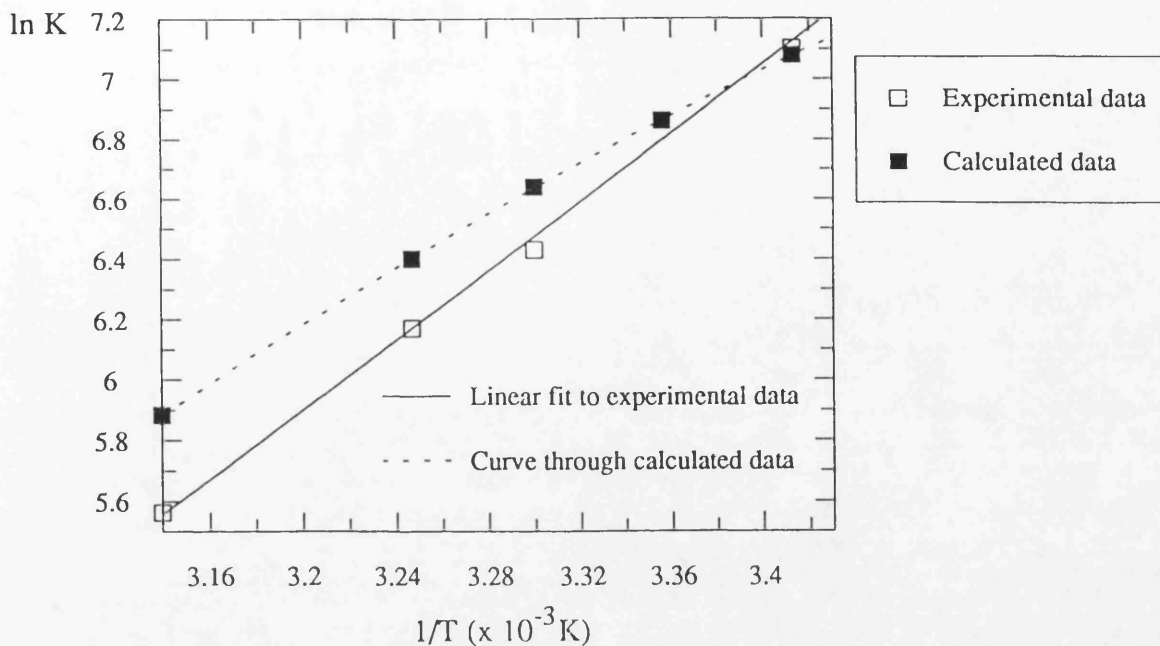


Figure 6.18 van't Hoff plot for ristocetin ( $0.5 \text{ mgml}^{-1}$ ) and N-acetyl D-alanine

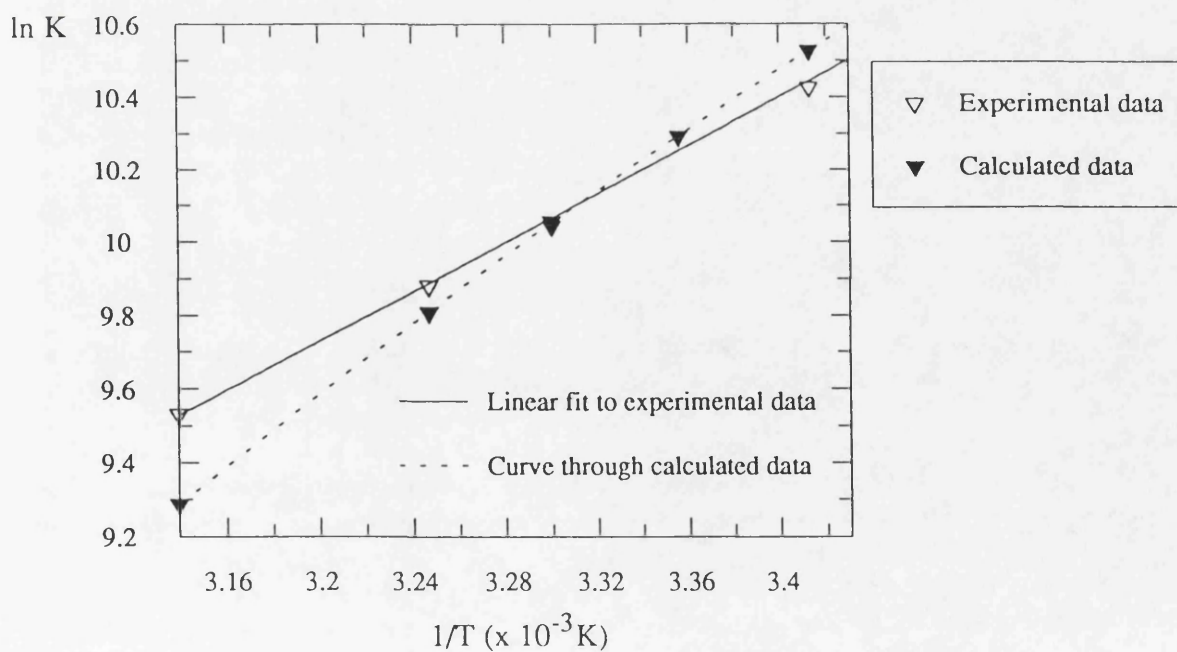


Figure 6.19 van't Hoff plot for ristocetin ( $0.5 \text{ mgml}^{-1}$ ) and N-acetyl-D-ala-D-ala

## 7 DISCUSSION (VANCOMYCIN & RISTOCETIN)

### 7.1 Previous studies

The results presented in chapter 6 were obtained from a series of experiments studying ligand binding to vancomycin and ristocetin with the aim of extending previous thermodynamic studies with these antibiotics. In particular, we wished to study the relative binding modes of several peptide molecules to the antibiotics and to interpret the results in terms of the molecular interactions formed between the ligands and the host molecule.

The types of experiment that have been used in the past to determine the thermodynamics of complex formation between vancomycin or ristocetin and ligands have included UV difference spectroscopy and titration microcalorimetry. The calorimetric titrations, which were used to study the binding of ac-D-ala, ac-D-ala-D-ala, ac-gly-D-ala and ac-D-ala-gly to ristocetin and vancomycin at temperatures of 25, 30 and 37 °C, were carried out with an LKB batch microcalorimeter with titration assembly, and an LKB flow microcalorimeter (Rodriguez-Tebar *et al.*, 1986). Some of the data from these experiments are shown in tables 7.1 and 7.2.

**Table 7.1** Thermodynamics parameters of peptide binding to vancomycin (Rodriguez-Tebar *et al.*, 1986)

	Temp (°C)	$-\Delta G^{\circ}$ (kJmol <sup>-1</sup> )	$-\Delta H^{\circ}$ (kJmol <sup>-1</sup> )	$-\Delta S^{\circ}$ (Jmol <sup>-1</sup> K <sup>-1</sup> )	$-\Delta C_p^{\circ}$ (Jmol <sup>-1</sup> K <sup>-1</sup> )
Ac-D-ala	25	14.0 (0.3)	30.6 (1.2)	56 (5)	
	30	13.9 (0.5)	30.9 (0.8)	56 (4)	93 (15)
	37	13.4 (0.4)	31.7 (1.3)	59 (5)	
Ac-D-ala- D-ala	25	25.8 (0.4)	30.4 (1.6)	15 (6)	
	30	23.4 (0.6)	33.4 (1.8)	33 (8)	582 (45)
	37	20.7 (0.8)	36.5 (1.7)	51 (8)	

There are similarities between the work of Rodriguez-Tebar *et al.* and the results presented in chapter 6: although the magnitude of the numbers might not agree at least the general trends are the same. For example at 25 °C, acetyl D-ala-D-ala binds to both antibiotics with a higher affinity than does acetyl D-ala and both ligands bind to ristocetin with higher affinity than to vancomycin. However, the  $\Delta C_p^{\circ}$  values vary significantly between the two studies, possibly due to the generally larger errors associated with the  $\Delta H^{\circ}$  values determined with the LKB calorimeter. Also, these experiments (Rodriguez-Tebar *et al.*, 1986) were performed over a narrower temperature range and the antibiotic concentrations are not clearly specified and therefore the differences in results could arise from dimerisation effects.

**Table 7.2** Thermodynamics parameters of peptide binding to ristocetin (Rodriguez-Tebar *et al.*, 1986)

	Temp (°C)	$-\Delta G^{\circ}$ (kJmol <sup>-1</sup> )	$-\Delta H^{\circ}$ (kJmol <sup>-1</sup> )	$-\Delta S^{\circ}$ (Jmol <sup>-1</sup> K <sup>-1</sup> )	$-\Delta C_p^{\circ}$ (Jmol <sup>-1</sup> K <sup>-1</sup> )
Ac-D-ala	25	17.4 (0.5)	28.3 (1.4)	37 (6)	
	30	17.2 (0.3)	29.2 (1.7)	39 (7)	332 (59)
	37	16.2 (0.3)	32.2 (1.6)	52 (6)	
Ac-D-ala- D-ala	25	28.8 (0.4)	25.4 (1.6)	-11 (6)	
	30	23.4 (0.3)	28.0 (1.5)	15 (6)	582 (45)
	37	20.7 (0.3)	30.1 (1.8)	30 (7)	

Another thermodynamic study of antibiotic-peptide complex formation involved using UV difference spectroscopy to determine association constants (Williamson *et al.*, 1984). The experiments were conducted at four temperatures, between 28 and 65 °C, and the enthalpy values were estimated from van't Hoff plots. The buffer system used in these experiments was 0.02 M sodium citrate at pH 5.0 and the results are given in table 7.3. Again, in this study the same general trends are observed even though there are numerical differences.

**Table 7.3** UV studies (Williamson *et al.*, 1984)

		dipeptide	tripeptide
Vancomycin	$\Delta G^\circ$ (kJmol <sup>-1</sup> )	25.9 (0.4)	35.6 (0.4)
	$\Delta H^\circ$ (kJmol <sup>-1</sup> )	32 (8)	73 (10)
Ristocetin	$\Delta G^\circ$ (kJmol <sup>-1</sup> )	31.4 (0.4)	33 (0.4)
	$\Delta H^\circ$ (kJmol <sup>-1</sup> )	31.4 (8)	42 (8)

## 7.2 Present work

The calorimetric experiments clearly show that the binding affinities of the ligands to the antibiotics increase as the length of the peptide increases, with the exception of D-ala-D-ala. To rationalize these results, we must consider the known structures of the antibiotic/ligand complexes (figure 7.1).

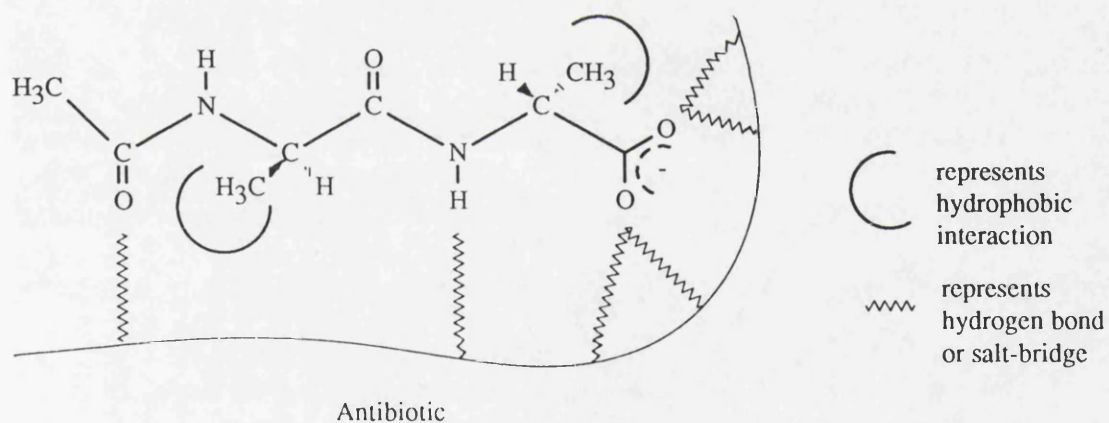


**Figure 7.1** Interactions between ristocetin or vancomycin and N-acetyl D-ala-D-ala

For example, the complex between the antibiotics and N-ac-D-ala-D-ala is stabilised by five hydrogen bonds; three of these are to the carboxylate group and two to amide groups in the peptide. The other possibly significant contribution to binding is the hydrophobic interaction between the alanine methyl groups and surrounding benzene rings of the antibiotic.

In the N-ac-D-ala complex, four of the five hydrogen bonds should still be in place, however the hydrophobic interaction with the second alanine methyl group will not be present. Hydrogen bond formation is thought to be accompanied by very small enthalpic changes but by larger entropic changes and similarly the hydrophobic effect is mainly an entropy driven effect. This is qualitatively reflected in the calorimetric results: the enthalpy values for ristocetin with N-ac-D-ala and N-ac-D-ala-D-ala are very similar, but  $\Delta S^\circ$  is more negative by about  $20 \text{ Jmol}^{-1}\text{K}^{-1}$ .

The antibiotic complexes with D-ala-D-ala should involve four hydrogen bonds and hydrophobic interactions between the two methyl groups and the antibiotic. However, D-ala-D-ala does not appear to bind to either ristocetin or vancomycin. The reason for this must presumably be concerned with the free, charged amino group. The other alternative is that the peptide does bind but with  $\Delta H^\circ$  approximately equal to zero, however, UV difference spectroscopy has also failed to find evidence for complex formation.

The heat capacity changes were large and negative for all the antibiotic/analogue peptide complexes. The observed negative  $\Delta C_p^\circ$  values probably arise from the transfer of the peptide from water to a more hydrophobic environment and from the conformational change which takes place on binding resulting in the burial of some hydrophobic side-chains of the antibiotic.

The  $\Delta C_p^\circ$  values given in chapter 6 were calculated from the temperature dependence of the enthalpy changes, however,  $\Delta C_p^\circ$  can also, in principle, be estimated from the degree of curvature in the van't Hoff plot. Plotting  $\ln K$  versus  $1/T$  will produce a linear relationship with gradient equal to  $-\Delta H^\circ/R$ , providing  $\Delta C_p^\circ$  is equal to zero. If  $\Delta C_p^\circ$  is not equal to zero then a curve is obtained in the van't Hoff plot. Hence it should be possible to calculate  $\Delta C_p^\circ$  values from the association constants determined in the calorimetric experiments.

Van't Hoff plots for each antibiotic/peptide complex were constructed using the association constants measured in the calorimetric titrations. From inspection of these plots, the gradients appear to be linear rather than curved (within experimental error). Theoretical curves were drawn on the van't Hoff plots using the  $\Delta C_p^\circ$  values determined from the relationship between  $\Delta H^\circ$  and  $T$  (see figures 6.16 to 6.19). In most cases the experimental and calculated points are similar. The largest deviation occurs with ristocetin and N-ac-D-alanine. these van't Hoff plots demonstrate the inaccuracy that can arise when using the van't Hoff equation to determine  $\Delta H^\circ$  and  $\Delta C_p^\circ$ .

### 7.3 Dimerisation Effects

It has been documented that free and complexed ristocetin dimerises even at low concentrations (Waltho & Williams, 1989). An association constant of  $2 \times 10^3 \text{ M}^{-1}$  for dimer formation of the ristocetin/tripeptide complex has been calculated from NMR measurements. Similarly, vancomycin is known to aggregate and an association constant for dimer formation of  $8 \times 10^2 \text{ M}^{-1}$  has been proposed (Nieto & Perkins, 1971a). It is possible that the antibiotic-peptide complexes will have different dimerisation constants compared to the free antibiotics. Ristocetin is believed to form dimers more readily in the presence of tripeptide since the carboxylate anion can

interact indirectly with the protonated amine of ristosamine in the other half of the dimer (Waltho & Williams, 1991). Also, the hydrogen bonds between the ristocetin molecules are more buried from the surrounding water and hence are strengthened when the peptide is bound.

Using the dimerisation constants for both antibiotics, it can be estimated that a substantial amount of the dimeric species of vancomycin or ristocetin is present at concentrations of  $0.5 \text{ mgml}^{-1}$ , but, when the antibiotic is diluted by a factor of 5, the monomeric species is prevalent. However it should be noted that the dimerisation constant for ristocetin applies only to the ristocetin/tripeptide complex and not to free ristocetin, which may dimerise to a lesser extent. Assuming that the ligands bind differently to the dimer than to the monomer, the thermodynamic parameters should show concentration dependent differences.

There is some evidence from the calorimetric experiments of dimer formation in the case of vancomycin with the peptides, N-acetyl D-ala-D-ala and the tripeptide ligand. Unusual binding isotherms are observed at a high concentration of vancomycin, whereas, the more usual 1:1 binding isotherms are observed at lower antibiotic concentrations. In an attempt to rationalize the binding curves for  $0.5 \text{ mgml}^{-1}$  vancomycin with N-ac D-ala-D-ala, the data were analysed using the two sets of sites binding model, with the antibiotic concentration set at half its real value (i.e. assuming that the antibiotic was fully dimerised). The data could be analysed in this way, but only if the peptide binds at one site on the dimer with an endothermic  $\Delta H^\circ$  value and at the other site with an exothermic  $\Delta H^\circ$  value. This model was deemed to be unsatisfactory in explaining ligand binding to vancomycin (since the antibiotic is unlikely to be 100% dimerised and since the two binding sites of the dimer should be very similar) and an alternative model was proposed. In this new model, it is assumed that the ligand is binding to both the monomeric form (giving  $K_1$  and  $\Delta H_1$ ) and the

dimeric form (giving  $K_2$  and  $\Delta H_2$ ) of vancomycin and that the dimer binding sites are identical. The formation of the dimer from two monomers ( $K_d$  and  $\Delta H_d$ ) is also included in the calculation. Using this model and estimating the various binding constants, dimerisation constants and enthalpy values, sample titration data could be generated which show very close similarities to the observed titration data. An example is given in figure 7.2. In this example the following values were assigned:

$$K_1 = 5000 \text{ M}^{-1} \quad \Delta H_1 = -37 \text{ kJmol}^{-1}$$

$$K_2 = 100000 \text{ M}^{-1} \quad \Delta H_2 = -58 \text{ kJmol}^{-1}$$

$$K_d = 10 \text{ M}^{-1} \quad \Delta H_d = 0$$

It is also possible to calculate the dimerisation constant ( $K_{d'}$ ) and enthalpy change ( $\Delta H_{d'}$ ) for the following association, where A represents the antibiotic and X represents the ligand:



This is done using the equations:

$$K_{d'} = K_d \cdot K_2^2 / K_1^2 \quad \text{and} \quad \Delta H_{d'} = \Delta H_d + 2(\Delta H_2 - \Delta H_1).$$

$K_{d'}$  is calculated to be  $4000 \text{ M}^{-1}$  and  $\Delta H_{d'}$  is equal to  $-42 \text{ kJmol}^{-1}$  for the vancomycin-N-acetyl-D-ala-D-ala example. Hence dimerisation is enhanced by the presence of the peptide ligand.

Although this model explains the observed titration data, it is not possible to obtain the thermodynamic parameters directly from the calorimetric data because of the large number of variables in the analysis.

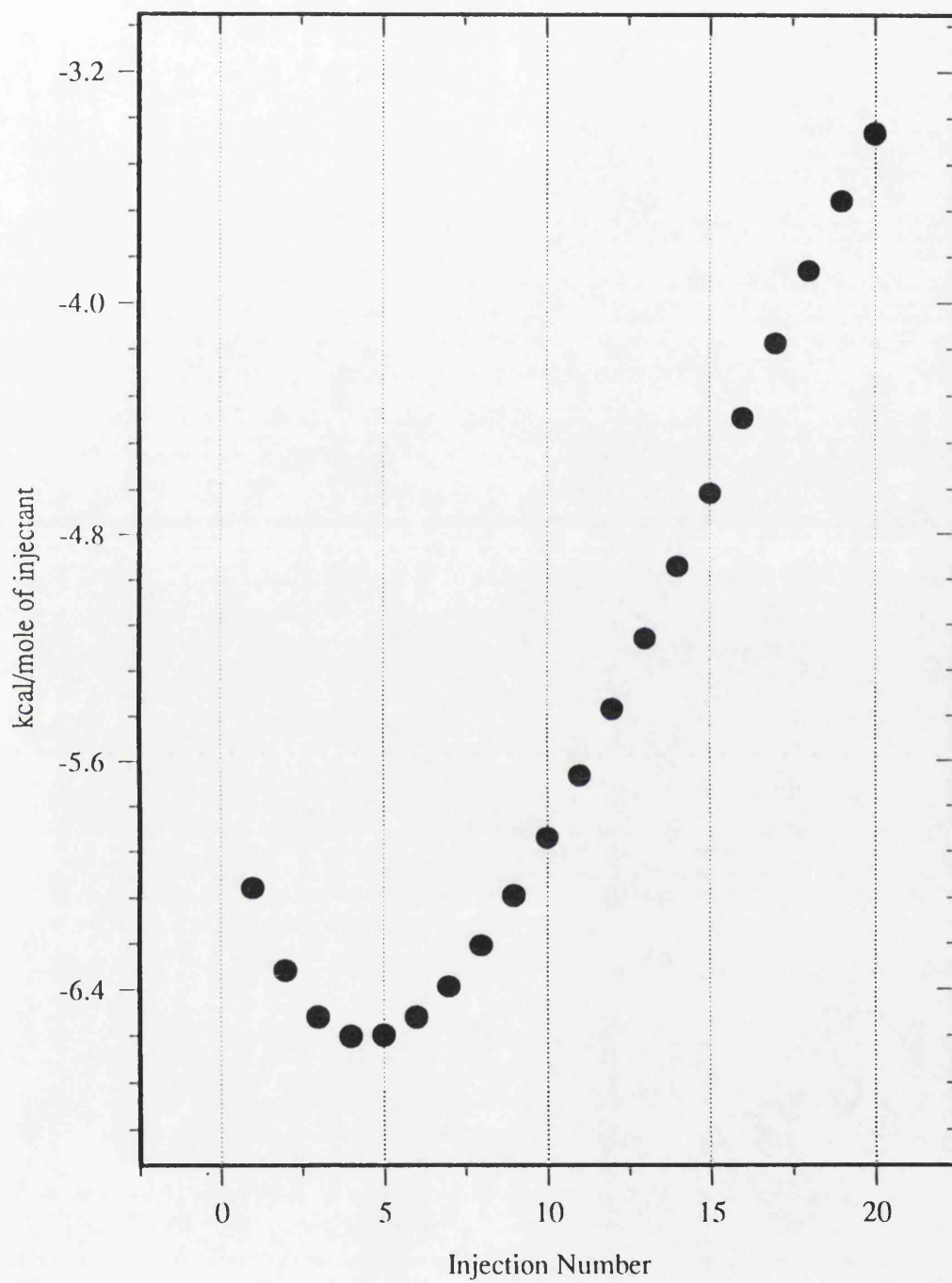


Figure 7.2 Example of simulated titration data for vancomycin ( $0.5 \text{ mgm}l^{-1}$ ) and N-acetyl D-ala-D-ala

## 8 CONCLUSIONS

The aim of this thesis was to study the thermodynamics of molecular recognition. The first model system, PGK, proved to be a more complex system than originally thought. However, microcalorimetry was able to characterize the thermodynamic parameters associated with the binding of substrates and ligands to the enzyme. The high affinity binding of 3-phosphoglycerate to PGK is mainly entropy driven, with a small exothermic contribution to binding. Titrations of PGK with 3-phosphoglycerate in different buffer systems yielded an assortment of  $\Delta H^\circ$  and  $K_a$  values, which can be explained by substrate deprotonation upon binding to the enzyme. The release of protons to the buffer during binding gives rise to an additional heat effect which is detected by the calorimeter. Several anions were observed to inhibit the binding of 3-phosphoglycerate, for example, sulphate, chloride and triphosphate.

The nucleotide substrates appear to bind to PGK at more than one site. The binding curves could be analysed assuming either a single binding site or two different binding sites but during studies of the formation of the ternary complex, it became obvious that ADP must bind to more than one site. One of these binding sites appears to be competitive with 3-phosphoglycerate and thus the presence of ADP in the reaction cell leads to a significant decrease in the binding affinity of 3-phosphoglycerate.

Two mutant forms of PGK were also studied by microcalorimetry. The mutation in the interdomain region of PGK has little effect on the thermodynamics of

substrate binding. However as might be expected, the mutation in the active site area results in very different thermodynamic behaviour.

The antibiotic model system was an easier system to study by microcalorimetry. The binding isotherms, in the majority of cases, could be analysed assuming a single binding site per antibiotic molecule. There was a clear trend between binding affinity and the length of the peptide ligand. Two concentrations of antibiotic were used during the experiments and it was found that the binding parameters for the associations of vanomycin with N-acetyl D-ala-D-ala and the tripeptide were dependent on the antibiotic concentration. This suggested that the antibiotic was dimerising at the higher concentration. The unusual binding curves which were observed in these experiments could be simulated assuming that the ligand binds preferentially to the dimer molecule. The change in heat capacity associated with binding was measured using two methods: the van't Hoff relationship and the dependence of  $\Delta H^\circ$  on temperature. The results for  $\Delta C_p^\circ$  were consistent with a reduction in the hydrophobic surface area accessible to solvent upon complex formation.

## Appendix A Protein Engineering

### Overview of site-directed mutagenesis

Protein engineering is concerned with the modification of protein structures. The aim is to improve the properties of a protein in a specific way i.e. change the substrate specificity of an enzyme or increase the stability of a protein. The structure of a protein can be altered in several ways: amino acid residues can be modified directly by chemical reactants or indirectly by altering the gene encoding for the protein. This second technique, protein engineering, enables amino acid residues to be substituted with any other naturally occurring amino acid.

The instructions for the biosynthesis of a protein are contained within a segment of the DNA called a gene. The gene is first transcribed to produce a complementary nucleic acid, messenger RNA, which is then translated into the protein chain. Each amino acid is designated by a sequence of three nucleotides (or codon) and therefore changing the nucleotide sequence of the codon introduces an amino acid replacement: this process is known as site-directed mutagenesis.

Once the gene has been altered it is cloned (reproduced identically) in a microorganism. However if a fragment of DNA is inserted directly into a cell it will not be replicated since it lacks the necessary coding regions to effect replication. The DNA fragment must be joined to another DNA molecule which is capable of directing its own replication. The carrier DNA is called a vector.

## Recombinant DNA technology

The methods used in recombinant DNA technology require several key enzymes: restriction endonucleases, DNA ligase and DNA polymerase. Genes can be removed from a chromosome using restriction endonucleases, and inserted into a vector using DNA ligase. This ability to form novel DNA molecules is known as recombinant DNA technology.

Restriction endonucleases are enzymes found in bacteria which were discovered to be able to kill viruses by splicing the viral DNA. Each enzyme recognises a sequence of usually 4 or 6 bases and then cuts the DNA in this region. The recognition sequences are symmetrical, that is, there are the same bases in each strand but they run in opposite directions. Restriction enzymes may cut in the centre of the sequence to give "blunt ends" or several base pairs apart to leave single-stranded tails or "sticky ends".

Restriction endonucleases are used in genetic engineering to cut a DNA molecule into fragments which can then be separated by gel-electrophoresis and the fragment containing the desired gene isolated. Fragments of DNA which have been cut with the same restriction enzyme to give complementary sticky ends can be covalently joined by DNA ligase. DNA ligase from phage T4 is also able to join molecules with blunt ends but with very low efficiency. DNA ligase and the restriction endonucleases allow DNA sequences to be recombined *in vitro* at will.

DNA polymerase I can synthesize double-stranded DNA from a template-primer complex. In addition to its 5' to 3' polymerase activity, this enzyme has two exonuclease activities: one acting in the 5' to 3' direction and the other in the 3' to 5' direction. The Klenow fragment of DNA polymerase I has the polymerase and 3' to 5' exonuclease activities only. In the presence of excess nucleoside phosphates, its

exonuclease activity is suppressed and it can be used to generate double-stranded DNA from a single-stranded DNA template and primer.

## **Vectors**

Vectors are usually plasmids or bacteriophages. A plasmid is a small, circular molecule of double-stranded DNA with the ability to undergo autonomous replication. The requirements of a vector are that it must have single restriction sites and clear selection markers. Selection markers are, for example, a resistance to an antibiotic: cells that have taken up the plasmid can be identified by plating the culture on media containing the antibiotic, only the cells containing the plasmid will be able to grow. Plasmids need to be small to increase the efficiency of transformation. A plasmid can be used as a cloning vector in two unrelated hosts, this requires two different origins of replication and the vector is called a shuttle vector.

The foreign DNA gene is inserted into the plasmid by cutting the DNA molecule with a restriction enzyme and then inserting the fragments into plasmid vectors cut open with the same enzyme. DNA ligase completes the newly formed plasmid. It is possible to achieve over-expression of a protein in the microorganism by inserting multiple copies of the plasmid into the cell and so a high yield of the protein can be obtained.

## **Transformation**

The recombinants are introduced into the host cell by the process of transformation. This requires extreme conditions and is a low efficiency process. The selection markers are used at this stage to select colonies which have taken up the

plasmid. Since all the colonies will not contain the gene of interest a selection procedure is required. The host cells can then be cultured and protein extracted.

### **Site-Directed Mutagenesis**

This method allows single amino acid substitutions to be made in any part of the protein molecule. The vectors used for site-directed mutagenesis usually are based on M13: a bacteriophage which replicates inside a host cell as double-stranded DNA but the DNA is later packaged and passed on as single-stranded DNA which can easily be isolated from the phage particles. The double-stranded form of the M13 vector is isolated from infected cells and genes to be cloned are inserted. Single-stranded versions of the cloned gene are obtained from the phage particles.

An oligonucleotide, 15-20 bases long, is synthesized; this is easily done using e.g. automated solid-state phosphoramidite techniques. This oligonucleotide is complementary to the gene around the site of mutation but contains a mismatch at the base that is to be mutated. The oligonucleotide hybridizes to the single-stranded DNA and then DNA polymerase synthesizes the remainder of the strand. DNA ligase joins the ends of the synthetic primer to the new DNA. This vector can now be introduced into *E.coli* and the progeny cells will contain either the wild-type or mutant gene. The M13 vector is then isolated, the mutant gene excised, inserted into a suitable vector and used to transform an appropriate organism (Zoller & Smith, 1982)(figure A.1).

### **Comparison of wild-type and mutant enzymes**

Once a site-directed mutant has been prepared, its behaviour can be compared with wild-type to give an indication of the effect of the mutation. Most mutations are

designed to delete a single interaction, such as a hydrogen bond or salt-bridge. The only difference between the wild-type and mutant enzyme should be at the changed side-chain, however, it is possible that the mutant may be structurally altered or incorrectly folded and it is therefore necessary to verify the structure of the mutant so that a meaningful comparison can be made.

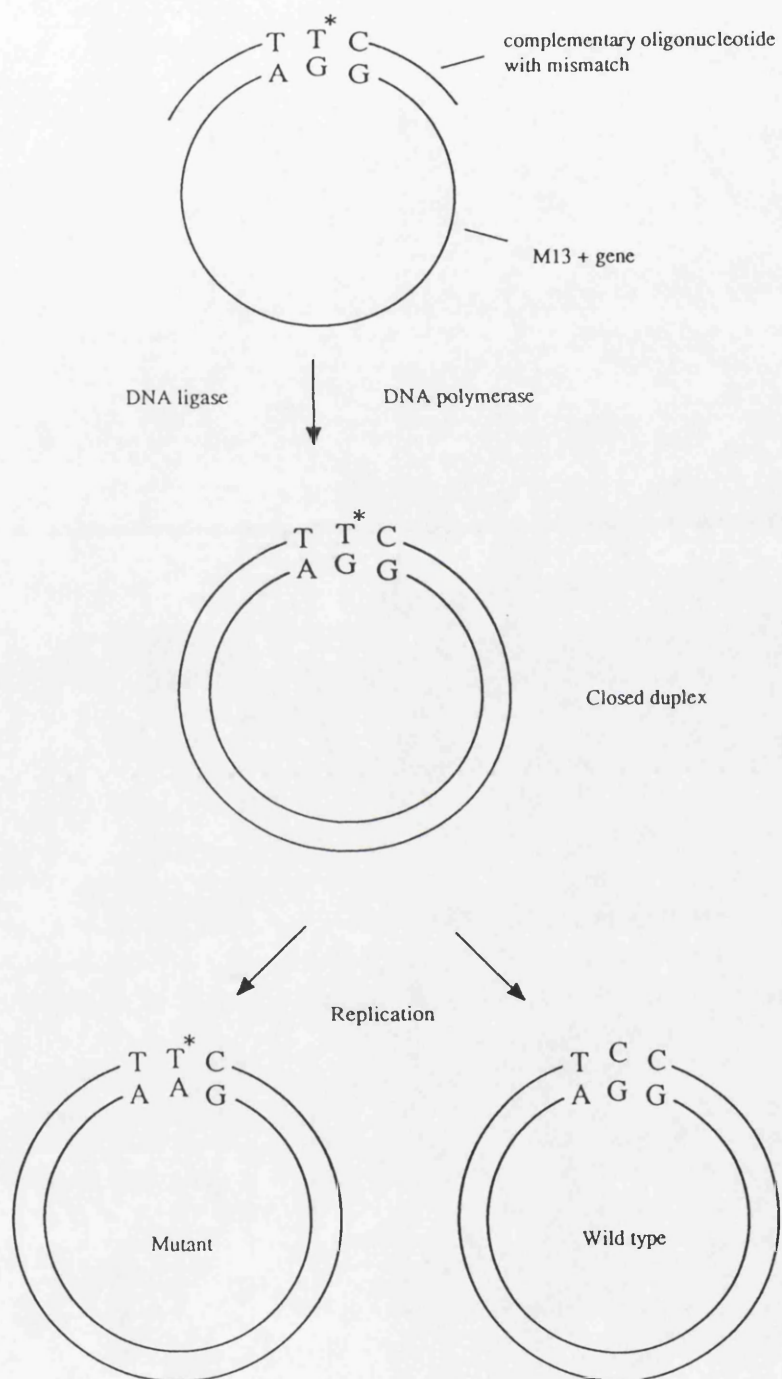


Figure A.1 Strategy for site-directed mutagenesis

## Appendix B Analysis of enzyme kinetic data

The Michaelis-Menten equation (eqn. 1.15) can be re-arranged in several ways to give straight-line relationships:

$$\frac{1}{V} = \frac{K_M}{V_{\max}} \frac{1}{[S]} + \frac{1}{V_{\max}} \quad \text{Lineweaver-Burk}$$

$$\frac{[S]}{V} = \frac{1}{V_{\max}} [S] + \frac{K_M}{V_{\max}} \quad \text{Eadie-Hofstee}$$

$$V = -K_M \frac{V}{[S]} + V_{\max} \quad \text{Hanes}$$

If the kinetic data fitted the Michaelis-Menten equation perfectly then all the above plots would yield the same  $K_M$  and  $V_{\max}$  values. In practice, because there are errors in the results which are distorted differently in each plot, each analysis gives a different answer. In this thesis, all three plots were used and the  $K_M$  and  $V_{\max}$  values obtained were averaged.

## Appendix C Abbreviations

### 1. Amino acid abbreviations

Amino acid	3 letter code	1 letter code	Amino acid	3 letter code	1 letter code
Glycine	Gly	G	Glutamic acid	Glu	E
Alanine	Ala	A	Glutamine	Gln	Q
Valine	Val	V	Arginine	Arg	R
Leucine	Leu	L	Histidine	His	H
Isoleucine	Ile	I	Phenylalanine	Phe	F
Serine	Ser	S	Cysteine	Cys	C
Threonine	Thr	T	Tryptophan	Trp	W
Aspartic acid	Asp	D	Tyrosine	Tyr	Y
Asparagine	Asn	N	Methionine	Met	M
Lysine	Lys	K	Proline	Pro	P

### 2. Buffer salts

PIPES	piperazineN,N'-bis(2-ethanesulphonic acid)
MES	2-(N-morpholino)ethanesulphonic acid
MOPS	3-(N-morpholino)propanesulphonic acid
Tris	tris(hydroxymethyl)aminomethane
TRICINE	N-tris(hydroxymethyl)methylglycine
TEA	triethanolamine

## REFERENCES

- Adams, B., Pain, R.A. (1986) *FEBS lett.* **196**, 361
- Anderson, C.M., Zucker, F.H., Steitz, T.A. (1979) *Science* **204**, 375
- Bailey, J.M., Lin, L-N, Brandts, J.F., Mas, M.T. (1990) *J. Prot. Chem.* **9**, 59
- Banks, R.D., Blake, C.C.F., Evans, P.R., Haser, R., Rice, D.W., Hardy, G.W., Merret, M., Phillips, A.W. (1979) *Nature* **279**, 773
- Barna, J.C.J., Williams, D.H., Williamson, M.P. (1985) *J. Chem. Soc. Chem. Commun.* 254
- Bartlett, P.A., Marlowe, C.K. (1987) *Science* **235**, 569
- Bash, P.A., Singh, U.C., Brown, F.K., Langridge, R., Kollman, P.A. (1987) *Science* **235**, 574
- Bennett, W.S., Steitz, T.A. (1978) *Proc. Natl. Acad. Sci. U.S.A.* **75**, 48
- Benzinger, T.H., Kitzinger, C., (1960) *Methods Biochem. Anal.* **8**, 309
- Blake, C.C.F., Evans, P.R. (1974) *J. Mol. Biol.* **84**, 585
- Blake, C.C.F., Rice, D.W. (1981) *Phil. Trans. R. Soc. Lond. B* **293**, 93
- Blake, C.C.F., Rice, D.W., Cohen, F.E. (1986) *Int. J. Pep. Protein Res.* **27**, 443
- Brandts, J.F., Lin, L.-N. (1990) *Biochemistry* **29**, 6927
- Brandts, J.F., Lin, L.-N., Wiseman, T., Williston, S., Yang, C.P. (1990) *International laboratory* 29
- Bryant, T.N., Watson, H.C., Wendell, P.L. (1974) *Nature* **247**, 14
- Bucher, T. (1955) *Methods Enzymol.* **1**, 415
- Calvet, E., Prat, H. (1963) In *Recent Progress in Microcalorimetry*, Pergamon, London
- Chatterjee, A.N., Perkins, H.R. (1966) *Biochem. Biophys. Res. Commun.* **24**, 489
- Chen, A.-T., Wadso, I. (1982) *J. Biochem. Biophys. Methods* **6**, 307
- Cooper, A., Sanders, B., Dryden, D.T.F. (1989) *J. Mol. Liq.* **42**, 99

- Cortijo, M., Baron, C., Jimenez, J.S., Mateo, P.L. (1982) *J. Biol. Chem.* **257**, 1121
- Creighton, T.E. (1984) In *Proteins, Structures and Molecular Properties*
- Cronin, C.N., Kirsch, J.F. (1986) *Biochemistry* **27**, 4572
- Davis, J.F., Delcamp, T.J., Prendergast, N.J., Ashford, V.A., Freisheim, J.J., Kraut, J. (1990) *Biochemistry* **29**, 9467
- Eftink, M., Biltonen, R. (1980) In *Biological Microcalorimetry*, Ed. Beezer, A.E., Academic Press, New York, pp. 343-412
- Estell, D.A., Graycar, T.P., Miller, J.V., Powers, D.B., Burnier, J.P., Ng, P.N., Wells, J.A. (1986) *Science* **233**, 659
- Fairbrother, W.J., Walker, P.A., Minard, P., Littlechild, J.A., Watson, H.C., Williams, R.J.P., (1989) *Eur. J. Biochem.* **183**, 57
- Fairbrother, W.J., Graham, H.C., Williams, R.J.P. (1990a) *Eur. J. Biochem.* **190**, 161
- Fairbrother, W.J., Graham, H.C., Williams, R.J.P. (1990b) *Eur. J. Biochem.* **190**, 407
- Fersht, A., Shi, J.-P., Knill-Jones, J., Lowe, D.M., Wilkinson, A.J., Blow, D.M., Brick, P., Carter, P., Waye, M.Y., Winter, G. (1985) *Nature* **314**, 235
- Fersht, A. (1985) In *Enzyme Structure and Mechanism*, W.H. Freeman
- Fersht, A. (1987) *Trends Biochem. Sci.* **12**, 301
- Fesik, S.W., O'Donnell, R.T., Gampe, R.T., Olejniczak, E.T. (1986) *J. Am. Chem. Soc.* **108**, 3165
- Fleischman, S.H., Brooks, C.L. (1990) *Proteins* **7**, 52
- Frieden, E. (1975) *J. Chem. Educ.* **52**, 754
- Ghuysen, J.M. (1980) *Top. Antibiotic Chem.* **5**, 9
- Gilson, M.K., Rashin, A., Fine, R., Honig, B. (1985) *J. Mol. Biol.* **183**, 503
- Gilson, M.K., Honig, B. (1987) *Nature* **330**, 84
- Graham, H.C., Williams, R.J.P. (1991) *Eur. J. Biochem.* **197**, 81
- Graham, H.C., Williams, R.J.P., Littlechild, J.A., Watson, H.C. (1991) *Eur. J. Biochem.* **196**, 261
- Grenthe, I., Ots, H., Ginstrup, O. (1970) *Acta. Chem. Scand.* **24**, 1067
- Harlos, K., Vas, M., Blake, C.F. (1992) *Proteins* **12**, 133
- Harris, C.M., Harris, T.M (1982a) *J. Am. Chem. Soc.* **104**, 363

- Harris, C.M., Harris, T.M. (1982b) *J. Am. Chem. Soc.* **104**, 4293
- Herrin, T.R., Thomas, A.M., Perun, T.J., Mao, J.C., Fesik, S.W. (1985) *J. Med. Chem.* **28**, 1371
- Hu, C.Q., Sturtevant, J.M. (1987) *Biochemistry* **26**, 178
- Johnson, C.M., Cooper, A., Brown, A.J.P. (1991) *Eur. J. Biochem.* **202**, 1157
- Kalman, J.R., Williams, D.H. (1980a) *J. Am. Chem. Soc.* **102**, 897
- Kalman, J.R., Williams, D.H. (1980b) *J. Am. Chem. Soc.* **102**, 906
- Kannan, R., Harris, C.M., Harris, T.M., Waltho, J.P., Skelton, N.J., Williams, D.H. (1988) *J. Am. Chem. Soc.* **110**, 2946
- Kati, W., Wolfenden, R. (1989) *Science* **243**, 1591
- Kauzmann, (1959) *Adv. Prot. Chem* **14**
- Kellis, J.T., Nyberg, K., Fersht, A.R. (1989) *Biochemistry* **28**, 4914
- Klotz, I.M., Franzen, J.S. (1962) *J. Am. Chem. Soc.* **84**, 3461
- Kraut, J. (1988) *Science* **242**, 533
- Laemmli, U.K. (1970) *Nature* **227**, 680
- Larsson-Raznikiewicz, M. (1964) *Biochim. Biophys. Acta.* **85**, 60
- Larsson-Raznikiewicz, M. (1967) *Biochim. Biophys. Acta.* **132**, 33
- Larsson-Raznikiewicz, M. (1970) *Eur. J. Biochem.* **17**, 183
- Larsson-Raznikiewicz, M., Arvidsson, L. (1971) *Eur. J. Biochem.* **22**, 506
- Larsson-Raznikiewicz, M. (1973) *Arch. Biochem. Biophys.* **158**, 754
- Leo, A., Hansch, C., Elkins, D. (1971) *Chem. Rev.* **71**, 525
- Lin, L.-N., Mason, A.B., Woodworth, R.C., Brandts, J.F. (1991) *Biochemistry* **30**, 11660
- Mas, M.T., Chen, C.Y., Hitzeman, R.A., Riggs, A.D. (1986) *Science* **233**, 788
- Mas, M.T., Resplandor, Z.E., Riggs, A.D. (1987) *Biochemistry* **26**, 5369
- Mas, M.T., Bailey, J.M., Resplandor, Z.E. (1988) *Biochemistry* **27**, 1168
- Mas, M.T., Resplandor, Z.E. (1988) *Proteins* **4**, 56
- Matthews, S.A., Bolin, J.T., Burridge, J.M., Filman, D.J., Volz, K.W., Kaufman, B.T., Beddell, C.R., Chapness, J.N., Stammers, D.K., Kraut, J. (1985) *J. Biol. Chem.* **260**, 381

- McCammon, J.A., Harvey, S.C. (1987) In *Dynamics of Proteins and Nucleic Acids*, Cambridge Univ. Press, Cambridge
- McDonald, R., Steitz, T.A., Engelman, D.M. (1979) *Biochemistry* **18**, 338
- Meot-Nir, M. (1984) *J. Am. Chem. Soc.* **106**, 1257
- Meot-Nir, M., Sieck, L.W. (1986) *J. Am. Chem. Soc.* **108**, 7444
- Minard, P., Hall, L., Betton, J.-M., Missiakas, D., Yon, J.M. (1989) *Protein Eng.* **3**, 55
- Minard, P., Bowen, D.J., Hall, L., Littlechild, J.A., Watson, H.C., (1990) *Protein Eng.* **3**, 515
- Monk, P., Wadso, I. (1968) *Acta Chem. Scand.* **22**, 1842
- Mori, N., Singer-Sam, J., Riggs, A.D. (1986) *FEBS Lett.* **204**, 313
- Morin, P.E., Freire, E. (1991) *Biochemistry* **30**, 8494
- Nageswara Rao, B.D., Cohn, M., Scopes, R.K. (1978) *J. Biol. Chem.* **253**, 8056
- Nieto, M., Perkins, H.R. (1971a) *Biochem. J.* **123**, 773
- Nieto, M., Perkins, H.R. (1971b) *Biochem. J.* **123**, 789
- Oefner, C., D'Arcy, A., Winkler, F.K. (1988) *Eur. J. Biochem.* **174**, 377
- Osguthorpe, P.D., Roberts, V.A., Osguthorpe, D.J., Wolff, J., Gennest, M., Hagler, A.T. (1988) *Proteins* **4**, 31
- Pauling, L. (1946) *Chem. Eng. News* **24**, 1375
- Perkins, H.R. (1969) *Biochem. J.* **111**, 195
- Pickover, C.A., McKay, D.B., Engelman, D.M., Steitz, T.A. (1979) *J. Biol. Chem.* **254**, 11323
- Privalov, P.L. (1974) *FEBS Lett.* **40**, S140
- Radzicka, A., Wolfenden, R. (1988) *Biochemistry* **27**, 1664
- Ray, B.D., Moore, J.M., Nageswara Rao, B.D. (1990) *J. Inorg. Biochem.* **40**, 47
- Reynolds, P.E. (1961) *Biochim. Biophys. Acta.* **52**, 403
- Rodriguez-Tebar, A., Vazquez, D., Perez Velazquez, J.L., Laynez, J., Wadso, I. (1986) *J. Antibiotics* **39**, 1578
- Rossmann, M.G. (1974) *Nature* **250**, 194
- Roustan, C., Fattoum, A., Jeanneau, R., Pradel, L.-A., (1980) *Biochemistry* **19**, 5168

- Russell, A.J., Thomas, P.G., Fersht, A.R. (1987) *J. Mol. Biol.* **193**, 803
- Sanders, B. (1989) Ph.D. Thesis, University of Glasgow
- Schierbeck, B. Larsson-Raznikiewicz, M. (1979) *Biochim. Biophys. Acta.* **568**, 195
- Scopes, R.K. (1975) *Methods Enzymol.* **42**, 127
- Scopes, R.K. (1978) *Eur. J. Biochem.* **85**, 503
- Scopes, R.K. (1978) *Eur. J. Biochem.* **91**, 119
- Sedmak, J.J., Grossberg, S.E. (1977) *Anal. Biochem.* **79**, 544
- Sehl, L.C., Castellino, F.J. (1990) *J. Biol. Chem.* **265**, 5482
- Sharp, K.A., Nicholls, A., Friedman, R., Honig, B. (1991) *Biochemistry* **30**, 9686
- Sheldrick, G.M., Jones, P.G., Kennard, O., Williams, D.H., Smith, G.A. (1978) *Nature* **271**, 223
- Sherman, M.A., Dean, S.A., Mathiowetz, A.M., Mas, M.T. (1991) *Protein Eng.* **4**, 935
- Shortle, D., Stites, W.E., Mecker, A.K. (1990) *Biochemistry* **29**, 8033
- Sinev, M.A., Razgulyaev, O.I., Vas, M., Tinchenco, A.A., Ptitsyn, O.B. (1989) *Eur. J. Biochem.* **180**, 61
- Spragg, S.P., Wilcox, J.K., Roche, J.J., Barnett, W.A. (1976) *Biochem. J.* **153**, 423
- Street, I.P., Armstrong, C.R., Withers, S.G. (1986) *Biochemistry* **25**, 6021
- Sturtevant, J.M. (1974) *Ann. Rev. Biophys. Bioeng.* **3**, 35
- Tanswell, P., Westhead, E.W., Williams, R.J.P. (1976) *Eur. J. Biochem.* **63**, 249
- Tompa, P., Hong, P.T., Vas, M. (1986) *Eur. J. Biochem.* **154**, 643
- Vas, M., Batke, J. (1984) *Eur. J. Biochem.* **139**, 115
- Wadso, I. (1968) *Acta Chem. Scand.* **22**, 927
- Walker, P.A., Littlechild, J.A., Hall, L., Watson, H.C. (1989) *Eur. J. Biochem.* **183**, 49
- Wallas, C.H., Strominger, J.L. (1963) *J. Biol. Chem.* **238**, 2264
- Waltho, J.P., Williams, D.H. (1989) *J. Am. Chem. Soc.* **111**, 2475
- Waltho, J.P., Williams, D.H. (1991) *Ciba Foundation Symposium* **158**, 73

- Watson, H.C., Walker, N.P.C., Shaw, P.J., Bryant, T.N., Wendell, P.L., Fothergill, L.A., Perkins, R.E., Conroy, S.C., Dobson, M.J. (1982) *EMBO J.* **1**, 1635
- Watson, H.C., Littlechild, J.A. (1990) *Biochem. Soc. Trans.* **18**, 187
- Weiner, S.J., Kollman, P.A., Case, D.A., Singh, U.C., Ghio, C., Alagona, G., Profeta, S., Weiner, P. (1984) *J. Am. Chem. Soc.* **106**, 765
- Wells, J.A., Powers, D.B., Bott, R.R., Graycar, T.P., Estell, D.A. (1987) *Proc. Natl. Acad. Sci. USA* **84**, 1219
- Williams, D.H., Rajananda, V., Kalman, J.R. (1979) *J. Chem. Soc. Perkin Trans. 1*, 787
- Williams, D.H., Rajananda, V., Williamson, M.P., Bojesen, G. (1980) *Top. Antibiotic Chem.* **5**, 119
- Williams, D.H., Butcher, D.W. (1981) *J. Am. Chem. Soc.* **103**, 5697
- Williams, D.H., Williamson, M.P., Butcher, D.W., Hammond, S. (1983) *J. Am. Chem. Soc.* **105**, 1332
- Williams, D.H. (1984) *Acc. Chem. Res.* **17**, 364
- Williams, D.H., Waltho, J.P. (1988) *J. Pharmacol.* **37**, 133
- Williams, D.H., Cox, J.P.L., Doig, A.J., Gardner, M., Gerhard, U., Kaye, P.T., Lal, A.R., Nicholls, I.A., Salter, C.J., Mitchell, R.C. (1991) *J. Am. Chem. Soc.* **113**, 7020
- Williamson, M.P., Williams, D.H. (1981) *J. Am. Chem. Soc.* **103**, 6580
- Williamson, M.P., Williams, D.H., Hammond, S.J. (1984) *Tetrahedron* **40**, 569
- Williamson, M.P., Williams, D.H. (1985) *J. Chem. Soc. Perkin Trans. 1*, 949
- Wilson, C.A.B., Tuite, M.F., Dobson, M.J., Kingsman, S.M., Kingsman, A.J., Glover, L.A., Hardman, N., Watson, H.C., Fothergill, L.A., (1984) *Biochem. Soc. Trans.* **12**, 278
- Wilson, C.A.B., Hardman, N., Fothergill-Gilmore, L.A., Gambin, S.J., Watson, H.C. (1987) *Biochem. J.* **241**, 609
- Wilson, H.R., Williams, R.J.P., Littlechild, J.A., Watson, H.C. (1991) *Eur. J. Biochem.* **170**, 529
- Wilson, J.E., Chin, A. (1991) *Anal. Biochem.* **193**, 16
- Wiseman, T., Williston, S., Brandts, J.F., Lin, L.-N. (1989) *Anal. Biochem.* **179**, 131
- Wolfenden, R. (1969) *Nature* **223**, 704
- Wright, P.E. (1989) *Trends Biochem. Sci.* **14**, 255

Wrobel, J.A., Stinson, R.A. (1978) *Eur. J. Biochem.* **85**, 345

Zoller, M.J., Smith, M. (1982) *Nucleic Acids Res.* **10** 6487

Faraday Transactions: Biophysics and Biophysical  
Chemistry Special Issue

Author for Proofs & Correspondence:

Dr. Alan Cooper, Chemistry Department, Glasgow  
University, Glasgow G12 8QQ, Scotland

**Microcalorimetry of Enzyme-Substrate Binding: Yeast  
Phosphoglycerate Kinase**

Katherine E. McAuley-Hecht & Alan Cooper

Chemistry Department, Glasgow University,  
Glasgow G12 8QQ, Scotland

---

ABSTRACT

The binding of substrates and various other anions to yeast phosphoglycerate kinase (PGK) has been studied by titration microcalorimetry. Binding of 3-phosphoglycerate to a single high-affinity site ( $K$  ca.  $2 \times 10^5 \text{ M}^{-1}$ ) is entropy driven ( $\Delta G^0 \approx -30 \text{ kJ mol}^{-1}$ ,  $\Delta H^0 \approx -6 \text{ kJ mol}^{-1}$ ,  $\Delta S^0 \approx +80 \text{ J K}^{-1} \text{ mol}^{-1}$ ), with additional heat effects arising from deprotonation of the substrate near neutral pH. This binding is inhibited by a range of other anions (chloride, sulphate, triphosphate, other substrates), probably through competition for the same basic site. Nucleotide substrates (ATP and ADP) appear to bind to two separate sites on the enzyme, one of which is competitive with the phosphoglycerate site and other anions. Microcalorimetry of non-productive ternary complex formation (PGK:ADP:3-PG) reflects this multiplicity of sites. Comparative experiments with two site-directed mutants of PGK (His388→Gln and Arg168→Lys) are also reported.

---

## INTRODUCTION

The thermodynamic forces responsible for biomolecular recognition processes and interactions are of fundamental interest. Direct measurement of the energetics of ligand binding to enzymes under physiological conditions is now feasible using the improved calorimetric techniques that have recently become available.<sup>1</sup> Phosphoglycerate kinase (PGK; EC 2.7.2.3) is a particularly interesting case in this regard since it is possible in principle to study binding of individual substrate molecules in addition to the more usual analogues and inhibitors. PGK catalyses reversible phosphoryl transfer between 1,3-diphospho-D-glycerate (1,3-DPG) and adenosine diphosphate (ADP) to produce 3-phospho-D-glycerate (3-PG, phosphoglycerate) and adenosine triphosphate (ATP) in a key step of glycolysis. X-ray diffraction studies of the structures of PGK from various species<sup>2-4</sup> have shown that the single polypeptide chain is organised into two structurally distinct domains of approximately equal size, with primary binding sites for nucleotide and glycerate substrates located on opposite domains in sites close to the interdomain cleft. Mg-ATP or Mg-ADP molecules bind competitively in a shallow depression on the C-domain in a site typical of a nucleotide fold. Early ambiguities regarding the precise location of the phosphoglycerate and diphosphoglycerate binding site have recently been resolved by studies of the pig muscle enzyme<sup>4</sup> which confirm that 3-PG binds in a very basic site on the N-domain. In view of the distance between these binding sites, a hinge-bending model has been proposed for PGK in which movement around the waist region (or hinge) between the two domains expels water and brings the substrates into an orientation and proximity which facilitate phosphoryl transfer.<sup>2,3</sup> Whether this arises from concerted ligand-induced conformational motion, or simply a change in thermal flexibility of the hinge<sup>5-7</sup> is still to be confirmed. Consequently the binding of substrate molecules to these separate sites, together with the possible interactions between them in ternary enzyme-substrate complexes, is of considerable interest. We report here on studies of such processes by sensitive titration microcalorimetry techniques, using wild-type and site-directed mutant enzymes isolated from over-producing strains of yeast.

## MATERIALS AND METHODS

Glyceraldehyde 3-phosphate dehydrogenase (GAPDH; yeast, EC 1.2.1.12), adenosine (free base), adenosine 5'-diphosphate (ADP; monocyclohexylammonium salt), adenosine 5'-triphosphate (ATP; disodium salt), reduced  $\beta$ -nicotinamide adenine dinucleotide (NADH), D(-)-3-phosphoglycerate (3-PG; disodium salt), and triphosphate (pentasodium tripolyphosphate) were obtained from Sigma. All other reagents were of AnalaR grade. Wild-type and

mutant PGKs were prepared in-house from over-producing yeast strains, as described below.

### Yeast Transformation and Culture

Plasmids pMA27 and pMA40b, containing the wild-type and His388->Gln PGK genes respectively (courtesy of Dr. L.A. Gilmore),<sup>8</sup> were used to transform the *S.cerevisiae* host Y22 (ade<sup>-</sup>, his<sup>-</sup>, ura<sup>-</sup>, trp<sup>-</sup>, met<sup>-</sup>, leu<sup>-</sup>) using the method of Beggs.<sup>9</sup> Transformants were isolated by leucine selection and, after full marker analysis, suitable colonies were grown in 10 litre batch culture at 30°C using a medium comprising yeast extract 10 g l<sup>-1</sup>, bactopectone 10 g l<sup>-1</sup> and glucose 20 g l<sup>-1</sup>. Similar procedures were used to prepare Arg168->Lys PGK using yeast cultures supplied by Dr.J. Littlechild. SDS-PAGE analysis of crude cell extracts indicated that PGK was produced in high yield by all these cells.

### PGK Isolation and Purification

PGK was purified from harvested yeast cells as previously described<sup>10</sup> with the addition of an ion-exchange step using DEAE-Sephadex between the (NH<sub>4</sub>)<sub>2</sub>SO<sub>4</sub> precipitation and S-200 gel filtration procedures.<sup>11</sup> PGK from the (NH<sub>4</sub>)<sub>2</sub>SO<sub>4</sub> fractionation was dialysed against 10mM TRIS-MOPS pH 7.0, and applied to the DEAE-Sephadex column (2.2 x 20 cm) eluting with this buffer. The enzyme was not retained under these conditions and peak fractions were pooled and concentrated by (NH<sub>4</sub>)<sub>2</sub>SO<sub>4</sub> precipitation prior to the final S-200 gel filtration stage. Purified protein was subsequently stored as an ammonium sulphate precipitate at 4°C until use.

### PGK Assay

PGK activity was measured at 25°C in the conventional "reverse" direction using the coupled assay of Scopes<sup>12</sup> using a high sulphate, fixed Mg<sup>2+</sup> concentration system.<sup>13,14</sup> The assay buffer comprised 30mM triethanolamine-HCl, pH 7.5, 40mM (NH<sub>4</sub>)<sub>2</sub>SO<sub>4</sub>, 1mM Mg acetate, 0.15mM NADH and 0.2 mg ml<sup>-1</sup> GAPDH. Substrates were prepared in assay buffer separately and contained additional Mg acetate at 0.091 and 0.975 mol mol<sup>-1</sup> for 3-PG and ATP, respectively, in order to maintain a free Mg<sup>2+</sup> concentration of 1mM.<sup>13</sup> The reaction was initiated by the addition of 20 µl of PGK solution to 0.98 ml of assay mix and the rate calculated using a millimolar extinction coefficient of 6.22 for NADH at 340nm. One unit of activity is defined as 1 µmol of NADH oxidised min<sup>-1</sup>.<sup>12</sup> Kinetic parameters were derived from least-squares analysis of Eadie-Hofstee plots. This assay procedure, when allowed to go to completion under the appropriate conditions, was also used in occasional trials to check the concentrations of substrates in experimental mixtures.

The concentration of PGK (both wild-type and mutants) was determined by UV absorbance, using an extinction coefficient of 0.495 at 280nm for a 1 mg ml<sup>-1</sup> solution<sup>15,16</sup> and assuming a relative molecular mass of 45000.

### Titration Microcalorimetry

Enzyme-ligand titration isotherms were measured at 25°C using a Microcal Omega titration microcalorimeter, and data were analyzed in terms of various binding schemes by non-linear regression using the Microcal ORIGIN software package.<sup>1</sup> A typical titration sequence involved 20 injections, at 3 minute intervals, of 5µl aliquots of substrate (or ligand) solution into the stirred calorimeter cell (total volume = 1.4ml) containing appropriate enzyme solution, so that each titration was complete in about 1 hour. Control experiments for heats of dilution of ligand and enzyme were performed under identical conditions and used for data correction in subsequent analysis. Protein samples for microcalorimetry (typical concentration about 0.1mM, 5 mg ml<sup>-1</sup>) were dialysed extensively against the appropriate buffer, centrifuged to remove any undissolved material, and briefly degassed prior to loading in the calorimeter cell. Known weights of substrate and ligand were dissolved in the same dialysis buffer, to minimize dilution artifacts, and loaded in the injection syringe at typically 10-20mM concentrations. All experiments were repeated at least twice, and usually more, using different batches of enzyme. Literature values<sup>17,18</sup> of buffer ionization enthalpies ( $\Delta H_I$ ) were confirmed by calorimetric titration with standard HCl. This also served to verify the calorimetric calibration.

### RESULTS & DISCUSSION

Enzymes isolated here from over-producing strains of yeast - necessary to yield the relatively large (gram) quantities required for titration calorimetry - were homogeneous by SDS-polyacrylamide gel electrophoresis analysis and had  $K_m$  and specific activity ( $V_{max}$ ) values comparable to published data for PGK.<sup>8,11,19,20</sup> In particular, the wild-type enzyme typically had a specific activity of about 600 units mg<sup>-1</sup> with  $K_m(\text{ATP}) = 0.29\text{mM}$  and  $K_m(3\text{-PG}) = 0.52\text{mM}$ . The mutant enzymes were somewhat less active, with  $V_{max} = 130$  and  $150$  units mg<sup>-1</sup> for His388->Gln and Arg168->Lys mutants respectively.  $K_m$  values were 0.12(ATP) and 0.19(3-PG), and 0.79(ATP) and 1.79(3-PG) mM for His388->Gln and Arg168->Lys, respectively.

Using this material we have examined the binding of three substrates (3-PG, ATP, ADP) and other anions (sulphate, triphosphate) to PGK by titration microcalorimetry under a range of conditions. Most work has concentrated on the

wild-type enzyme, with parallel experiments in some cases using the site-directed His388->Gln mutant PGK and, to a lesser extent because of poor expression and reduced yield, the Arg168->Lys mutant for comparison. Non-productive ternary complexes of PGK with ADP and 3-PG have also been examined. Binding studies with the fourth substrate, 1,3-diphosphoglycerate, were not feasible because of its poor stability in water, though some experiments containing this as part of an ADP:1,3-DPG mixture were done. Examples of typical thermograms, illustrating various significant features for titration of wild-type PGK with substrate (ATP in this case) are given in Figure 1. Initial injection of substrate to the enzyme solution gives an exothermic response, under most conditions (e.g. Fig.1A), whose magnitude decreases with subsequent injections, eventually reaching levels representative of simple dilution of the injected ligand (Fig.1B), as expected for simple binding to protein sites. The heat of dilution of the protein (Fig.1C) is of order 5  $\mu$ J per injection, and is usually negligible. The integrated heat effects from such experiments, after correction for heats of dilution (Fig.1D), can be fit to various theoretical binding schemes, including a simple 1:1 complex model which yields both the binding constant (K) and enthalpy ( $\Delta$ H) for the process. However, it became clear during the course of these studies that such a model was not always appropriate, especially in experiments involving nucleotide binding to the enzyme. For example, the best-fit line (single-site model) for the ATP binding data shown in Figure 1D, shows small but significant systematic deviations from the observations. Furthermore, the calorimetric titration curves observed here for PGK are quite sensitive to ionic strength and other anion effects. Consequently we have to take into account several competing processes, mainly concerned with non-specific and/or competitive anion binding in and around the enzyme active sites, that complicate detailed interpretation, as will emerge in the following discussion of the binding of individual ligands. As an empirical guide, thermodynamic binding parameters determined by calorimetry for the various substrates assuming 1:1 complex formation are summarized in Table 1, under a range of conditions for both wild-type and mutant enzymes.

### Phosphoglycerate Binding

Contrary to previous preliminary observations by other workers using less sensitive calorimetric techniques,<sup>21</sup> the titration of wild-type PGK with 3-PG gives an exothermic response (Figure 2A) which fits satisfactorily to a single binding site model, giving binding parameters illustrated in Table 1. These binding parameters are, however, very sensitive to the nature of the buffer and the presence of other anions. The dependence on buffer salts is particularly informative as it reflects changes in protonation of the enzyme/ligand system during

binding.<sup>18,22,23</sup> Significant differences in measured  $\Delta H^0$  of binding of 3-PG to PGK in different buffers, even at the same pH, can be correlated with the different enthalpies of ionization of the buffer salts. The  $pK_a$  ( $-\text{COOH}$ ) of phosphoglycerate in solution is about 6.84,<sup>24</sup> so a significant fraction will be protonated near neutral pH. However nmr,<sup>24</sup> X-ray diffraction,<sup>4</sup> and other studies<sup>25</sup> indicate that it is the predominantly unprotonated carboxylate ( $-\text{COO}^-$ ) form of 3-PG that binds to the protein active site. Consequently, in a well-buffered system near neutral pH,  $\text{H}^+$  ions must be released during binding to be picked up by the conjugate base component of the buffer mixture. In a calorimetric experiment this gives rise to an additional source of heat proportional to the number of protons released ( $\delta\nu$ ) and to the heat of ionization of the particular buffer ( $\Delta H_I$ ) so that the observed apparent enthalpy ( $\Delta H_{\text{obs}}$ ) is given by:-

$$\Delta H_{\text{obs}} = \Delta H_0 - \delta\nu \cdot \Delta H_I$$

where  $\Delta H_0$  is the binding enthalpy in the absence of buffer effects. The data of Table 2 are broadly consistent with this. Assuming a  $pK_a$  of 6.84 for the free ligand, and that only the fully ionized form of 3-PG binds to the enzyme, gives consistent estimates for  $\Delta H_0$  of about  $-6.2 \text{ kJ mol}^{-1}$ . Thus most of the exothermicity of binding of 3-PG (except at high pH) arises from buffer protonation effects and not directly as a consequence of the binding interactions themselves. The binding affinity of fully ionized 3-PG can be estimated from the high pH measurements to be about  $2 \times 10^5 \text{ M}^{-1}$  under these conditions, corresponding to a  $\Delta G^0$  of about  $-30 \text{ kJ mol}^{-1}$ . Consequently the binding is mainly entropy driven ( $\Delta S^0 \approx +80 \text{ J K}^{-1} \text{ mol}^{-1}$ ), reflecting possibly the predominantly electrostatic nature of the interactions in the basic patch region of the protein, involving displacement of solvated water molecules.<sup>26</sup>

Interestingly, the above analysis seems to imply that the effect of changing pH, in the pH 6-8 range at least, lies solely with the effect on the state of ionization of the 3-PG ligand, and that no functionally important protein groups titrate in this region - at least none that affect 3-PG binding. As suggested by nmr experiments,<sup>24</sup> it may well be that the various histidine side chains in the binding site region have anomalous  $pK$ 's because of the strong electrostatic interactions with adjacent groups. Unfortunately, further calorimetric investigation of this is complicated by a range of non-specific ion effects which severely limit the range of buffers available and make interpretation ambiguous. In addition to phosphate, which is well known to interfere with PGK ligand binding and kinetics,<sup>13,14,27</sup> we have shown in trial experiments that binding of 3-PG is inhibited by the presence of anions such as chloride ( $\text{Cl}^-$ , 10-60 mM), sulphate ( $\text{SO}_4^{2-}$ , 1-2 mM), triphosphate (mainly  $\text{HP}_3\text{O}_{10}^{4-}$  near neutral pH, 1 mM), and in general by increasing ionic strength.  $\text{Mg}^{2+}$

also has an inhibitory effect, possibly due to complexation with 3-PG. The sulphate effect is particularly interesting, since sulphate is known from kinetic studies to act both as an activator or, at higher concentrations, as an inhibitor of the enzyme action.<sup>13</sup> Calorimetric measurements of 3-PG binding under standard conditions (pH 6-7) show that  $K_a$  for 3-PG falls from a value of about  $1.4 \times 10^5 \text{ M}^{-1}$  in the absence of sulphate to about  $29000 \text{ M}^{-1}$  in the presence of  $1.3 \text{ mM SO}_4^{2-}$ . Assuming simple competitive binding of sulphate for the same site on the enzyme, this implies a  $K_a$  for sulphate binding of about  $3000 \text{ M}^{-1}$ , compared to a value of about  $4000 \text{ M}^{-1}$  determined by direct calorimetric titration of PGK with sulphate (see Fig. 4 and discussion below). The apparent heat of binding of 3-PG was also reduced to about  $-7.8 \text{ kJ mol}^{-1}$  under these conditions, consistent with simultaneous displacement of sulphate. No 3-PG binding could be observed in the presence of  $1 \text{ mM}$  triphosphate, suggesting a  $K_I > 10000 \text{ M}^{-1}$  for this ligand consistent with the binding constant of about  $60000 \text{ M}^{-1}$  determined by direct titration (Fig.4 and below).

The phosphoglycerate binding thermogram is most dramatically affected by the presence of ADP which, at millimolar concentrations, reverses the strong exothermic 3-PG binding to give a much weaker endothermic effect (Figure 3). This is discussed in more detail below in the context of ternary enzyme-substrate complexes.

### Nucleotide Binding

Binding to PGK of the nucleotide substrates ATP and ADP is mutually competitive: that is, calorimetric titration of the enzyme with ADP (say) in the presence of saturating concentrations of ATP (or vice versa) shows no additional heat effect, except at relatively high concentrations, confirming that these molecules share the same enzyme binding site(s). However, unlike 3-PG titration, there is some ambiguity regarding the appropriate binding model to be used for analysis. Although binding isotherms for Mg.ADP or Mg.ATP under standard conditions can in many cases be fit with a simple 1:1 complex model (Table 1), there is additional evidence (both from our own work on ternary complexes and inhibition effects - see below - and from other studies<sup>14,28,29</sup>) that the data are more consistent with (at least) two separate binding sites of relatively high ("site a") and low ("site b") affinities, respectively. Consequently, nucleotide binding data have been further analysed in terms of a 2-site model, and parameters are given in Table 3 for comparison. In most cases the fit of the calorimetric data to a 2-site model is more satisfactory (for nucleotides) than a single-site approximation, and the factor of about 20 difference in apparent binding affinities of the two sites is compatible with previous estimates.<sup>14</sup> Interestingly, in the presence of 3-PG the weaker nucleotide binding site

was much less apparent, and a single binding site model was equally satisfactory.

The more complicated binding pattern for ADP and ATP makes detailed interpretation of buffer or ionic strength effects difficult. Although there do appear to be some differences in thermodynamic binding parameters in different buffers at different pH, there is insufficient evidence to judge whether these arise from changes in protonation of either substrate or protein groups. Again, however, the range of buffers and conditions that could be examined was limited by non-specific and ionic strength effects that interfere with binding at the nucleotide site. Binding isotherms were also affected by  $Mg^{2+}$  concentrations (it is known that both substrates bind in the  $Mg^{2+}$  form<sup>2,3</sup>), and several non-specific buffer effects could be ascribed to possible magnesium ion complexation by components of the buffer mixture.

#### Ternary PGK:ADP:3-PG Complexes

Figures 2 and 3 shows examples of typical calorimetric results for ternary complex formation. In such experiments PGK was first titrated to saturation with one ligand (ADP, say), and then with the second (3-PG; see Fig.2C for example), or vice versa (as in Fig.3B), following alternate routes to the non-productive ternary complex in the thermodynamic cycle shown in Scheme 1. Each titration yields apparent  $K$  and  $\Delta H^0$  estimates, and accumulated results - assuming single and separate binding sites for each ligand - are given in Table 1.

#### (SCHEME 1)

When analyzed according to this simple scheme, the binding of the two substrates are clearly not independent of each other since the presence of one markedly affects both the apparent  $K$  and  $\Delta H^0$  of binding of the other. Specifically, binding of 3-PG to PGK in the presence of excess ADP gives a small endothermic response (as opposed to the exothermic binding in the absence of ADP), and the apparent binding affinity is also reduced ( $K_2 < K_3$ ). In contrast, although the presence of 3-PG makes subsequent binding of ADP less exothermic, the apparent  $K$  for ADP binding is actually enhanced under these conditions ( $K_4 > K_1$ ).

Although at first sight such results might appear to lend support to the notion of major ligand-induced conformational change in the protein, there are some anomalies about the data as they stand which need explanation. Firstly the calorimetric enthalpies do not appear to satisfy Hess's law: that is, the sum of the enthalpies of formation of the PGK:ADP:3-PG ternary complex should be the same whatever the order of addition

of the substrates. Examination of data in Table 1 (columns 1 + 3 versus 2 + 4) suggests that this is not generally the case. Similarly, for thermodynamic consistency,  $K_1K_3$  must equal  $K_2K_4$  (or the equivalent for sums of  $\Delta G^0$ ). But the agreement here is equally unsatisfactory: with  $K_2K_4 > K_1K_3$ , in general. Although such differences might conceivably be a result of combined experimental error, much more significant is the consistent lack of reciprocity in these results. In other words, whereas the presence of ADP apparently inhibits 3-PG binding ( $K_3 < K_2$ ), if we change the order of addition, 3-PG seems to activate ADP binding ( $K_4 > K_1$ ). This cannot be consistent with any simple scheme of interacting binding sites which requires  $K_3/K_2 = K_4/K_1$ , which is patently not the case here. Our model must therefore be incorrect or incomplete.

A more rational explanation for the above observations emerges if we accept (as discussed above) that there are, in fact, two separate binding sites for ADP: one high-affinity site (probably the crystallographically identified "active site" on the C-domain), and a second low-affinity site at which ADP binds competitively with 3-PG. Several consequences would follow from such a model. Firstly, in the presence of excess ADP, binding of 3-PG would be inhibited by ADP already bound at the low-affinity site. Moreover, in order for 3-PG to bind, it must first displace ADP from this site. This endothermic displacement of ADP (ca. +57 kJ mol<sup>-1</sup> at pH 7, Table 1) more than offsets the subsequent exothermic 3-PG binding (ca. -15 kJ mol<sup>-1</sup>), to give an apparent endothermic binding of 3-PG to form the ternary complex (ADP is still bound at the high-affinity site). Reversing the order of addition, the presence of excess 3-PG inhibits subsequent binding of ADP at its low-affinity site, possibly to such an extent that this site is either not observed or significantly weakened in these experiments such that we see mainly the effect of binding to the high-affinity ADP site. In other words, 3-PG apparently activates ADP binding by suppressing binding at the low-affinity site.

The values obtained for apparent binding constants and enthalpies for ternary complex formation seem to bear out this scheme. For example, assuming that ADP binds competitively at the 3-PG site with  $K$  of order 2500 M<sup>-1</sup> (Table 3), titration of PGK with 3-PG in the presence of 1 mM ADP would be inhibited and would give an apparent association constant for 3-PG reduced by a factor of order 5 from that observed in the absence of ADP. Prior to addition of 3-PG, the low-affinity ADP site would be roughly 70% occupied with ADP. The endothermic displacement of this would more than compensate the (smaller) exothermic effect of binding 3-PG, so the overall apparent enthalpy might be of order +15 kJ mol<sup>-1</sup>, in general agreement with observation (Table 1). Conversely, in the presence of millimolar concentrations of 3-PG, the relatively high affinity of 3-PG would strongly inhibit low affinity binding of ADP ( $K_{App} < 20$

$M^{-1}$ ), such that only the high affinity binding site of ADP would be observed under the titration conditions used here.

Given this complexity of binding sites it is, unfortunately, not yet possible from these data alone to determine whether there is any major interaction between the active sites in the ternary complex that might be related to catalytic function.

### Binding of Other Ligands

Indirect evidence for at least one sulphate binding site on PGK comes from its inhibitory effect on 3-PG binding, for example (see above). Calorimetric titration with sulphate (Fig.4) demonstrates this binding directly, and the thermogram may be analyzed in terms of a single, relatively weak, entropy-driven, ligand binding:  $K$  approx  $4000 M^{-1}$ ,  $\Delta H^0 \approx -7 kJ mol^{-1}$ ,  $\Delta S^0 \approx +45 J K^{-1} mol^{-1}$ . This is consistent with the  $K_I$  of about  $3000 M^{-1}$  estimated from sulphate inhibition above.

Direct interaction of triphosphate can also be seen (Fig.4). Binding in this case is somewhat tighter ( $K \approx 60000 M^{-1}$ ), but still entropy driven ( $\Delta H^0 \approx -17 kJ mol^{-1}$ ,  $\Delta S^0 \approx +35 J K^{-1} mol^{-1}$ ). And again this is consistent with binding at or near the 3-PG site, with consequent inhibition of 3-PG binding, as observed above.

With adenosine, only very weak binding could be detected by calorimetry under standard conditions at final ligand concentrations up to about 2.5 mM. This supports the picture that electrostatic interactions are predominant in PGK-ligand binding.

Although binding of 1,3-diphosphoglycerate has not been studied directly, because of its lack of commercial availability and instability in solution, we have made preliminary experiments in forming the catalytically active ternary complex. In these experiments PGK was titrated with an equimolar mixture of ATP + 3-PG containing a trace of PGK, made up immediately prior to the start of the experiment, to give an equilibrium mixture containing ADP + 1,3-DPG. Such titrations (Figure 4) are exothermic (apparent  $\Delta H^0 \approx -35 kJ mol^{-1}$ ), with an apparent  $K$  of order  $2-3 \times 10^4 M^{-1}$ . This is somewhat smaller than might have been anticipated from the reported very high affinity of 1,3-DPG for PGK,<sup>14</sup> though interpretation of this kind of experiment involving multiple ligands with several potentially interacting binding sites is not straightforward, and the definitive calorimetric experiments have yet to be devised.

## PGK Mutants

Calorimetric titration experiments with two site-directed mutants of PGK have been performed for comparison with the detailed wild-type study. The first of these mutants, His388->Gln, involves change of a single amino acid remote from the probable active site(s) of the protein, but located in the hinge region possibly implicated in the hinge-bending mechanism of catalytic activity.<sup>24</sup> Changing the histidine residue at position 388 to a glutamine residue affects a crucial interaction with a glutamic acid residue, identified by crystallography, and results in possible changes in dynamic flexibility of the hinge.<sup>5,6,11</sup> The Arg168->Lys mutant, on the other hand, is a charge-conservative mutation of a residue involved in the 3-PG binding site. Both these mutants are catalytically active, but do show differences in binding parameters for various substrates (Table 1).

For His388->Gln the overall pattern of substrate binding parameters is broadly similar to that of the wild-type enzyme, as might be anticipated for a mutation remote from the active sites, though there are some quantitative differences that might be significant. In particular, although the apparent binding affinities and nucleotide enthalpies are very similar to wild-type under similar conditions, phosphoglycerate binding to this mutant appears to be somewhat more exothermic. Binding of 3-PG in the presence of ADP to form the ternary complex remains exothermic, unlike the endothermic response seen with the unmodified enzyme, and the apparent inhibitory effect of ADP on 3-PG binding is also reduced. This may simply mean that the low-affinity site (site b) has an even lower affinity for ADP in this mutant. Alternatively this might reflect some changes in overall interaction between the two protein domains brought about by mutation in the hinge region.

Only a limited number of experiments have been performed with the Arg168->Lys mutant, and the only significant change compared to wild-type (Table 1) is a roughly 4-fold reduction in binding affinity for 3-PG. This is reasonable considering the location of this mutation in the phosphoglycerate binding site, where Arg-168 interacts directly with the phosphate oxygens of 3-PG.<sup>4</sup>

## Errors

Although the accuracy of calorimetric measurements is intrinsically quite high with modern instrumentation, and routine calibration of our system yields errors in absolute enthalpies of better than  $\pm 1\%$ , there are many factors which combine to reduce the real accuracy of parameters derived from calorimetric titrations of biological molecules as reported here. In particular, estimates of binding enthalpies rely on accurate knowledge of protein concentration in the experiment,

which we have determined here using careful 280nm absorbance measurements. However, protein molar extinction coefficients ( $\epsilon_{280}$ ) are only known to  $\pm 5\%$ , at best,<sup>16</sup> and even this does not take into account any inactive, non-binding protein molecules that might arise due to partial degradation of the enzyme during storage or even during the course of an experiment (though tests of enzyme activity before and after calorimetric titrations showed no measurable loss of activity in occasional trials). Errors in ligand concentration, estimated here by weight assuming 100% purity and cross-checked enzymologically and (in the case of nucleotides) by  $A_{260}$  measurements, can give rise to incorrect  $\Delta H^0$  and  $K$  values. This, together with variations observed with repeat experiments with different enzyme preparations, even assuming that the correct binding model has been chosen, suggests that the estimated errors on  $\Delta H^0$  are no better than  $\pm 10\%$ , and that absolute  $K$  values are probably accurate to within a factor of 2. However, despite these relatively large (but realistic) uncertainties in absolute values for  $K$  and  $\Delta H$ , since all data were analyzed using the same overall assumptions we can be reasonably confident that the overall trends reported here are correct.

#### SUMMARY & CONCLUSIONS

Using direct titration microcalorimetry techniques to study substrate binding to yeast phosphoglycerate kinase under near-physiological conditions, we have established the following:

- (1) Binding of 3-phospho-D-glycerate to a single, high affinity site on the enzyme is entropy driven ( $\Delta G^0 \approx -30 \text{ kJ mol}^{-1}$ ,  $\Delta H^0 \approx -6 \text{ kJ mol}^{-1}$ ,  $\Delta S^0 \approx +80 \text{ J K}^{-1} \text{ mol}^{-1}$ ).
- (2) Displacement of hydrogen ions from the carboxyl group of 3-PG, to bind as the carboxyate, gives an additional exothermic heat effect arising from protonation of buffer molecules in solution.
- (3) Binding of 3-PG is competitively inhibited by a range of anions, including ADP.
- (4) Nucleotide substrates, ADP and ATP, bind to two sites on the enzyme, one of which is competitive with 3-PG.
- (4) Ternary enzyme-substrate complex studies are complicated by the multiplicity of nucleotide binding sites, and there is no direct calorimetric evidence yet for major ligand-induced changes in the protein.

This study demonstrates both the feasibility of direct measurement of biomolecular interactions by modern calorimetric techniques, and the inherent complexity of such processes. In particular, the potential multiplicity of competing binding processes, together with the

polyelectrolyte nature of both binding sites and ligands, makes interpretation of the fundamental thermodynamic parameters for such interactions in aqueous systems a major challenge.

Acknowledgements: We are grateful to Drs. C.M. Johnson, A.J.P. Brown, L.A. Gilmore, J.A. Littlechild, H.C. Watson, Miss L. Whytelaw, and Mrs. M. Nutley for advice and help. Financial support for equipment and a research studentship (K.E.M-H.) was provided by SERC.

## References

1. T.Wiseman, S.Williston, J.F.Brandts, and L-N.Nin, *Analyt.Biochem.*, 1989, 179, 131-137.
2. R.D.Banks, C.C.F.Blake, P.R.Evans, R.Haser, D.W.Rice, G.W.Hardy, M.Merrett, and A.W.Phillips, *Nature*, 1979, 279, 773-777.
3. H.C.Watson, N.P.C.Walker, P.J.Shaw, T.N.Bryant, P.L.Wendell, L.A.Fothergill, R.E.Perkins, S.C.Conroy, M.J.Dobson, M.F.Tuite, A.J.Kingsman, and S.M.Kingsman, *EMBO J.*, 1982, 1, 1635-1640.
4. K.Harlos, M.Vas, and C.C.F.Blake, *Proteins: Structure, Function, and Genetics*, 1992, 12, 133-144.
5. A.Cooper, B.Sanders, and D.T.F.Dryden, *J.Mol.Liquids*, 1989, 42, 99-111.
6. D.T.F.Dryden, P.G.Varley, and R.H.Pain, *Eur.J. Biochem.*, 1992, 208, 115-123.
7. G.Haran, E.Haas, B.K.Szpiowska, and M.T.Mas, *Proc.Natl.Acad.Sci. USA*, 1992, 89, 11764-11768.
8. C.A.B.Wilson, N.Hardman, L.A.Fothergill-Gilmore, S.J.Gamblin, and H.C.Watson, *Biochem.J.*, 1987, 241, 609-614.
9. J.D.Beggs, *Nature*, 1978, 275, 104-109.
10. P.Minard, D.J.Bowen, L.Hall, J.A.Littlechild, and H.C.Watson, *Protein Eng.*, 1990, 3, 515-521.
11. C.M.Johnson, A.Cooper, and A.J.P.Brown, *Eur.J. Biochem.*, 1991, 202, 1157-1164.
12. R.K.Scopes, *Methods Enzymol.*, 1975, 42, 127-138.
13. R.K.Scopes, *Eur.J.Biochem.*, 1978, 85, 503-516.
14. R.K.Scopes, *Eur.J.Biochem.*, 1978, 91, 119-129.
15. T.Bucher, *Methods Enzymol.*, 1955, 1, 415-422.
16. S.C.Gill and P.H. von Hippel, *Anal.Biochem.*, 1989, 182, 319-326.
17. J.J.Christensen, L.D.Hansen, and R.M.Izatt, *Handbook of Proton Ionization Heats*, (Wiley, New York, 1976).
18. A.Cooper and C.M.Johnson, in *Methods in Molecular Biology: Physical Methods of Analysis*, ed. C.Jones, B.Mulloy, and A.H.Thomas (Humana Press, Clifton, N.J., in press).

19. M.T.Mas, Z.E.Resplandor, and A.D.Riggs, *Biochemistry*, 1987, 26, 5369-5377.
20. M.T.Mas, J.M.Bailey, and Z.E.Resplandor, *Biochemistry*, 1988, 27, 1168-1172.
21. C.Q.Hu and J.M.Sturtevant, *Biochemistry*, 1987, 26, 178-182.
22. J.M.Sturtevant, in *Experimental Thermochemistry*, Vol.II, ed. H.A.Skinner (Interscience, New York, 1962), pp. 427-442.
23. A.Cooper and C.A.Converse, *Biochemistry*, 1976, 15, 2970-2978.
24. H.R.Wilson, R.J.P.Williams, J.A.Littlechild, and H.C. Watson, *Eur.J.Biochem.*, 1988, 170, 529-538.
25. G.A.Orr and J.R.Knowles, *Biochem.J.*, 1974, 141, 721-723.
26. W.Kauzmann, *Adv.Protein Chem.*, 1959, 14, 1-63.
27. M.M.Khamis and M.Larsson-Raznikiewicz, *Acta Chem.Scand. Ser.B*, 1987, 41, 348-355.
28. M.Larsson-Raznikiewicz, *Arch.Biochem.Biophys.*, 1973, 158, 754-762.
29. M.Vas and J.Batke, *Eur.J.Biochem.*, 1984, 139, 115-123.

Figure Legends

- FIG.1: Titration calorimetry for the addition of ATP (14.9mM, 20 x 5 $\mu$ l injections) to wild-type PGK (0.115mM) in 50mM Tris/MOPS buffer, pH 7.0, containing 4mM magnesium acetate, 0.1mM DTT and 0.05% Na azide, at 25°C. The upper panel shows the calorimetric raw data (negative response is exothermic) for the titration (A), together with controls for ATP dilution (B) and protein dilution (C) under identical conditions. The lower panel (D) shows the normalized, integrated enthalpy per titration injection, after correction for dilution heats, together with the best fit line to a single binding site model.
- FIG.2 (A) Calorimetric response for titration of PGK (0.10mM) with 3-PG (10mM, 15 x 5 $\mu$ L injections) in 50mM MES buffer, pH 6, 25°C, containing 4mM magnesium acetate, 0.1mM DTT and 0.05% Na azide. (B) Titration with 3-PG (20 injections) under identical conditions, with the addition of 1.2mM ammonium sulphate. (C) Titration with 3-PG (20 injections) as in (A) but with the prior addition of ADP (1.3mM) to the sample cell mixture.
- FIG.3 Normalized integrated heats, corrected for dilution, for addition of ADP (20mM, 20 x 5 $\mu$ l) to PGK (0.1mM) in 50mM MES buffer, pH 6, 25°C, containing 4mM magnesium acetate, 0.1mM DTT and 0.05% Na azide: (A) without 3-PG (open symbols), (B) in the presence of 0.6mM 3-PG (closed symbols). Data in (A) have been fit (solid line) to a 2-site model with parameters indicated in Table 3, whereas data in (B) fit satisfactorily to a single binding site model (Table 1).
- FIG.4 Thermograms for binding of assorted ligands to wild-type PGK (ca. 0.1mM) in 50mM MES buffer, pH 6, 25°C, containing 4mM magnesium acetate, 0.1mM DTT and 0.05% Na azide: (A) Sulphate (as ammonium sulphate); (B) triphosphate; (C) an equimolar, equilibrium mixture of ADP and 1,3-DPG (prepared by mixing ATP and 3-PG with a trace of PGK immediately prior to the experiment).

Table 1: Apparent PGK-substrate binding parameters ( $K_{App}$  / $M^{-1}$  and  $\Delta H_{App}$  / $kJ mol^{-1}$ ) determined from calorimetric titrations assuming 1:1 complex formation[a].

	PGK + ATP	PGK + ADP	PGK + 3-PG	PGK:ADP + 3-PG[b]	PGK:3-PG + ADP[c]
Wild-type, pH 7		(1)	(2)	(3)	(4)
$K_{App}$	6850	3550	180000	27000	11500
$\Delta H_{App}$	-34.3 (1.5)	-57.5 (4.9)	-15.5 (0.7)	+ 9.4 (0.6)	-10.1 (1.9)
Wild-type, pH 6					
$K_{App}$	6600	5900	113000	18200	19000
$\Delta H_{App}$	-34.8 (0.7)	-34.8 (0.8)	-19.1 (0.6)	+ 2.8 (0.4)	-13.9 (1.3)
His388->Gln, pH 6					
$K_{App}$	7800	8370	118000	55000	27000
$\Delta H_{App}$	-34.7 (4.0)	-33.2 (3.5)	-25.8 (2.6)	-10.7 (1.2)	-14.7 (2.0)
Arg168->Lys, pH 6					
$K_{App}$	5000	5300	28000	-	-
$\Delta H_{App}$	-33.1 (5.0)	-23.6 (2.0)	-13.8 (2.0)	-	-

[a] Routine buffer composition: 50mM Tris/MOPS (pH 7) or 50mM MES (pH 6) containing 4mM Mg acetate, 0.1mM dithiothreitol, and 0.05% sodium azide as anti-microbial agent. All measurements at 25°C. Quantities in brackets are standard deviations from multiple determinations of enthalpy values. Standard deviations on K values are in the range  $\pm 50\%$ , or less.

[b] Binding of 3-PG after prior titration with nucleotide. [ADP] = 1.4 mM in final mixture.

[c] Binding of ADP after prior titration with phosphoglycerate. [3-PG] = 0.6 mM in final mixture.

Table 2: Apparent enthalpies ( $\text{kJ mol}^{-1}$ ) of binding of 3-phosphoglycerate to wild-type PGK under different buffer conditions.

Buffer[a]	$\Delta H_I$ [b]	$\Delta H_{App}$	$\delta\nu_{H^+}$ [c]	$\Delta H_0$ [d]
Tricine, pH 8	31.2	-8.4	0.065	-6.4
Tris/MOPS, pH 7	23.5	-15.5	0.41	-5.9
PIPES, pH 7	11.3	-10.9	0.41	-6.3
MES, pH 6	14.6	-19.1	0.87	-6.3

[a] 50mM buffer, containing 0.1mM dithiothreitol and 0.05% Na azide. (Abbreviations: Tricine = N-tris(hydroxymethyl)methylglycine; Tris = tris(hydroxymethyl)aminomethane; MOPS = 3-(N-morpholino)propanesulphonic acid; PIPES = piperazine-N,N'-bis(2-ethanesulphonic acid); MES = 2-(N-morpholino)ethanesulphonic acid.)

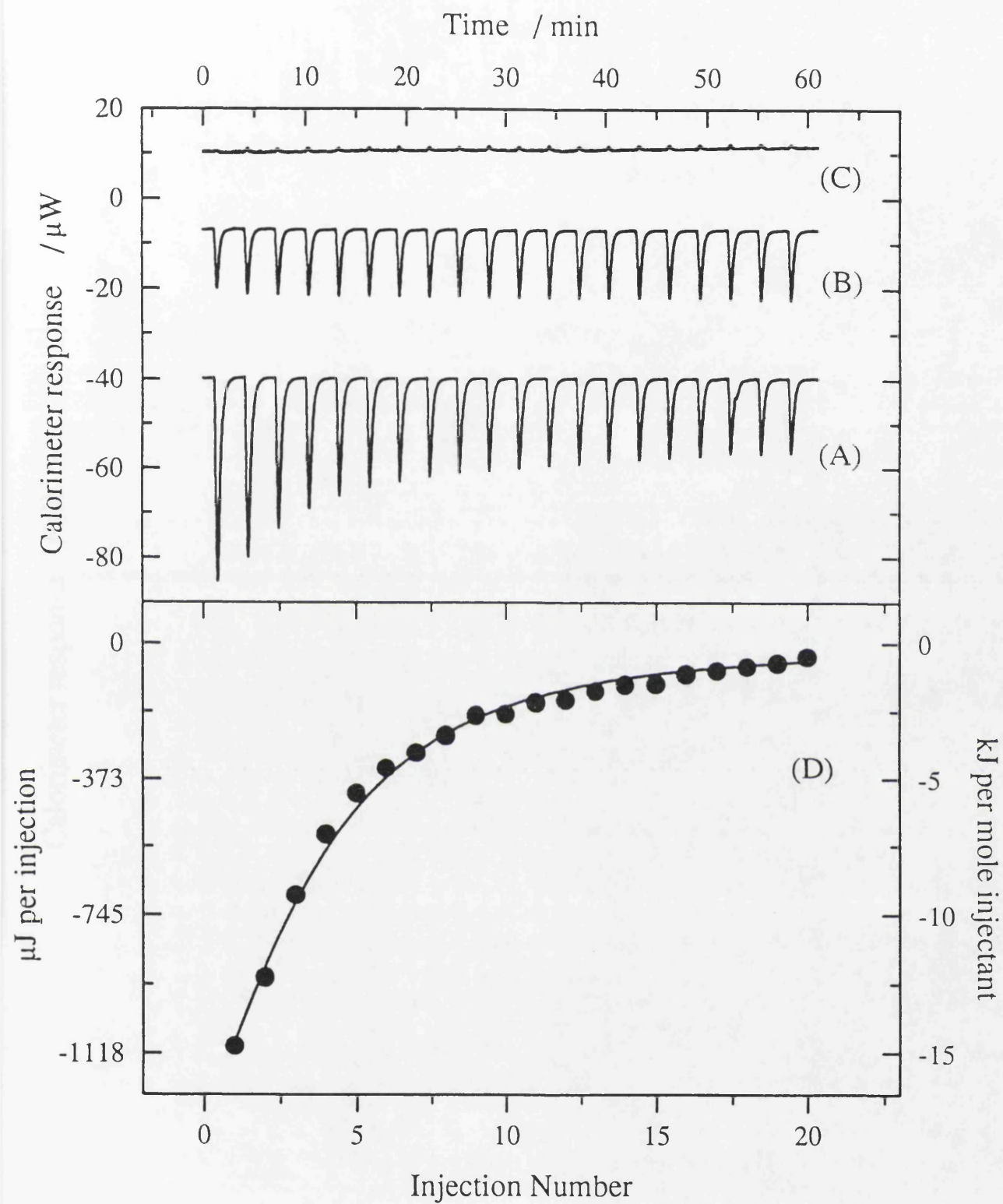
[b] Hydrogen-ion dissociation enthalpy of the buffer.

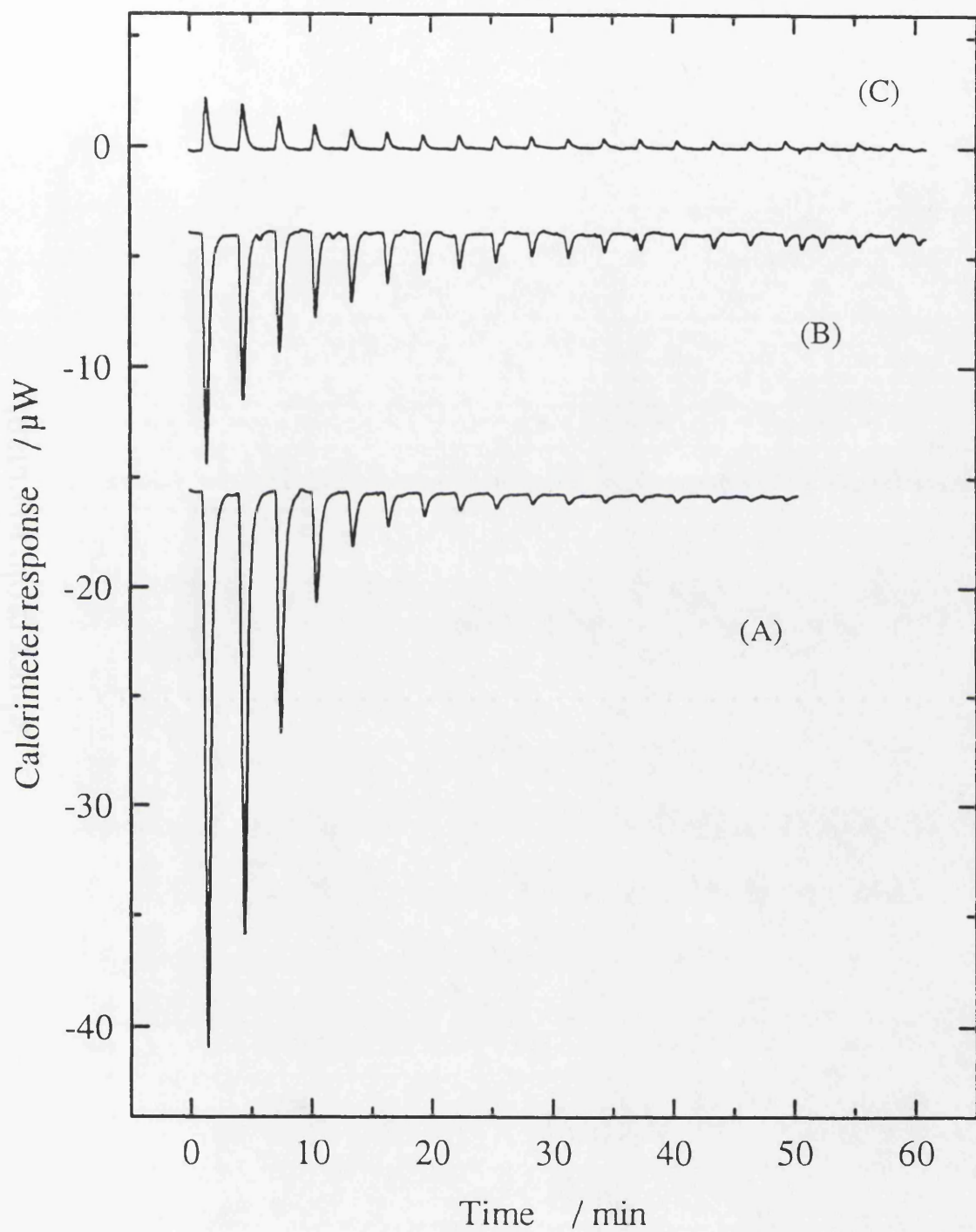
[c] Fractional protonation of 3-PG in solution assuming  $pK_A = 6.84$ .

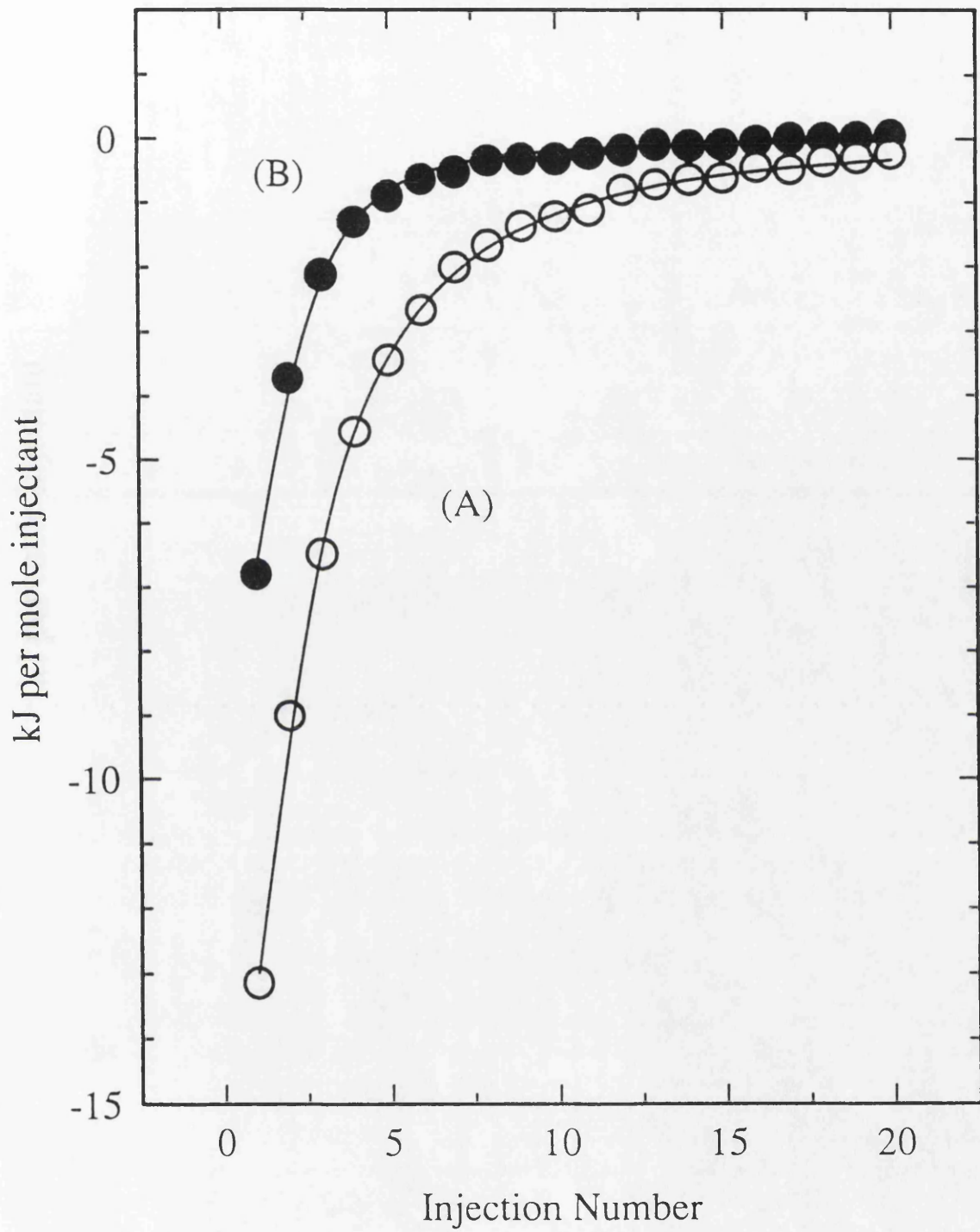
[d] 3-PG binding enthalpy corrected for buffer protonation heats assuming that only the fully ionized form binds to the enzyme.

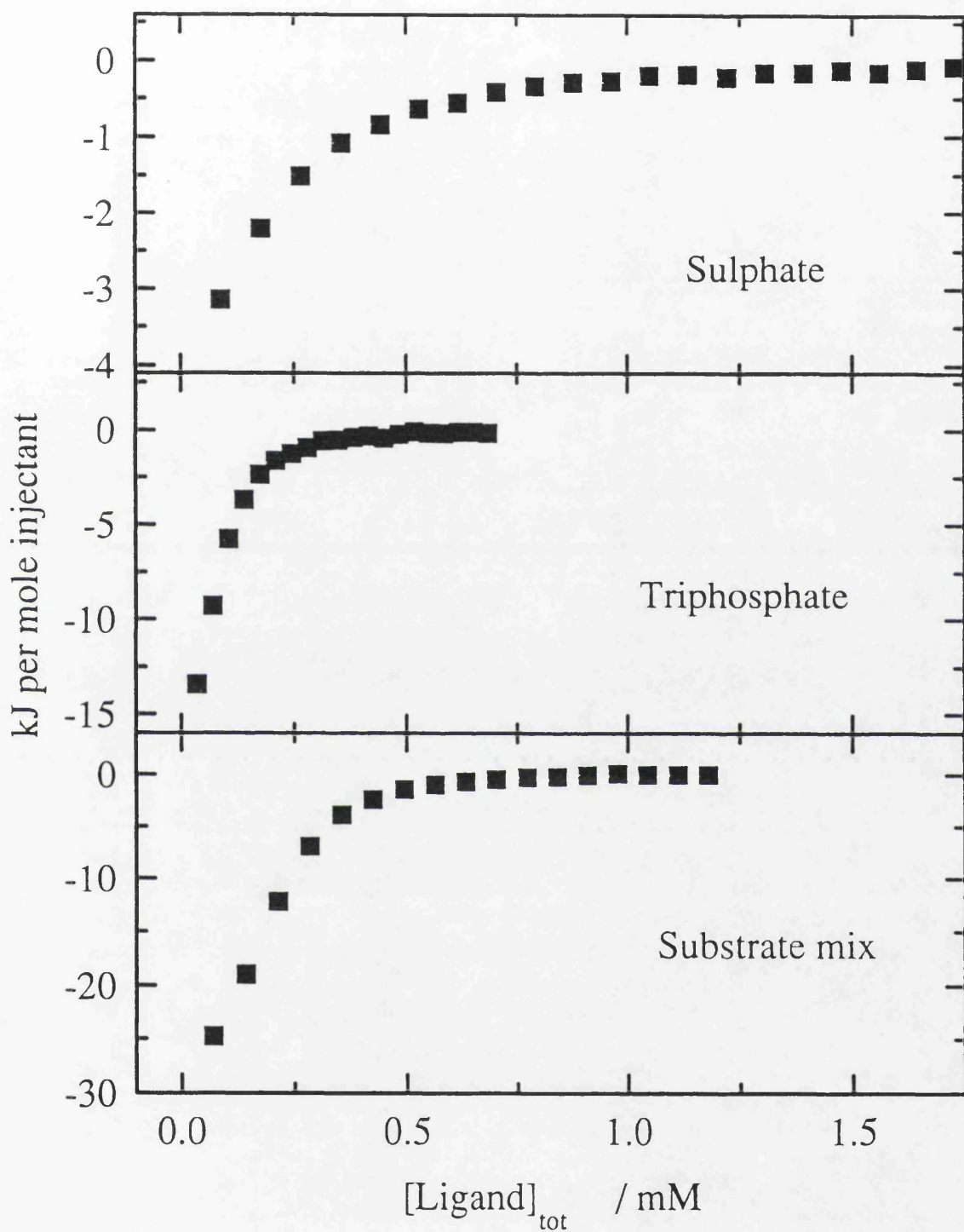
Table 3: Examples of alternative 2-site binding parameters for ADP and ATP to wild-type PGK. Experimental conditions as described in Table 1.

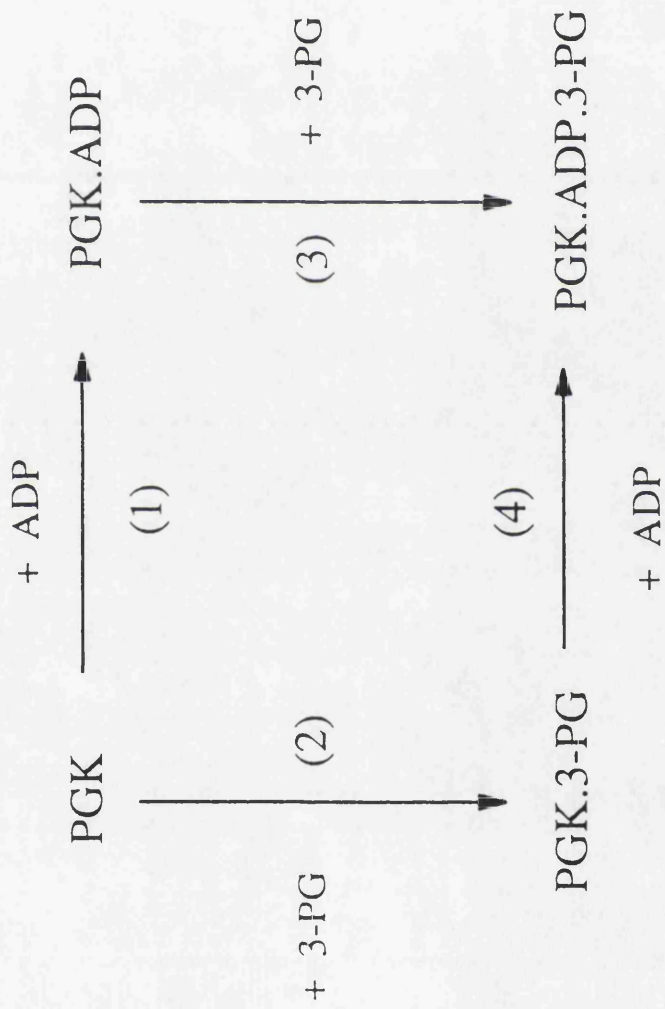
Substrate	<u>Site a</u>		<u>Site b</u>	
	$K_a$ /M <sup>-1</sup>	$\Delta H_a$ /kJ mol <sup>-1</sup>	$K_b$ /M <sup>-1</sup>	$\Delta H_b$ /kJ mol <sup>-1</sup>
ADP: pH 7	44000	-15.9 (1.7)	2400	-41.1 (3.0)
pH 6	35000	-15.8 (1.3)	2600	-24.8 (1.0)
ATP: pH 7	29000	-19.1 (3.0)	1020	-23.8 (9.9)
pH 6	25000	-19.5 (1.9)	1500	-28.9 (2.8)











Scheme 1

Royal Society discussion meeting, April 28-29, 1993:

"The Chemistry of Biological Molecular Recognition"

---

Microcalorimetry and the molecular recognition of peptides and proteins

Alan Cooper and Katherine E. McAuley-Hecht

Department of Chemistry, Glasgow University, Glasgow G12 8QQ,  
Scotland, U.K.

Keywords: Thermodynamics  
Non-covalent interaction  
Vancomycin  
Cyclodextrin  
Protein folding  
Stability

## SUMMARY

Isothermal titration (ITC) and differential scanning calorimetry (DSC) techniques are now routinely applicable to the study of non-covalent interactions in biomolecular recognition. Examples from our own current work on peptide antibiotic interactions and protein folding illustrate what may be achieved. ITC binding studies of vancomycin antibiotics with model peptides give information about the thermodynamics of group interactions, and also demonstrate possible complexities due to ligand-induced aggregation processes. The thermal stability of proteins in mixed aqueous solvents, studied by DSC, shows how the balance of forces responsible for folding stability may switch, without markedly perturbing the native structure. Separate experiments on the molecular recognition of unfolded polypeptide chains by cyclodextrins is consistent with simple binding of these cyclic polysaccharides to exposed aromatic groups on the thermally denatured protein.

## 1. INTRODUCTION

Biomolecular recognition processes rely on a subtle balance of non-covalent forces to control conformation and mediate binding. The folding of polypeptides and other biopolymers into unique conformations constitutes a molecular self-recognition process in which the system, comprising macromolecule plus solvent, recognizes that, for certain specific polymer sequences, limited regions of conformation space are more favourable. Once folded, these specific conformations are then likely to provide specific binding sites for the recognition other molecules (ligands) that themselves depend on non-covalent interactions. This is fundamentally a thermodynamic problem. Although we might be able to name the sort of interactions involved (H-bonds, hydrophobic, electrostatic, Van der Waals forces, etc.) we, as yet, have little success in predicting their relative contributions ab initio. This arises because, unlike covalent forces that are overwhelmingly enthalpic and can be computed with quite high precision, the free energy changes associated with non-covalent interactions involve a delicate balance between (often large) enthalpic and entropic contributions in which solvent molecules play a major role.

There are several consequences of this. From the molecular modelling point of view the lack of appropriate 2-body potential functions describing non-covalent forces leads to computational difficulties. Indeed, the inherently many-body nature of non-covalent interactions means that solvent must be explicitly included in any attempts to describe the overall energetics. And, indeed, even quite simple changes in solvent can alter the balance and nature of the interactions quite significantly. For example, as we shall see below, in recent work on the folding of a small protein we have shown how transfer from aqueous to water/methanol mixtures can change the apparent stabilizing interactions from predominantly hydrophobic (in water) to predominantly H-bonding (in MeOH mixtures) - at least as a first approximation - without significantly affecting the native conformation of the protein (Woolfson et al., 1993).

In such a complex theoretical situation it is particularly

important that we have reliable empirical approaches based on measurement of thermodynamic parameters for appropriate systems under relevant conditions. Although calorimetry gives the most direct thermodynamic information, until relatively recently the techniques were rather insensitive and tedious to use for most biological systems, and we have had to rely on less satisfactory indirect techniques. However, instrumental speed and sensitivity has improved dramatically in recent years so that direct calorimetric studies of interesting biomolecular systems is now routine, and instruments are commercially available for both isothermal titration (ITC) and differential scanning (DSC) work (Privalov & Potekhin, 1986; Sturtevant, 1987; Wiseman et al., 1989; Wadsö, 1991; Cooper & Johnson, 1993a,b,c). Here we will illustrate current applications and salient points of the technique with some recent examples from our own work on topics related to the folding and interaction of proteins and peptides, including studies on the effects of cyclic polysaccharides (cyclodextrins) and non-aqueous solvents on protein stability, and (in collaboration with Dr. D.H. Williams and his group) measurements on the vancomycin class of antibiotics.

## 2. ISOTHERMAL TITRATION MICROCALORIMETRY

ITC is used typically to study the thermodynamics of binding and other processes that can be initiated by mixing in solution. Earlier methods, based on the "heat-leak" principle pioneered in the biomolecular field by Sturtevant (1974) and Wadsö (1983,1991), have been superceded by more recent instruments using efficient mixing and active feedback methods (Wiseman et al., 1989), or kinetic deconvolution techniques (Bastos et al., 1991), that are much faster and rather more convenient in use. Typical biomolecular thermal titrations involving, say, 20 or more injections of ligand into a macromolecule solution may now be done in 1 hour, or less, using reasonable amounts of material, and with an ultimate working sensitivity of the order of 5  $\mu$ J per injection. Current work in our laboratory includes measurement of enzyme-substrate complexes (McAuley-Hecht & Cooper, 1993), protein-nucleic acid interactions, and, as described below, peptide antibiotic binding.

(a) Peptide Antibiotic Interactions

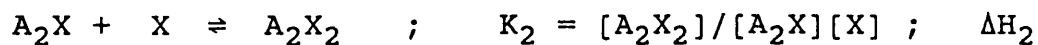
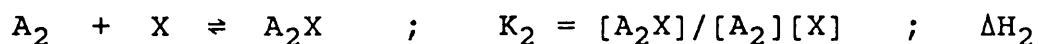
The binding of small peptide analogues of bacterial cell wall components to the vancomycin class of antibiotics is of both clinical and academic interest (Wright & Walsh, 1992), providing a potentially simple experimental model for biomolecular recognition studies. Dudley Williams and his group have done much to clarify the structural details by high resolution NMR and are now showing how the basic interactions may be broken down into the component parts (Williams et al., 1990, 1991, 1993). To complement this work we are now doing systematic calorimetric measurements of these binding processes in solution.

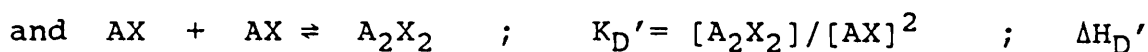
The experiments are, in principle, relatively straightforward. Sequential addition of ligand (peptide) solution to the calorimeter cell containing antibiotic (or vice versa) gives a series of heat pulses associated with binding. In simple cases the size of each heat pulse (after appropriate corrections for heats of mixing and dilution) is proportional to the extent of complex formation and the enthalpy ( $\Delta H$ ) of the process. Consequently one obtains a thermal titration curve which may be analysed to give both  $\Delta H$  and the binding constant ( $K$ ), which immediately leads directly to  $\Delta G^0$  and  $\Delta S^0$ . Examples showing the isothermal titration microcalorimetry of binding of di-N-acetyl-L-Lys-D-Ala-D-Ala (DALAA) to vancomycin under various conditions are shown in Figure 1. Measurements at different temperatures give the temperature dependence of  $\Delta H$  ( $\Delta C_p$ ), which may be significant, and data for a range of ligands are given in Table I.

Though the range of ligands studied is still far from comprehensive, data such as these form the basis for attempts to determine the individual functional group components of the interaction, and the availability of enthalpy and entropy data, in addition to free energy, will be a stringent test of such predictions. Some such small group contributions can be obtained experimentally. For example, what is the contribution of the peptide  $-\text{COO}^-$  group to the overall interaction? Binding of the acetate anion itself is rather too weak to measure directly by calorimetry - or, rather, the acetate concentrations required in the titration are so high that heats of dilution obscure the desired binding heats - but it can be determined by competition experiments. Figure 1 shows

that increasing concentrations of acetate in the reaction mixture progressively inhibit binding to vancomycin of the much stronger ligand, DALAA. The apparent enthalpy of DALAA binding is also reduced, and the effect is seen also with other antibiotics. The data are consistent with simple competitive binding of acetate and DALAA for the same antibiotic binding site, so that titration with DALAA in the presence of acetate requires displacement of the acetate, and may be analysed to give the acetate binding parameters shown in Table I.

Here is not the place to attempt any interpretation of these data, but it is important to point out some of the complications that can arise. For example, during the course of these experiments it became clear that the binding of many ligands was not a straightforward process. In particular, the apparent  $K$  and  $\Delta H$  values showed some dependence on total antibiotic concentration and, in some cases at higher antibiotic concentration, the thermal titration curves showed anomalous behaviour (Figure 2) inconsistent with simple 1:1 complex formation. Such observations suggest that aggregation of the antibiotics is significant even at the relatively low concentrations used in these experiments (0.04 to 1mM), and it is for this reason that previous calorimetric measurements using less sensitive techniques show some differences with the results presented here (Rodríguez-Tebar et al., 1986; Arriaga et al., 1990). Ligand-induced changes in the aggregation state of the antibiotics have also been inferred from NMR experiments (Waltho & Williams, 1989; Gerhard et al., 1993). The calorimetric observations may be described in terms of a simple ligand-induced dimerization or dissociation model which, in the simplest case, assumes two identical, non-interacting binding sites on the antibiotic dimer. This involves the following equilibria (A = antibiotic, X = ligand):





Not all these parameters are independent, of course. For example:

$$K_D' = K_D \cdot K_2^2 / K_1^2 \quad \text{and} \quad \Delta H_D' = \Delta H_D + 2(\Delta H_2 - \Delta H_1)$$

which emphasises an important principle of thermodynamic linkage (Wyman, 1964) that, in this case for instance, if ligand binding is more favourable to the dimer ( $K_2 > K_1$ ) then ligand binding will also induce dimerization ( $K_D' > K_D$ ), and vice versa.

With so many free variables it has not yet been possible for us to obtain unique sets of parameters by fitting the data. We can, however, model the observations with physically reasonable numbers that may be tested by other kinds of experiment. For example, the vancomycin/N-ac-D-ala-D-ala data of Fig.2 may be modelled approximately by the following parameters:

$$\begin{array}{llll} K_1 & = & 5000 & \text{M}^{-1} & ; & \Delta H_1 & = & -37 & \text{kJ mol}^{-1} \\ K_2 & = & 100000 & \text{M}^{-1} & ; & \Delta H_2 & = & -58 & \text{kJ mol}^{-1} \\ K_D & = & 10 & \text{M}^{-1} & ; & \Delta H_D & = & 0 & \end{array}$$

giving:

$$K_D' = 4000 \text{ M}^{-1} \quad ; \quad \Delta H_D' = -42 \text{ kJ mol}^{-1}$$

This implies that this ligand binds preferentially to the vancomycin dimer, and that the relatively weak tendency toward dimerization of the free antibiotic is significantly enhanced by the presence of peptide ligand. We should emphasise that these are model parameters only, but similar order of magnitude estimates are found for other ligands studied.

Although we have concentrated here on the observations with vancomycin, we have also done most of these experiments with other members of the vancomycin family, including ristocetin, eremomycin, and derivatives. However, despite their familial relationship, their behaviour towards ligand binding can be quite different. For example, with ristocetin we also observe anomalous concentration-dependent ligand binding isotherms

but, in this case, the data are more consistent with ligand-induced dissociation, rather than the association we see with vancomycin. This illustrates the potential complexity of even apparently simple molecular recognition systems, and emphasises the difficulties in generalizing from one system to another.

### 3. DIFFERENTIAL SCANNING CALORIMETRY

Differential scanning calorimetry is a relatively simple and familiar technique involving measurement of the differential heat energy uptake in the sample during a change in temperature. For systems showing a sharp thermal transition, such as lipid bilayer phase changes, DNA/RNA melting, or protein unfolding transitions, the resultant peak in excess heat capacity may be analyzed to give overall enthalpy, heat capacity, and other thermodynamic components of the process. The main technical difficulty with biological materials is that one ideally needs to work in dilute (< 1mg/ml) aqueous solutions where the heat capacity of the sample may be overwhelmed by that of the water, but specialist instruments based on the designs of Privalov and Brandts are available (Privalov & Potekhin, 1986; Cooper & Johnson, 1993b).

#### (a) Protein Folding Forces

Protein folding and unfolding has been extensively characterized by DSC studies, in parallel with other methods, though the precise balance of thermodynamic forces responsible for the stabilization of protein conformations is still unclear - see Dill (1990) for review.

Building upon earlier work by Velicelebi & Sturtevant (1979) we have recently looked at the thermal unfolding of a small protein, ubiquitin, in mixed water/methanol mixtures (Woolfson *et al.*, 1993). High resolution NMR of this protein has shown that it retains its native conformation even up to 40% MeOH. In the absence of methanol, ubiquitin is quite stable, but undergoes a cooperative thermal unfolding transition at elevated temperatures (Figure 3). The details of this endothermic transition are typical of small globular proteins

in aqueous solution, including the distinctive increase in excess heat capacity of the unfolded chain with respect to the folded protein. This positive  $\Delta C_p$  mimics the thermodynamics of transfer of organic molecules from non-polar to aqueous phases, and is usually taken as the signature of hydrophobic stabilization of the folded protein (Kauzmann, 1959). In the presence of methanol, although its stability is reduced somewhat, the protein still undergoes a cooperative endothermic transition but with  $\Delta C_p = 0$ , in contrast to the behaviour in pure water. The transition is also significantly more endothermic ( $\Delta H$  more positive) than would be expected in water at the same temperature. NMR experiments indicate that, although thermal unfolding is not apparently as complete as it is in water, aromatic side chains do become exposed in the high temperature state of ubiquitin in water/methanol mixtures. Consequently, although the protein may fold entirely adequately in mixed solvents, such folding lacks the thermodynamic characteristics of the hydrophobic interaction.

This illustrates, perhaps, some of the important principles and major difficulties in describing the thermodynamic basis of protein folding. Although much structural emphasis is placed on hydrogen bonding within protein structures, the thermodynamic contribution of such interactions to the stability of the folded protein in water is relatively small or non-existent. This is because polar, H-bonding groups usually have a strong affinity for water that, in small molecules at least, makes them more soluble in water than in non-polar environments. Consequently, although it is energetically important that all H-bonds be made, it is relatively unimportant whether these are intra-molecular bonds with other peptide or side chain groups, or inter-molecular with solvent water. The tightly packed, extensive H-bonded network we see within proteins is a necessary but not sufficient thermodynamic condition for folding, and the driving force is (probably) provided by the hydrophobic contribution. However, replace some of the solvent water with less polar molecules, and this balance may change. Hydrophobic residues may now favour the unfolded state, exposed to the non-polar solvent, but transfer of hydrogen-bonding groups would be less favourable because they would now be unable to make H-bonds with solvent. As far as the protein is concerned, at low temperature, the compact extensively H-bonded structure is favourable in either solvent, though the thermodynamic

characteristics might be quite different. Experimentally it is quite difficult to separate different contributions such as these since it is impossible to find solvent mixtures that change hydrophobicity, for example, without at the same time altering hydrogen bond affinities - indeed this is inevitable since the "hydrophobic effect" is really only another consequence of the hydrogen bond in water.

(b) Molecular Recognition of Unfolded Proteins

The standard picture of the unfolding of a globular protein involving exposure of non-polar residues leads directly to a simple method to recognise the unfolded state using cyclodextrins. These cyclic polysaccharides can bind to a wide range of non-polar molecules in water, usually by complexation within the relatively hydrophobic cavity of the toroidal molecule (Bender & Komiyama, 1978; Saenger, 1980; Szejtli, 1982). The broad specificity of this process is well established and has stimulated a wide range of applications, including recently such delightful examples as the formation of "molecular necklaces" of  $\alpha$ -CD molecules threaded onto single polymer chains (Harada & Kamachi, 1992), and the inclusion of  $C_{60}$  into  $\gamma$ -CD to give water-soluble fullerenes (Andersson *et al.*, 1992). This remarkable versatility prompted the thought that cyclodextrins might also affect the thermal stability of proteins and other macromolecules (Cooper, 1992). Since the unfolding of a globular protein normally involves the exposure of buried hydrophobic amino acid side-chains (Kauzmann, 1959; Privalov & Gill, 1988), the binding of cyclodextrins to these exposed residues might destabilize its native conformation by shifting the equilibrium in favour of the unfolded polypeptide chain. This indeed appears to be the case. Differential scanning calorimetry (DSC) measurements of a series of proteins shows that  $\alpha$ -CD promotes unfolding, and that increasing cyclodextrin concentrations progressively reduce the thermal stability of the proteins in a manner consistent with weak non-covalent attachment of  $\alpha$ -CD molecules onto the unfolded chain. This novel means of perturbing conformation in solution is proving useful in probing the thermodynamics and kinetics of protein folding.

Figure 4(a)-(d) gives examples of DSC traces showing the endothermic unfolding transitions of a representative series

of proteins in aqueous buffers, with and without  $\alpha$ -CD. With the exception of PGK, and provided samples are not kept at high temperature for too long, all these thermograms are fully reversible and are typical of simple cooperative thermal unfolding transitions of proteins.  $\alpha$ -cyclodextrin reduces the mean unfolding transition temperature ( $T_m$ ) for all proteins examined, and the effect is approximately linear with [ $\alpha$ -CD] up to saturating concentrations (about 14% w/v at room temperature), as illustrated in Figure 5. Similar effects are seen with  $\beta$ -cyclodextrin and with its more soluble hydroxypropyl derivative (Fig. 4e).

Two other effects are apparent in Figure 4. Firstly, alongside the reduction in  $T_m$  there is a consistent decrease in the transition enthalpy ( $\Delta H_m$ ) with increasing cyclodextrin concentration. Part of this arises from the normal temperature dependence of  $\Delta H_m$  for globular proteins, which is a manifestation of the heat capacity increment ( $\Delta C_p$ ) on unfolding (Kauzmann, 1959; Privalov & Gill, 1988). However, even when corrected for this effect, the observed transition enthalpies are consistently lower than expected at these temperatures in the absence of CD, by up to about 40 kJ mol<sup>-1</sup> at the highest available concentrations. Secondly, the  $\Delta C_p$  values themselves are also consistently lower in the presence of CD, as indicated by the post-transition heat capacity baselines (except for PGK where this is obscured by the exothermic aggregation of the protein). Both these effects are consistent with the binding of cyclodextrin molecules to hydrophobic sites exposed on the unfolded polypeptide. Heats of complex formation between  $\alpha$ -CD and aromatic groups are small but exothermic (typically -4 to -20 kJ mol<sup>-1</sup>; Lewis & Hansen, 1973; Cooper & MacNicol, 1978) and complex formation with such groups on the unfolded polypeptide would both reduce the overall transition enthalpy and, by burying these groups within the CD cavity, also reduce the  $\Delta C_p$  effect.

Mole-for-mole, the destabilizing effects of cyclodextrins are comparable to or even greater than conventional chemical denaturants such as urea or guanidine hydrochloride under similar conditions. Unlike urea or GuHCl, however, where the denaturing mechanism is far from clear, the cyclodextrin destabilizing effect can be described in terms of a quite simple binding model.

Assume, for simplicity, that there are  $n$  identical and independent ligand (L) binding sites exposed when the native protein (N) undergoes the 2-state transition to the unfolded state (D). The unfolding transition may be described by the simple equilibrium:



with subsequent ligand binding given by:



.. ..



where  $K$  is the intrinsic binding constant for ligand at any one site. Following standard methods, and bearing in mind the combinatorial factors, one may derive an overall apparent equilibrium constant for the unfolding process:

$$K_{App} = [D]_{tot}/[N]_{tot} = K_0(1 + K[L])^n$$

which shows, as expected, that unfolding of the protein is promoted by increasing ligand concentrations. For the interpretation of DSC experiments, this is best expressed in terms of the effect on  $T_m$ , the mid-point temperature of the transition, obtained as follows.

The Gibbs free energy of unfolding at any temperature ( $T$ ) is given by:

$$\begin{aligned} \Delta G &= -RT \cdot \ln K_{App} \\ &= \Delta G_0 - nRT \cdot \ln(1 + K[L]) \quad \dots\dots\dots \text{Equ. (1)} \end{aligned}$$

where  $R$  is the gas constant, and  $\Delta G_0 = -RT \cdot \ln K_0$  is the free energy of unfolding in the absence of ligand. This may be further expressed in terms of the enthalpy of the transition ( $\Delta H_0$ ) at the mid-point temperature ( $T_{m0}$ ) in the absence of ligand:

$$\Delta G_0 = \Delta H_0(1 - T/T_{m0})$$

(Ignoring, for simplicity, any possible temperature dependence of the enthalpy. This is a reasonable approximation over the narrow temperature ranges considered here, but  $\Delta C_p$  effects may be incorporated if required.)

In the presence of ligand, the mid point of the unfolding transition will occur at temperature  $T_m$  when, by definition,  $\Delta G = 0$ . Re-arrangement of Equ.(1) under these conditions gives:

$$\Delta T_m/T_m = -(nRT_{m0}/\Delta H_0) \cdot \ln(1 + K[L]) \quad \dots(2)$$

where  $\Delta T_m = T_m - T_{m0}$  is the shift in transition temperature of the protein brought about by the presence of ligand.

At low concentrations, with a weakly-binding ligand ( $K[L] \ll 1$ ), this takes on the approximate linear form:

$$\Delta T_m = -nKRT_{m0}^2 \cdot [L]/\Delta H_0 \quad \dots(3)$$

These simple expressions allow one to estimate the number of ligand binding sites and their average intrinsic binding constants.

{Equivalent expressions for a model in which ligand binds to the native, rather than unfolded form of the protein are identical to Equ.2 & 3, except for a change of sign.}

Figure 5 shows data for three different proteins plotted according to Equ.2, from which one may estimate the apparent numbers of binding sites and binding constants listed in Table II. Despite the simplifying assumptions, it is clear that this basic model is reasonably successful in explaining the observations, with estimates of  $n$  comparable to the number of available aromatic side-chains in these proteins and with weak  $K$  values expected for such cyclodextrin complexations at higher temperatures (Cooper & MacNicol, 1978).

Further work in this area is concentrating on the effects of these and chemically-modified cyclodextrins on the kinetics and reversibility of folding, and the use of polymerised

cyclodextrins both to improve the recognition selectivity and to separate folded and unfolded proteins by chromatographic techniques.

#### 4. EXPERIMENTAL METHODS

Calorimetric experiments reported here were done using Microcal MC2-D (DSC) or Omega (ITC) instruments as described elsewhere (Cooper, 1992; Cooper & Johnson, 1993a,b,c; McAuley-Hecht & Cooper, 1993), and analyzed using the ORIGIN suite of programs from Microcal Inc. Proteins, peptides, and cyclodextrins were from commercial suppliers (Sigma, Aldrich), with the exception of some modified peptides and antibiotics courtesy of Dr. D.H. Williams and his group. Protein concentrations were determined from 280nm absorbance measurements (Gill & von Hippel, 1989).

#### 5. ACKNOWLEDGEMENTS

Much of the work reported here arises from generous collaboration with Drs. Dudley H. Williams, Joel P. Mackay, Ute Gerhard, and other members of the Cambridge group, for which we are most grateful. Financial assistance for the calorimetric and other facilities in Glasgow, together with a research studentship (K.E.McA-H.) was provided by SERC.

## REFERENCES

- Andersson, T., Nilsson, K., Sundahl, M., Westman, G. & Wennerström, O. 1992 C<sub>60</sub> Embedded in  $\gamma$ -cyclodextrin: a water-soluble fullerene. J.Chem.Soc. Chem.Commun., 1992, 604-606.
- Arriaga, P., Laynez, J., Menendez, M., Cañada, J. & Garcia-Blanco, F. 1990 Thermodynamic analysis of the interaction of the antibiotic teicoplanin and its aglycone with cell-wall peptides. Biochem.J. 265, 69-77.
- Bastos, M., Hägg, S., Lönnbro, P. & Wadsö, I. 1991 Fast titration experiments using heat conduction microcalorimeters. J.Biochem.Biophys.Methods 23, 255-258.
- Bender, M.L. & Komiyama, M. 1978 Cyclodextrin Chemistry (Springer, New York).
- Cooper, A. 1992 Effect of cyclodextrins on the thermal stability of globular proteins. J.Amer.Chem.Soc. 114, 9208-9209.
- Cooper, A. & Johnson, C.M. 1993a Introduction to microcalorimetry and biomolecular energetics. In Methods in Molecular Biology: Protocols for Optical Spectroscopy and Macroscopic Techniques (ed. C. Jones, B. Mulloy & A.H. Thomas), chapter 9, Humana Press Inc., Totowa, NJ.
- Cooper, A. & Johnson, C.M. 1993b Differential scanning calorimetry. In Methods in Molecular Biology: Protocols for Optical Spectroscopy and Macroscopic Techniques (ed. C. Jones, B. Mulloy & A.H. Thomas), chapter 10, Humana Press Inc., Totowa, NJ.
- Cooper, A. & Johnson, C.M. 1993c Isothermal titration microcalorimetry. In Methods in Molecular Biology: Protocols for Optical Spectroscopy and Macroscopic Techniques (ed. C. Jones, B. Mulloy & A.H. Thomas), chapter 11, Humana Press Inc., Totowa, NJ.

Cooper, A. & MacNicol, D.D. 1978 Chiral host-guest complexes: interaction of  $\alpha$ -cyclodextrin with optically active benzene derivatives. J.Chem.Soc. Perkin II, 1978, 760-763.

Dill, K.A. 1990 Dominant forces in protein folding. Biochemistry 29, 7133-7155.

Gerhard, U., Mackay, J.P., Maplestone, R.A. & Williams, D.H. 1993 The role of sugar and chlorine substituents in the dimerization of vancomycin antibiotics. J.Amer.Chem.Soc. 115, 232-237.

Gill, S.C. & von Hippel, P.H. 1989 Calculation of protein extinction coefficients from amino acid sequence data. Analyt.Biochem. 182, 319-326.

Harada, A. & Kamachi, M. 1992 The molecular necklace: a rotaxane containing many threaded  $\alpha$ -cyclodextrins. Nature,Lond. 356, 325-327.

Kauzmann, W. 1959 Some factors in the interpretation of protein denaturation. Adv. Protein Chem. 14, 1-63.

Lewis, H.A. & Hansen, L.D. 1973 Thermodynamics of binding of guest molecules to  $\alpha$ - and  $\beta$ -cyclodextrins. J.Chem.Soc. Perkin II 1973, 2081-2085.

McAuley-Hecht, K.E. & Cooper, A. 1993 Microcalorimetry of enzyme-substrate binding: yeast phosphoglycerate kinase. J.Chem.Soc. Faraday Trans. 89, (in press)

Privalov, P.L. & Gill, S.J. 1988 Stability of protein structure and hydrophobic interaction. Adv. Protein Chem. 39, 191-234.

Privalov, P.L. & Potekhin, S.A. 1986 Scanning microcalorimetry in studying temperature-induced changes in proteins. Meth.Enzymol. 131, 4-51.

Rodríguez-Tebar, A., Vázquez, D., Velázquez, J.L.P., Laynez, J. & Wadsö, I. 1986 Thermochemistry of the interaction between peptides and vancomycin or ristocetin. J.Antibiot. **39**, 1578-1583.

Saenger, W. 1980 Cyclodextrin inclusion compounds in research and industry. Angew.Chem., Int. Ed. Engl. **19**, 344-362.

Sturtevant, J.M. 1974 Some applications of calorimetry in biochemistry. Ann.Rev.Biophys.Bioeng. **3**, 35-51.

Sturtevant, J.M. 1987 Biochemical applications of differential scanning calorimetry. Ann.Rev.Phys.Chem. **38**, 463-488.

Szejtli, J. 1982 Cyclodextrins and Their Inclusion Complexes (Akademiai Kiado, Budapest).

Velicelebi, G. & Sturtevant, J.M. 1979 Thermodynamics of the denaturation of lysozyme in alcohol-water mixtures. Biochemistry **18**, 1180-1186.

Wadsö, I. 1983 Biothermodynamics and calorimetric methods. Pure Appl.Chem. **55**, 515-528.

Wadsö, I. 1991 Microcalorimetry, with special reference to aqueous systems including uses in biology. In Experimental Chemical Thermodynamics - Solution Chemistry (ed. K.N. Marsh & P.A.G. O'Hare) Blackwell, Oxford.

Waltho, J.P. & Williams, D.H. 1989 Aspects of molecular recognition: Solvent exclusion and dimerization of the antibiotic ristocetin when bound to a model cell-wall precursor. J.Amer.Chem.Soc. **111**, 2475-2480.

Williams, D.H., Stone, M.J., Mortishire-Smith, R.J. & Hauck, P.R. 1990 Molecular recognition by secondary metabolites. Biochem.Pharmacol. **40**, 27-34.

- Williams, D.H., Cox, J.P.L., Doig, A.J. et al. 1991 Towards the semiquantitative estimation of binding constants. Guides for peptide-peptide binding in aqueous solution. J.Amer.Chem.Soc. **113**, 7020-7030.
- Williams, D.H., Searle, M.S., Mackay, J.P., Gerhard, U. & Maplestone, R.A. 1993 Toward an estimation of binding constants in aqueous solution: studies of associations of vancomycin group antibiotics. Proc.Natl.Acad.Sci.USA **90**, 1172-1178.
- Wiseman, T., Williston, S., Brandts, J.F., & Nin, L-N 1989 Rapid measurement of binding constants and heats of binding using a new titration calorimeter. Analyt.Biochem. **179**, 131-137.
- Woolfson, D.N., Cooper, A., Harding, M.M., Williams, D.H. & Evans, P.A. 1993 Protein folding in the absence of the solvent ordering contribution to the hydrophobic interaction. J.Mol.Biol. **229**, 502-511.
- Wright, G.D. & Walsh, T.W. 1992 D-Alanyl-D-alanine ligases and the molecular mechanism of vancomycin resistance. Acc.Chem.Res. **25**, 468-473.
- Wyman, J. 1964 Linked functions and reciprocal effects in hemoglobin: a second look. Adv.Protein Chem. **19**, 223-286.

Table I: Thermodynamic parameters for binding of assorted peptide ligands to vancomycin at 25°C, determined by isothermal titration microcalorimetry at pH 7.0 in 0.1M phosphate buffer.\*

Ligand	K M <sup>-1</sup>	$\Delta G^0$ kJ mol <sup>-1</sup>	$\Delta H$ kJ mol <sup>-1</sup>	$\Delta S^0$ J K <sup>-1</sup> mol <sup>-1</sup>	$\Delta C_p^0$ J K <sup>-1</sup> mol <sup>-1</sup>
N-acetyl-gly-gly	ca. 200	ca. -13	ca. -35	ca. -74	-
N-acetyl-D-ala	300	-14.1	-35.8	-73	525
N-ac-D-ala-D-ala	6600	-21.8	-35.6	-46	330
N-ac-gly-D-ala	5600	-21.4	-35.6	-48	-
N,N'-diacetyl-L-lys-D-ala	520000	-32.6	-53.3	-69	-
N-fumaryl-D-ala	2900	-19.8	-43.9	-81	-
N-succinyl-D-ala	1250	-17.7	-42.9	-85	-
Acetate**	6.5	-4.6	-24	-65	-

\* Measured with an antibiotic concentration of 0.1mM, or less, in cases where aggregation is significant.

\*\* Determined by competitive binding with N,N'-diac-L-lys-D-ala-D-ala

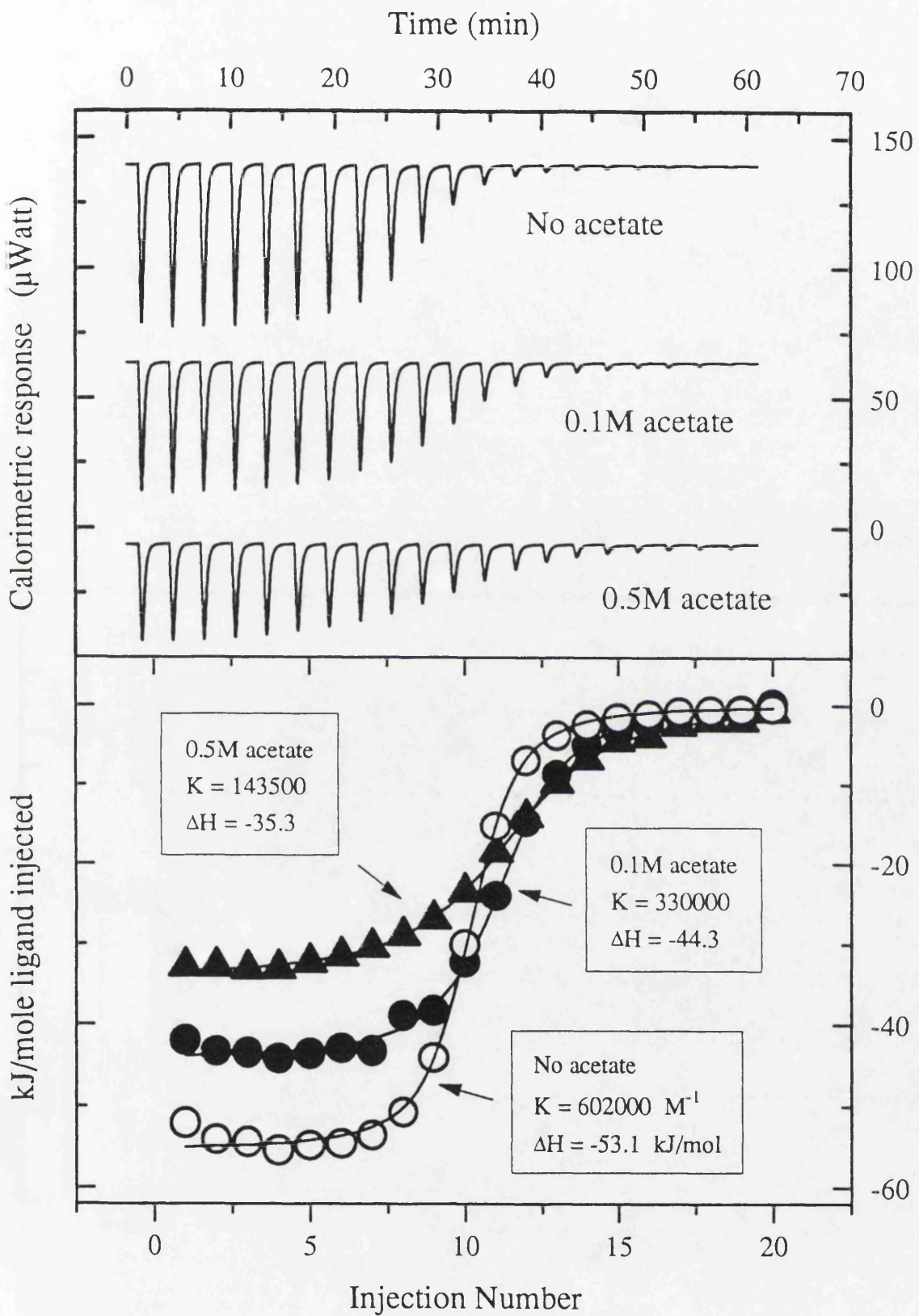
Table II: Protein-Cyclodextrin Binding Parameters determined from  $\Delta T_m$  versus  $[\alpha\text{-CD}]$  using equ.2.

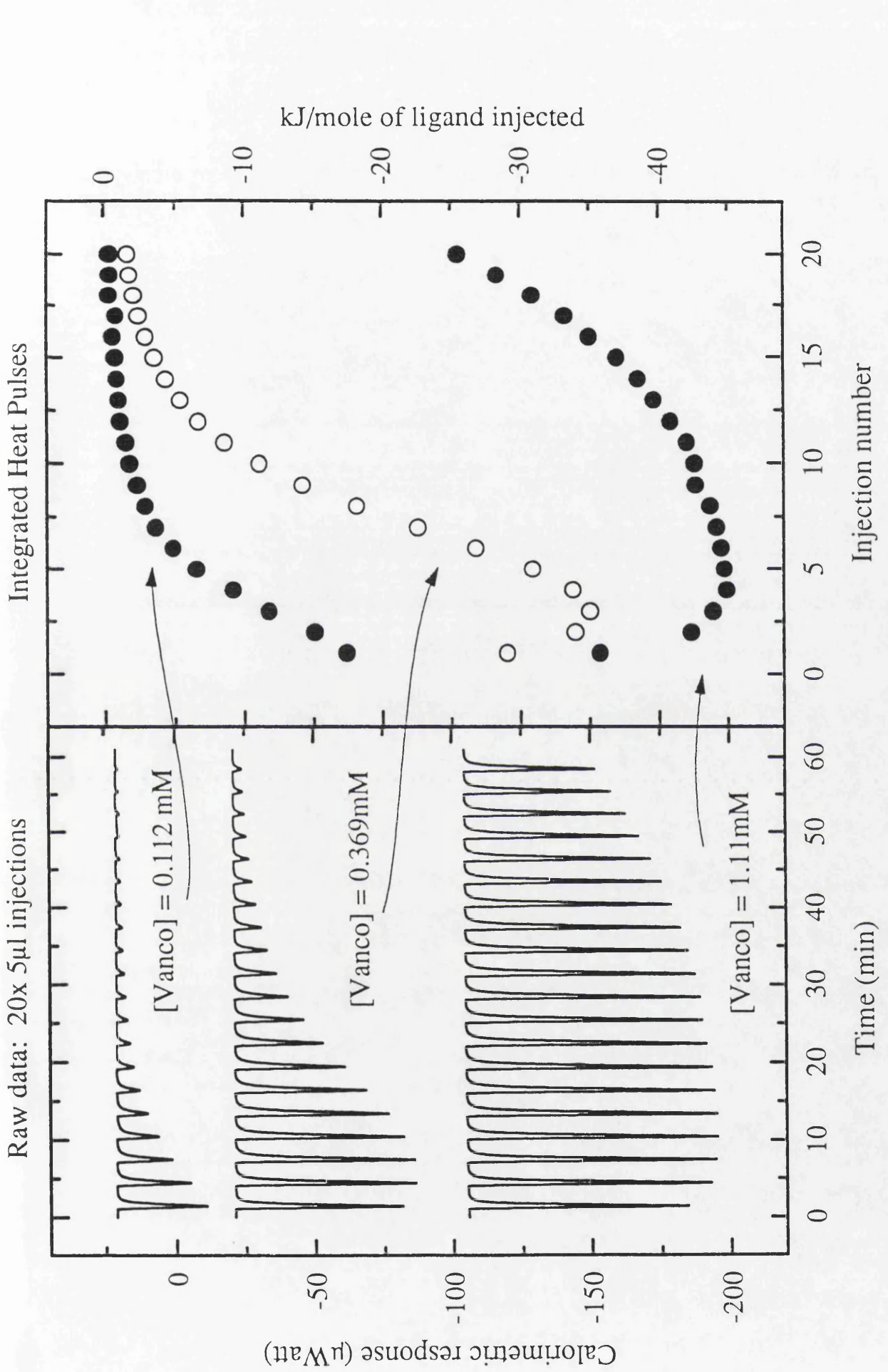
	Aromatic Side Chains				Total	$n_{\text{expt}}$	$K_b$ ( $M^{-1}$ )*
	Trp	Tyr	Phe				
Lysozyme	6	3	3		12	ca. 12	ca. 2
RNase	0	6	3		9	5.4	2.2
Ubiquitin	0	1	2		3	3.7	7.4

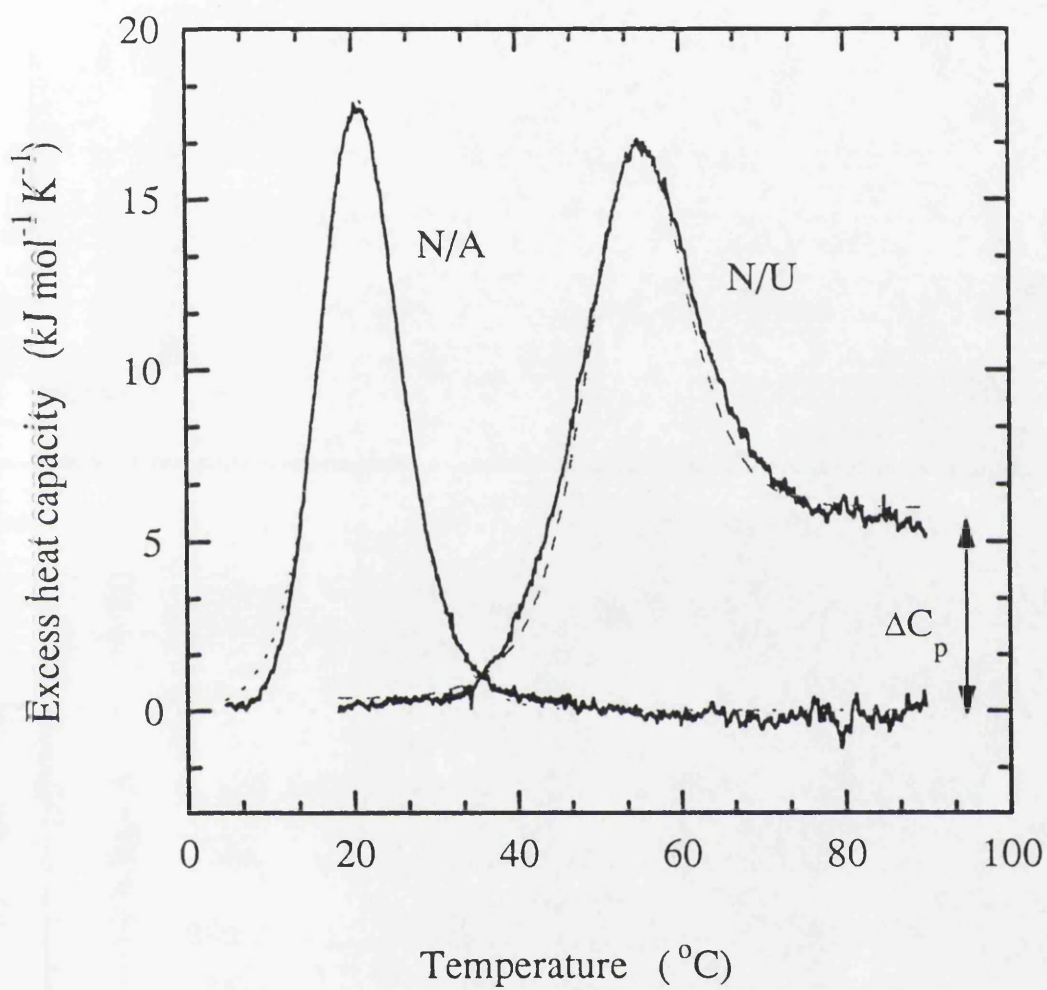
\* For comparison, the typical  $\alpha\text{-CD}$  binding constant for an aromatic amino acid (phenylalanine) in solution is approximately  $9 M^{-1}$  at  $65^\circ\text{C}$  (estimated from Cooper & MacNicol, 1978).

## FIGURE LEGENDS

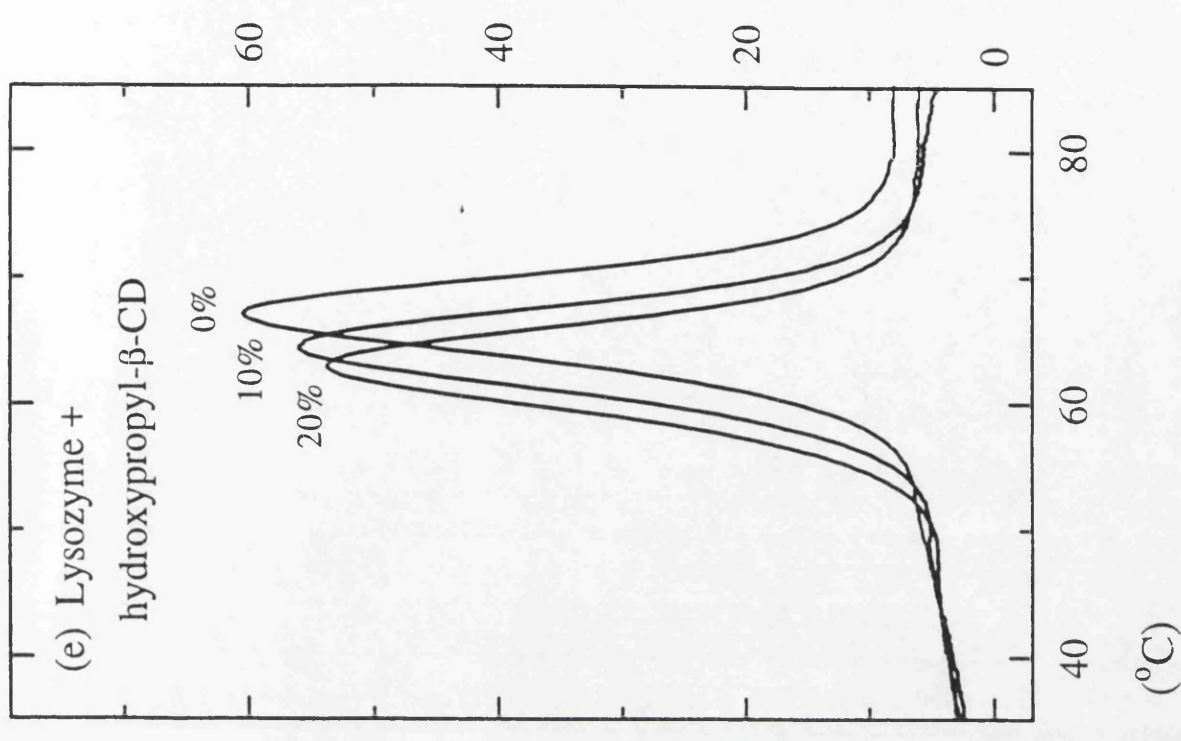
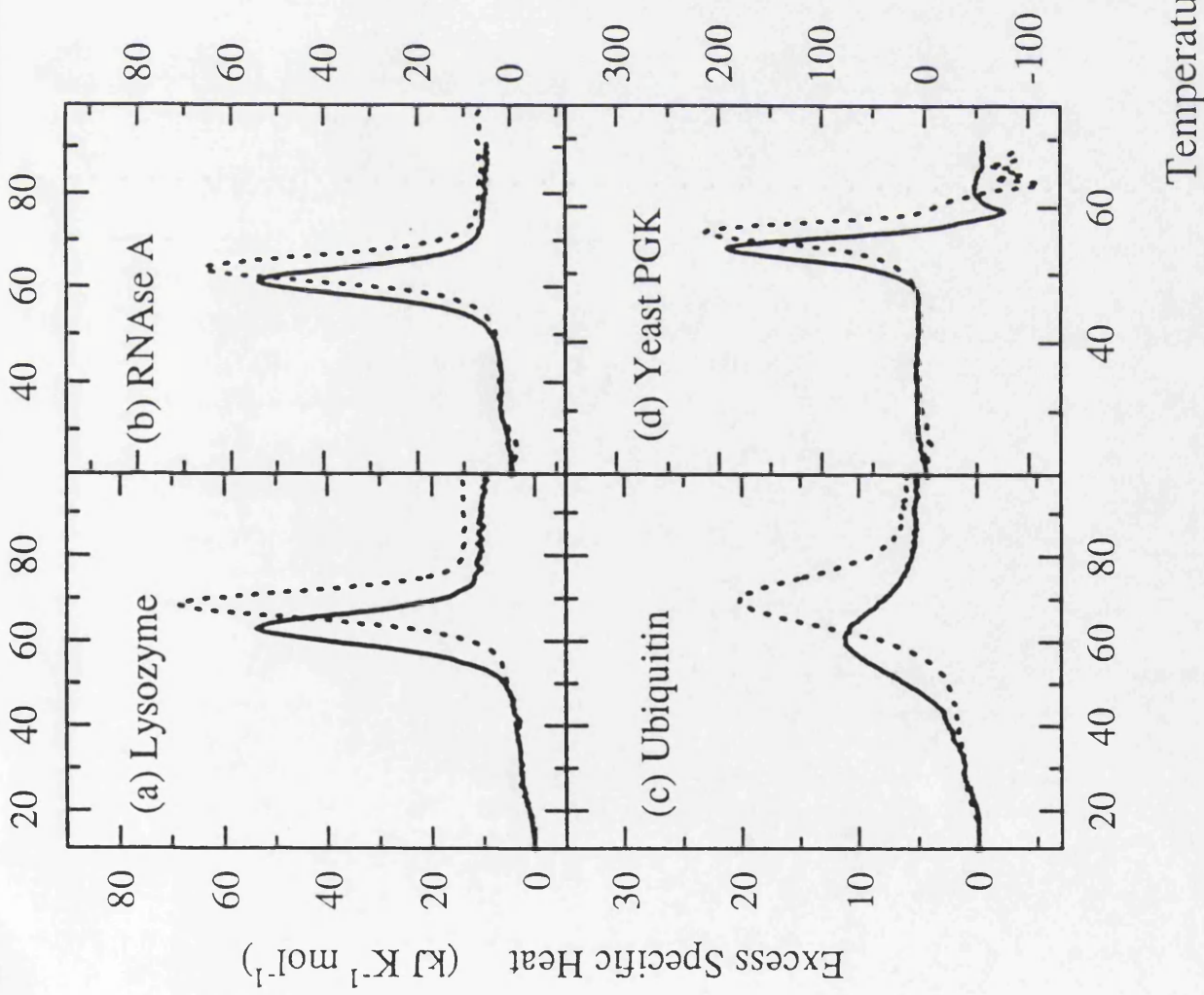
- Fig.1 Isothermal calorimetry data for the titration of vancomycin (0.3mM) with 20 x 5 $\mu$ l injections of N,N'-diacetyl-L-lys-D-ala-D-ala (7mM) in 0.1M phosphate buffer, pH 7, at 25°C. The upper part of the figure gives the raw data showing the sequence of exothermic heat pulses for three separate titrations at different acetate concentrations. The lower figure gives the integrated heat energy per injection, together with theoretical fits to each thermal titration curve, illustrating the competitive inhibition by acetate. The reaction cell volume of the calorimeter is about 1.4ml.
- Fig.2 ITC data for binding of N-acetyl-D-ala-D-ala to vancomycin at 25°C, pH 7. Each experiment consists of an identical sequence of 20 x 5 $\mu$ l injections of peptide ligand (12.3mM) into vancomycin solutions at three different concentrations (0.112, 0.369, and 1.11mM).
- Fig.3 Baseline-corrected DSC data for the thermal transition of ubiquitin in aqueous buffer (N/U) and 40% methanol/water mixtures (N/A).
- Fig.4 (a)-(d) DSC data for the thermal unfolding of proteins in the absence (dotted lines) and presence (solid lines) of  $\alpha$ -cyclodextrin. (e) shows similar data for lysozyme with various concentrations of hydroxypropyl- $\beta$ -cyclodextrin.
- Fig.5 The decrease in thermal transition temperatures ( $\Delta T_m$ ) as a function of  $\alpha$ -cyclodextrin concentration for three different proteins. The lines are non-linear regression fits to equ.2 with the parameters given in Table II.

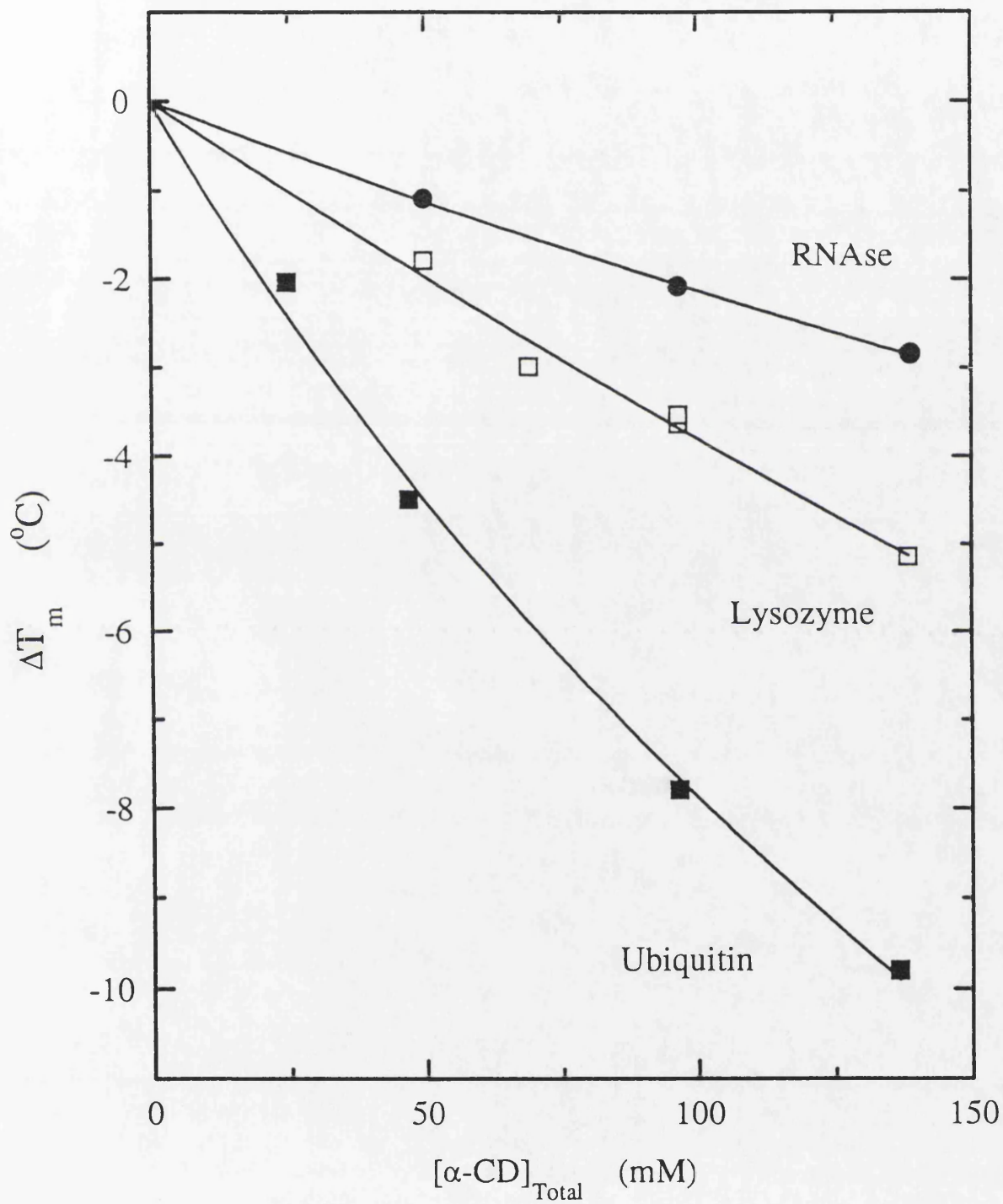






Cooper & McAuley-Hecht: Fig.3





GLASGOW  
UNIVERSITY  
LIBRARY